Study of Ventilation Flow in a Room Induced by Solar Chimneys

By

Kashif Nazir

Supervisor :**Dr. B. Phuoc Huynh**
Co-Supervisor :**Dr. Tien Thanh Nguyen**

A Thesis Submitted to the Graduate Research School, University of Technology Sydney for the Degree of Master of Science (Research)

School of Electrical, Mechanical & Mechatronics System
Faculty of Engineering & IT, University of Technology Sydney

January, 2018

CERTIFICATE OF ORIGINAL AUTHORSHIP

I certify that the work in this thesis has not previously been submitted for a degree nor has it been submitted as part of requirements for a degree except as fully acknowledged within the text.

I also certify that the thesis has been written by me. Any help that I have received in my research work and the preparation of the thesis itself has been acknowledged. In addition, I certify that all information sources and literature used are indicated in the thesis.

Production Note:
Signature removed prior to publication.

Signature of Student:

Dated: 16-01-2018

Acknowledgements

I am extremely grateful to Dr. Phuoc Huynh for his invaluable technical guidance and attentive, friendly support throughout this degree. He guided and supported me in every aspect to achieve this target. I was also very lucky to learn from Dr. Thanh Nguyen, who helped me in every phase, whenever required, during my study. I would like to thank Management / Staff of Faculty of Engineering & Information Technology and Graduate Research School for their support and help.

I would also like to thank my wife who supported me all the time especially during this study period. I would like to dedicate this study to my wife and parents, who always prayed for me to accomplish this task.

Table of Contents

List of Figures

List of Tables

Abstract

A Solar Chimney is a structure for ventilation purpose installed on the roof or side of any building to induce the stagnant air present in the room / building naturally to the outside using solar heat and attracts the fresh air from outside into the building. Many researchers and scientists have carried out studies based on computation and experiments for different type of solar chimney systems. Despite the fact that extensive work has already been carried out in this field but still huge potential exists to make this system more effective and economical.

The focus of the study and research is on solar chimney based ventilation systems. The use of Computational Fluid Dynamics (CFD) in solar chimney based system has been investigated and CFD models have been developed for research. In this study, naturally induced flow through a Two and Three Dimensional square rooms having dimensions (3 Meter × 3 Meter) and (3 Meter × 3 Meter × 3 Meter) respectively have been developed and investigated through numerical analysis. The numerical analysis has been carried out using Computational Fluid Dynamics (CFD) software. An inclined solar chimney has been used on the roof of the above mentioned square room to induce air flow through the room.

Based on the previous research in this field, the chimney height has been taken as 1.5 meter (effective length 2.12 meter), width of the chimney (0.3 meter for 2D room and 0.4 meter for 3D room). The chimney inclination angle is 45 degree with roof top and solar heat flux rate for chimney heated wall has been fixed as 300 W/m^2. The room air inlet is square shaped having dimensions 0.4 meter × 0.4 meter. The purpose is to investigate the effect of change of room air inlet position (Bottom, Center,

Top of the room side wall) to ultimately design / suggest most effective scenario.

The graphical and numerical analysis shows that by changing the room air inlet location, the air flow rate and flow pattern significantly changes. The best pattern is the one where air is evenly distributing in the room and passes through the sitting area of the occupants i.e. around floor of the room. Keeping this important factor in view, the desired air flow pattern, in both 2D and 3D simulations, has been seen in a model with air inlet location at top of the side wall.

Nomenclature / List of Symbols Used

The nomenclatures of terminologies and symbols used in the study are given below:

T	**Temperature**
P_t	**Total Pressure**
K	**Thermal Conductivity**
k	**Turbulent Kinetic Energy**
g	**Gravity**
T_{ref}	**Reference Temperature**
ρ	**Density**
μ	**Dynamic Viscosity**
v	**Kinematic Viscosity**
ε	**Dissipation Rate**
U	**Velocity in Horizontal Direction**
V	**Velocity in Vertical Direction**
W	**Velocity in Z-direction**
ΔP	**Pressure Difference**
VM	**Velocity Magnitude**
P	**Static Pressure**
Cp	**Specific Heat**
Q	**Heat Flux**
RH	**Wall roughness Height**

H_s	**Stack Height**
S_{ij}	**Mean strain-rate tensor**
τ_{ij}	**Reynolds stress tensor**
Re	**Reynolds Number**
Ra	**Rayleigh Number**
Pr	**Prandtl's Number**
C_D	**Closure Coefficient**
f	**External forces acting on a body**
β	**Volumetric Expansion Coefficient**
ℓ	**length**
P_s	**Stack Pressure**

All length values used / given in the study are in meters, Velocity in Meter/Sec and Pressure values in N/m^2, if otherwise specified.

Chapter 1

INTRODUCTION

1.1 History of Solar Chimney Based Research and Factors for Motivation

Energy, now a day, is a life line for human existence. Every aspect of our day to day life is dependent on energy. Our success and existence in future completely depends on the ways that how we utilize currently available energy resources and most importantly, the discovery of new methods to utilize energy resources which are environmentally friendly, cheaper and available in abundant quantities. Secondly, reduction in energy consumption by using natural sources of energy directly for our day to day uses and environment friendly energy production is an essential requirement to survive and protect our planet.

With continuous development in each sector, the requirement of mechanization and energy increases. Some Energy expert says that, *Alternative or renewable energy resources can never replace currently used resources like fossil fuels as there usage has increased manifold while the discovery of alternate resources is at minimum level.*

Below chart gives the idea about consumption of different energy resources:

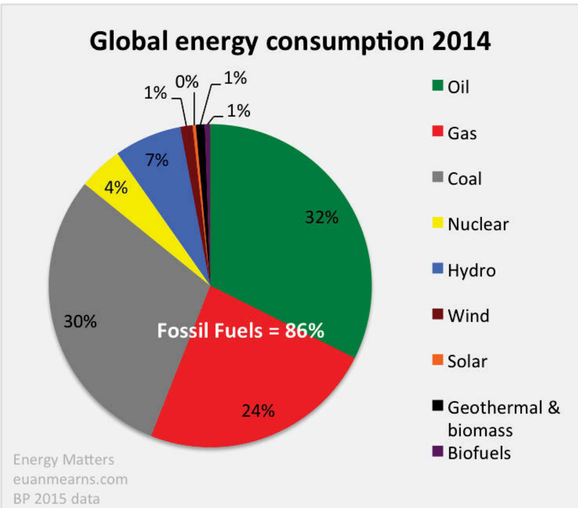

Figure: 1.1 : Global Energy Consumption (Source: "Energy Matters" - euanmearns.com, BP 2015 Data)

Many countries, particularly, developing countries have very less energy resources but their energy demand is increasing day by day at very higher rate due to substantial increase in their population. This scarcity of energy has badly suffered the living standards of people of these countries. The question has arisen now in every mind that how and from where this huge demand of energy can be met while presently used natural energy sources like oil, gas and coal reserves, are depleting rapidly. The following drawbacks of conventional energy sources are also contributing scientific diversion towards more environmental friendly resources:

1.1.1 Expensive

The conventional energy resources have become very expensive to utilize because of multiple factors. These factors may include higher production costs, transportation and storage charges etc. For example, Natural Gas is one of the most widely used conventional energy source. It may be a cheaper energy source when directly used as a Natural Gas but due to its non-availability in most of the countries, the same is being transported by producing countries to other countries by converting Natural Gas to Liquefied Natural Gas (LNG). The conversion of Natural Gas to LNG and its transportation is an expensive procedure. The tanker for LNG transportation, LNG Storage Facilities and re-gasification of LNG to Natural Gas requires huge capital and running expenditure. The conversion of Natural gas to LNG, transportation and re-conversion to Natural Gas make this energy source very expensive. The figure 1.2 below is showing LNG storage and transportation facility.

Figure: 1.2 : LNG storage tanks and a membrane-type tanker at Tokyo Electric Power Co's Futtsu Thermal Power Station in Futtsu, east of Tokyo. (Source: ISSEI KATO/Reuters/File - csmonitor.com)

1.1.2 Depleting Resources

Another drawback of conventional energy sources is that they are depleting very rapidly. Due to exponential increase in energy consumption, the available energy resources are depleting fast. Most of the countries have already depleted their Natural gas and Oil resources which were once available in huge quantities.

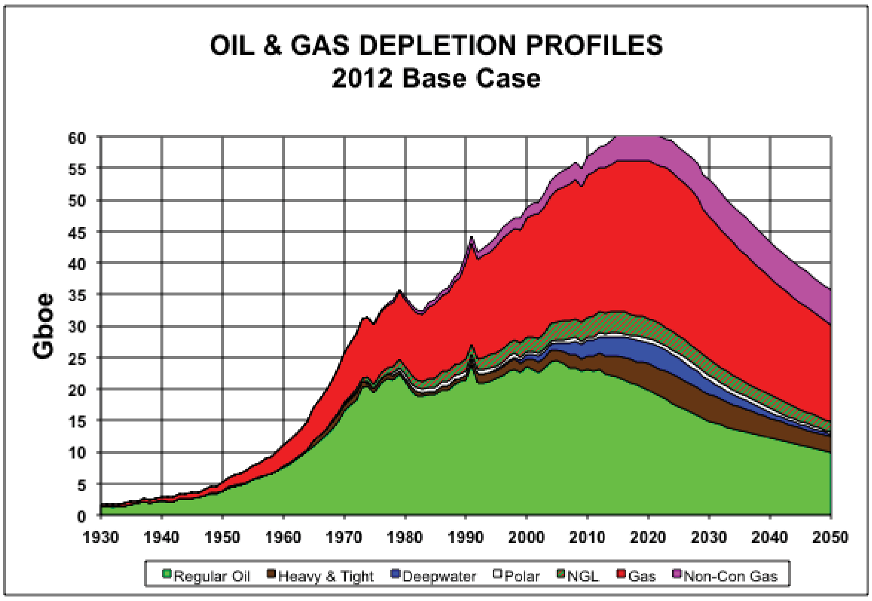

Figure: 1.3 : Graph showing depletion model of conventional energy resources. (Source: Colin J. Campbell, April 2015, "Changing in Human Circumstances" - resilience.org)

1.1.3 Pollution

Environmental pollution is a major concern in utilization of conventional energy resources. The burning of petroleum products emits plenty of carbon dioxide and other poisonous gases which are not only harmful for human health but also causing global warming.

Figure : 1.4: Pollution Caused by Power Plants using Oil and Gas
(Source : Photo by Kris Krug - nationalobserver.com)

1.1.4 Difficult to Handle

The resources of currently utilized conventional energy which include oil, coal and natural gas etc., in any form, are difficult to handle. Our history is full of disasters caused during exploration or use of these resources.

Figure :1.5: Example of Disasters / Accidents Caused during Exploration / Storage of Oil and Gas (Left: BP oil Rig explosion – Source: Release by US Coast Guard & Seen on Wikipedia. Right: Amuay oil refinery in Venezuela – Source: EJAtlas.)

Each year hundreds of precious human lives and millions of dollars of investment are lost in oil and gas related accidents. Although, human has tried to overcome these accidents and to some extent has succeeded to reduce them but these cannot be avoided at all. The preventive measures taken to avoid disasters related to conventional energy resources has significantly increased the capital and running costs of the projects.

1.2 Alternate Energy Resources

Keeping in view the continuous increase in demand of energy and disadvantages of conventional energy resources as explained above, the need is to divert towards other more reliable natural resources which are endless like Sun and from where we may get a clean and cheaper energy using simplest means. The scientists and researchers are continuously trying to develop new technique to use naturally available resources of energy, particularly renewable energy. The Renewable Energy is a term used in the case where energy is produced from environmental friendly resources available naturally. These resources may include Solar Energy (utilization of heat from Sun), energy from wind, energy production using rain, conversion of naturally produced sea waves energy into mechanical energy and geothermal heat. Renewable energy is also termed as naturally replenished energy. These resources may include:

1. Solar Energy

Figure: 1.6: Example of Solar Energy Utilization – Solar Panels (Source: Photo taken from Solartribune.com)

2. Wind Energy

Figure:1.7: Example of Wind Energy Utilization – Wind farm in Bangui Bay, Philippines. (Source: http://www.eco-business.com/news/the-blue-circle-vestas-to-expand-wind-energy-in-southeast-asia/)

3. Energy from Tides (Sea waves)

Figure:1.8: Example of Energy / Electricity production from Sea Waves
(Source: http://cmheavyindustries.com/wave-energy)

4. Hydro Electricity / Power

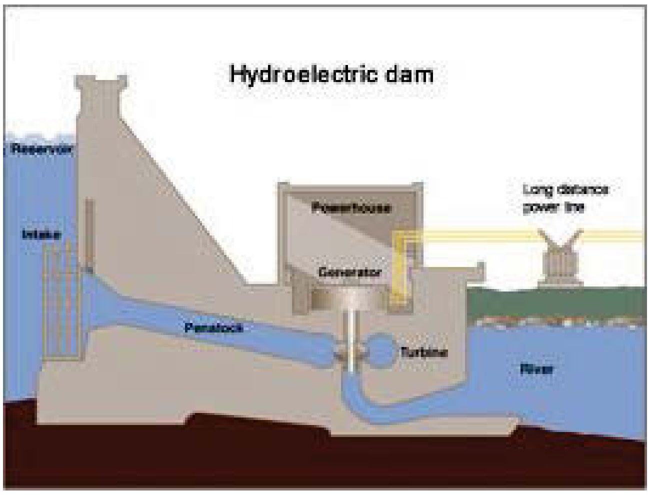

Figure:1.9: Example of Electricity Production from Water – Hydro (Source: Tennessee Valley Authority - public domain): photo taken from <https://www.eia.gov/energyexplained/index.cfm?page=hydropower_home>

5. Geothermal Energy

Figure:1.10: Example of Geo Thermal Energy Plant - Nesjavellir Geothermal Power Station in Iceland (Source: Photo by Gretar Ívarsson, geologist at Nesjavellir (Public Domain), taken from Wikipedia)

6. Bio Energy (Bio Mass & Bio Fuels)

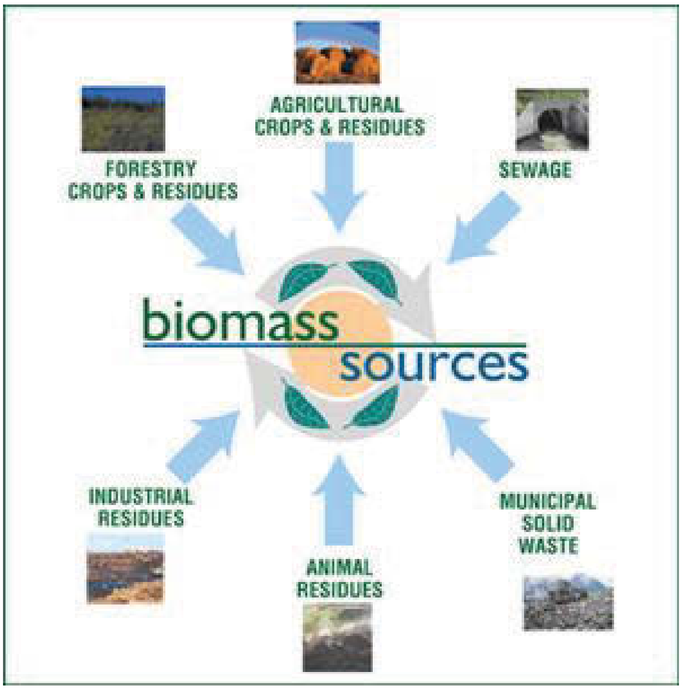

Figure:1.11: An example of different Biomass Sources from which Bio Energy can be produced (Source: Photo taken from Global Energy Network Institute; www.geni.org/globalenergy/library/articles-renewable-energy-transmission/bioenergy)

1.3 Solar Energy

The Sun is a largest source of natural heat and energy for our planet Earth. We need to develop more scientific methods to utilize this natural source of energy for our day to day needs. This can be a cheapest and environment friendly source of energy. There are many direct and indirect ways to utilize solar energy. Some of these methods may be:

1. Electricity production using Solar panels

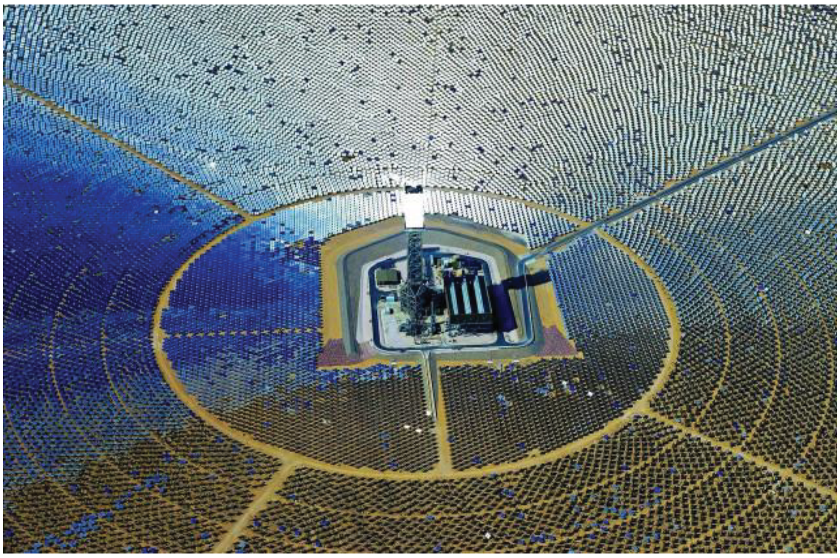

Figure:1.12: An example of Electricity Production from Solar Panels – Bright Source Solar Power Plant in California's Mojave Desert (Source: extremetech.com)

2. Electricity production through Solar Chimney Power Plants

Figure:1.13: An example of Solar Chimney power Plant - Solar Updraft Tower System Arizona by Enviromission (Source: photo taken from cleantechnica.com)

3. Solar Water heating Systems

Figure:1.14: An example of Water Heating based on Solar Energy – Domestic Solar Water Heater (Source: Photo taken from www.solar-geyser.com)

4. Natural Ventilation of the Building using Solar Chimney

Figure:1.14a: An example of Solar Chimney Installed at a Building for Natural Ventilation - Tanga School Falkenberg, Sweden
(Source: Photo Taken from “new-learn.info”)

In this era where we are continuously expanding / developing our cities with large buildings and infrastructures, the requirement of energy has substantially increased. The utilization of different mechanical equipment, consumption of different kinds of material by human and frequent movement of persons inside the building always contribute in increment of pollutant elements inside the building which may affect the human health adversely. This adverse effect has highlighted the need to remove these non-desirable elements. The natural ventilation removes this pollutant air present inside the building by inducing fresh from the outside without consuming any energy. This introduction of fresh air in the building provides better health and comfort to the occupants of the building.

Most of the energy in the building is utilized to give the comfort to the humans living in it or working in it. Some part of the energy is also utilized for the safety of the equipment and machinery installed in it like IT Servers, Computers etc. Most of the designers and researchers are putting their all-out efforts to use cheaper and environment friendly means for the ventilation of these buildings and trying to reduce energy consumption / costs. The most efficient way to achieve this ventilation could be through the installation of Solar Chimney which will use solar heat to induce natural flow in the building. Ample work has been done in this field but still much is needed to make it more economical and effective for our future needs.

1.4 Chimney and Natural Ventilation

In order to avoid currently faced economical, availability and safety issues related to use of conventional energy resources, it is an essential requirement of this time that we make effective utilization of available renewable energy resources. Only through this way, we may be able to cop increasing demand of energy in our day to day life and buildings. Ventilation of any type of building is an essential requirement due to many internal and external factors. One way is to ventilate building using mechanical sources which require energy in huge quantities and other method is Natural Ventilation using Solar Chimney, the use of which will give huge energy saving. Solar Chimneys (SC) are integrated with the building at different locations depending on the design, which uses the natural sunlight to replace the old / stale air present in the building by inducing fresh air from outside. This natural ventilation is based on buoyancy-driven airflow.

The use of chimneys and natural ventilation is a part of every type of architectural era in one way or the other. The advancement in the field of architecture made useful discoveries in the field of natural ventilation. The natural ventilation is a cheapest and the oldest method being employed from small houses to large buildings. Below are pictorial examples of chimneys on old and new buildings.

Figure 1.15 Chimneys, Hampton Court Palace, Surrey, UK. Different patterns and designs on the old chimneys. (Source: By Christine Matthews – taken from "geograph.org.uk")

Figure 1.16 Chimneys built for natural ventilation at The Energy and Resources Institute (TERI), Delhi, India. (Source: "teriin.org/technology/energy-efficient")

1.5 Solar Chimney

The Solar Chimney construction is different from conventional chimney, which has been in use since hundreds of years. The main difference is that the one wall of the Solar Chimney is transparent which allows the passage of solar heat through this wall and heats up other walls of the solar chimney, particularly, the wall opposite to transparent wall which is constructed as absorber. The conventional chimney has all solid walls. Due to solar heat passage inside the solar chimney, the air present in the solar chimney gets heated up and starts to rise up. This rise up of air after increase in temperature is due to buoyancy effect. Due to this buoyancy phenomenon, airflows through the solar chimney channel. As the air flow starts in the solar chimney channel, same effect is transferred down in the building and air present in the building / room is also pulled out of the building through the chimney. The air gap created in the building due to removal of stale air is filled by fresh air which comes inside the building naturally. This is the way how natural ventilation in a building is accomplished.

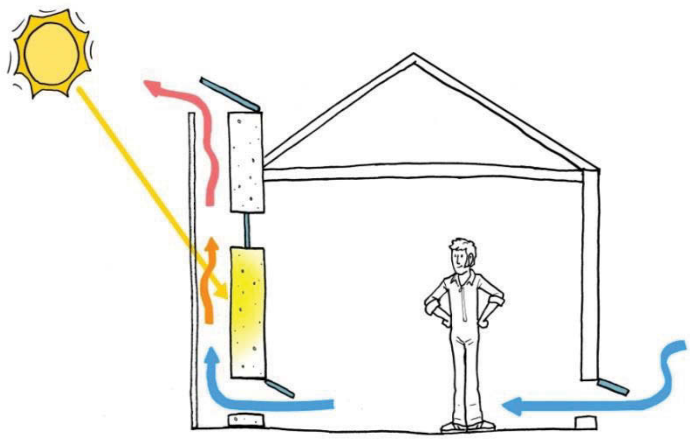

Figure 1.17 Typical Sketch of a Room Fitted with Side Wall Solar Chimney (Source “https://sustainabilityworkshop.autodesk.com/buildings/trombe-wall-and-attached-sunspace”)

The use of solar chimney is being implemented around the world and plenty of researchers are working in the field to enhance natural ventilation rates (air flow). Below is couple of examples showing solar chimneys installed at different locations.

Figure 1.18. Solar Chimneys installed at the roof of Sidwell Friends School, Washington DC. (Source: By Peter Aaron/OTTO, taken from kierantimberlake.com)

Figure 1.19 Solar Chimney at Urban Ecology Center, Menomonee Valley, USA. (Source: urbanecologycenter.org)

The geometry and construction of the Solar Chimney channel is mainly explained by effective height & length of the chimney and width of the chimney. The important parts / elements of the Solar Chimney are presented in Fig. 1.20 below.

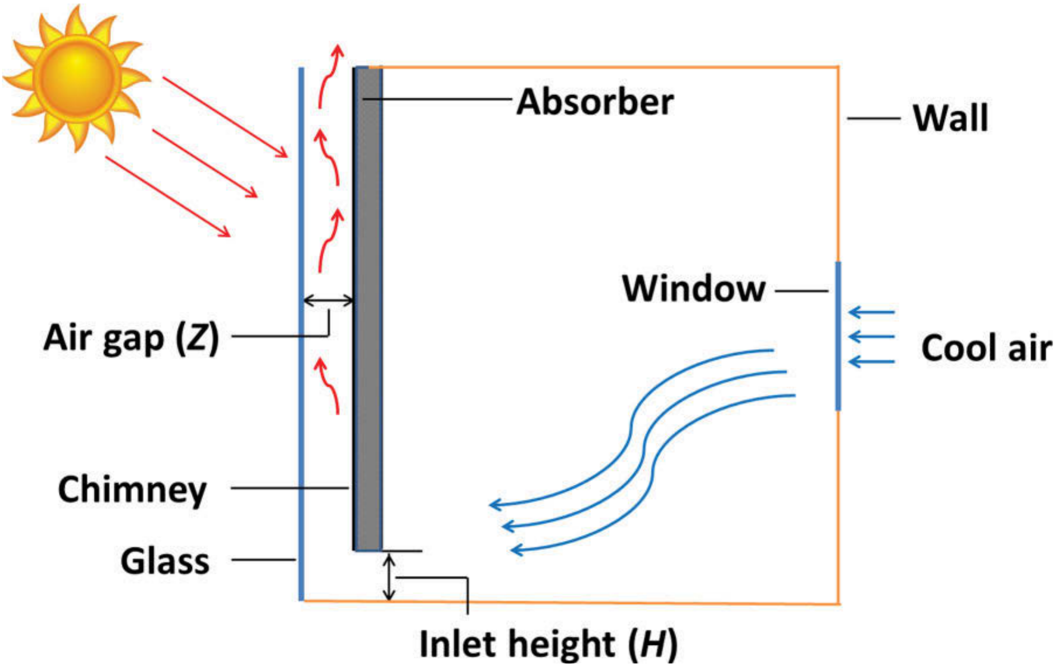

Figure 1.20: Showing parts of a typical Solar Chimney (Source: Photo taken from solarenergyengineering.asmedigitalcollection.asme.org)

Solar Chimney can be installed in any building and with many possibilities as described in Fig. 1.21 below,

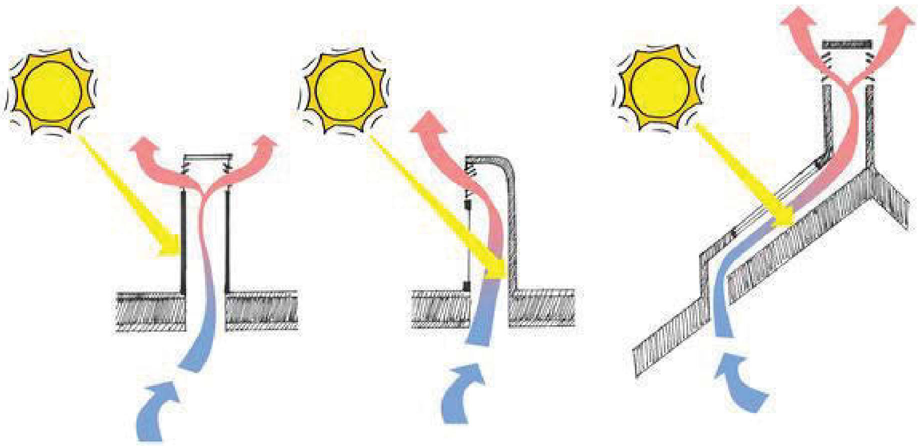

Figure 1.21: Different solar chimney designs, from a simple black-painted pipe to integrated Trombe *roof structure* (Source: sustainabilityworkshop.autodesk.com/buildings)

Below is a general schematic diagram of a multistory building with the installation and functioning of Solar Chimney.

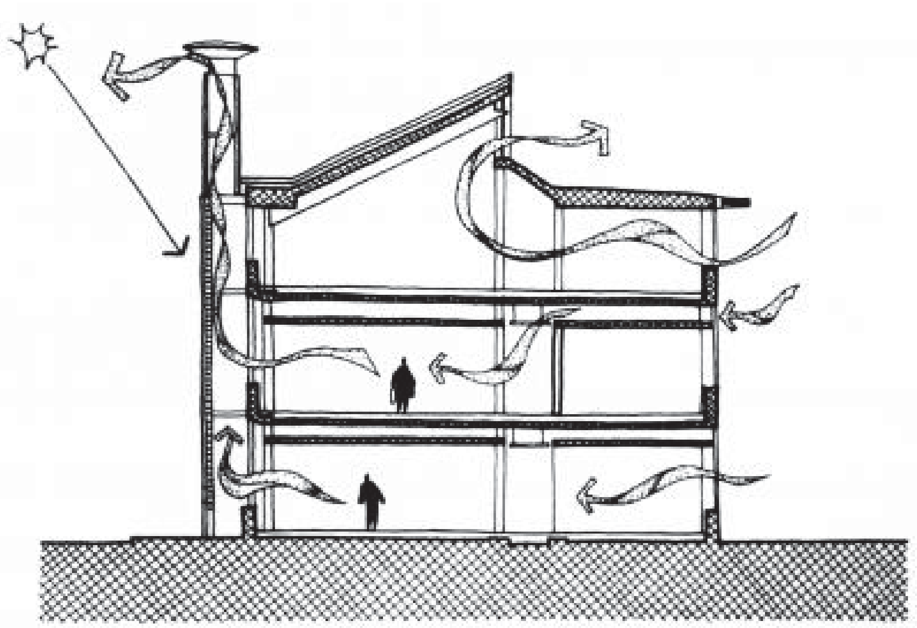

Figure: 1.22: The Building Showing Stack Effect: The hot air rises in a building due to buoyancy effect produced by chimney and low pressure produced in chimney area sucks in fresh air from outside (Source: Image from Sun, Wind, and Light, by G.Z. Brown and Mark DeKay, published by Wiley)

1.6 Principle and Performance of a Solar Chimney

The basic principle of any Solar Chimney is wind driven ventilation which is created by solar stack. The major contributing factor of natural ventilation is hot and lighter air in the stack which is produced due to solar heat being entered in the chimney through Sun light. This heated and lighter air rises up in the chimney and ultimately goes out of the chimney / building. The air which goes out of the chimney / building is compensated by introduction of fresh air which enters in the building through inlet opening naturally. The naturally ventilation is also assisted and enhanced by push effect of the wind present outside the building.

Performance of the Solar Chimney basically depends on Air Flow rates and Patterns through the building. The air temperature is also a primary factor in performance evaluation of Solar Chimney. The height / width of the solar chimney, outside wind temperature & wind rate and solar heat intensity also significantly contribute in the performance of the Solar Chimney.

1.7 Research Objectives

Primarily, the focus of this research is to study different possibilities of integration of Solar Chimney on a room with objective of finding the ways to enhance natural ventilation flow rate and achieve the desired flow rates. Different factors effecting solar chimney performance shall be analyzed numerically for the performance improvement. Starting from simple and basic design of the solar chimney, the more specific and effective designs based on previous research and experiments shall be numerically simulated and results will be analyzed and compared.

The main focus of this research is to study and investigate the effects of some key factors on the performance of a typical inclined Solar Chimney fitted on the roof of a real sized room by using a commercial Computational Fluid Dynamics (CFD) software package, CFD-ACE+ from ESI group, as follows:

A. Building a computational model (a room fitted with solar chimney).

B. Investigate the ventilation performance of a 2D (Two-Dimensional) room under effects of chimney and different room inlet locations using CFD.

C. Study the air flow patterns / flow rates through a 3D (Three-Dimensional) room with different air inlet locations and configurations of solar chimney, using CFD.

The above objectives have been achieved through following steps:

1) Literature review in the field of natural ventilation using solar heat to ascertain the extent of advancement in the subject.

2) Determine the most appropriate characteristics and parameters to be used in numerical simulation of solar chimney fitted room based on experiments and simulation carried out previously.

3) Developments of a basic two dimensional room model fitted with straight solar chimney on a small scale and perform numerical analysis of natural ventilation through this room using commercial Computational Fluid Dynamics (CFD) software.

4) Developments of a basic two dimensional room model fitted with inclined solar chimney on a small scale and perform numerical analysis. Selection of appropriate inclination angle based on previous research in the field.

5) Developments of a real sized (3 meter × 3 meter) two dimensional room model fitted with inclined solar chimney and perform numerical analysis to achieve natural ventilation through the room.

6) Study the Grid Convergence of the two dimensional real sized room model by increasing the number of cells gradually and then analyze the results of numerical simulation to achieve optimum / desired model which provides accurate solution / results.

7) Analyze the results of numerical simulation by changing location of room air inlet in a two dimensional room i.e. room inlet at bottom, middle and top of the room side wall.

8) Developments of a basic three dimensional room model fitted with inclined solar chimney on a small scale and perform numerical analysis.

9) Developments of a real sized (3 meter × 3 meter × 3 meter) three dimensional room model fitted with inclined solar chimney and perform numerical analysis to achieve natural ventilation through the room.

10) Study the Grid Convergence of the three dimensional real sized room model by increasing the number of cells gradually and then analyze the results of numerical simulation to achieve optimum / desired model which provides accurate solution / results.

11) Designing of inlet box around air inlet opening of the real sized room to numerically investigate the air flow patterns and mass flow rate at room inlet.

12) Study and investigate the effect of size / location of inlet box on air flow rates and patterns.

13) Numerically investigate the effect of location of roof top solar chimney i.e. left side, right side and middle of the roof top, on flow rates and flow patterns.

14) Analyze the results of numerical simulation by changing location of room air inlet in a three dimensional room i.e. room inlet at bottom, top and on same side of solar chimney (opposite to solar chimney) of the room side wall.

15) To propose an optimized model of real sized room fitted with Solar Chimney based on the analysis of simulations results and investigations.

16) Comparison of achieved results and discussion of results based on results of previous research in the field. Present some suggestions for improved Solar Chimney Design based on the research results.

Chapter 2

Basic Concepts of Fluid Mechanics and Solar Chimney Literature Review

2.1 Objectives of Literature Review

In this chapter, basic concepts of Fluid Dynamics, books written on Solar chimney, theoretical concepts that has been used during this research, various categories of papers and studies including experimental, numerical and analytical models of Solar Chimney based on Computational Fluid Dynamics (CFD) has been investigated and discussed.

The objective of literature review is to study the history, progress and innovation carried out in the field of Solar Chimney. This literature study gives us the idea about how and in which way we should proceed further. It also drives us in the way where there is still margin of more investigations, innovations and achievements.

Basic Concepts of Fluid Mechanics

2.2 Theoretical Concepts

Another purpose to present this chapter is to go through the theoretical concepts and basic principles which are essential part of this research and have been used during computational analysis of this research.

2.2.1 Fluid Dynamics

Fluid dynamics is an important part of engineering and physical sciences studies whereby properties of the fluids related to their flow / movements are studied. This is one of the branches of fluid mechanics. The other branch of fluid mechanics is called fluid statics. As clear from the name of the branch, it deals with the study of those fluids which are at rest. It is an important field whereby moving fluids and their properties / behavior is studied in order to make effective use of these fluids.

2.2.2 Fluid Flow

The study of flow properties of fluid, whether it is gas or liquid, is extremely important before putting it to any task. The one of the important and most widely use of liquid and gases is normally for heating & cooling applications which may be either in any process industry or in commercial / residential building. Most of the times, the flow of the fluid in any system is achieved by the use of some mechanical means. When these mechanical means are used, extreme care / attention is required towards some physical parameters like temperature, friction, pressure drop, head loss etc. as they are directly related to performance of the system and ultimately energy consumption. These important physical parameters are governed by many things which also include piping joints, diameter of the pipes, fittings used, number of valves etc.

The systems for the flow of liquid and gases are designed by keeping in view all the above factors. The basic purpose during any fluid flow is to minimize losses due to frictional or other reasons and to make the process most economical. For the purpose of flow, normally pipes and ducts are used. The most commonly used pipes are circular pipes and reason behind the use of these pipes is that they can withstand a large pressure difference between inside and outside environment.

The analysis of flow through a circular pipe has revealed that velocity of the fluid is near to zero at the wall due to frictional conditions and is maximum at the center of the pipe. Therefore, in fluid flow calculations, average velocity (V_{avg}) is taken which is considered as constant throughout the cross section of the pipe in incompressible flow. In practical scenario, the average velocity may change due to change in other physical conditions, particularly, temperature but we still consider it constant based on the judgment that slight loss in accuracy is acceptable when we get good convenience by working with constant properties like velocity, temperature etc.

The change in physical parameters like temperature of the fluid is very negligible without the presence of any external contributing source. The same has been proven practically / experimentally. A simple example of this may be taken as that of fluid flow in a circular pipe without introduction of any internal or external heating source. If we measure the inlet and outlet temperature of the fluid, there will be very negligible change in temperature which could be due to friction of fluid and pipe. This nominal change is normally ignored in calculations as it will not have significant effect on end results.

2.2.3 Laminar and Turbulent Flow

Another important factor in fluid flow studies and calculation is behavior of fluid flow in a pipe i.e. flow is stream line or it is not stream line. The first scenario where flow is smooth streamlines with ordered motion is called laminar flow while in other scenario where flow is highly disturbed with huge velocity fluctuations, is called turbulent flow. Normally, the flow is stream line at low velocities and become turbulent at higher velocities.

In practical situations, most of the flows are turbulent. The Laminar flow is only seen in a condition where very highly viscous liquid is flowing through a small diameter pipe. The flow condition from laminar to turbulent does not change instantly but there is always certain transition period present for this change. A simple example which explains the laminar and turbulent behavior of the fluid is of cigarette fumes. It has been noticed that the smoke of the cigarette rises as a smooth plume initially, say few centimeters, and then starts moving randomly in all directions. So initially it started to flow as laminar but then flow converted to turbulent due to external parameters.

2.2.4 Laminar Flow in Pipes

As discussed above, laminar flow is a flow in smooth lines with steady state velocity and velocity profile remains the same during the flow. The velocity remains the same and smooth in axial direction while there will be no velocity / motion towards radial direction.

The term called Reynolds Number (Re) is normally used to differentiate between laminar and turbulent flows. Generally, if $Re \leq 2300$, the flow is stream line and it will be laminar. The figure 2.1 below is showing laminar flow in a pipe.

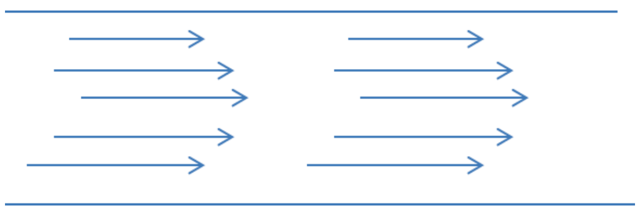

Figure 2.1 : Example of Laminar Flow in a Pipe (self)

2.2.5 Turbulent Flow in Pipes

Turbulent flow phenomenon is an essential part of our day to day life and in every aspect of engineering practice where fluid flow is involved. In general, most of the flows we deal during any experimentation or analysis are turbulent in nature. It is, therefore, very important in any engineering field involving fluid flows, to analyze and understand the turbulence effects on the system particularly wall shear stresses produced due to this flow.

The turbulence flow phenomenon is very complex mechanism and phenomenal research work has been carried out in this field but still there is much to explore. In such scenarios, we normally follow and utilize already developed empirical relationships and experiment results related to particular area and field and same is almost the case with turbulent flows.

The difference of laminar and turbulent flow is that in case of laminar, the flow is streamline, therefore momentum and energy transfer always occurs by molecular diffusion while in case of turbulent, eddies transfer energy, momentum and mass to other parts of the fluid rapidly and in more quantity. Therefore, there will always be higher values of heat transfer, mass transfer and friction in turbulent flows than the laminar flows.

Turbulent flow is created basically due to rapid fluctuations of moving fluid particles which are called eddies and it happens throughout the flow. These random fluctuations in flow also create this additional mechanism whereby transfer of momentum and energy also starts in the flow at higher rates.

The figure 2.2 below is giving an idea of turbulent flow in a pipe.

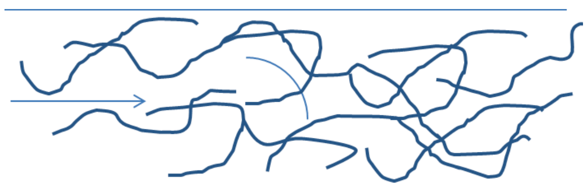

Figure 2.2 : Example of Turbulent Flow in a Pipe (self)

2.2.6 Reynolds Number

The change of flow condition from laminar to turbulent or vice versa normally depends on type of fluid and condition of the pipe through which fluid is flowing. These factors may include flow velocity, temperature of the fluid, type of the fluid, pipe surface condition like roughness, number of fittings and bends involved in the piping etc.

Significant research was carried out in 18th century to understand the phenomenon whereby laminar flow changes to turbulent or vice versa. The most important breakthrough was achieved by Osborne Reynolds in 1880s who discovered and presented the theory that this transition of flow from one state to other i.e. laminar to turbulent depends mainly on inertial and viscous forces of the flowing fluid and also give the relationship to calculate this phenomenon which is the ratio of inertial forces to viscous forces present in the fluid. He named this ratio as Reynolds number and presented the relationship to calculate this number for a fluid flowing in a circular pipe as:

$$Re = \frac{\rho U D}{\mu} \quad \rightarrow \quad \textbf{2.1}$$

Where, μ is viscosity of the fluid, ρ is density, D is diameter of the pipe and U is the velocity of the fluid.

The Reynolds number is a dimensionless quantity. As Reynolds number is a ratio of inertial forces to viscous forces, the flow would be turbulent in nature when inertial forces are large compared to viscous forces i.e. with higher value of Reynolds number. Similarly, low value of Reynolds number is achieved when viscous forces are large enough to suppress the effect of inertial forces during fluid flow. In this situation, flow would be laminar in nature.

The different barrier has been defined by Reynolds where the flow situation changes from one condition to other. Normally, laminar flow condition does not change to turbulent condition instantly rather there is always a transition phase in between laminar and turbulent flow. The flow initially shifts to transition phase from laminar phase and then changes to turbulent phase. The value of Reynolds number is called critical (Re_{cr}) where the flow condition changes to turbulent phase. The value of Reynolds number for this flow condition change depends mainly on type of fluid and pipe condition. Generally, for a flow through a circular pipe, the value of critical Reynolds number is considered as 2300.

Although it is desirable to have the exact value of Reynolds number where fluid flow changes its condition from laminar to transition and from transition to turbulent but in reality, it is very difficult to have these exact values for each fluid. In practical scenario, the shift from one flow condition to other condition mainly depends on different physical parameters of fluid and pipe internal conditions.

Under normal circumstances of fluid flow in a circular pipe, the following values have been defined to get the idea of change in flow condition with respect to Reynolds number. That is,

$Re \leq 2300$	**Laminar Flow**
$2300 \leq Re \leq 4000$	**Transitional flow**
$Re \geq 4000$	**Turbulent Flow**

In case the fluid is in transitional flow regime, the flow condition of the fluid repeatedly changes from laminar to turbulent and vice versa. The figure 2.3 below is giving an idea of all three conditions i.e. laminar, transition and turbulent flow, during a fluid flow in a pipe:

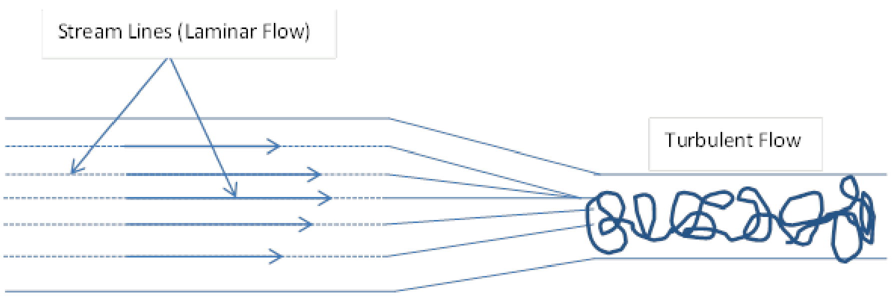

Figure 2.3 : Laminar to Turbulent Flow Transition in a Pipe (self)

2.2.7 Basic Equations of Fluid Flow

In order to understand and calculate the different parameters of fluid flow, many relationships and equations has been developed. These equations evaluate and explain the relationship between different flow variables involved with respect to actual conditions and time. From these basic equations, more specific relationships have been developed for particular fluids and specific flow conditions.

2.2.8 The Navier-Stokes Equations

The development of Navier-Stokes and continuity equations have made the analysis of fluid flow more comprehensive and are the basic equations in analysis of any fluid flow phenomenon numerically or experimentally. These equations give the idea of physical parameters involved in any fluid flow scenario. The basic of all simulation models depends on these equations in one way or other. These basic laws of motion are also applicable for all type of substances including solids. The only difference between solids and liquids is that when stress is applied on a fluid, it will deform and will return to original condition even if the application of force is stopped. In fluid flow calculations, this behavior must be accounted for during analysis.

The Newton's second law of motion states that the rate of change of momentum of a body is proportional to the unbalanced forces acting on it and this change is always in the direction of the applied force. There are always number of forces which are present in fluid flow and acting on a fluid particle. These forces must be known and should be calculated in order to have better idea of fluid flow phenomenon.

The following forces may act on fluid particle:

- Forces created due to viscosity of the fluid
- Gravity force and electromagnetism forces. These are called body forces
- Rotation of the fluid also produces some forces.
- Any type of Pressure forces

Navier and Stokes played the leading role in development of basic equation that is why they have been named after them. Firstly, Navier derived an equation of motion based on the assumption that fluid flow is laminar and relation of shear rate and shear stress is linear. Afterwards, Stokes also derived an equation of motion with the same basics but in a little different form. Both times, the equations were derived for viscous fluids. Based on these two derived equations, the governing fluid flow equation is known as Navier-Stokes equations. Although Navier-Stokes equation was basically derived and developed for laminar flow but it can be utilized for turbulent flows with little changes / modifications.

The Navier-Stokes equations elaborate the motion of fluid substances and can be derived by considering the dynamic equilibrium of a fluid element.

Navier-Stokes Equation for Incompressible Flow of Newtonian (Constant Viscosity) Fluid

$$\frac{\partial u}{\partial t} = -(u.\nabla)u + \nabla.(v\nabla u) - \frac{1}{\rho}\nabla p + f \qquad \longrightarrow \textbf{2.2}$$

Or it may be written as

$$\frac{\partial u}{\partial t} = -(u.\nabla)u + v\nabla^2 u - \frac{1}{\rho}\nabla p + f \qquad \longrightarrow \textbf{2.3}$$

Continuity and Navier-Stokes equations for incompressible flow of Newtonian fluid in Cartesian coordinates may be written as:

Continuity:

$$\frac{\partial u}{\partial x} + \frac{\partial V}{\partial y} + \frac{\partial w}{\partial z} = 0 \quad \longrightarrow \mathbf{2.4}$$

Where u , v and w are velocity components in x, y, z directions

Navier – Stokes:

X – Component:

$$\rho\left(\frac{\partial u}{\partial t} + u\frac{\partial u}{\partial x} + V\frac{\partial u}{\partial y} + w\frac{\partial u}{\partial z}\right) = -\frac{\partial p}{\partial x} + \mu\left(\frac{\partial^2 u}{\partial x^2} + \frac{\partial^2 u}{\partial y^2} + \frac{\partial^2 u}{\partial z^2}\right) + \rho g_x \longrightarrow \mathbf{2.5}$$

Y – Component:

$$\rho\left(\frac{\partial V}{\partial t} + u\frac{\partial V}{\partial x} + V\frac{\partial V}{\partial y} + w\frac{\partial V}{\partial z}\right) = -\frac{\partial p}{\partial y} + \mu\left(\frac{\partial^2 V}{\partial x^2} + \frac{\partial^2 V}{\partial y^2} + \frac{\partial^2 V}{\partial z^2}\right) + \rho g_y \longrightarrow \mathbf{2.6}$$

Z – Component:

$$\rho\left(\frac{\partial w}{\partial t} + u\frac{\partial w}{\partial x} + V\frac{\partial w}{\partial y} + w\frac{\partial w}{\partial z}\right) = -\frac{\partial p}{\partial z} + \mu\left(\frac{\partial^2 w}{\partial x^2} + \frac{\partial^2 w}{\partial y^2} + \frac{\partial^2 w}{\partial z^2}\right) + \rho g_z \longrightarrow \mathbf{2.7}$$

The equations described above will not have proper analytic solution, therefore, these are simplified in order to get the appropriate solution. We normally use some dimensionless numbers to simplify and solve these equations. These dimensionless numbers may include Reynolds number and the Rayleigh number.

As explained previously, the Reynolds number is a ratio of inertial forces to viscous forces. Based on this fact, these two forces play an important role in any fluid flow system. The following relationship explains the Reynolds number as already explained.

$$Re = \frac{\rho U D}{\mu}$$

The change of flow condition i.e. laminar or turbulent depends on the value of this number and same has been explained in detail in previous section.

The Rayleigh number is another important relationship of forces which describe the heat transfer phenomenon in any fluid flow system particularly in flows which are driven due to buoyancy. If the value of Rayleigh number in any fluid flow is below the critical value for that fluid, the transfer of heat normally occurs in the form of conduction and on the other hand if value is greater than critical value, the transfer of heat occurs in the form of convection. The relation below explains the Rayleigh number.

$$Ra = \frac{g\beta \Delta T C_p \rho^2 D^3}{\mu K} \longrightarrow \textbf{2.8}$$

Where K denotes thermal conductivity.

The Rayleigh number is also used to get the idea about the flow induced by the buoyancy forces during natural convection. The value of this Rayleigh number tells us the condition of flow i.e. when the value of $Ra < 10^8$, it indicates that induced flow is in laminar state and state of the flow would be transitional to turbulent between the Rayleigh number range of $10^8 < Ra < 10^{10}$.

2.2.9 Heat Transfer and Energy Conservation Equation

There are three basic conservation equations i.e. conservation of mass, conservation of heat and conservation of momentum. These are governing equations in any process involving mass, heat or momentum. The accurate solution of these equations is essentially required to ensure that obtained results are accurate and showing factual position of the system.

The importance of Energy Conservation Equation is extremely high in this study. The results of any study and computation depend on correct solution of this equation which must be near to reality. There are many ways to write and express energy equation but ultimate solution procedure is same. The differential form of energy equation can be written in following form. This form is normally called total enthalpy form.

$$\frac{\partial(\rho H)}{\partial t} + \nabla.(\rho\bar{V}H) = \nabla.(K_{(eff)}\nabla T + \frac{\partial p}{\partial t} + \nabla.(\bar{V}.\bar{\bar{\tau}}) + \rho\bar{V}.\left(\sum_{i}^{nForces} \bar{f_i}\right) + \sum_{i=1}^{nSource} S_{H_i} \quad \longrightarrow \quad \mathbf{2.9}$$

In, above equation, "ρ" represents the density, "H" is representing stagnation or may also be called as total enthalpy and "t" stands for time.

The term "$K_{(eff)}$" has been used to represent thermal conductivity (effective). This term includes effects of both, laminar and turbulent conditions. The "T" stands for temperature, "p" denotes the pressure, $\bar{f_i}$ represents the body force vector from force source or force contribution

i and S_{Hi} denotes the energy contribution from energy source "i". $\bar{V}$ is vector form of velocity component and $\bar{\bar{\tau}}$ is vector form of shear stress.

The above mentioned total enthalpy form "H" is associated with other fluid thermodynamic properties through the relationship defined below;

$$H = e + \frac{p}{\rho} + \frac{1}{2}(u^2 + V^2 + w^2)$$

In above relationship, the term "e" denotes the static internal energy, "p" and "ρ" represents the pressure and density of the fluid respectively, whereas, terms "u", "v", and "w" representing velocity components in x, y, and z coordinate directions, respectively.

2.2.10 Pressure Losses

Every physical system involves plenty of pressure losses and theses pressure losses can be represented in variety of terms. The normally attributed pressure losses in any system relates to friction i.e. due to contact of flowing fluid with the walls of the system or pipe. The contribution of other major losses is attributed to fitting losses. There are plenty of fittings, joints and bends which are required to be used in any piping system. These fittings like Tees, Elbows, Valves etc. make a major contribution in pressure loss of any system.

The Bernoulli equation represents and calculates the effect of above mentioned pressure losses through following equation:

$$\frac{1}{2}\rho v^2 + P_s + \rho g h + \Delta P_{fan} = P_t + \frac{1}{2}\rho v^2 \sum K_{drop} \quad \rightarrow \quad \textbf{2.10}$$

The term ($\sum K_{drop}$) in above equation represents the aggregated effect of pressure drop in any piping system as explained above i.e. due to contact of fluid with walls of the pipe and use of fittings.

2.2.11 Importance of Buoyancy and Stack Effect

The physical phenomenon called Buoyancy is an important physical property of any fluid. This property has particularly significant role in present research as whole system of natural ventilation depends on this property of the fluid. Buoyancy is a type of force in a fluid due to which it rises up in a pipe, vessel or system. The driving force behind this phenomenon is change in density of the fluid. The density of the fluid normally changes with change in temperature of the fluid.

The phenomenon of buoyancy and stack effect are closely linked. In stack effect, the temperature of the associated environment is increased through some natural or other means which ultimately affects the density of the fluid present in nearby area. The fluid starts to rises up due to change in density. This movement remains continue as soon as above condition of temperature and density is intact. This continuous movement of the fluid through buoyancy effect using stack is called Stack Effect.

The above explained movement of the fluid creates a differential pressure in a stack and this difference can be calculated with the use of following relationships;

$$\Delta Pstack = gH_s\Delta\rho \quad \longrightarrow \quad \textbf{2.11}$$

$$\Delta Pstack = \rho g H_s \frac{\Delta T}{T_i} \quad \longrightarrow \quad \textbf{2.12}$$

The term T_i in above relationship represents temperature at inner side of the solar chimney whereas ΔT is used to show difference in temperature of chimney i.e. temperature of outside and inside.

2.2.12 Boundary Layer

The effect of forces on a fluid varies from location to location. Some forces have major contribution near the wall of the system i.e. at boundary layer and others contribution is significant in the center of the pipe. In order to achieve accurate results, the effect of these forces must be accounted for in every system. The pressure loss, as explained above, has significant contribution on a fluid present near wall of the pipe which is also called boundary layer. The term viscosity represents the effect of contact of liquid with wall of the pipe. The viscosity is always considerably high at boundary of the pipe / system as compared to center or other locations. The same phenomenon happens in a chimney where boundaries of the chimney affect the flow of the fluid and ultimately ventilation rate.

There are certain types of boundary layers which are created in a system. The type of boundary layer depends on the type of system, fluid and flow conditions present near the boundary wall.

2.2.13 Laminar and Turbulent Boundary Layer

In any flow system, the boundary layers can be laminar or turbulent depending on fluid and flow conditions. The Reynolds number is a primary indicator to differentiate whether flow is laminar or turbulent. The laminar boundary layer is formed during flow with lower Reynolds number whereas flow with high Reynolds number results in formulation of turbulent boundary layer.

2.2.14 Thermal Boundary Layer

A layer of stagnant fluid is formed between moving fluid and solid surface at boundary wall called thermal boundary layer. The thickness of this layer depends on the type of fluid, its velocity, density, temperature etc.

The functionality and performance of the solar chimney is significantly affected by thermal layer. The high rate of heat transfer from solid wall to fluid (air) in any solar chimney is desirable, which is affected by this thermal layer. The reduction in heat transfer due to thickness of thermal layer may result in reduced stack effect.

The thickness of thermal boundary layer and its effects are normally evaluated using a term called Prandtl number. The value of this Prandtl number gives the idea about the thermal boundary layer, particularly, its thickness. The following relationship is used to determine the value of Prandtl number;

$$P_r = \frac{C_p \mu}{K} \quad \rightarrow 2.13$$

Where,

C_p = $Specific\ heat$

μ = $Viscosity$

K = $Thermal\ Conductivity$

The thermal boundary layer is analogous to velocity boundary layer. The thickness of the thermal boundary depends on the value of Prandtl number. If Prandtl number value is greater than one, thermal boundary layer thickness will be higher and vice versa.

2.2.15 The Turbulence Models

In day to day life and in almost all practical situations, turbulent flows are normally experienced. The magnitude of turbulence depends on the type of system, fluid and flow conditions. The plenty of work has been carried out in the field of turbulence modelling and number of turbulence models has been developed to be used in a particular situation.

2.2.16 Importance of Turbulence in Practical Situations

The success is to use an appropriate model for a particular situation and achieve a desired output. The selection of right turbulence model is extremely important for particular research. The selection of turbulence model largely depends on the value of Reynolds number. The more we know about the parameter of the fluid and system being used, we will be in a better position to select a right model.

A perfect and useful turbulence model must fulfill following requirements:

- Should be accurate and obtained results correspond near to reality.
- The model should be simple in understanding and use,
- It must have wide applicability,
- And the most importantly, it must be economical to use and run.

2.2.18 The Turbulence Energy Equation

The Kinetic energy term is frequently used in fluid thermodynamics and is an important parameter. The turbulence kinetic energy is used to consider and calculate the kinetic energy of turbulence part of fluid flow.

Many scientists and researchers have developed the turbulent energy equation but Prandtl (1945) is considered as pioneer in this field who developed and presented the Turbulence Energy Equation.

Below is the modeled form of turbulence kinetic energy equation;

$$\frac{\partial k}{\partial t} + U_j \frac{\partial k}{\partial x_j} = \tau_{ij} \frac{\partial U_i}{\partial x_j} - \varepsilon + \frac{\partial}{\partial x_j}\left[\left(v + \frac{v_T}{\sigma_k}\right)\frac{\partial k}{\partial x_j}\right] \quad \longrightarrow \quad \mathbf{2.14}$$

Where τ_{ij} is called Reynolds-Stress Tensor and can be calculated using the following relationship;

$$\tau_{ij} = 2v_T S_{ij} - \frac{2}{3} k\delta_{ij} \quad \longrightarrow \quad \mathbf{2.15}$$

Where,

S_{ij} is mean Strain-rate Tensor

v_T is kinematic eddy viscosity

σ_k is a Closure Coefficient

2.2.17 Turbulence Models – One Equation and Two Equations

The Turbulence is a key feature of any flowing fluid and with the passage of time, intense research in the field of flow turbulence has been carried out which resulted in development of different type of models but following two models are basic models;

a) One-Equation Models
b) Two-Equation Models

The both above models have been frequently used in turbulence modelling and computations but Two-Equation models have more significance and are being used more frequently because of their completeness. Both the models use Boussinesq eddy-viscosity approximation, which is an important factor in fluid mechanics.

2.2.19 One-Equation Models

The use of One-Equation Models is very limited to specific problems. This model solves a single conservation equation for turbulent viscosity. This model is economical in use but it cannot be normally used for general flows.

The Prandtl's proposed following One-Equation Model by introducing closure coefficient C_D:

$$\frac{\partial k}{\partial t} + U_j \frac{\partial k}{\partial x_j} = \tau_{ij} \frac{\partial U_i}{\partial x_j} - C_D \frac{k^{3/2}}{l} + \frac{\partial}{\partial x_j}\left[\left(v + \frac{v_T}{\sigma_k}\right)\frac{\partial k}{\partial x_j}\right] \longrightarrow \mathbf{2.16}$$

Where C_D can be calculated using following relationship;

$$\varepsilon = \frac{C_D k^{3/2}}{l} \longrightarrow \mathbf{2.17}$$

2.2.20 Two-Equations Models

Amongst all the available models in recent times, the Two-Equations Models presented the great advantage in solving turbulence based flow problems and computations. All Two-Equation Models have used Boussinesq approximation as basis of modelling.

Below is the discussion on important Two-Equation models.

A) The k-ω Model

The k-ω model is a Two-Equation model which solves the two equations. First one is Kinetic Energy "k" equation and second is transport equation for "**ω**". In this model "**ω**" is an inverse time scale and it is associated with the turbulence.

In this model, the turbulent viscosity is calculated using the following relationship;

$$v_T = \rho \frac{k}{\omega}$$

B) The Standard k-ε Model

Another Two-Equation Model is k-ε model. This model is much popular and being most widely used in last few decades. The different modifications have been performed in the model to make to more appropriate for general use, particularly, introduction / redefining of closure coefficients. The model is relatively simple to implement but it is normally used for fully turbulent flows.

The standard equations for turbulence and dissipate rate in above model are:

Turbulence Kinetic Energy:

$$\frac{\partial k}{\partial t} + U_j \frac{\partial k}{\partial x_j} = \tau_{ij} \frac{\partial U_i}{\partial x_j} - \varepsilon + \frac{\partial}{\partial x_j}\left[\left(v + \frac{v_T}{\sigma_k}\right)\frac{\partial k}{\partial x_j}\right] \quad \longrightarrow \textbf{2.18}$$

Dissipation Rate:

$$\frac{\partial \varepsilon}{\partial t} + U_j \frac{\partial \varepsilon}{\partial x_j} = C_{\varepsilon_1} \frac{\varepsilon}{k} \tau_{ij} \frac{\partial U_i}{\partial x_j} - C_{\varepsilon_2} \frac{\varepsilon^2}{k} + \frac{\partial}{\partial x_j}\left[\left(v + \frac{v_T}{\sigma_\varepsilon}\right)\frac{\partial \varepsilon}{\partial x_j}\right] \quad \longrightarrow \textbf{2.19}$$

The Kinematic Eddy Viscosity or turbulent viscosity can be calculated using following relationship:

$$v_T = C_v k^2/\varepsilon$$

The following are the values of five Closure Coefficients (constants) used in above equations:

- C_v = 0.09
- C_{ε_1} = 1.44
- C_{ε_2} = 1.92
- σ_k = 1.0
- σ_ε = 1.3

As explained above, the standard k-ε model is normally used for models involving flow at high Reynolds number. This model does not give appropriate results in area near to walls as flow becomes nearly stagnant in that area resulting in very low turbulence.

2.2.21 Low-Reynolds-Number k-ε Models

The Standard k-ε model is most widely used model but still there are some disadvantages in general use which necessitated the need to modify this model for use in all flow conditions. As explained above, it does not give appropriate results near walls of the piping system or model, therefore, some additional wall function are required to be used to accommodate this disadvantage. This model is also poor in dealing with flows where high pressure difference exists.

For compensation of these weak points, researchers and scientists developed new models and modified standard Standard k-ε model. The Chien (1982) modified the Standard k-ε model and developed low-Reynolds-number k-ε model to cover the weaknesses in the earlier model related to near wall areas. This model of Chien is particularly useful for flows with low Reynolds number. Keeping in view the above advantage of low-Reynolds-number k-ε model, the same has been used in current research during CFD simulations.

➢ *Low-Reynolds-Number k-ε Model of Chien*

Keeping in view the drawbacks of Standard k-ε model, Chien made few modifications in this model and re-defined flow properties near the walls. He simplified the physical properties in boundary areas with almost zero values of following three basic properties of the fluid and flow:

$$U \approx 0 \qquad k \approx 0 \qquad \varepsilon \approx 0$$

In case of the Standard k-ε model, the turbulent kinetic energy dissipation is considered to be very negligible in near-wall areas due to the isotropic or negligible turbulence within this area. The above assumption / calculation can be true for main stream flows i.e. flow in the central area which is free from wall or boundary effects but not acceptable for boundary or near-wall areas. Chien added some particular terms in his modified model to address this issue

Chien also studied function of dissipation rate and further divided dissipation rate into below mentioned two parts:

- Isotropic part
- Anisotropic part

The term "ε" present in transport equation of dissipation rate represents and calculates the isotropic portion of dissipation rate only. He calculated the effect of anisotropy part through asymptotic analysis and added the expression for the same in dissipation rate present in transport equation of turbulent kinetic energy ($\boldsymbol{k}$). He also introduced damping functions for accurate calculations of turbulent viscosity alongwith introduction of term called "destruction of dissipation" in transport equation of dissipation "ε".

The generalized form of Chien low-Reynolds Number $\boldsymbol{k}$-**ε** model can be written in following form:

$$\frac{\partial}{\partial t}(\rho k) + \frac{\partial}{\partial x_j}(\rho u_j k) = \frac{\partial}{\partial x_j}\left[\left(v + \frac{v_\tau}{\sigma_k}\right)\frac{\partial k}{\partial x_j}\right] + \rho(P - \varepsilon - D) \longrightarrow \textbf{2.20}$$

$$\frac{\partial}{\partial t}(\rho \varepsilon) + \frac{\partial}{\partial x_j}(\rho u_j \varepsilon) = \frac{\partial}{\partial x_j}\left[\left(v + \frac{v_T}{\sigma_s}\right)\frac{\partial \varepsilon}{\partial x_j}\right] + C_{S_1} f_1 \frac{\rho P \varepsilon}{k} - C_{S_1} f_2 \frac{\rho \varepsilon^2}{k} + E \longrightarrow \textbf{2.21}$$

$$v_T = C_v f_v \frac{\rho k^2}{\varepsilon} \longrightarrow \textbf{2.22}$$

The model parameters appearing in the preceding equations are:

- C_v = 0.09
- C_{S_1} = 1.35
- C_{S_2} = 1.8
- σ_k = 1.0
- σ_s = 1.3

Constants

$$f_v = 1 - exp\,(-0.0115y^{+})\,, \qquad f_1 = 1.0$$

$$f_2 = 1 - 0.22exp\left[-\left(\frac{Re_\tau}{6}\right)^2\right]$$

$$D = \frac{2vk}{y^2} \qquad E = -2v\left(\frac{\varepsilon}{y^2}\right)\exp(-0.5y^{+})$$

In above expressions, "y" is considered as the normal distance from the particular cell center to the wall, whereas, y+ is dimensionless, sublayer-scaled, distance. For best computational results, the model should be designed in such a way that location of the cell center must be well within the laminar sublayer. This means that the value of y+ must be near to one i.e. (y+ ~ 1). In order to fulfill above condition, fine grids are required to be created, particularly, near boundary areas.

The term "f" is denoting damping function and "D" represents dissipation rate. Above equations contains empirical damping functions f_v , f_1 , f_2 and "E". The term "P" is turbulence-energy production.

2.3 The Chimney and Natural Ventilation

The Chimney is a historical structure being used for centuries in living constructions. The structure and shape of the chimney may vary from region to region and culture to culture but basic purpose is same i.e. to remove the non-desirable elements such as stale air, smoke etc. out of the room or building. The basic principle behind chimney is stack effect.

The figure below is showing principle of natural ventilation in a multistory building.

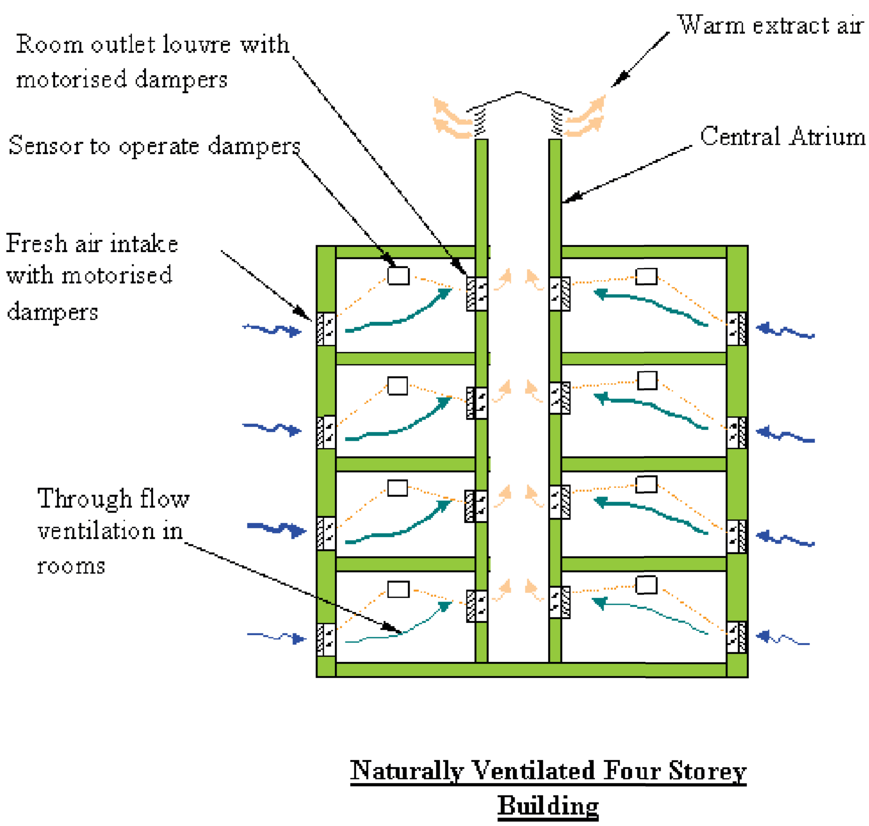

Figure 2.4 : Natural Chimney functionality in a multistory building
(Source : www.arca53.dsl.pipex.com)

2.3.1 Solar Chimney

The major difference between the normal chimney and solar chimney is that solar chimney uses solar heat to increase the temperature of air present inside it. The solar chimney face facing the sun is transparent and it allows the sun rays to pass through it. When these rays enter the chimney, they heat up the air present in the space and also heat is absorbed on the absorber plate present opposite to the transparent face. Due to this heat, hot air rises up in the chimney due to buoyancy and induces fresh air from the outside which is called natural ventilation.

The solar chimneys are also being used to produce electricity. The chimneys used to produce electricity are normally very huge in size compared to chimneys used on the buildings. The example of same can be found in Manzanares, Spain where a solar tower has been built whose height is 195m while it is giving maximum output power of 50 KW.

Figure 2.5 below is showing an arrangement of standard Solar Chimney and giving basic structure / working idea.

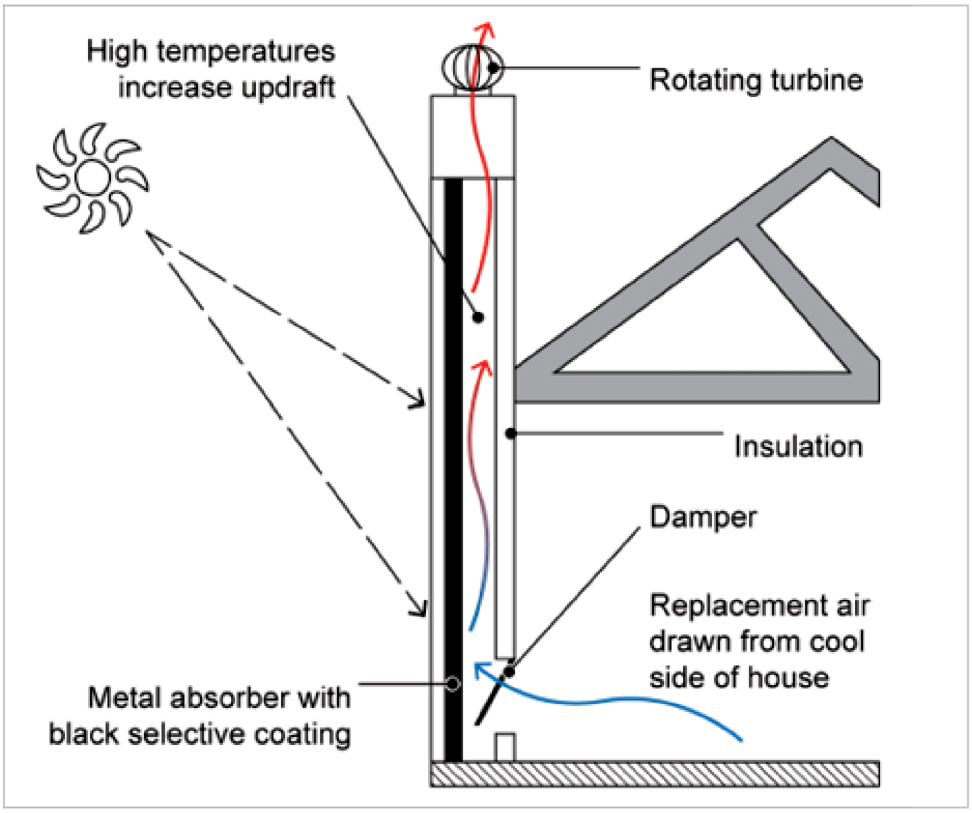

Figure 2.5: Standard Solar Chimney (Source: Green Builder Solar Guidelines (Residential), photo taken from www.yourhome.gov.au/passive-design/passive-cooling)

In this research, the main focus is that how the natural ventilation can be increased using standard solar chimney.

2.4 Computational Fluid Dynamics (CFD)

Computational fluid dynamics (**CFD)** is a technique in the field of **fluid mechanics** that uses numerical techniques and algorithms to solve and analyze the situations which involves fluid flows.

The governing equations for computational fluid dynamics are a set of Partial Differential Equations known as the Navier-Stokes equations. These equations are based on conservation of mass, momentum, and energy. Theoretically, turbulent flow problems can be solved using the unsteady Navier-Stokes equations but due to certain limitations in numerical simulations, only flow problems with low Reynolds number flows can be solved. In order to make count of turbulence in fluid flows, simplified form of Navier-Stokes equations are used which is known as Reynolds Averaged Navier-Stokes (RANS) equations.

Fluid Mechanics and Fluid Dynamics application can be found in almost every aspect of our day to day life. Enormous research has been carried out in this field during 19^{th} century. But recent advances in software developments and particularly Computational Fluid Dynamics have open new field advancement particularly with reference to motion of the fluids. Through CFD, the behavior of fluids any flow system can be seen and analyzed. These all analysis are carried out through flow basic equations and in CFD, they are generally called governing equations.

The bases of the computations in CFD are conservation laws of Physics and then governing equations are derived from it. The basic laws are:

- Law of Mass conservation
- Newton's second law of motion
- First law of thermodynamics

The involvement and advantage of CFD in almost every industrial application of fluid flow has made it powerful tool. Whether it is a university based research or some industrial problem, the use of CFD has become essential before on ground application. These pre-implementation analyses have given huge advantage in better understanding and successful completion of any project. The developers and researchers have described many advantages if the CFD is employed any flow analysis and same advantage has proven too time to time.

The following advantages of the use of CFD have forced the new researchers to utilize it in more efficient and effective manner. These are the few basic advantages and actual benefits are not limited to these:

1. By utilizing CFD in any fluid flow calculations, one can study and analyze the each and every term of governing equations separately. The detailed analyses are available after computation.
2. The other main advantage of CFD is that it provides the very cost effective and time saving means to simulate actual flow scenario as compared to experimental or analytical approach which are costly and time consuming. It also has the advantage to cater complex geometries and difficult flow conditions. The multiphase and multi fluid flows can also be simulated in CFD with reasonable accuracies.
3. The CFD has the ability to simulate those conditions which cannot be practically performed or cannot be repeated in normal situations like huge disasters (Tsunami) or nuclear tests / accidents etc. By using CFD, these disasters can be simulated as happened actually and their analyses can be used to identify the causes, prevent theses disasters in future or preventive measures can be defined.

4. CFD also provide an opportunity to analyze visually every aspect of fluid motion in detail. Every streamline of fluid motion can be visualized and comprehensive information can be obtained.

The steps in CFD process consist of pre-processing stage like development of model, defining physical and boundary conditions, than is the solver stage whereby process is simulated as per defined criteria and governing equations are solved. The last step is analyses of simulation results. The results may be analyzed mathematically and by visualizing flows.

2.4.1 Basic Computational Techniques

Every software package has some basic techniques to be utilized for calculating the solution. CFD has also some basic computational techniques which will be analyzed shortly.

2.4.2 Discretization

Converting Derivatives to Discrete Expressions

In CFD, we get a numerical solution of a differential equation at discrete points which are called grids. By connecting these grid points, we obtain a flow pattern after simulation. These grid points are defined in a certain domain and the domain is our area of interest. Whatever the domain is, solver will calculate the solution within that domain. The clarity of this point can easily be made by considering an experiment whereby we are measuring velocity at some equally distant points using some measuring device. After taking data at all the points in the defined field / domain of flow, we may imagine the flow condition by connecting all these points. Same thumb rule is being followed in computational fluid dynamics.

Similarly if we require data in between the measurement points, we may use interpolation which can be linear or higher order interpolation. The same technique is followed in CFD solver.

2.4.3 Spatial Discretization

Spatial Discretization is a method whereby the continuous solution is discretized in smaller increments to make it acceptable to any computational solver and then the solver solve the governing equation at these discretized points. The accuracy of any solution largely depends on development of these discrete points. The differential equation is discretized in the flow domain.

2.4.4 Discretization Methods

There are many ways to derive a differential equation after discretization. But the most common methods being used are listed below.

1) The Finite Difference Method
2) The Finite Element Method
3) The Finite Volume Method

2.5 CFD and Solar Chimney Systems

Behavior of Solar Chimney systems can be evaluated by using CFD analysis. In other words, some phenomena such as vortex regions, velocity and total pressure profiles can be predicted and analyzed by computational fluid mechanics techniques.

Computational fluid dynamics (CFD) technique in evaluation of fluid flow phenomenon has been well established in last two decades and many researchers have validated the results of CFD with that of practical experimentations. The number of simulations related to natural ventilation has also been performed using CFD packages and results have been cross verified with practical experiments. The use of CFD has made possible to predict more reliable results for natural ventilation before going into practical implementation. This prediction of almost accurate results has provided savings in term of time and expenditures. Almost each and every project is going through simulation process before actual implementation in the field.

The numerous researchers have validated CFD as a best tool for prediction of fluid flows, particularly in the study of natural ventilation. They have placed CFD as most widely used software for accurate simulations with reasonable accuracy of results. The applicability of CFD has been confirm and tested by these researchers in almost every field of engineering.

The researchers have made all out efforts in successful utilization of CFD and most importantly, had success in obtaining desired results. These ventilation studies have been carried out by Wang, Jiang and Haghighat [18], Li and Fuchs [19], Borchiellini, Fracastoro, Perino [20], Chen [21 & 22], Yau [12], Yau and Lee [13], Versteeg and Malalasekera [14], Emmerich and McGrattan [15], Murakami [16], Zhang and Chen [17].

The computational study of natural ventilation based on solar chimney systems is being extensively carried out through the use of CFD packages. By using the CFD, we get that information which is not available through any other means. Through computations of any flow system, we get each and every bit of information which we need by only employing the right software package with accurate conditions. We can simulate any type of two dimensional and three dimensional models and get the solution of Navier-Stokes equations in no time. CFD can handle almost all type of geometries whether simple or complex with the availability of variety of results which may include information about flow patterns, temperature distribution and pressure variation etc. within a specified model space.

Now we will go through some of the natural ventilation researches carried out in the field, particularly, by the usage of CFD packages.

Solar Chimney Literature Review

2.6 Solar Chimney Systems Modeling and Analysis

The concept of Solar Chimney was originated in early 80s when mathematical models of Trombe wall and the Solar Roof Collector were developed. The earlier research in the field of natural ventilation was carried out by Akbarzadeh et al. in 1982. They build a modified Trombe wall of 0.235m placed at the roof of a building in the University of Melbourne, Australia and conducted experiments. During the analysis, turbulence flow was present through the Trombe wall. It has been observed that height of the building air inlet location and width of the wall significantly affects the heat transfer rate.

In 1989, Das and Kumar performed experimentation on solar chimney model. They built a flat-plate inclined solar chimney. The walls of the solar chimney were made of 3mm mild steel plates. The height of the chimney was two meter while the width was 0.1m. The collector of this inclined solar chimney was made of wood and black paint was employed to increase absorption of solar heat. The experimentation results showed that a maximum temperature of 56.5 ^{o}C was obtained in solar chimney. The air flow rate achieved was 0.255 m/s.

The effect of solar chimney width on the performance of natural ventilation was numerically studied by Zamora and Kaiser [33]. They used Phonics code by changing Rayleigh number within the range of 10^5 - 10^{12} and keeping heat flux, wall temperatures and boundary conditions constant. The researchers developed a correlation for the optimum aspect ratio based on range of Rayleigh number. The correlation revealed that the optimum aspect ratio decreases with the increase of the Rayleigh number.

Studies based on analytical, computational and experimental methods have been frequently performed to evaluate integration and performance of solar chimney. Analytical studies are normally carried out with many assumptions for the sake of simplifications. But computational methods have open new horizon in the field of natural ventilation using solar chimney. We can easily study and predict flow patterns through the solar chimney and within the building / room using CFD techniques. The use of CFD has greatly influence our knowledge and widen our view in this field. The studies carried out in the field of solar chimney based natural ventilation can be generally classified into following four groups;

- Research / study carried out on laboratory size / small scale models.
- Research carried out on real sized / large scale models.
- Practical experimentations performed on small and large scale solar chimney models

- Studies performed on models with controlled indoor environment.

The basic purpose of all the research carried out in this field is to find and suggest optimum design of solar chimney in order to increase natural ventilation rate with minimum expenditures. There are many parameters which affect the thermal performance of the solar chimney and ultimately increase or decrease the natural ventilation rate. The most important parameters are chimney aspect ratio, height of solar chimney and air inlet opening, angle of the chimney with respect to roof of the building, capability of the chimney to pass and absorb solar heat, area of inlet and outlet openings.

There are two major research areas which have been pointed out by most of the researchers and further discussion will be carried out on these areas in coming sections. These areas are;

(a) The effect of geometry on the performance of solar chimney / natural ventilation.

(b) The effect of solar chimney tilt angle on ventilation performance.

The above stated factors greatly influence the results of solar chimney and therefore considered as the key factors in determining the solar chimney thermal performance. Other parameters as explained above have also great contribution in increasing / decreasing the performance of solar chimney based systems.

The researchers have worked on every aspect of the solar chimney and associated building in order to enhance the natural ventilation. Lee and Strand [6] research was concentrated on the solar heat absorption capacity of a solar chimney. They analyzed that by increasing the solar heat absorptance of a chimney from 0.25 to 1.0, an increment of nearly 57% can be achieved in the flow rate passing through the chimney. This shows that higher absorptance capacity of the solar chimney is desirable for increased natural ventilation.

The same phenomenon of solar heat absorptance was also analyzed by Pavlou et al. [7]. It was suggested in the research that the absorber surface should have the highest absorptance to emittance ratio in order to maximum solar chimney thermal performance. It was also analyzed that the effect of the solar heat absorptance at the outer surface of the chimney (surface facing the Sun) on thermal performance is negligible.

Many researchers investigated the integration of solar chimney on multistory buildings. Macias et al in 2006 studied the performance of the solar chimney in a multistory building using two simulation models. These models were TRNSYS and TAS. Calderaro and Agnoli in 2007 also employed first model against energy upgrade investigation of a huge building with solar chimney in the presence of other sources of energy. The thermal performance of the solar chimney with reference to construction elements was also analyzed by Pavlou and Santamouris in 2007, using the TRNSYS 15.1 model. The said solar chimney was attached to a room. The construction parameters investigated were related to glazing type, walls thermal resistance and thickness of the solar chimney.

2.7 Effect of Geometry on Ventilation

The thermal performance of the solar chimney and natural ventilation rate is greatly influenced by the geometry of the building and solar chimney. The construction of room, solar chimney and air inlet / outlet dominantly affects the efficiency of the solar chimney. Plenty of work has been carried out to study effect of geometry on thermal performance, particularly flow rate. The performance in terms of flow rate can also be presented in terms of Air Changes per Hour (ACH). This is the ratio of air volume flow rate to the total volume of the room i.e.

$$\mathbf{ACH} = \frac{\mathbf{Q} \times \mathbf{3600}}{\mathbf{V'}}$$

The above expression has been defined by ASHRAE, where the *Q is* volumetric flow rate of air in m^3/s and V' is room volume in m^3.

2.7.1 Studies on Large Scale/ Full Size Models

Bansal et al. [3] is one of the pioneer researchers in the field of natural ventilation using solar chimney. He carried out the investigation using a steady state mathematical model. The area of the collector of the solar chimney, used for these analyses, was 2.25 m^2 and chimney width was 15 cm. The different solar radiation values were used to evaluate the performance. It was noted that with heat flux rate of 200 to 1000 W/m^2, 140-330 m^3/h air flow rate can be obtained.

Bansal et al. [4] also studied the wind tower based natural ventilation system. This system was assisted by solar chimney. The solar chimney was fixed at the exit end of the outlet apertures of the room with an inclination angle of 30°. In order to concentrate on the performance of the solar chimney, the stack effect in the wind tower was neglected. The analysis of this model revealed that air flow rate up to 1.4 kg/s can be achieved by keeping the heat flux rate at 700 W/m^2. The air flow rate with respect to external ambient flow rate was also studied. Air Changes per Hour of 35 to 73 can be obtained with ambient wind speed of 1.0 m/s.

The study on full scale model was carried out by Arce et al. [1]. The solar wall prepared for investigation was 4.5 meter in height and was 1 meter in width. The absorber wall was made of reinforced concrete with thickness of 0.15 meter and painted black to increase absorbance. The height of the stack was 3.5 meter and aspect ratio was 11 with air gap of 0.3 meter. They reported up to 374 m^3/h air flow with the heat flux rate of 604 W/m^2. They concluded that the outside wind velocity and pressure gradient between inlet and outlet openings have major influence on the performance of solar chimney based systems.

An office room of one story building with floor area of 36 m^2 was numerical analyzed by Miyazaki et al. [2] with the help of CFD. In order to validate the numerical results of this simulation, they were compared with results of earlier experiments carried out by Bouchairin1994. The comparison made of the results numerically obtained by changing width of the solar chimney i.e. 0.2m, 0.3m and 0.5m. It was reported that the results obtained with solar chimney width of 0.3 meter were in accordance with the experimental results.

Experimental investigation was carried out in case of residential ventilation using four types of solar chimneys by Mathur et al. [26]. They studied the effect of cylindrical solar chimney having height of 2 meter and width of 28 cm in continuation to their earlier investigations ([25] and [27]), they used it with and without outer covering. It was suggested that, cylindrical chimney is easy to install at existing buildings and give higher performance with inclination angle of 45° and heat flux rate of 949.53 W/m^2. The ventilation rate was increased up to 15.94% with this arrangement.

Numerical and analytic investigation of the performance of solar chimney model with reference to air inlet opening size and width of the solar chimney was carried out by Bassiouny and Koura [23]. The physical parameters considered for these analysis were same as that of taken by earlier researchers for same type of studies like Bansal et al. [3], Ong & Chow [24] and Mathur et al. [25]. The ACH was analyzed by increasing air inlet opening size and solar chimney width by three times each. The results obtained showed that the ACH was increased by 11% in case of air inlet opening while the result was 25% increase in case of solar chimney width. Therefore it was suggested that increase in chimney width has more positive effect on natural ventilation rate than air inlet opening.

Different air gap or solar chimney widths have been investigated by researchers. The chimney width in between 0.3 to 0.5 meter has been reported as optimum width like at [1], [2] and [25]. The air reverse circulation phenomenon has also been reported by researchers at higher chimney widths like Chen et al. [28] observed reverse circulation at the width of 0.4 meter.

Some researchers also tested and analyzed performance of the models fitted with metallic solar chimney. A real sized model with metallic solar chimney was tested in Thailand [29]. The height of the chimney was 2 meter with a width of 0.145 meter. The model base area was 11.55 m^2 and a height was 2.68 m. The mass flow rate obtained was up to 0.02 kg/s.

2.7.2. Studies on Small Scale Models

Plenty of research has been carried out on small scale models as they are easy to investigate with reference to simulation and experimentation.

An experimental investigation was carried out by Bansal et al. [30]. They used window as solar chimney. Three different combinations of chimney width and air inlet opening size were analyzed. Aluminum sheet of 1 mm thickness was used. The model was made of wooden box having dimensions 1m × 1m × 1 m. When they kept the air inlet opening at the height of 0.13 meter with solar chimney width of 0.13 meter, maximum flow velocity of 0.24 m/s was obtained. The results of experiment were validated with mathematical model which showed difference of 2% to 6% between two results.

Mathur et al. [25] investigated the effect of aspect ratio on the performance of solar chimney by considering nine combinations of absorber height and width. The small scale solar chimney up to 1m height was considered for this investigation. They reported maximum ventilation of 5.6 ACH in a room of 27 m^3 and heat flux of 700 W/m^2 against model having aspect ratio of 2.83 for a 1 m high chimney with different absorber height ranging from 0.7 m to 0.9 m.

The concept of natural ventilation in high rise buildings with the help of solar chimneys is also getting attention. The researchers in Thailand [32] have experimentally investigated the integration of solar chimney in high rise buildings. The two small scale models of three stories each were constructed with dimensions of 1.2 m × 2 m × 1 m. They used different model configurations to analyze their effect. In first model, air inlet openings were made at each floor while there was only one outlet opening at third floor while in other case, the air inlet and outlet openings were made on each floor. The setup in case of second model showed better results than the first one.

2.8 Research Based on Controlled Environment

The analysis of solar chimney based systems largely depends on solar radiation which is very hard to predict and control. The experiments require accurate supply of this heat for better results. This requirement has lead the researchers to perform experiment indoor where the supply of heat can be controlled and maintained at required rate using different heating systems.

The variation of mass flow rate was analyzed by Burek and Habeb [34] experimentally with reference to different heat inputs and channel depths in a controlled indoor environment. The dimensions of the experimental model were 102.5 cm × 92.5 cm (height × width) with varying channel depth from 20 to 110 mm. The heat ranging from 200 to 100 W was supplied through electrical system for a collector area of 1 m^2. The results showed that mass flow rate is directly dependent on heat input.

2.9 Studies Based on Experiments

The simulation analysis of any Solar Chimney alone or a whole room / building fitted with solar chimney is first major step in determining do-ability and performance of the design. But analyses of practical experiments are equally essential to certify results achieved from simulation analysis. Many researchers have gone through practical experiments of solar chimney alone or in combination of simulation in order to determine / analyze performance of results achieved from computer model and actual experimental model. The few studies based on solar chimney practical experiments have been discussed below.

A solar chimney model with built in latent heat source was fabricated by Y. Kaneko, K. Sagara, T. Yamanaka, H. Kotaniin Department of Architectural Engineering, Osaka University which was also the site for experimentation. The built in latent heat source was based on an Aluminum (Al) plate and PCM (Sodium Sulfate Decahydrate "Na_2SO_4 $10H_2O$") for latent heat storage. The 06 number PCM encapsulated in the rectangular container of dimensions of 0.6m length × 0.25m width × 0.025m thickness were utilized. The solar chimney was placed with 45^o angle with respect to the horizontal. They used pyranometer to measure solar heat.

The results of above experimentation showed airflow rate of 100 to 400 m^3/hr. In order to verify experimental results, numerical simulation was also performed. The temperature data obtained through simulation was in line with that of experimental data.

Burek and Habeb in 2007 studied the performance of a vertical solar chimney having dimensions 1.025 m high and 0.925 m wide experimentally. The absorber was made of Aluminum plate with matt black paint. The heat was provided through electrical heating system with a range from 2 to 1000 W/m^2. The results validated the earlier numerical and experimentation result that mass flow rate is directly dependent on heat input.

2.10 Effect of Solar Chimney Angle on Performance

Initially, research was performed on straight solar chimney but with the passage of time, the solar chimney inclination has given new horizon to improve the ventilation rate. As the heat input or heat absorbed by the absorber plays a vital role in the thermal performance and ventilation rate, same can be increased by integrating chimney at some suitable angle in order to get / absorb maximum solar heat in a given situation. Researchers have performed number of numerical and experimental studies on inclination angle of solar chimney starting from 10 degree to 70 degree with roof top and proposed most appropriated inclination angles. The most benefitted inclination range, suggested by researchers is between 45 degree to 65 degree. It also depends on the actual site location where solar chimney setup is being installed.

The experimental investigation based on aspect ratio and inclination angle of solar chimney was studied by Chen et al. [28] with different solar heat inputs. The solar chimney of height 1.5 meter and with width of 0.62 meter was made for experimentations. The experiments were performed on same length of the chimney by changing inclination angle. An electrical heating system was utilized to provide heat flux from 200 to 600 W/m^2. The experiments were performed with different inclination angle of this solar chimney. The results showed that the maximum flow rate was noted as 0.035 m^3/s at 45 degree tilt angle. It was also confirmed that this flow rate was approximately 45% more than that of achieved with straight solar chimney.

The effect of solar chimney inclination angle was experimentally, analytically and numerically was investigated by Sakonidou et al. [36]. For simulation, they developed a two dimensional CFD model in FLUENT. Different simulations were performed by changing chimney length from 1meter to 12 meter and chimney tilt angle from 30 degree to 90 degree. The experimental chimney was of parallelepiped shape with dimensions of 1 m × 0.74 m × 0.11 m (height × width × air gap). The absorber was built with aluminum sheet painted with black colour. The insulation was also arranged for absorber with 5 cm fiberglass. It has been reported that air flow rate increases with increase in chimney height. The analytical model showed an appropriate angle 65 degree for chimney inclination while the CFD gave the 60 degree.

Harris and Helwig [35] also numerically studied the change in inclination angle on performance of the chimney. They reported that with 67.5 degree tilt angle of solar chimney, the air flow rate has been incremented by 11% as compared to straight solar chimney.

2.11 Outcome of Literature Review

The extensive research has been carried out on almost every aspect of the Solar Chimney during last three decades but still new achievements are being obtained with every new simulation and experimentation. Plenty of literature is available about the research carried out on different aspects of Solar Chimney and by reviewing this literature, some parameters can be fixed based on results and analysis. These help us to focus our future research on such parameters where there is still margin of improvement available or where we can achieve more fruitful results.

By reviewing plenty of literature, I have been able to fix the value of some parameters for ease of research / simulation as proper research cannot be performed in multi dimensions with limited time period. It is better to concentrate on few parameters in order to get useful results in shorter time. In the present research, I have concentrated on room air inlet locations and study air flow pattern / pressure around inlet / outlet openings of the room. This has been achieved by designing environmental boxes around inlet / outlet openings of the room.

Secondly, after literature review, I have been able to fix some parameters where plenty of research has already been carried out and it is clearly evident from literature that certain value of a parameter will give desired results. These parameters include inclination angle of the solar chimney, height and width of the solar chimney

Chapter 3

Two-Dimensional Modeling and Simulation

3. Abstract

This chapter describes the two dimensional modeling and simulation of the room fitted with solar chimney. Initially, a small scale model has been designed and simulated to get the familiarization of software package, its use and results obtained. After successful simulation on a small scale model, a real sized room fitted with solar chimney has been designed.

The final room was selected after number of simulations of different models having different sizes of the room and different inclination of solar chimney.

The grid convergence tests were carried out on selected model. After achieving the grid convergence, the final model was simulated with different air inlet locations and analyses were performed; the detailed discussion on this is presented in this chapter.

3.1. Two-Dimensional Modeling and Simulation of a Small Size Room

As a first step, a two dimensional room at smaller scale with the width and the height of 0.5m each, which has been fitted with a straight chimney at roof top of length 0.25m, was modeled using CFD-ACE+, a CFD software package from the ESI group. In this case, the width of solar chimney and room air inlet opening is 0.025m each. In this model, the solar chimney is placed on the room roof opposite to inlet opening. The purpose of this small scale modeling was to understand the basic parameters and functioning of the CFD software before going into real sized room modeling. The figure below shows air flow through this small size room;

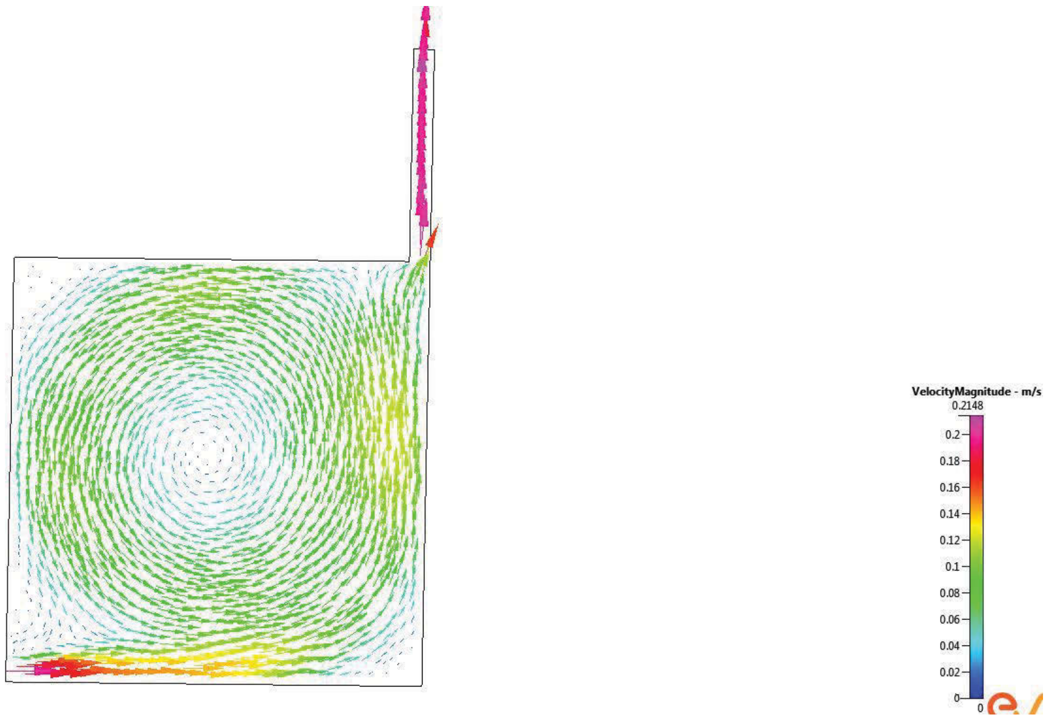

Figure 3.1 : Air Flow through small size room fitted with straight solar chimney (image from CFD Viewer)

In order to get further idea about behavior of room model and to select a proper model for detailed analysis, initially different models were prepared and simulated based on literature review. These basic room models, with less number of cells, were made and simulated by changing following;

1. By changing the room width and height.
2. By changing the chimney height.
3. By changing location of the chimney at roof top.
4. By changing angle of the chimney with respect to roof top.
5. By changing width of the chimney.

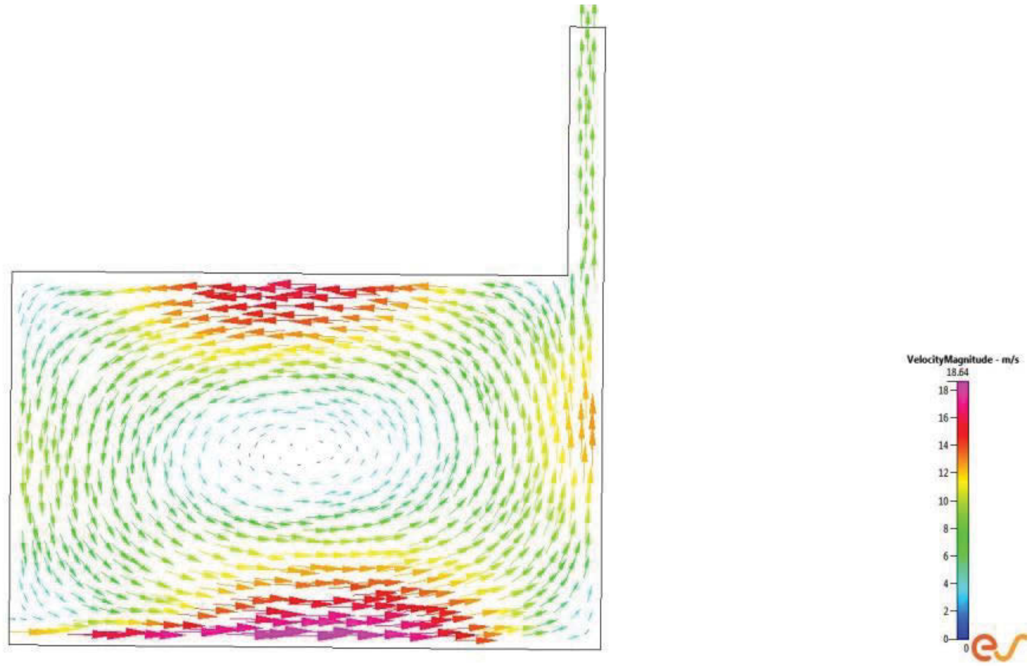

Figure:3.2: Air Flow through a room (3 meter × 5 meter) fitted with straight solar chimney of 2 meter height.

3.2. Two-Dimensional Modeling and Simulation of a Real Size Room

After getting the idea of functionality of software and modules to be used, a real sized room with dimensions of 3m width and 3m height was created. The room air inlet opening and the width of the solar chimney was 0.3m. Initially, analysis on straight solar chimney was performed. The purpose was to get the idea about flow rates and air patterns in the real sized room. Analyses were carried out by changing different parameters for different simulation and their effect on the output parameters.

The detailed analysis were not carried out as much work has already been carried out on straight chimney and literature review reveals that inclined solar chimney with and angle of 45^0 gives maximum heat absorption by solar chimney and ultimately results in more air flow rate from the room.

The figure below shows air flow and temperature patterns after simulation of real size room (3 meter × 3 meter) with 1.5 meter chimney height.

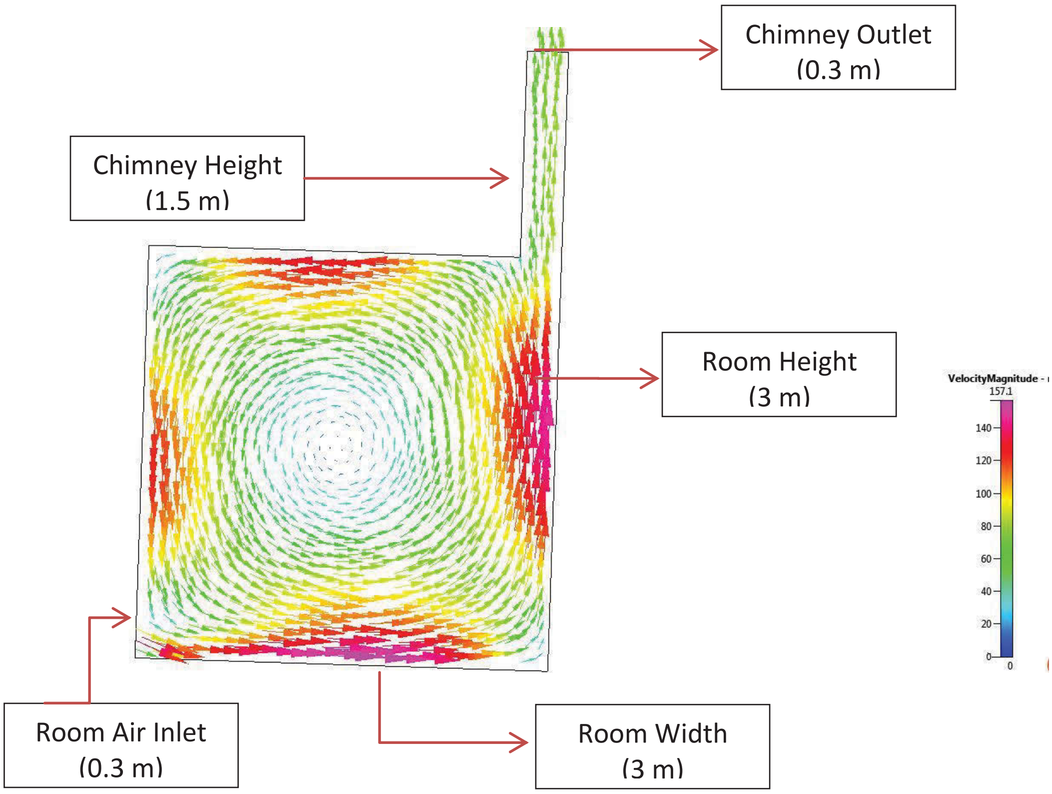

Figure 3.3: Air Flow through Real Size room fitted with straight solar chimney

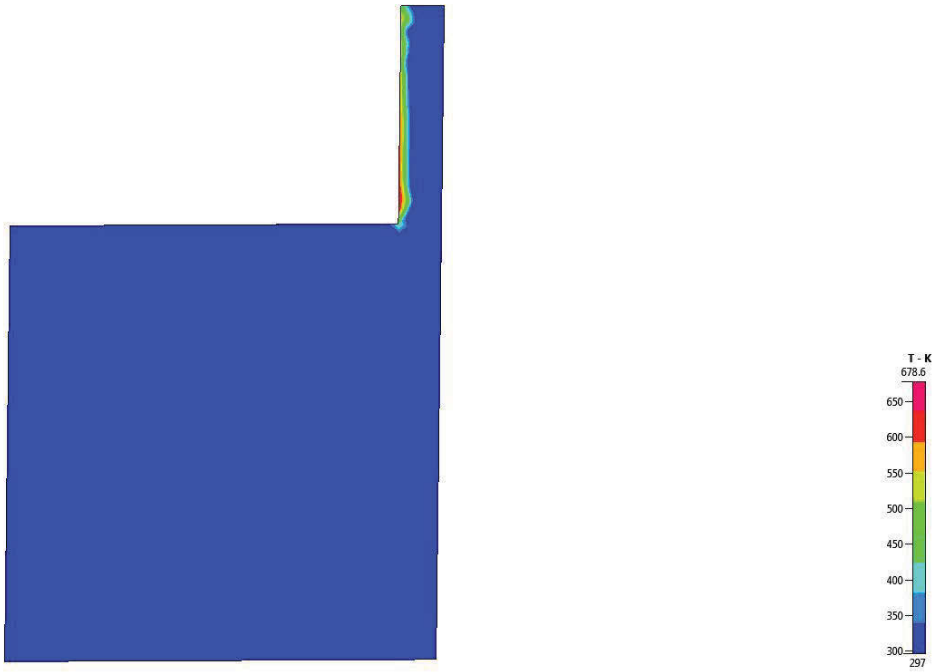

Figure: 3.4: Temperature pattern in a Real Size room Fitted with straight solar chimney

Later on, a solar chimney with an angle of 45^0 from roof top was considered based on literature review (this angle gives the maximum solar heat absorbance as per most of experimental and numerical analysis). The effective length of solar chimney in this case is 2.12m. The Figure 3.4 shows a real sized room (3 meter × 3 meter) fitted with 45^0 inclined solar chimney.

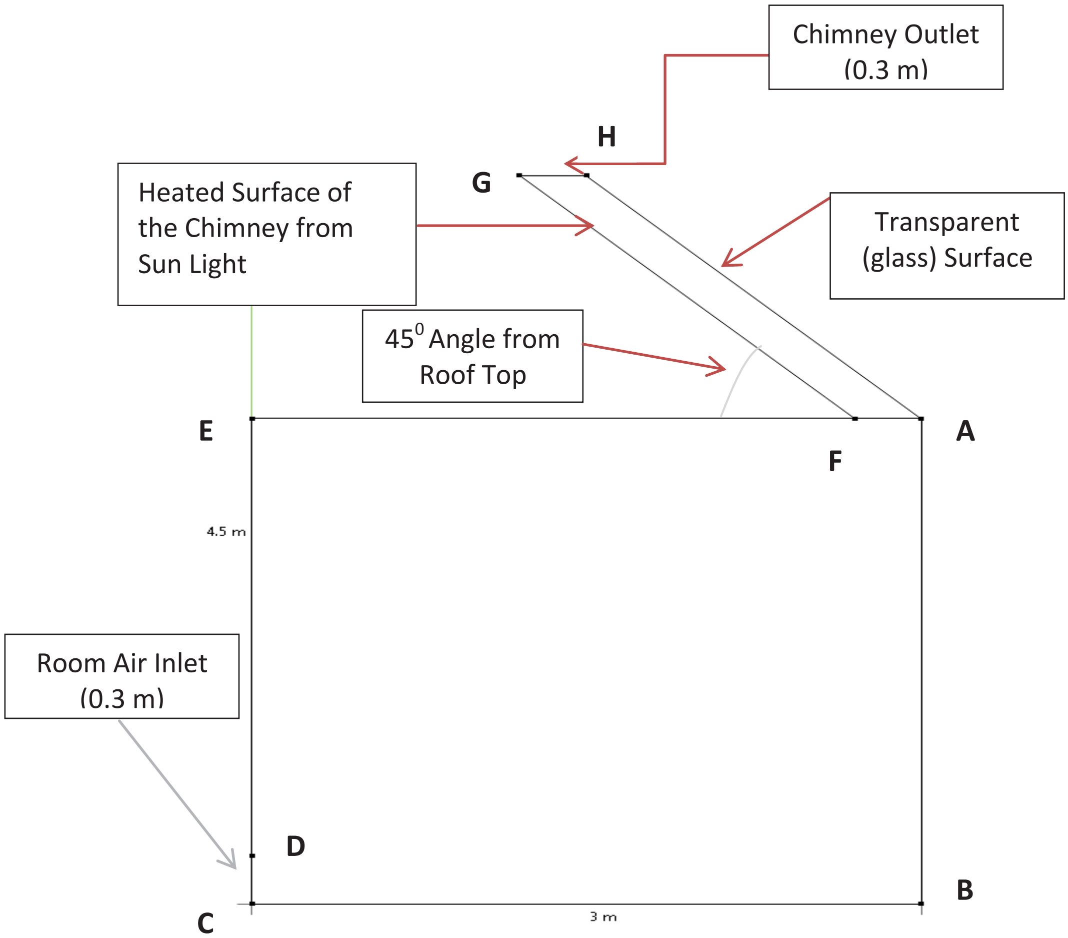

Figure 3.5: Model of a real sized room fitted with inclined solar chimney

The different parts of the above 2D model are described as follow;

AB ------------- Right side wall of the room having height 3m.

BC ------------- Floor of the room having width 3m.

CD ------------- Air Inlet of the room (0.3m)

DE ------------- Left side wall of the room (3m height)

EF ------------- Roof of the room (3m width)

FA -------------Chimney inlet interface (0.3m)

FG -------------Solar chimney inside wall (heated wall) – 1.5m high from roof top with effective length of 2.12m

AH ------------- Solar chimney upper wall (transparent)

GH ------------- Solar Chimney outlet (0.3m)

Further analyses were performed on the above real sized room fitted with a solar chimney with an angle of 45^0 from roof top.

3.3. Designing of a Real Sized 2D Room in CFD GEOM

The models are designed in CFD-GEOM module of CFD ACE+ software. The both geometry and grids were created in the CFD-GEOM. Structured meshes are used in each model. The Figure 3.6 below is showing finalized two-dimensional model with grids and meshes (structured mesh) in CFD-GEOM.

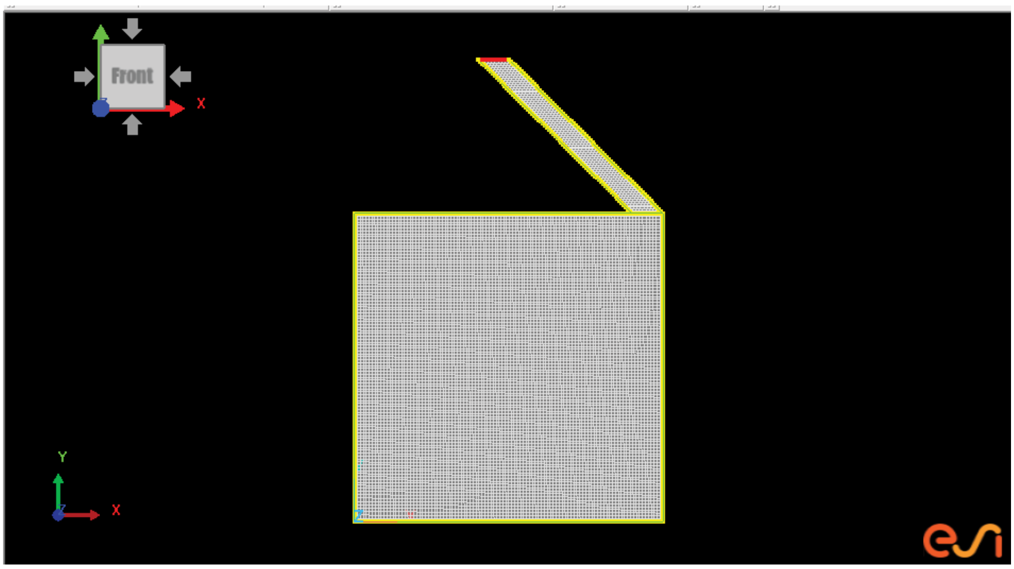

Figure 3.6: Finalized Two Dimensional Model with Grids and Faces

3.4. Simulation Steps of a Real Sized 2D Room in CFD ACE+ GUI (Software Solver)

The models are simulated in CFD-ACE GUI module of CFD ACE+ software. The Figure 3.7 below is showing exported DTF file in CFD Solver for simulation.

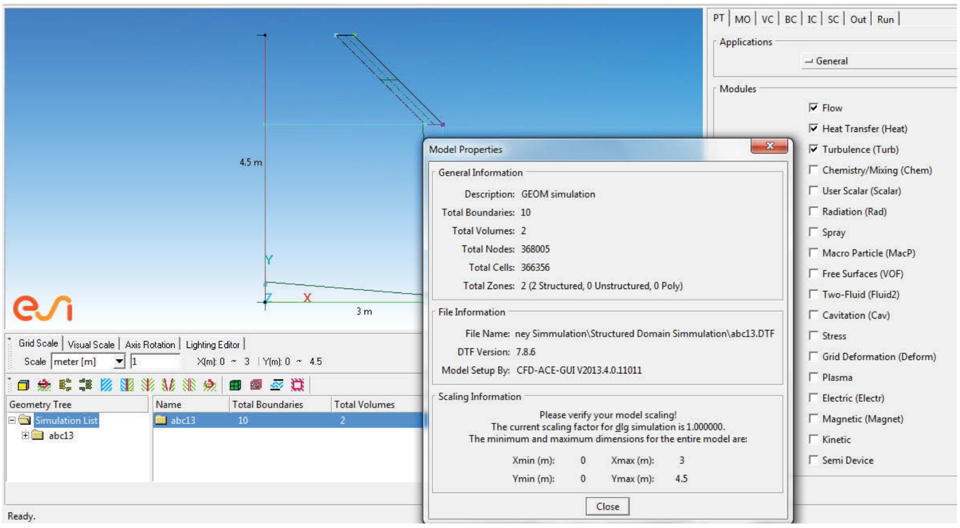

Figure 3.7: Exported DTF model (Figure: 3.6) in CFD-ACE GUI Module for Simulation

The following major steps were involved during simulation of above model;

- **Selection of Modules in CFD-ACE GUI for simulation**
- **Gravity and Boussinesq Force Selection**
- **Turbulence Model Selection**
- **Selection of volume conditions / properties**
- **Defining Inlet Boundary Conditions**
- **Defining Chimney outlet Boundary Conditions**
- **Solar Chimney Heat Flux Rate**
- **Defining Initial Conditions**
- **Defining number of iterations and convergence criteria**

3.5. Physical Conditions for the Model and Simulation in the CFD Solver

After the pre-processing stage in CFD-GEOM module by defining the geometry, mesh type and boundary conditions of the models, CFD-GUI module is used as the graphical user interface to the CFD-ACE-SOLVER.

The present simulation is performed in full-scale models and the air properties are assumed to be constant and corresponding to air temperature as 300 K and air standard pressure at sea level as 101.3 kpa. The boussinesq approximation has also been assumed for the buoyancy force arising from density variation as a result of temperature change. The following values of molecular properties are used (using common notation):

ρ (Density) = 1.161 kg/m^3

μ (Dynamic viscosity) = 1.846×10^{-05} kg/m-s

v (kinematic viscosity) = 1.5×10^{-05} m^2/s

Cp = 1007 J/kg-k

K (Thermal Conductivity) = 0.0263 W/m-k

Prandtl No. = 0.9

Reference Temperature = 297 K

Thermal Expansion Coefficient = 0.003367 K^{-1}

The following three modules were selected in the CFD ACE+ Solver (CFD-GUI);

1) **Flow Module**
2) **Heat Transfer Module**
3) **Turbulence Module**

A Reynolds-Averaged Navier-Stokes (RANS) formulation is used.

The low Reynolds Number k-ε turbulence model of Chien [37] is adopted, where k stands for turbulent kinetic energy and ε is its dissipation rate.

3.5.1 Boundary Conditions

The boundary conditions for the variables like velocity components, pressure and temperature areas follows;

- All openings on the flow domain's boundary i.e. room inlet opening and solar chimney outlet opening have been assigned with ambient conditions based on normal atmosphere around the room. The fluid has been considered at atmospheric pressure with a constant gauge value of p = 0 N/m^2 and temperature as T = 297K.
- The value of heat flux "Q" for lower wall (heated face) of the chimney (wall facing roof of the room) has been fixed as 300 W/m^2 with Zero Velocity while the upper face (wall) has been designed as transparent to allow passing of solar heat up to lower face. Although, the higher value of solar heat flux favours the natural ventilation but this constant value of solar heat flux has been

considered based on literature review, whereby, it has been analyzed that in most of the normalized area, the average heat flux provided by actual sun radiation is around this value. So the consideration of this value keeps the research more practicable.

- The remaining surfaces like walls of the room, roof & floor of the room have been assumed as adiabatic walls with velocity value as zeros. The adiabatic condition has been considered based on the fact that walls of the buildings are normally constructed to avoid losses of internal cooling or to protect inner environment from outside harsh weather. So in case of concrete walls, the heat transfer is very negligible through walls and therefore, adiabatic conditions may be considered for walls.
- Based on the previous research in the field as explained in Chien [30] and to keep turbulence model results equaling to laminar model, the value of k and ε have been taken as 1.00E-05 which is near to Zero for all solid surfaces. Where k is turbulent kinetic energy and ε is its dissipation rate.
- At all openings, the constant value of Temperature, k and ε shall apply only on those sections of an opening if inflow is occurring. If during computation, outflow is observed on any sections, the constant value of temperature, k and ε shall be ignored and actual values shall be calculated. Similarly, the constant pressure condition applies only on those sections of an opening where there is outflow. If the computation reveals inflow on any sections, the constant pressure condition there will be ignored, and pressure will be computed instead.

The other parameters considered for simulation are tabulated below;

Table: 3.1 : Physical Parameters Considered during Numerical Simulation

Physical Parameters Taken for Simulation of 2D Room Fitted with Inclined Solar Chimney			
Modules		**Body Forces**	
Flow		Gravity in Y-Direction (m/s^2)	-9.81
Heat Transfer		**Boussinesq Approximation**	
Turbulance		Reference Temperature (K)	297
		Volume Coefficient of Thermal Expension (1/K)	0.003367
Turbulance Model			
K Epsilon Family			
Low Re (Chien)			
Standard Wall			
Convergence Criteria	0.0001		

Boundary Conditions		**Initial Conditions**	
Room Inlet (Fixed Pressure)			
P (N/m^2)	0	P (N/m^2)	0
T (K)	297	T (K)	297
Kinetic Energy (m^2/s^2)	1.00E-05	Kinetic Energy (m^2/s^2)	1.00E-05
Dissipation Rate (m^2/s^3)	1.00E-05	Dissipation Rate (m^2/s^3)	1.00E-05
Room Outlet (Fixed Pressure)			
P (N/m^2)	0		
T (K)	297		
Kinetic Energy (m^2/s^2)	1.00E-05		
Dissipation Rate (m^2/s^3)	1.00E-05		
Chimney Inlet Wall			
Heat Flux (W/m^2)	300		

3.5.2 Pressure

When discussing a piping system, the term "pressure" is often used to describe a key fluid property that plays an important role in the operation of equipment like compressors, pumps, control valves, tanks, vessels, natural or force ventilation systems and other devices. However, like many terms used in engineering, there are nuances in meaning that must be taken into account to avoid miscommunication, confusion and costly mistakes. Quite often, key qualifiers that distinguish between total pressure, static pressure and dynamic pressure are not used. Sometimes the distinction is important, just as the difference between mass flow rate and volumetric flow rate must be made to be concise when discussing flow rate.

Definition and Units

The classical definition of pressure is the amount of force acting on a surface per unit area.

Pressure = *Force / Area*

This gives pressure the units of *pounds per square inch* (lb/in^2 or psi) or *newtons per square meter* N/m^2 (Pascal). Other units commonly used for pressure include the atmosphere, bar, kilopascal, torr, inches (or mm) of mercury and inches (or mm) of water.

Total Pressure

The total pressure is the force per unit area that is felt when a flowing fluid is brought to rest and is usually measured with a Pitot tube type instrument. The total pressure is the sum of the static pressure and the dynamic pressure.

$P_{total} = P_{static} + P_{dynamic}$

Total pressure is often referred to as the stagnation pressure.

Static Pressure

Static pressure is felt when the fluid is at rest or when the measurement is taken when traveling along with the fluid flow. It is the force exerted on a fluid particle from all directions, and is typically measured with gauges and transmitters attached to the side of a pipe or tank wall. Since static pressure is what most pressure gauges measure, static pressure is usually what is implied when the term "pressure" is used in discussions.

Dynamic Pressure

The difference between the total and static pressure is the dynamic pressure, which represents the kinetic energy of the flowing fluid. Dynamic pressure is a function of the fluid velocity and its density and can be calculated from:

$$P_{dynamic} = \rho v^2 / 2g$$

Depending on the application, the difference between total and static pressure may be negligible, but for others, neglecting the difference may result in costly mistakes.

For gas applications, the distinction between total and static pressure again will depend on the amount of dynamic pressure, but because the density of a gas is much lower than that of a liquid, a much higher velocity is needed before the difference between total and static pressure needs to be made.

Pressure is most important factor in natural ventilation. There are two types of pressure values appearing in software / simulation results i.e. Static Pressure and Total Pressure. The concerned value in this research is Static Pressure. The value of static pressure at solar chimney exit plays a significant role in ventilation systems. In natural ventilation systems, we normally keep this value as per atmospheric pressure.

The figure below shows the interface of the CFD ACE+ solver where different properties are defined for simulation purpose.

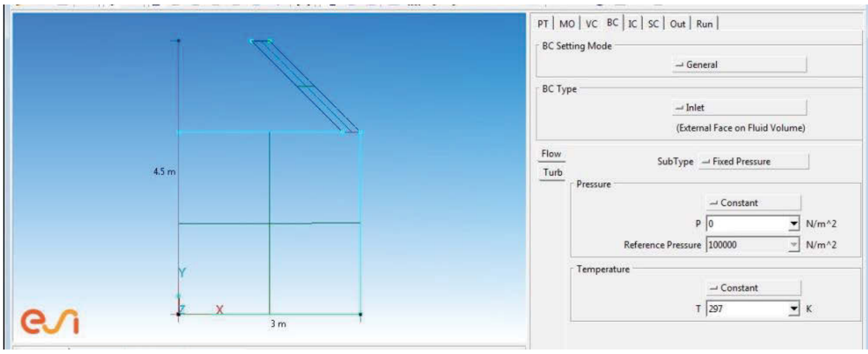

Figure: 3.8: Simulation in CFD-GUI Module of the CFD-ACE+ Solver

3.6. Simulation and Analysis of First (Basic) Model

The first model was prepared with very small number of grid points on CFD GEOM. The figure below shows first model which was simulated using following number of grid points;

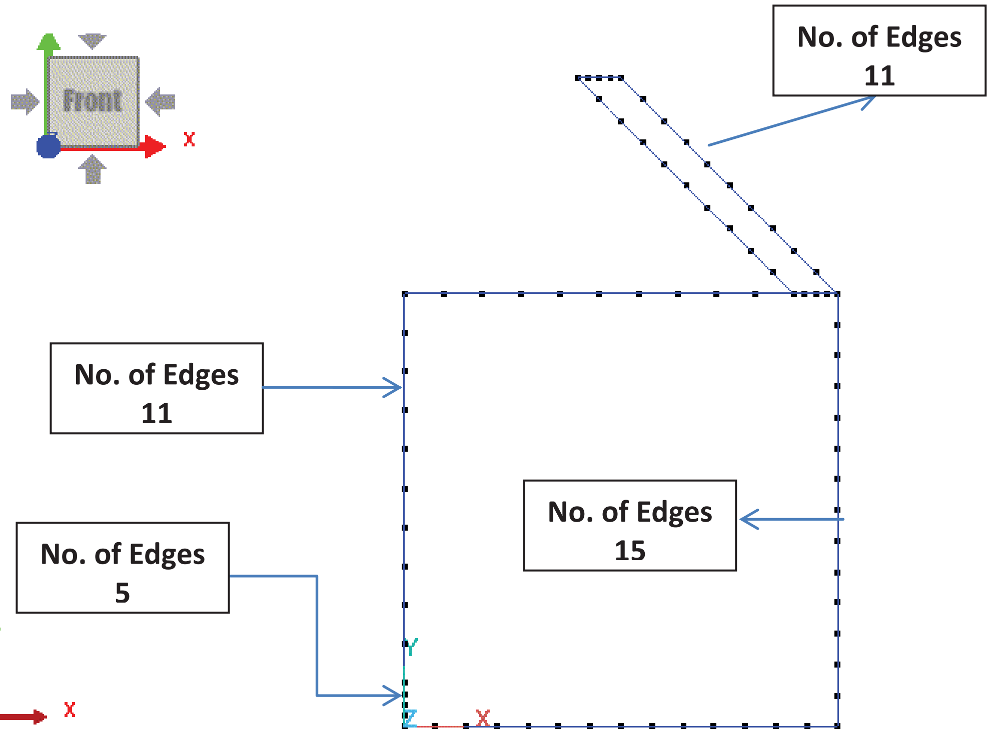

Figure 3.9: Model of a real sized room in CFD GEOM with Edges

The figure below shows meshing of first model in CFD GEOM.

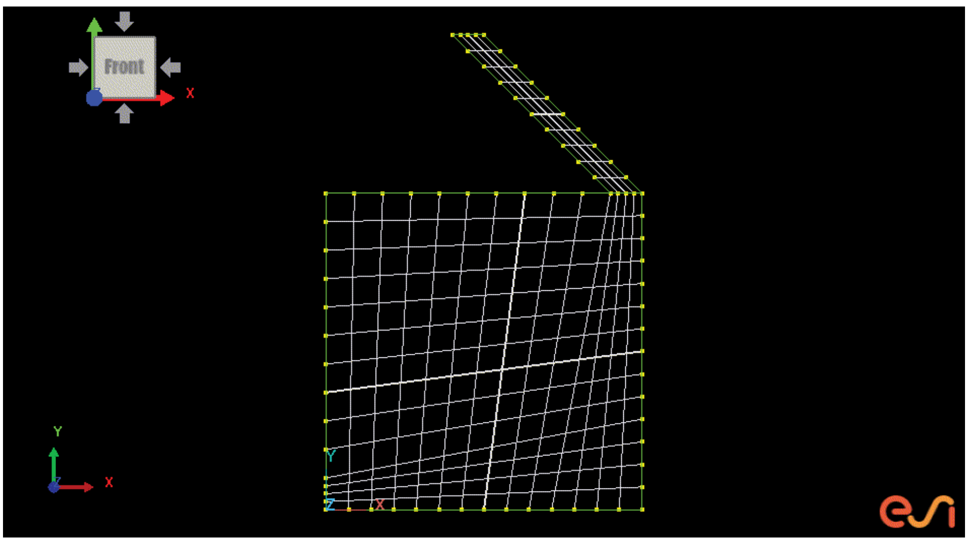

Figure 3.10: Model of a real sized room in CFD GEOM with Edges and Meshes

The above model was simulated with the parameters defined in the last section 3.1. The below are the graphical and numerical results obtained from this simulation;

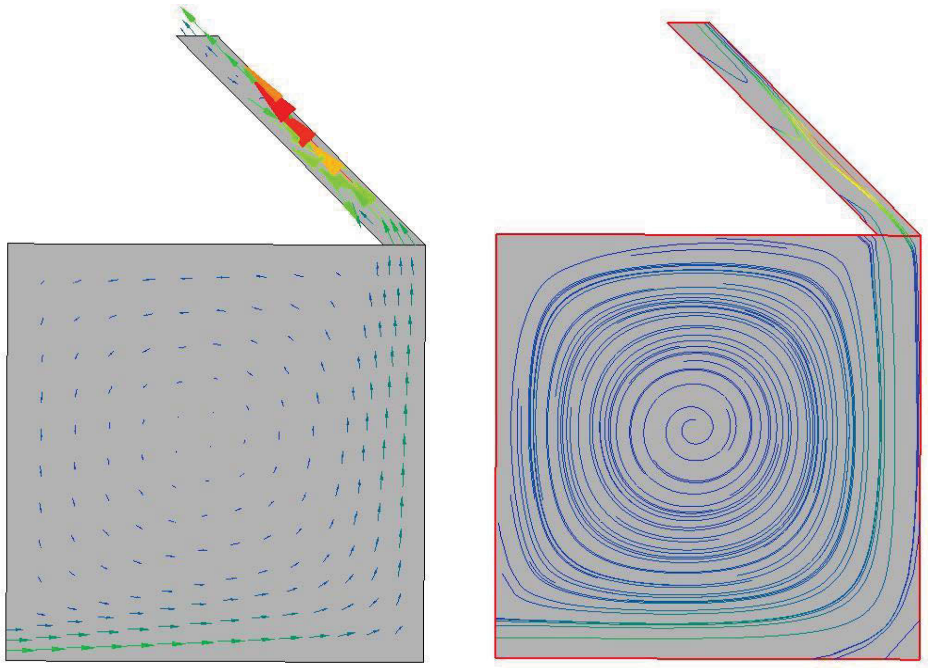

Figure 3.11: Flow Pattern through 2D Real Sized Room

The data table 3.2 below has been shown to give idea that what type of data has been collected against the simulation for further analysis. It is also giving the overview that the data has been collected at three different locations against each simulation.

Table: 3.2: Simulation Data of 2D Model-7 at Three Different Locations

Room Length	Room Width	Chimney Height / Length	
3 m	3 m	1.5 / 2.12 m	
Chimney Angle	Inlet / Outlet Opening		
45	0.3 meter		
Nodes		No.	210489
Faces		No.	419643
Cells		No.	209242
In Flow		KG/S	0.0171248
Out Flow		KG/S	0.0171249
Maximium Velocity		Met/S	1.089
Maximum Temp.		K	399.6
Converged at Iteration			5794

Simulation Data of 2D Model (Model-7 with Air Inlet at Bottom of the Side Wall)											
At Center of Room Air Inlet				At Chimney Inlet				At Chimney Outlet			
Coordinates of Location		Variable	Values	Coordinates of Location		Variable	Values	Coordinates of Location		Variable	Values
X (meter)	0.1	U (m/s)	0.04049	X (meter)	2.85	U (m/s)	-0.00207	X (meter)	1.29	U (m/s)	-0.33846
Y (meter)	0.15	V (m/s)	0.00231	Y (meter)	2.8	V (m/s)	0.033773	Y (meter)	4.43	V (m/s)	0.332922
		VM (m/s)	0.040556			VM (m/s)	0.033845			VM (m/s)	0.474757
		P (N/m^2)	-3.1E-05			P (N/m^2)	-8.1E-06			P (N/m^2)	-0.00171
		Pt (N/m^2)	0.000925			Pt (N/m^2)	0.000658			Pt (N/m^2)	0.136116
		T (K)	297			T (K)	297			T (K)	307.288

In order to further explain above data table, the graph in figure 3.11a below has been drawn which shows change of velocity at three different locations of the model:

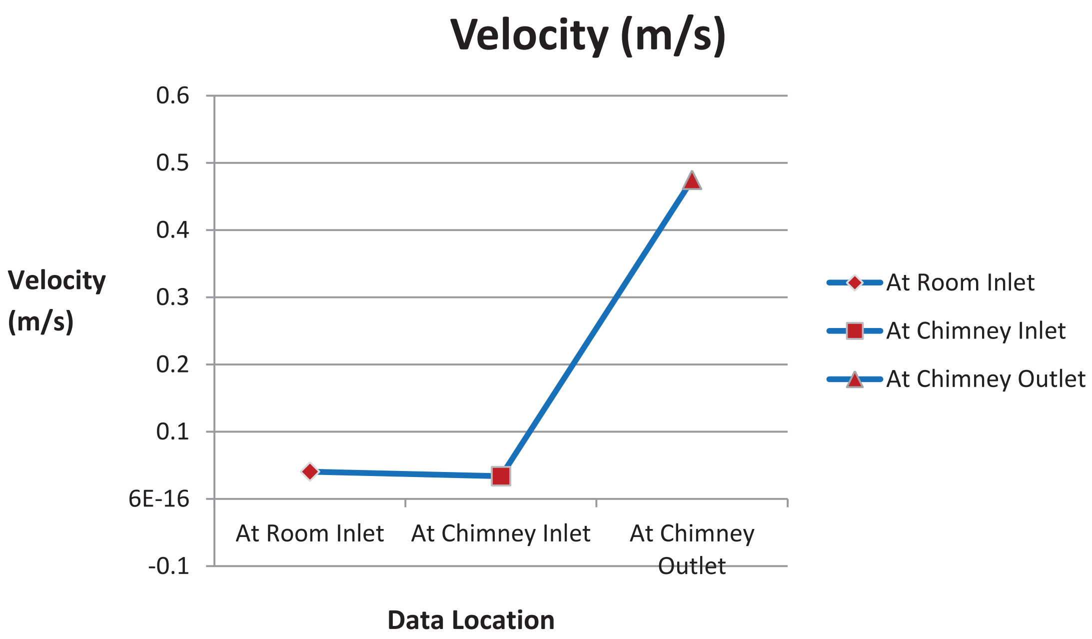

Figure: 3.11a: Showing change in velocity at three different locations of the Model

3.6.1 Grid Convergence Criteria

The Grid Convergence criteria of 0.0001 has been adopted for each simulation as shown in below screen shot:

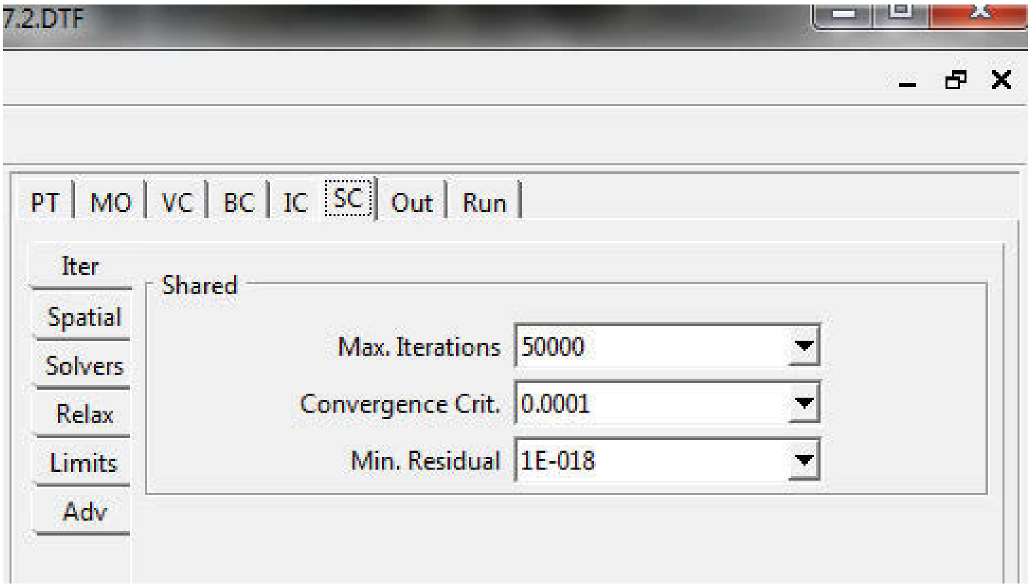

Figure 3.12: Showing number of Iterations and Grid Convergence Criteria for Simulation in the Solver

3.6.2 Normalized and Un-Normalized Residuals

The normalized and un-normalized residuals are used to measure the accuracy of the solution. It has been particularly taken care about the residuals values range after simulation. If the value of any parameter, in un-normalized residual graph, goes much out of range, the same has been re-simulated by changing grids spacing and other parameters.

The graphs below are showing the normalized and un-normalized solutions of one model.

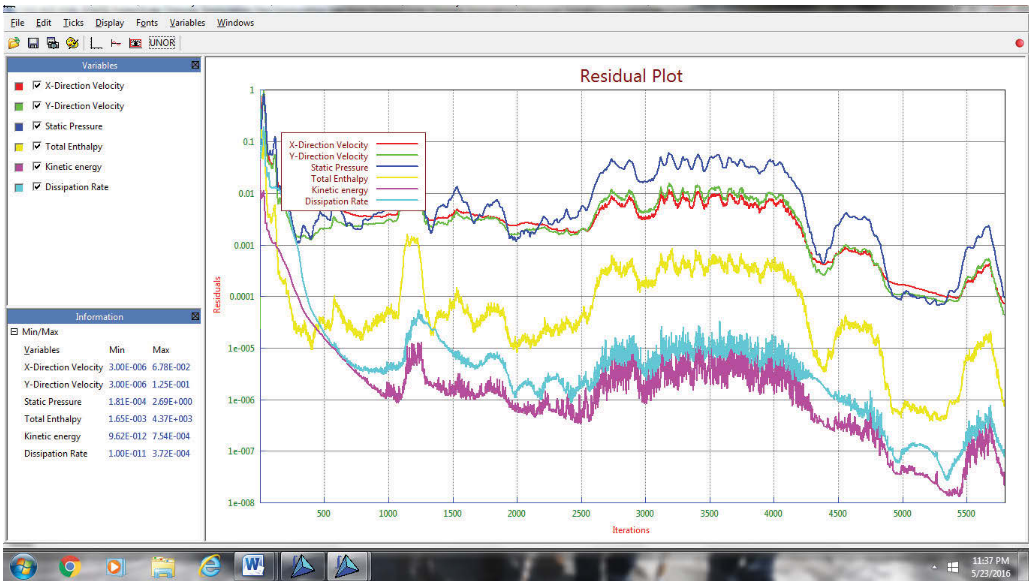

Figure 3.13: Normalized residual plot after convergence of model at desired level

Figure 3.14: Un-normalized residual plot after convergence of model at desired level

3.7. Grid Convergence Study

Regardless of the application, there is a need for control of numerical accuracy in Computational Fluid Dynamics (CFD). This need is just as critical in CFD work as it is in experiments where the experimenter is expected to provide estimates for the accuracy of his or her measurements. All CFD texts of any value stress this need. Grid Convergence Study is a way to authenticate the results of computations using some well-established methods.

3.7.1 Numerical Error

There could be a number of reasons which may contribute error in numerical simulation results. The best solution of the model is one which has been tested against illumination of these errors. The following numerical errors may be present in CFD simulations:

A) Discretization Error

Discretization error is the difference between the exact solution to the discrete equations and the exact solution to the continuous Partial Differential Equations. It is the most contributing numerical approximation error and is difficult to estimate in any modeling / simulation. The source of discretization error is the discretization of the domain and the Partial Differential Equations

Richardson Extrapolation method is being most widely used to estimate discretization error. Discretization error is estimated by changing the grids spacing of the model.

B) Round-off Error

A *round-off error* is the difference between the calculated approximate value and its exact mathematical value due to rounding. Round-off error may be present in numerical simulations due to the finite representation of data on digital computers. The accumulation of round-off error by repeated algebraic calculations in huge numbers can make it a significant source of error.

C) Iterative Error

Iterative errors may be present in a numerical solution with the use of iterative procedure is used to solve the discretized equations and is the difference between the solution at the current iteration and the exact solution to the discretized equations.

3.7.2 Verification and Validation of Computational Fluid Dynamics (CFD) Numerical Simulations

The verification and validation of results in any numerical simulation is essentially required to ensure that the results obtained are credible for decision making in design. Verification and validation determines the extent of errors in the simulation results. Up to a certain level, uncertainty and errors are acceptable but beyond that, modeling and simulation needs to be re-visited in order to contain errors within the desirable limits. Verification assessment examines for computer programming errors. Validation assessment determines if the computational simulation agrees with physical reality.

Grid convergence study or Grid convergence test or grid refinement study is normally used method to verify the solution results.

3.7.3 Spatial (Grid) Convergence

The analysis of Spatial Convergence of a simulation is a most commonly used method for determining the *ordered* discretization error in any CFD simulation. The basics of this method is to perform simulation on two or more successively finer grids and then analyze / compare solution results i.e. important parameters values at some key points.

By increasing the number of grid points, they become more refined and the number of cells in any flow domain of the model increases. This reduces the time step which produces more accurate results and ultimately, spatial and temporal discretization errors approaches to zero. But computer round-off errors remain there.

Methods to examine the spatial and temporal convergence of CFD simulations have been presented in the book by Roache. The method explained in above referred book is called Richardson's extrapolation which will also be explained in this chapter and same has been used by me during my research for Grid Convergence study.

3.7.4 Sequence of Grids Creation for a Grid Convergence Study

The simplest approach to generate the series of model with different number of grids is to start with the coarser or less number of grids. Starting with less number of grids and cells, it will be easy to get the convergence of the simulation with desired boundary conditions. It will also be easy to get the results in minimum possible time which will give the basic idea about the flows, temperature and pressure condition with the model. It will also give us the idea that we are going in the right direction.

In order to continue for grid convergence study, increase the number of grid points equally in each coordinate direction. In generating the fine grid, one can build in the **n** levels of coarser grids by making sure that the number of grid points in each coordinate direction satisfies the relation:

$$N = 2^n m + 1$$

Where **m** is an integer. For example, if two levels of fine grids are desired (i.e. coarse, medium, and fine grids) then the number of grid points in each coordinate direction must equal **4 m + 1**. The **m** may be different for each coordinate direction.

It is not essentially required to double the number of grid points in each coordinate direction to obtain the finer grid. *Non-integer* grid refinement or coarsening can be used. For example, the grid points may be increase to double in the start as the numbers of grid points are less and increasing to double will not have significant effect on the simulation / solution. But at later stages, the increase of grid points in double quantity may lead the solution out of range or solution may not converge at desired convergence criteria.

Non-integer grid refinement or coarsening will require the generation of a new grid. It is very important to maintain the same grid generation parameters as the original grid. If the same criteria is not followed for grid refinement, that may result in errors in solution / simulation results. Another important parameter which should be taken care during grid refinement is Grid Refinement Ration (r). And, r is defined as below:

$$r = \frac{h_2}{h_1}$$

Where h_1 and h_2 are uniform discrete cell lengths of fine grid and coarse grid respectively.

The grid refinement ratio should be a minimum of **r > = 1.1** to allow the discretization error to be differentiated from other error sources (iterative convergence errors, computer round-off errors, etc.).

3.7.5 Order of Grid Convergence

The order of grid convergence involves the behavior of the solution error defined as the difference between the discrete solution and the exact solution,

$$E = f(h) - f_{exact} = C\,h^p + \text{H.O.T.}$$

Where **C** is a constant, **h** is some measure of grid spacing, and **p** is the order of convergence. A "second-order" solution would have **p = 2**.

A CFD code uses a numerical algorithm that will provide a *theoretical order of convergence*, however, the boundary conditions, numerical models, and grid will reduce this order so that the *observed order of convergence* will likely be lower.

Neglecting higher-order terms and taking the logarithm of both sides of the above equation results in:

$$\text{Log}(E) = \log(C) + p\log(h)$$

The order of convergence **p** can be obtained from the slope of the curve of **log(E)** versus **log(h)**. If such data points are available, the slope can be read from the graph or the slope can be computed from a least-squares fit of the data. The least-squares will likely be inaccurate if there are only a few data points.

A more direct evaluation of **p** can be obtained from three solutions using a constant grid refinement ratio **r**,

$$P = \ln\left(\frac{f_3 - f_2}{f_2 - f_1}\right) / \ln(T)$$

The order of accuracy is determined by the order of the leading term of the truncation error and is represented with respect to the scale of the discretization, **h**. The local order of accuracy is the order for the stencil representing the discretization of the equation at one location in the grid. The global order of accuracy considers the propagation and accumulation of errors outside the stencil. This propagation causes the global order of accuracy to be, in general, one degree less than the local order of accuracy. The order of accuracy of the boundary conditions can be one order of accuracy lower than the interior order of accuracy without degrading the overall global accuracy.

3.7.6 Richardson Extrapolation Method for Grid Convergence Test

The best known way to demonstrate grid convergence is to repeat a computation with same model but with increased number of grid points and then compare the two solutions. Using results of simulation with two different grids, techniques such as Richardson Extrapolation (Roache 1998) can be used. Richardson Extrapolation is the discretization error estimator and is a recovery method. Discretization error is estimated by varying the grid spacing uniformly in all directions. This method is very simple to implement and should be used whenever possible.

A simulation will yield a quantity **f** that can be expressed in a general form by the series expansion:

$$f = f_{h=0} + g_1 h + g_2 h^2 + g_3 h^3 + \dots$$

where **h** is the grid spacing and the functions g_1, g_2, and g_3 are independent of the grid spacing. The quantity **f** is considered "second-order" if $g_1 = 0.0$. The $f_{h=0}$ is the continuum value at zero grid spacing.

If one assumes a second-order solution and has computed **f** on two grids of spacing h_1 and h_2 with h_1 being the finer (smaller) spacing, then one can write two equations for the above expansion, neglect third-order and higher terms, and solve for $f_{h=0}$ to estimate the continuum value,

$$Fh_{=0} \cong f_1 + \left(\frac{f_1 - f_2}{T^2 - f_1} \right)$$

The Richardson extrapolation can be generalized for a **p-th** order methods and **r**-value of grid ratio (which does not have to be an integer) as:

$$Fh_{=0} \cong f_1 + \left(\frac{f_1 - f_2}{T^p - f_1} \right)$$

Traditionally, Richardson extrapolation has been used with grid refinement ratios of **r = 2**. Thus, the above equation simplifies to:

$$f_{h=0} \cong \frac{4}{3} f_1 - \frac{1}{3} f_2$$

In theory, the above equations for the Richardson extrapolation will provide a fourth-order estimate of $f_{h=0}$, if f_1 and f_2 were computed using exactly second-order methods. Otherwise, it will be a third-order estimate.

In general, we will consider $\mathbf{f_{h=0}}$ to be **p+1** order accurate. Richardson extrapolation can be applied for the solution at each grid point, or to solution functionals, such as pressure recovery or drag. This assumes that the solution is globally second-order in addition to locally second-order and that the solution functionals were computed using consistent second-order methods. Other cautions with using Richardson extrapolation (non-conservative, amplification of round-off error, etc...) are discussed in the book by Roache.

For our purposes we will assume **f** is a solution functional (i.e. pressure recovery). The $\mathbf{f_{h=0}}$ is then as an estimate of **f** in the limit as the grid spacing goes to zero. One use of $\mathbf{f_{h=0}}$ is to report the value as an improved estimate of $\mathbf{f_1}$ from the CFD study, however, one has to understand the caveats mentioned above that go along with that value.

The other use of $\mathbf{f_{h=0}}$ is to obtain an estimate of the discretization error that bands **f** obtained from the CFD. This use will now be examined.

The difference between $\mathbf{f_1}$ and $\mathbf{f_{h=0}}$ is one error estimator, however, this requires consideration of the caveats attached to $\mathbf{f_{h=0}}$.

We will focus on using $\mathbf{f_1}$ and $\mathbf{f_2}$ to obtain an error estimate. Examining the generalized Richardson extrapolation equation above, the second term on the right-hand side can be considered to be an error estimator of $\mathbf{f_1}$. The equation can be expressed as:

$$A_1 = E_1 + O(h^{p+1}, E_1^2)$$

Where $\mathbf{A_1}$ is the actual fractional error defined as:

$$A_1 = (f_1 - f_{h=0}) / f_{h=0}$$

And $\mathbf{E_1}$ is the estimated fractional error for $\mathbf{f_1}$ defined as:

$$E_1 = \frac{\varepsilon}{T^p - 1}$$

Or the expression may be written as:

$$E_1 = \frac{\varepsilon}{r^2 - 1}$$

where the grid refinement ratio is:

$$\mathbf{r = h_2 / h_1}$$

where the relative error is defined as:

$$\varepsilon = \frac{f_2 - f_1}{f_1}$$

This quantity should not be used as an error estimator since it does not take into account **r** or **p**. This may lead to an underestimation or overestimation of the error. One could make this quantity artificially small by simply using a grid refinement ratio **r** close to 1.0.

The estimated fractional error $\mathbf{E_1}$ is an *ordered* error estimator and a good approximation of the discretization error on the fine grid if $\mathbf{f_1}$ and $\mathbf{f_2}$ were obtained with good accuracy (i.e. $\mathbf{E_1 < 1}$). The value of $\mathbf{E_1}$ may be meaningless if $\mathbf{f_1}$ and $\mathbf{f_{h=0}}$ are zero or very small relative to $\mathbf{f_2-f_1}$. If such is the case, then another normalizing value should be used in place of $\mathbf{f_1}$.

3.7.7 Grid Convergence Index (GCI)

As noted by Roache (1998), Richardson extrapolation is not limited to doubling or halving the grid-point spacing. For the generalized theory of Richardson extrapolation, we write:

$$Ø_{exact} \approx Ø_h + \frac{Ø_h - Ø_{rh}}{r^p - 1}$$

where p is the order of the finite-difference scheme and r is the grid-refinement ratio. By definition, if we halve the size of the grid-point spacing, then r = ½ and doubling the size corresponds to r = 2.

It is a straightforward matter to use Richardson extrapolation on two grids that differ in cell size by a factor of 2 because the grid-point locations on the coarse grid are identical to those on the fine grid at every other point. Nevertheless, the method applies to any value of r. Since the solutions have to be compared at the same physical point, interpolation is needed on one of the grids to establish solution values at the same points for comparison.

Building on Richardson extrapolation, Roache (1998) has developed the Grid Convergence Index (GCI) to help establish a uniform method for reporting the estimated error in a computation. By definition,

$$GCI = Fs \frac{|\epsilon_h|}{r^p - 1}$$

Where,

$$\epsilon_h = \frac{Ø_h - Ø_{rh}}{Ø_h}$$

The quantity Eh is the fractional error for the grid with spacing h. If two grids are used, Roache recommends using Fs 3. This will provide a conservative estimate of solution error for virtually all fluid-flow problems. If three different grids are used, Fs 1.25 is appropriate. In the latter case, the three-grid sequence of computations can be used to first establish the actual order of the method, p. Then, the index can be computed to provide a measure of how accurate the solutions on the finest grids are.

The GCI is especially useful as a measure of how accurately key quantities such as lift and drag coefficients, skin friction and surface-pressure coefficients have been computed. That is, its use is not confined to an overall measure of solution errors at specific grid points. It can be applied to any key feature of the solution that is of particular interest.

To determine the order of a finite-difference method, we observe that if it is pth_order accurate, then the solution error will change according to:

$$E_h \approx Ch^p \qquad \text{where} \qquad C = \text{Constant}$$

The value of p is the slope of E_h as a function of h on a log-log plot. At least three grids are needed to accurately determine p. It is simplest if the three grids have been done with constant r. That is, if the finest grid has spacing h, the next to finest would have rh and the coarsest would have r^2h.

Normally expressed as a percent, the GCI provides an excellent estimate of the error band that can be placed on a fine-grid solution. Roache suggests a grid convergence index **GCI** to provide a consistent manner in reporting the results of grid convergence studies and perhaps provide an error band on the grid convergence of the solution. The **GCI** can be computed using two levels of grid, however, three levels are recommended in order to accurately estimate the order of convergence and to check that the solutions are within the asymptotic range of convergence.

3.7.8 Near-Wall Grid-Point Spacing

There is another grid-related factor affecting solution accuracy. In order to resolve thin viscous layers, for example, highly stretched grids are normally used. Conventional central-difference approximations are only first-order accurate on such a grid, and care must be taken to account for this. Also, the location of the grid point nearest the surface has a nontrivial effect on the accuracy of skin friction and surface heat flux. Wilcox (1989), for example, has found that grid-insensitive computations using wall functions that account for pressure gradient, can be obtained with block-implicit methods provided

$$\mathbf{10 < Y_2^+ < 100 \qquad (wall\ functions)}$$

Where $\mathbf{Y_2^+}$ is the sublayer-scaled value of the first grid point above the surface. This range appears to hold for boundary-layer computations as well [Chambers and Wilcox (1977)], again provided pressure gradient is accounted for. When turbulence-model equations are integrated through the viscous sublayer, many researchers have shown that it is imperative to require $\mathbf{Y_2^+} < 1$. For shock separated flows, particularly at hypersonic speeds, Marvin and Huang (1996) recommend the more-stringent condition $\mathbf{Y_2^+} < 0.3$. When these limits are not adhered to, solution errors throughout the boundary layer generally are large.

3.7.9 Grid Convergence Study for Present Research

Grid Convergence test was employed to make sure that grids pattern employed for this simulation are adequate. More than 13 models were simulated with increased number of grid points and cells. Starting from 236 numbers of cells, the number of cells increased to 409561 numbers. Each time, the convergence was achieved up to the desired level (1.0×10^{-04}) and the results were analyzed.

To study the grid convergence, two points at different locations were taken and the important parameters at these points were noted. The percentage differences between values of same parameters in two simulations were analyzed. The process remains continues by making new models with increased number of cells unless grid convergence was achieved. More than 13 models were simulated by increasing number of grid points / cells.

The data table 3.3 below has been given to give idea about the number of simulations carried out with increasing number of cells and what type of data has been collected against these simulations for further analysis. It is also giving the overview that the data has been collected at three different locations against each simulation.

The table below shows a comparison of data against all these simulated models.

Table: 3.3 (a) : Table for Comparison of Simulation Data of 2D Models – Values Taken at Three Different Locations

Room Length	Room Width	Chimney Length	2D Model-1	2D Model-2	2D Model-3	2D Model-4	2D Model-5	2D Model-6	2D Model-7
3 meter	3 meter	2.12 meter							
Chimney Angle	Inlet / Outlet Opening								
45^o	0.3 meter								
Nodes		No.	275	1110	4460	17880	70900	102871	124511
Faces		No.	510	2139	8757	35433	141145	204931	248129
Cells		No.	236	1030	4298	17554	70246	102061	123619
In Flow		KG/S	0.172307	0.072841	0.0256465	0.0189446	0.0173202	0.0176459	0.0174705
Out Flow		KG/S	0.128382	0.0728886	0.02518	0.0189442	0.0173211	0.0176456	0.0174697
Max. Vel.		Met/S	2.431	0.5993	0.7468	0.9536	1.072	0.9973	1.037
Max. Temp.		K	541.4	405.8	382.7	389.1	398.4	396.1	397.2
Converged at Iteration			219	324	408	942	841	2484	2921
Data Locations									
At Room Inlet	Location	Variable							
X (meter)	0.1	U (m/s)	0.516571	0.212064	0.0692905	0.0466684	0.033104	0.0423587	0.0417772
Y (meter)	0.15	V (m/s)	-0.00148845	-0.0281994	-0.00012777	0.00077734	0.00713043	0.00123012	0.00121418
		VM (m/s)	0.516575	0.213999	0.069291	0.0466748	0.0338633	0.0423765	0.0417949
		P (N/m^2)	-0.00946235	-0.0045425	-0.000164723	-2.68E-05	4.82E-06	-4.29E-05	-4.21E-05
		Pt (N/m^2)	0.1411499	0.0223406	0.00262946	0.00123921	0.000671042	0.00100019	0.000972583
		T (K)	297	296.999	297	297	297	297	297
At Chimney Inlet									
X (meter)	2.85	U (m/s)	-0.0526889	-0.0580289	-0.00977815	-0.00185965	-5.41E-05	-0.00326516	-0.00322321
Y (meter)	2.8	V (m/s)	0.366939	0.265017	0.0730493	0.0442726	0.0310729	0.0350496	0.0342625
		VM (m/s)	0.376164	0.271314	0.0737162	0.0443118	0.031073	0.0352031	0.0344157
		P (N/m^2)	-0.0224751	-0.0117915	-0.00103612	6.74E-05	6.17E-05	-5.38E-05	-5.88E-05
		Pt (N/m^2)	0.067008	0.0311809	0.00214097	0.00120771	0.000622468	0.000667466	0.0006308
		T (K)	297.055	296.998	297.006	297	297	297	297
At Chimney Outlet									
X (meter)	1.29	U (m/s)	-0.00704094	-0.236495	-0.440796	-0.379393	-0.340003	-0.346723	-0.347941
Y (meter)	4.43	V (m/s)	0.0212206	0.262122	0.448033	0.373096	0.334733	0.33951	0.341946
		VM (m/s)	0.0223582	0.353041	0.62915	0.532131	0.477126	0.485267	0.487842
		P (N/m^2)	0.0515751	-0.00449052	-0.00339108	-0.0019918	-0.00169078	-0.00171347	-0.00178435
		Pt (N/m^2)	0.0863536	0.304846	0.272988	0.188945	0.135171	0.14179	0.147568
		T (K)	425.144	333.216	315.876	309.29	307.17	307.361	307.68

Table: 3.3 (b) : Table for Comparison of Simulation Data of 2D Models – Values Taken at Three Different Locations

Model Description			2D Model-8	2D Model-9	2D Model-10	2D Model-11	2D Model-12	2D Model-13	2D Model-14
Nodes		No.	210489	231347	263283	297436	333510	367889	411183
Faces		No.	419643	461477	525267	593493	665559	734244	820743
Cells		No.	209242	230131	261985	296058	332050	366356	409561
In Flow		KG/S	0.0171248	0.0170668	0.0169949	0.0169239	0.0168599	0.0168176	0.0168226
Out Flow		KG/S	0.0171249	0.017067	0.0169949	0.016923	0.0168588	0.016818	0.0168226
Max. Vel.		Met/S	1.089	1.089	1.085	1.093	1.108	1.117	1.122
Max. Temp.		K	399.6	400	400.4	400.8	401.2	401.4	401.6
Converged at Iteration			5794	6024	7512	6650	10963	8506	45098
Data Locations									
At Room Inlet	Location	Variable							
X (meter)	0.1	U (m/s)	0.0404898	0.0406924	0.0405157	0.0403307	0.0400564	0.0401073	0.0348766
Y (meter)	0.15	V (m/s)	0.00231009	0.00175689	0.00173421	0.00173538	0.00170333	0.0017005	0.00913418
		VM (m/s)	0.0405557	0.0407303	0.0405528	0.040368	0.0400926	0.0401433	0.0360529
		P (N/m^2)	-3.09E-05	-3.59E-05	-3.56E-05	-3.59E-05	-3.48E-05	-3.50E-05	9.90E-06
		Pt (N/m^2)	0.000924864	0.000927881	0.000919844	0.000910884	0.000899077	0.000901159	0.000765923
		T (K)	297	297	297	297	297	297	297
At Chimney Inlet									
X (meter)	2.85	U (m/s)	-0.00207105	-0.00273522	-0.00273531	-0.002895	-0.00277202	-0.00291304	-0.000790831
Y (meter)	2.8	V (m/s)	0.0337732	0.0339509	0.0337657	0.0341524	0.033576	0.0339649	0.031925
		VM (m/s)	0.0338447	0.0340718	0.033888	0.0342867	0.0337025	0.0341024	0.0319349
		P (N/m^2)	-8.10E-06	-2.86E-05	-3.02E-05	-3.13E-05	-3.47E-05	-3.22E-05	8.26E-05
		Pt (N/m^2)	0.00065778	0.000646913	0.000638128	0.000652835	0.000626531	0.000644756	0.000674911
		T (K)	297	297	297	297	297	297	297
At Chimney Outlet									
X (meter)	1.29	U (m/s)	-0.338461	-0.334596	-0.335445	-0.331965	-0.330895	-0.329771	-0.327653
Y (meter)	4.43	V (m/s)	0.332922	0.328953	0.329927	0.326512	0.325453	0.324318	0.322179
		VM (m/s)	0.474757	0.469216	0.470506	0.46563	0.464125	0.462527	0.459517
		P (N/m^2)	-0.00171278	-0.0016727	-0.00169519	-0.00167183	-0.00167405	-0.00166432	-0.00161699
		Pt (N/m^2)	0.136116	0.129588	0.132756	0.128387	0.127603	0.126908	0.123028
		T (K)	307.288	307.033	307.189	307.032	307.027	307.004	306.819

In order to further explain above data table, the graphs in figures 3.14a, 3.14b and 3.14c have been drawn which show change of flow through inlet and outlet, maximum temperature and maximum velocity with increasing number of cells:

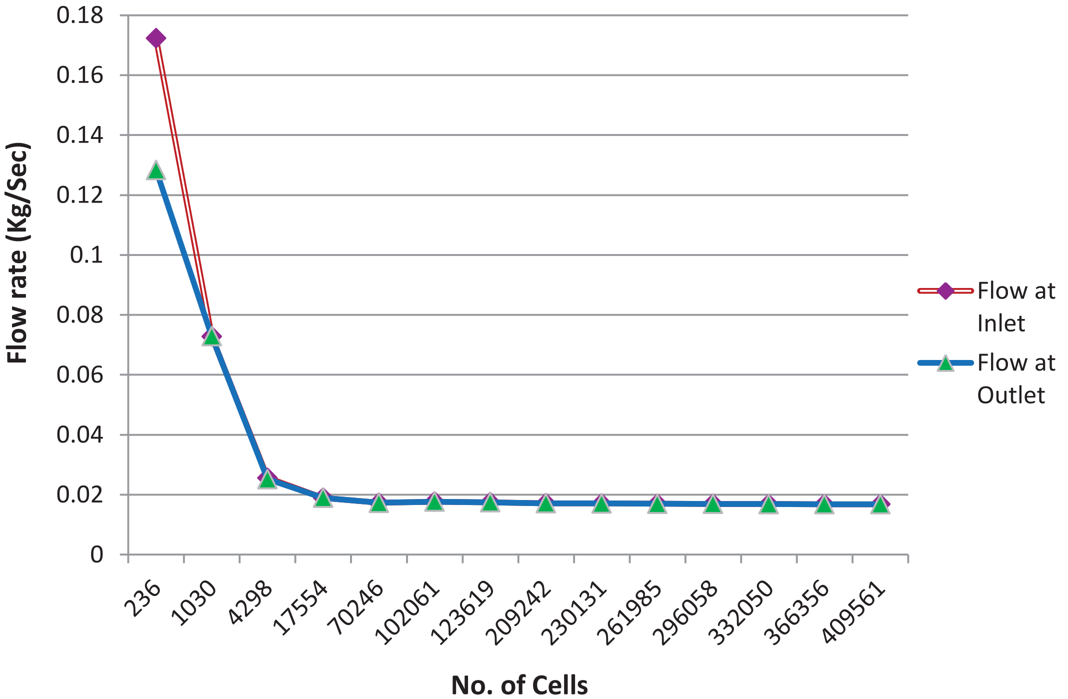

Figure:3.14a: Showing change in flow rate at inlet and outlet of the model with increase in number of cells

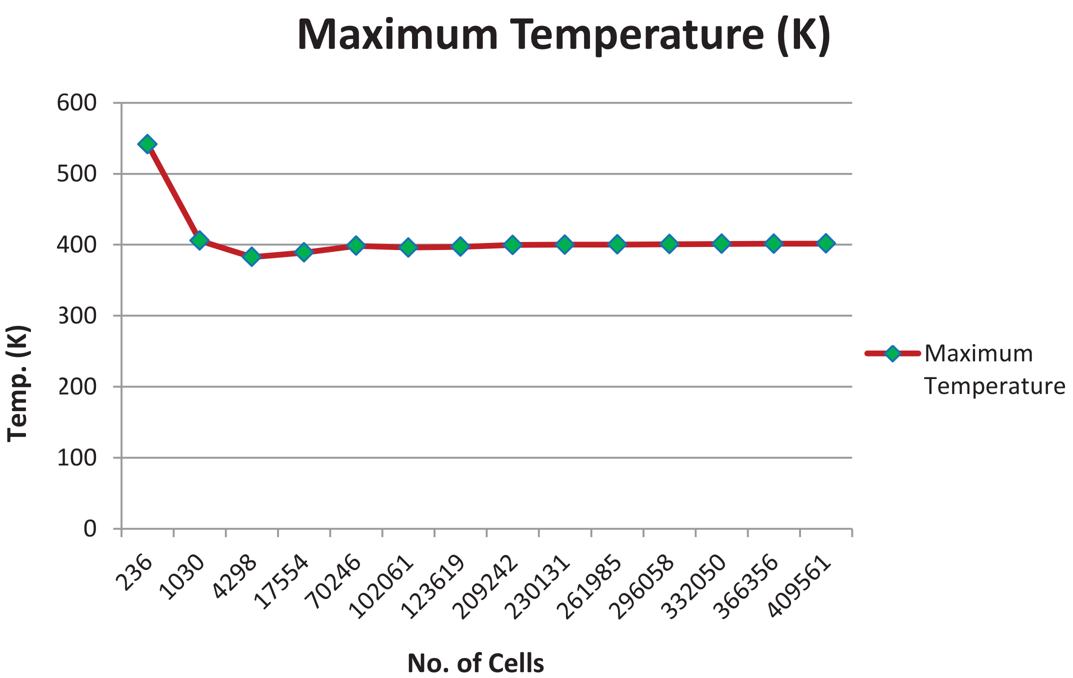

Figure:3.14b: Showing change in temperature with increase in number of cells

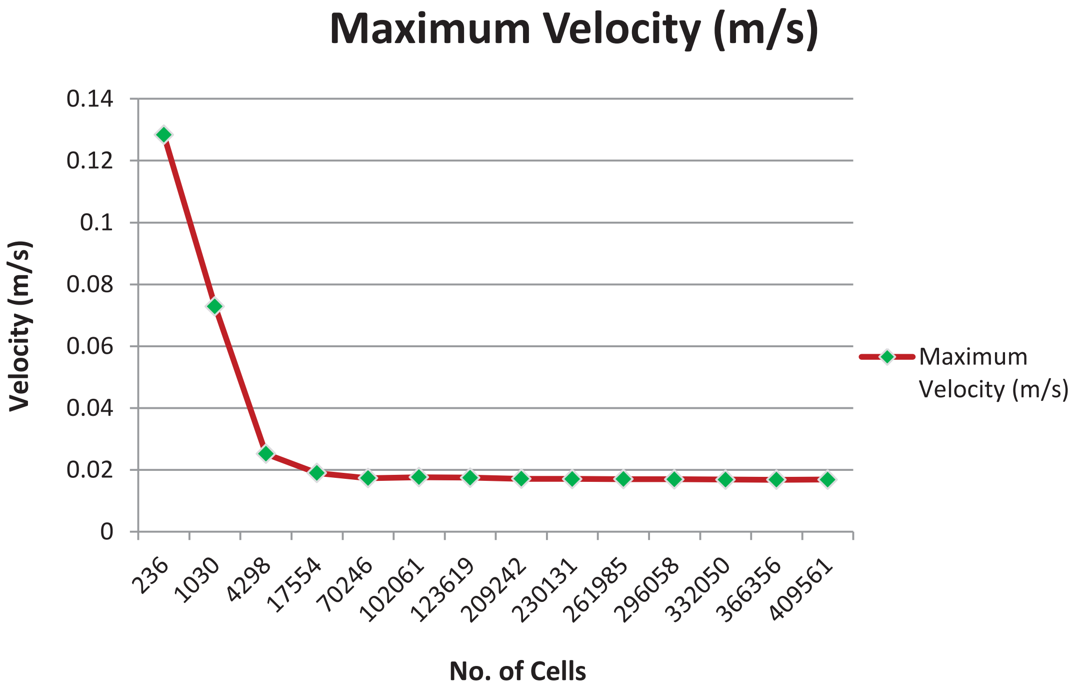

Figure:3.14c: Showing change in velocity with increase in number of cells

3.7.10 Solution Convergence and Mass Flow Rate Analysis

The above Two-Dimensional models have been simulated using physical parameters explained previously. The convergence criterion was kept at 0.0001 for each simulation and acceptable mass flow rate balance has been achieved in each model. The table below is explaining the mass flow rate balance achieved in each simulation of models presented in Table 3.3:

Model	No. of Cells	Flow Rate at Inlet (Kg/sec)	Flow Rate at Outlet (Kg/sec)	Difference of Inlet and Outlet (Kg/sec)
2D Model-2	1030	0.072841	0.0728886	4.76E-05
2D Model-3	4298	0.0256465	0.02518	0.0004665
2D Model-4	17554	0.0189446	0.0189442	4E-07
2D Model-5	70246	0.0173202	0.0173211	9.00E-07
2D Model-6	102061	0.0176459	0.0176456	3E-07
2D Model-7	123619	0.0174705	0.0174697	8E-07
2D Model-8	209242	0.0171248	0.0171249	1.00E-07
2D Model-9	230131	0.0170668	0.017067	2.00E-07
2D Model-10	261985	0.0169949	0.0169949	0
2D Model-11	296058	0.0169239	0.016923	9E-07
2D Model-12	332050	0.0168599	0.0168588	1.1E-06
2D Model-13	366356	0.0168176	0.016818	4.00E-07
2D Model-14	409561	0.0168226	0.0168226	0

Through above tabulated analysis, it is clear that after achieving convergence as per defined criteria, balance of mass is well verified.

The data of Model number 7 and Model number 9 against which grid convergence has been achieved are tabulated below:

Table: 3.4: Simulation Data of 2D Model-7 at Three Different Locations

Room Length	Room Width	Chimney Height / Length	
3 m	3 m	1.5 / 2.12 m	
Chimney Angle	Inlet / Outlet Opening		
45	0.3 meter		
Nodes		No.	210489
Faces		No.	419643
Cells		No.	209242
In Flow		KG/S	0.0171248
Out Flow		KG/S	0.0171249
Maximium Velocity		Met/S	1.089
Maximum Temp.		K	399.6
Converged at Iteration			5794

Simulation Data of 2D Model (Model-7 with Air Inlet at Bottom of the Side Wall)											
At Center of Room Air Inlet				**At Chimney Inlet**				**At Chimney Outlet**			
Coordinates of Location		Variable	Values	Coordinates of Location		Variable	Values	Coordinates of Location		Variable	Values
X (meter)	0.1	U (m/s)	0.04049	X (meter)	2.85	U (m/s)	-0.00207	X (meter)	1.29	U (m/s)	-0.33846
Y (meter)	0.15	V (m/s)	0.00231	Y (meter)	2.8	V (m/s)	0.033773	Y (meter)	4.43	V (m/s)	0.332922
		VM (m/s)	0.040556			VM (m/s)	0.033845			VM (m/s)	0.474757
		P (N/m^2)	-3.1E-05			P (N/m^2)	-8.1E-06			P (N/m^2)	-0.00171
		Pt (N/m^2)	0.000925			Pt (N/m^2)	0.000658			Pt (N/m^2)	0.136116
		T (K)	297			T (K)	297			T (K)	307.288

Table: 3.5: Simulation Data of 2D Model-9 at Three Different Locations

Room Length	Room Width	Chimney Height / Length	
3 m	3 m	1.5 / 2.12 m	
Chimney Angle	Inlet / Outlet Opening		
45	0.3 meter		
Nodes		No.	263283
Faces		No.	525267
Cells		No.	261985
In Flow		KG/S	0.016995
Out Flow		KG/S	0.016995
Maximium Velocity		Met/S	1.085
Maximum Temp.		K	400.4
Converged at Iteration			7512

Data & Locations (Model-9)											
At Center of Room Air Inlet				At Chimney Inlet				At Chimney Outlet			
Coordinates of Location		Variable	Values	Coordinates of Location		Variable	Values	Coordinates of Location		Variable	Values
X	0.1	U	0.040516	X	2.85	U	-0.00274	X	1.29	U	-0.33545
Y	0.15	V	0.001734	Y	2.8	V	0.033766	Y	4.43	V	0.329927
		VM	0.040553			VM	0.033888			VM	0.470506
		P	-3.6E-05			P	-3E-05			P	-0.0017
		Pt	0.00092			Pt	0.000638			Pt	0.132756
		T	297			T	297			T	307.189

The table below is showing analysis of a selected data taken at two different points for grid convergence study:

Table: 3.6 : Comparison of Velocity Magnitudes and Temperatures at two selected points for two different cases

Variable	Case -7 (G1)	Case -9 (G2)	Difference (%age)
Grid Patterns (Number of Cells)	209242	261985	25
Velocity Magnitude (m/s) at room inlet	0.0405557	0.0405528	0.01
Velocity Magnitude (m/s) at chimney inlet	0.0338447	0.033888	0.13
Temperature (K) at middle of the chimney near wall	383.652	384.484	0.22
Temperature (K) just before chimney outlet	307.288	307.189	0.03

From the above data, it is cleared that the difference of velocity magnitude at same location i.e. room air inlet opening between two different cases is only 0.01% against 25% increased number of cells. To study grid independency more rigorously, another location was taken at chimney inlet. The difference of velocity magnitude at this location between above two cases is only 0.13%. Also, the difference of temperature, just before the chimney outlet, between two cases is only 0.03%. The above results are showing good grid convergence.

By using Generalization Richardson 2nd order accurate Extrapolation, the estimated fractional error (E_1) which is an ordered error estimator for the fine grid solution (f_1), the coarse grid solution (f_2), and r-value of grid ration is as follows [11].

$$E_1 = \frac{\epsilon}{r^2 - 1}$$

whereϵ is defined below:

$$\epsilon = \frac{f_2 - f_1}{f_1}$$

Here, f_1 and f_2 are two separate discrete solutions which have been considered as the studied parameters (velocity magnitude or temperature).

And, r is the grid refinement ratio which is defined as below:

$$r = \frac{h_2}{h_1}$$

Where h_1 and h_2 are uniform discrete cell lengths of fine grid and coarse grid respectively.

The Table-4.2 shows the amount of estimated fractional error, using the Generalization of Richardson Extrapolation, for velocity magnitude and temperature at two different selected points.

Table: 3.7: Estimated fractional error by using Generalization of Richardson Extrapolation for velocity magnitude and temperature at two different selected points

Grid Patterns (Number of Cells)	Selected Point 1		Selected Point 2	
	E_1 for Velocity Magnitude	E_1 for Temperature	E_1 for Velocity Magnitude	E_1 for Temperature
G1 (209242)	0.000276	0.006075	0.003590	0.0008285
G2 (261985)				

As it is evident from the above table and graph that by increasing the number of grid cells, the amount of estimated fractional error E_1 for velocity and temperature in the two selected points are much less than 1 (E_1<< 1) which verifies the reasonable accuracy of the solutions.

Based on above grid convergence study, Model number 7 was selected for further analysis with reference to change in room air inlet location.

3.8 Effect of Room Air Inlet Locations

The change of room air inlet location significantly effects air flow rate and pattern in a room. In order to study this affect, following three models, with different room inlet location, were considered for further analysis and comparison of results.

The purpose was to compare air flow rate and flow patterns with changing inlet location in order to suggest best location for room air inlet to get maximum air flow rate.

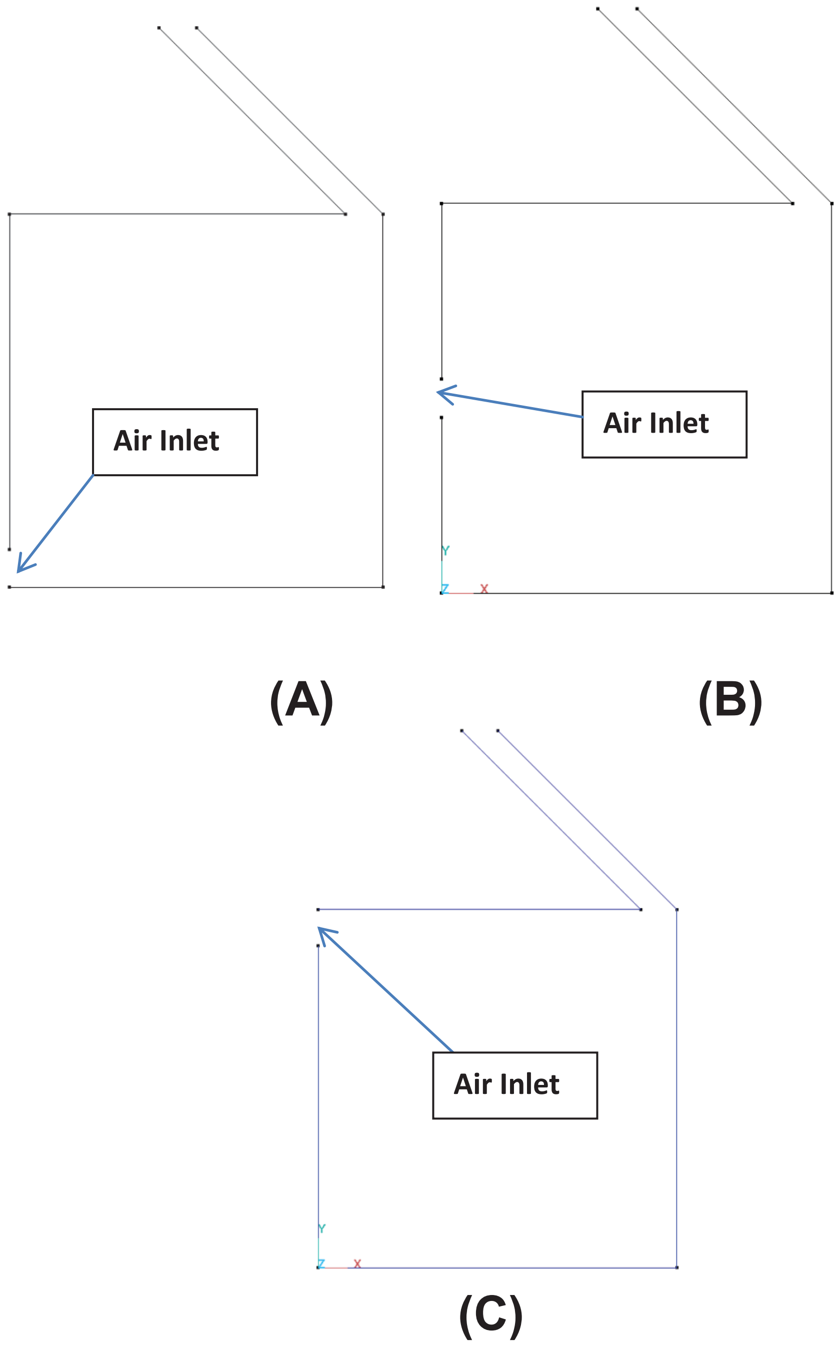

Figure 3.15: Model for different inlet opening locations. A) Inlet at bottom of the wall B) Inlet at middle of the wall C) Inlet at top of the room wall.

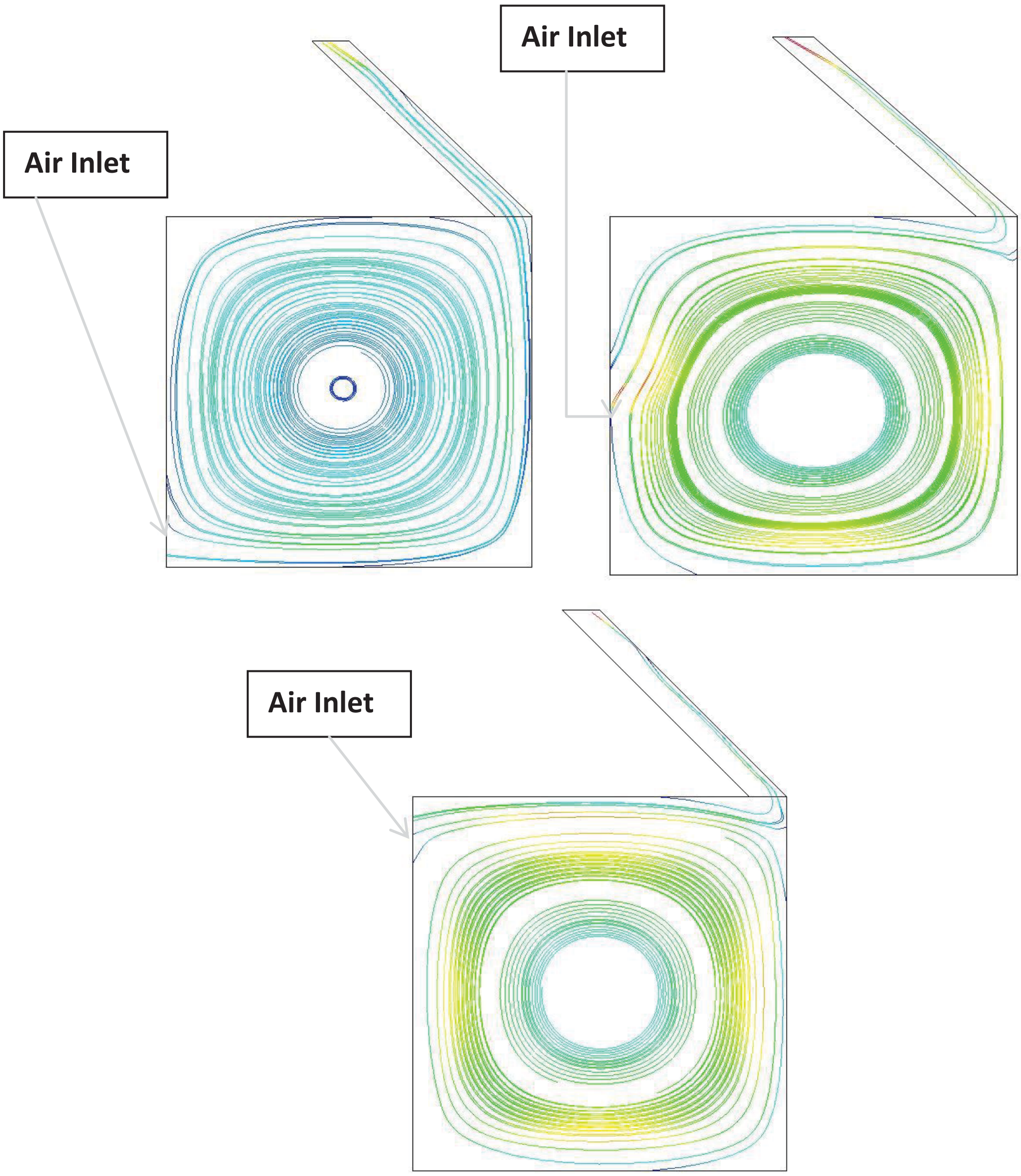

Figure 3.16: Air Flow Pattern after Simulation of Basic Model with different inlet opening locations analyzed in CFD View

3.8.1 Room with Air Inlet at Bottom of the Wall

Below are the simulation results of a basic model with room air inlet location at bottom of the side wall and which successfully fall in the criteria of grid convergence test i.e. Model-7. The graphical and numerical results obtained against this simulation are presented below.

Table: 3.8 : Simulation Data of 2D Model-7 with Room inlet opening at Bottom of the side wall

Room Length	Room Width	Chimney Height / Length	
3 m	3 m	1.5 / 2.12 m	
Chimney Angle	Inlet / Outlet Opening		
45	0.3 meter		
Nodes		No.	210489
Faces		No.	419643
Cells		No.	209242
In Flow		KG/S	0.0171248
Out Flow		KG/S	0.0171249
Maximium Velocity		Met/S	1.089
Maximum Temp.		K	399.6
Converged at Iteration			5794

Simulation Data of 2D Model (Model-7 with Air Inlet at Bottom of the Side Wall)											
At Center of Room Air Inlet				At Chimney Inlet				At Chimney Outlet			
Coordinates of Location		Variable	Values	Coordinates of Location		Variable	Values	Coordinates of Location		Variable	Values
X (meter)	0.1	U (m/s)	0.04049	X (meter)	2.85	U (m/s)	-0.00207	X (meter)	1.29	U (m/s)	-0.33846
Y (meter)	0.15	V (m/s)	0.00231	Y (meter)	2.8	V (m/s)	0.033773	Y (meter)	4.43	V (m/s)	0.332922
		VM (m/s)	0.040556			VM (m/s)	0.033845			VM (m/s)	0.474757
		P (N/m^2)	-3.1E-05			P (N/m^2)	-8.1E-06			P (N/m^2)	-0.00171
		Pt (N/m^2)	0.000925			Pt (N/m^2)	0.000658			Pt (N/m^2)	0.136116
		T (K)	297			T (K)	297			T (K)	307.288

The table above is showing a glimpse of data which has been collected after simulation for analysis purpose. The data has been taken at three different locations against for the purpose of Grid Convergence Study.

The first measurement point against above model has been taken at following axis locations:

1) **X = 0.1 meter**
   Y = 0.15 meter

The above location has been taken just after the entrance of the room inlet. This location is 0.1 meter away from entrance in X-Axis direction and at the height of 0.15 meter from the floor of the room. This position comes out to be at the center of the room inlet opening.

The second measurement point has been taken at following axis locations:

2) X = 2.85 meter
Y = 2.80 meter

The above location has been taken at the entrance of the solar chimney inlet. This location is 2.85 meter away from entrance in X-Axis direction and at the height of 2.8 meter from the floor of the room.

The third measurement point has been taken at following axis locations:

3) X = 1.29 meter
Y = 4.43 meter

The above location has been taken just before solar chimney outlet. This location is 1.29 meter away in X-Axis direction and at the height of 4.43 meter from the floor of the room. This position has been 0.07 meter before the solar chimney outlet and near the heated wall of the solar chimney in order to measure change in temperature due to heated wall.

All above mentioned data measurement locations has been shown in figure 3.17 below:

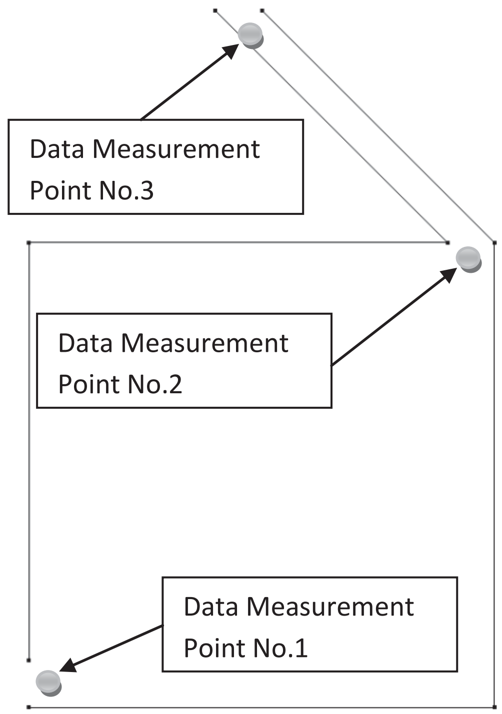

Figure 3.17: Model with inlet opening at bottom of the side wall – Showing location of data measurement points for analysis

The following important parameters which are considered important in the study of natural ventilation through solar chimney have been noted at each measurement location:

U---- Air velocity in horizontal direction (m/s)
V ---- Air velocity in vertical direction (m/s)
VM ---- Air velocity Magnitude at that location (m/s)
P ---- Static pressure at that location (N/m^2)
P_t ---- Total pressure at that location (N/m^2)
T ---- Air Temperature at that location (K)

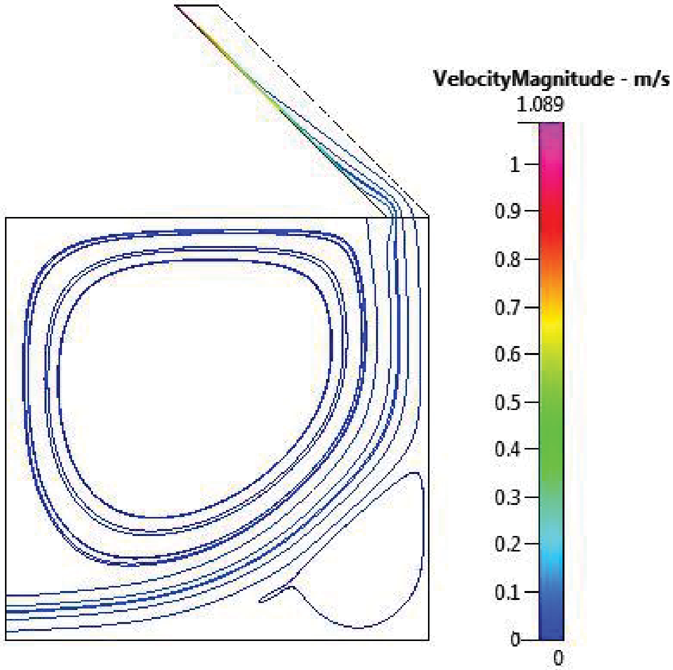

Figure 3.18: Model with inlet opening at bottom of the side wall – Showing velocity Magnitude after simulation.

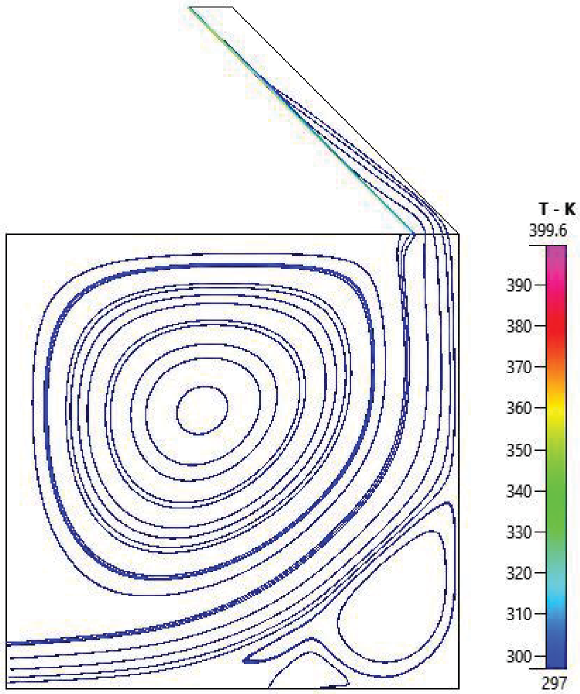

Figure 3.19: Model with inlet opening at bottom of the side wall – Showing Temperature profile after simulation.

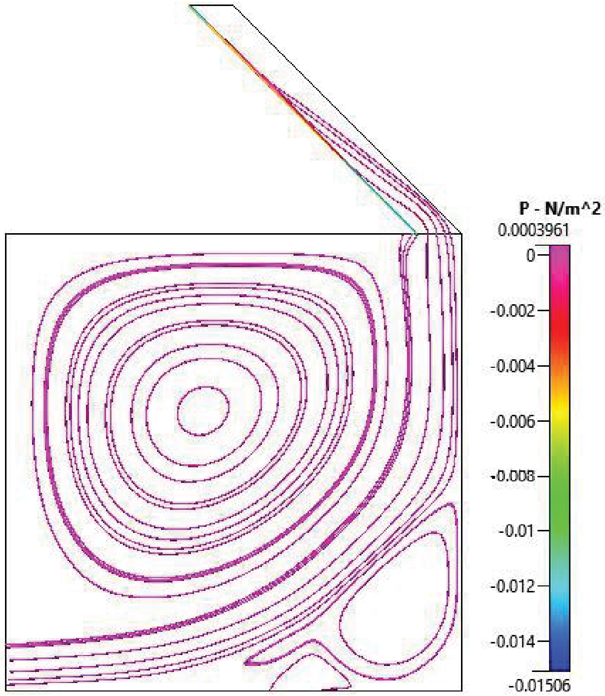

Figure 3.20: Model with inlet opening at bottom of the side wall – Showing Pressure profile after simulation.

3.8.2 Room with Air Inlet at Middle of the Wall

A new model with room air inlet location at middle of the wall was made having the same number of cells where grid convergence was achieved i.e. Model-7. The Model was simulated using the same parameters in order to compare results. The graphical and numerical results obtained against this simulation are presented below.

Table: 3.9 : Simulation Data of 2D Model-7 with Room inlet opening at Middle of the side wall

Room Length	Room Width	Chimney Height / Length	
3 m	3 m	1.5 / 2.12 m	
Chimney Angle	Inlet / Outlet Opening		
45	0.3 meter		
Nodes		No.	210402
Faces		No.	419643
Cells		No.	209242
In Flow		KG/S	0.0665684
Out Flow		KG/S	-0.065973
Maximium Velocity		Met/S	0.765692
Maximum Temp.		K	360.338
Converged at Iteration			21861

Simulation Data of 2D Model (Model-7 with Air Inlet at Middle of the Side Wall)											
At Center of Room Air Inlet				At Chimney Inlet				At Chimney Outlet			
Coordinates of Location		Variable	Values	Coordinates of Location		Variable	Values	Coordinates of Location		Variable	Values
X	0.1	U	0.096555	X	2.85	U	0.076824	X	1.29	U	-0.36245
Y	1.5	V	0.020293	Y	2.8	V	0.023331	Y	4.43	V	0.356989
		VM	0.098674			VM	0.080312			VM	0.508731
		P	6.15E-04			P	0.010825			P	-0.1908
		Pt	6.27E-03			Pt	0.014578			Pt	0.131249
		T	297.002			T	297.001			T	309.274

The table above is showing a glimpse of data which has been collected after simulation for analysis purpose. The data has been taken at three different locations against for the purpose of Grid Convergence Study.

The first measurement point against above model has been taken at following axis locations:

1) **X = 0.1 meter**
   Y = 1.5 meter

The above location has been taken just after the entrance of the room inlet. This location is 0.1 meter away from entrance in X-Axis direction and at the height of 1.5 meter from the floor of the room. This position comes out to be at the center of the room inlet opening.

The second measurement point has been taken at following axis locations:

2) **X = 2.85 meter**
   Y = 2.80 meter

The above location has been taken at the entrance of the solar chimney inlet. This location is 2.85 meter away from entrance in X-Axis direction and at the height of 2.8 meter from the floor of the room.

The third measurement point has been taken at following axis locations:

3) X = 1.29 meter
Y = 4.43 meter

The above location has been taken just before solar chimney outlet. This location is 1.29 meter away in X-Axis direction and at the height of 4.43 meter from the floor of the room. This position has been 0.07 meter before the solar chimney outlet and near the heated wall of the solar chimney in order to measure change in temperature due to heated wall.

All above mentioned data measurement locations has been shown in figure 3.21 below:

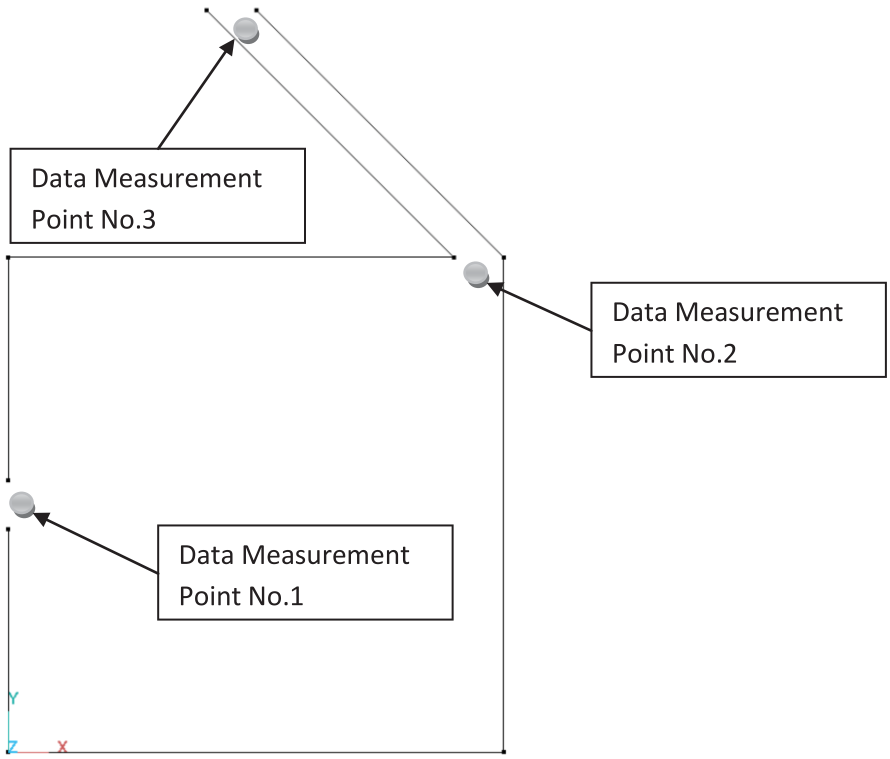

Figure 3.21: Model with inlet opening at middle of the side wall – Showing location of data measurement points for analysis

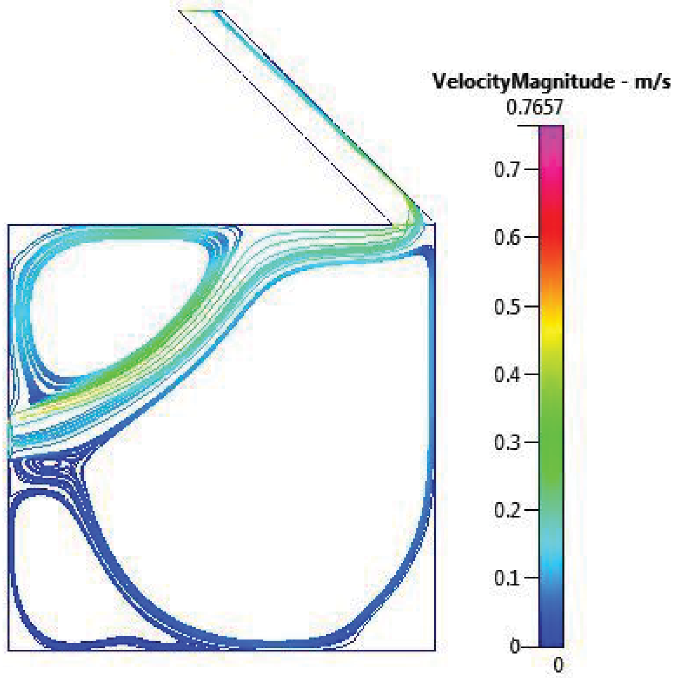

Figure 3.22: Model with inlet opening at middle of the side wall – Showing Velocity pattern after simulation.

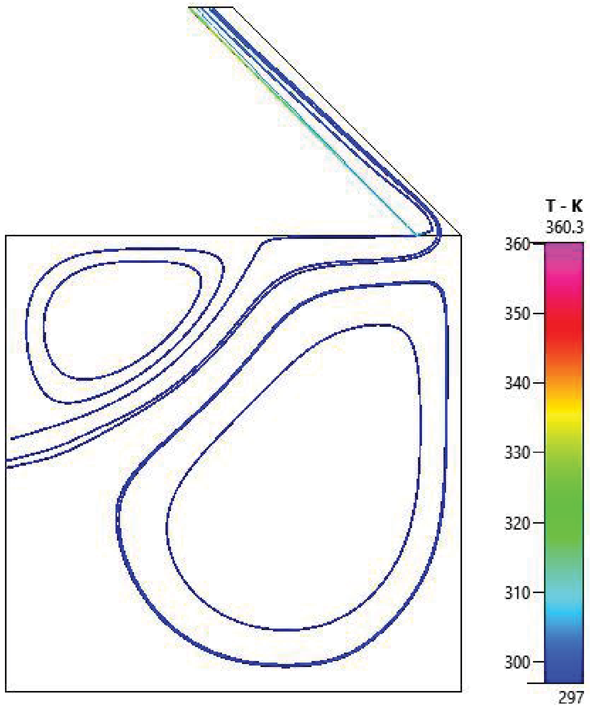

Figure 3.23: Model with inlet opening at middle of the side wall – Showing Temperature profile after simulation.

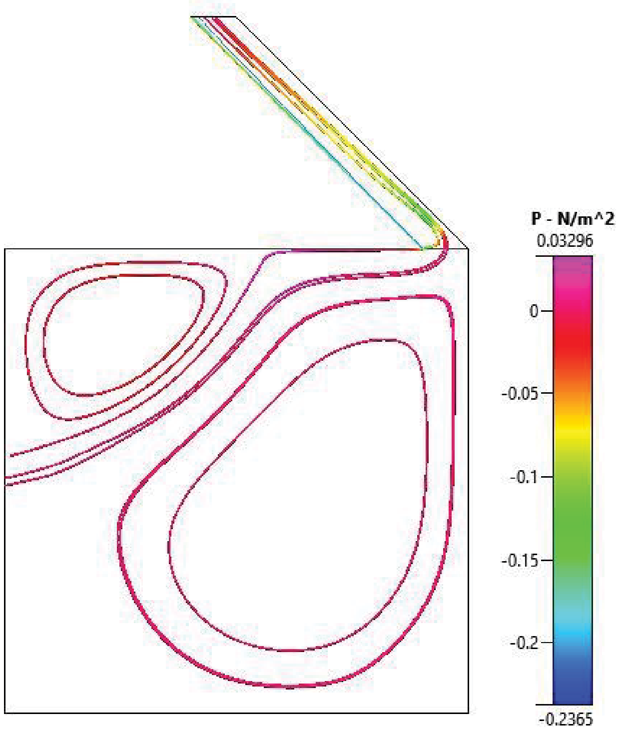

Figure 3.24: Model with inlet opening at middle of the side wall – Showing Pressure profile after simulation.

3.8.3 Room with Air Inlet at Top of the Wall

A new model with room air inlet location at top of the wall was made having the same number of cells where grid convergence was achieved i.e. Model-7. The Model was simulated using the same parameters in order to compare results. The graphical and numerical results obtained against this simulation are presented below.

Table: 3.10: Simulation Data of 2D Model-7 with Room inlet opening at Top of the side wall

Room Length	Room Width	Chimney Height / Length	
3 m	3 m	1.5 / 2.12 m	
Chimney Angle	Inlet / Outlet		
45	0.3 meter		
Nodes		No.	210402
Faces		No.	419643
Cells		No.	209242
In Flow		KG/S	0.0737158
Out Flow		KG/S	0.0736501
Maximium Velocity		Met/S	0.624
Maximum Temp.		K	363.581
Converged at Iteration			12491

Simulation Data of 2D Model (Model-7 with Air Inlet at Top of the Side Wall)											
At Center of Room Air Inlet				At Chimney Inlet				At Chimney Outlet			
Coordinates of Location		Variable	Values	Coordinates of Location		Variable	Values	Coordinates of Location		Variable	Values
X	0.1	U	0.218256	X	2.85	U	0.054188	X	1.29	U	-0.4163
Y	2.85	V	-0.00126	Y	2.8	V	0.03238	Y	4.43	V	0.416179
		VM	0.21826			VM	0.063131			VM	0.588651
		P	-7.65E-05			P	0.002975			P	-0.0142
		Pt	2.76E-02			Pt	0.005294			Pt	0.187062
		T	297			T	297.001			T	310.129

The table above is showing a glimpse of data which has been collected after simulation for analysis purpose. The data has been taken at three different locations against for the purpose of Grid Convergence Study.

The first measurement point against above model has been taken at following axis locations:

1) X = 0.1 meter
Y = 2.85meter

The above location has been taken just after the entrance of the room inlet. This location is 0.1 meter away from entrance in X-Axis direction and at the height of 2.85 meter from the floor of the room. This position comes out to be at the center of the room inlet opening.

The second measurement point has been taken at following axis locations:

2) X = 2.85 meter
Y = 2.80 meter

The above location has been taken at the entrance of the solar chimney inlet. This location is 2.85 meter away from entrance in X-Axis direction and at the height of 2.8 meter from the floor of the room.

The third measurement point has been taken at following axis locations:

3) X = 1.29 meter
Y = 4.43 meter

The above location has been taken just before solar chimney outlet. This location is 1.29 meter away in X-Axis direction and at the height of 4.43 meter from the floor of the room. This position has been 0.07 meter before the solar chimney outlet and near the heated wall of the solar chimney in order to measure change in temperature due to heated wall.

All above mentioned data measurement locations has been shown in figure 3.25 below:

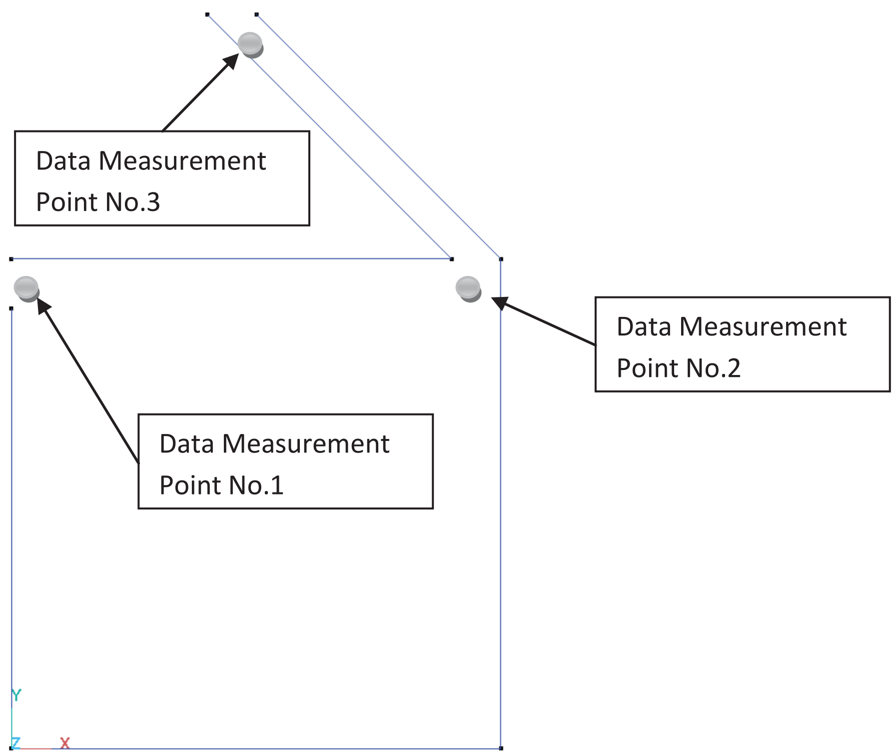

Figure 3.25: Model with inlet opening at top of the side wall – Showing location of data measurement points for analysis.

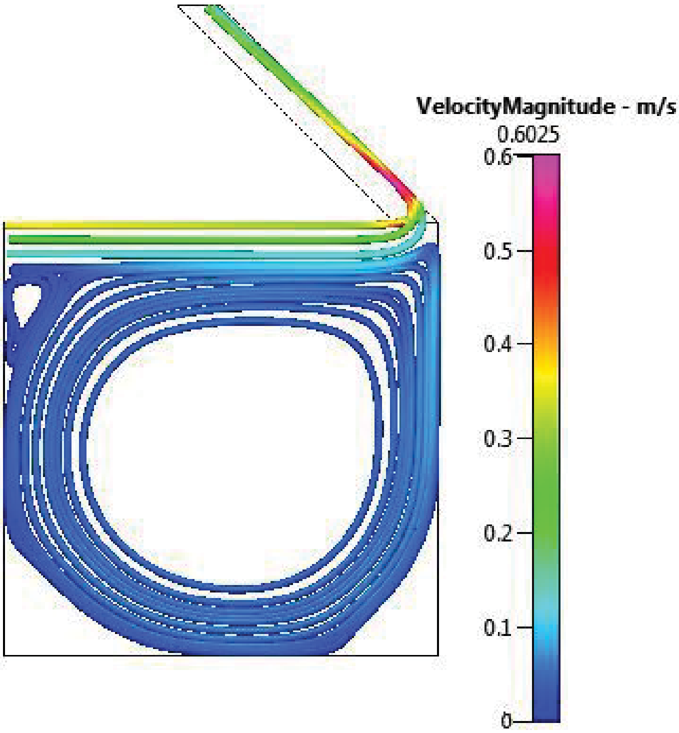

Figure 3.26: Model with inlet opening at top of the side wall – Showing Velocity pattern after simulation.

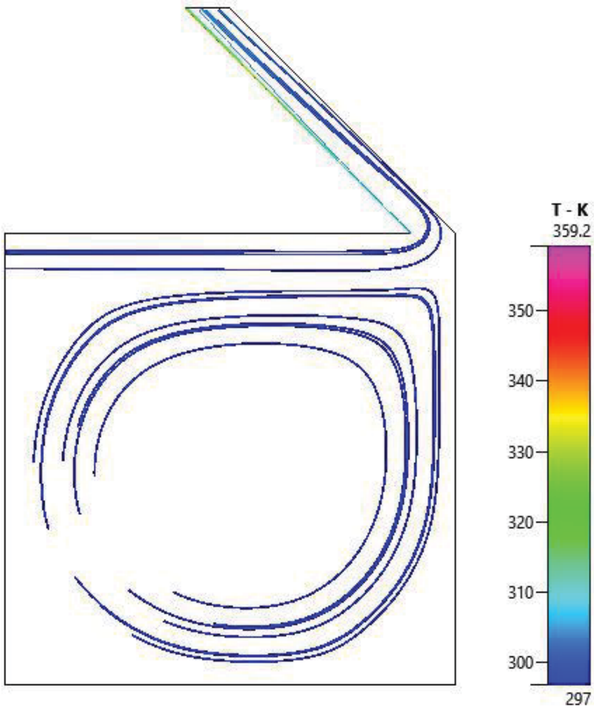

Figure 3.27: Model with inlet opening at top of the side wall – Showing Temperature profile after simulation.

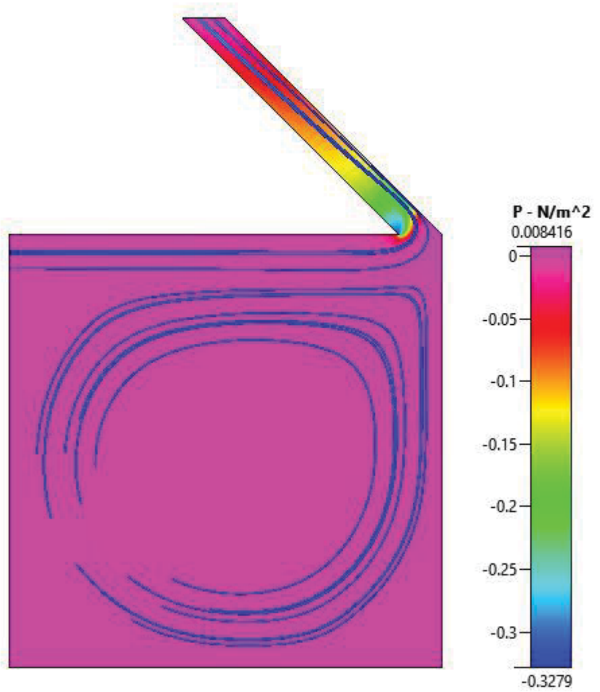

Figure 3.28: Model with inlet opening at top of the side wall – Showing Pressure profile after simulation.

3.8.4 Solution Convergence and Mass Flow Rate Analysis

After convergence, acceptable mass flow rate balance has been achieved in each model with different room inlet locations. The table and graph below in figure 3.28a is explaining the mass flow rate balance achieved in each three cases where room air inlet location has been changed.

Model Description	Air Mass Flow Rate at Inlet (Kg/sec)	Air Mass Flow Rate at Outlet (Kg/sec)	Difference (Kg/sec)
Model with room air inlet at bottom of the side wall	0.017125	0.017125	1.00E-07
Model with room air inlet at middle of the side wall	0.066568	0.065973	0.000595
Model with room air inlet at top of the side wall	0.073716	0.07365	6.57E-05

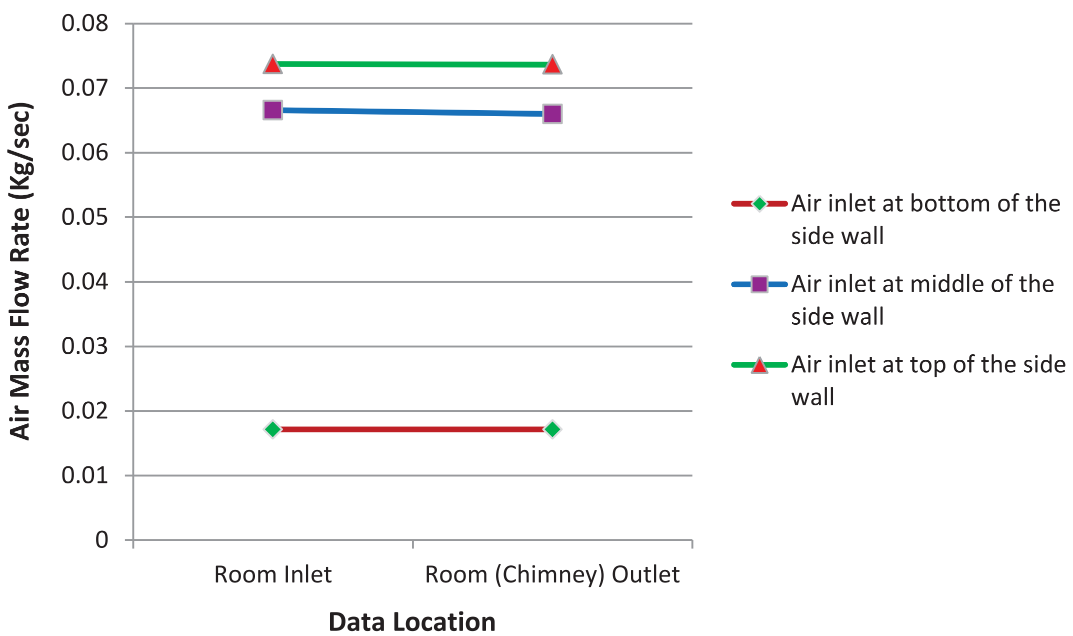

Figure:3.28a: Graph showing comparison of Total Mass Air Flow Rate at Room inlet and outlet.

Through above tabulated and graphical analysis, it is clear that after achieving convergence as per defined criteria, balance of mass is well verified.

The relative difference also comes well within acceptable limits i.e.

(In Flow – Out Flow) / Inflow

Model	Relative Difference
Model with room air inlet at bottom of the side wall	5.84E-06
Model with room air inlet at middle of the side wall	8.94E-03
Model with room air inlet at top of the side wall	8.91E-04

3.9 Analysis and Discussion on Simulation Results

With the change in room air inlet location, the air flow rate and pattern significantly changes. The table below summarizes and give comparison of some important parameters noted after simulation with each type of room model:

Room Air Inlet location	Air Inflow Rate (Kg/sec)	Maximum Velocity (m/s)	Maximum Temperature (K)
Bottom of the side wall	0.017125	1.089	399.6
Middle of the side wall	0.066568	0.766	360.34
Top of the side wall	0.073716	0.624	363.58

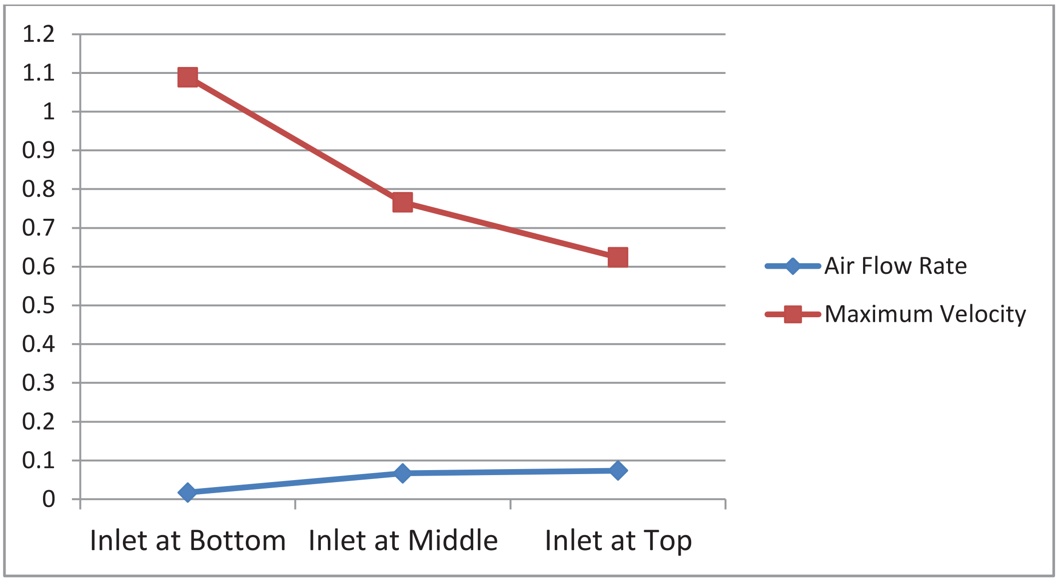

Figure:3.28b: Graph showing comparison of Air Flow Rate and Velocity with change in inlet location

The graphical and numerical analysis shows that with change of room air inlet location, while keeping all other parameters same, air flow rate and velocity significantly changes. It can be clearly observed from above graphical outputs, comparison table and graphs that by taking air inlet location towards top side of the room, the air flow rate increases and velocity decrease.

Another important factor in room ventilation is air flow pattern. The best pattern will be the one which will evenly circulate in the room and must pass through the sitting area of the occupants which is the floor of the room. Keeping this important factor in view, the best air flow pattern has been seen in a model where air inlet location is at the bottom of the wall (figure 3.18) and in a model where room inlet is at top of the wall (figure 3.26).

In these models, air is more evenly distributing in whole room as compared to other model which will give comfort to the occupants of the room. Further analysis will be carried out on a 3D model.

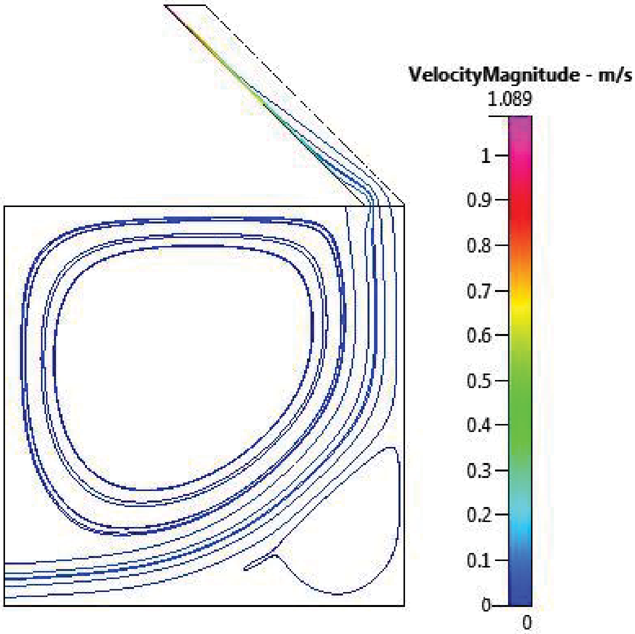

Figure 3.29: Model with inlet opening at bottom of the side wall – Showing air flow pattern after simulation.

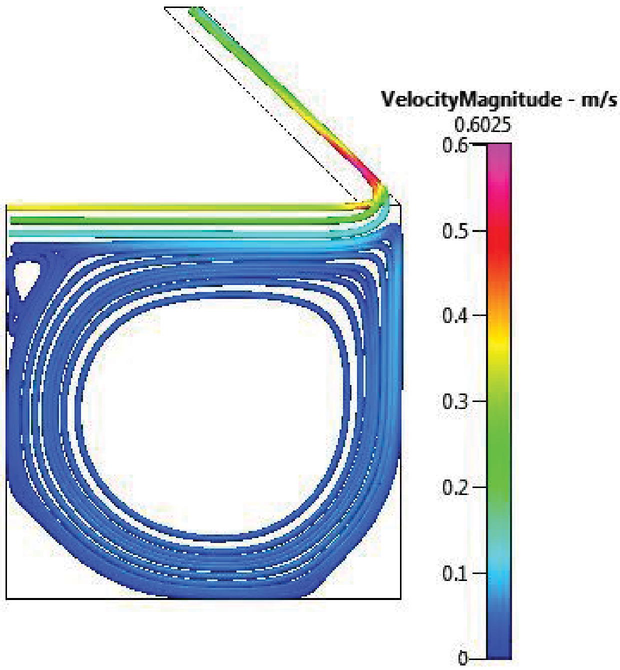

Figure 3.30: Model with inlet opening at top of the side wall – Showing air flow pattern after simulation.

In order to further analyze the behavior of air flow rate and velocity in three models, data of velocity magnitude measured along the room and curves drawn to identify the difference. The data points has been taken along the straight line in the room from left to right with a height of 01 meter from the floor. The data points has been taken at this level keeping in view the fact that this level is normally sitting area of the occupants and any better air flow / velocity at this level will directly provide comfort along with desired ventilation.

The figures and curves below are showing points in the room where data has been taken and value / trend of the data respectively.

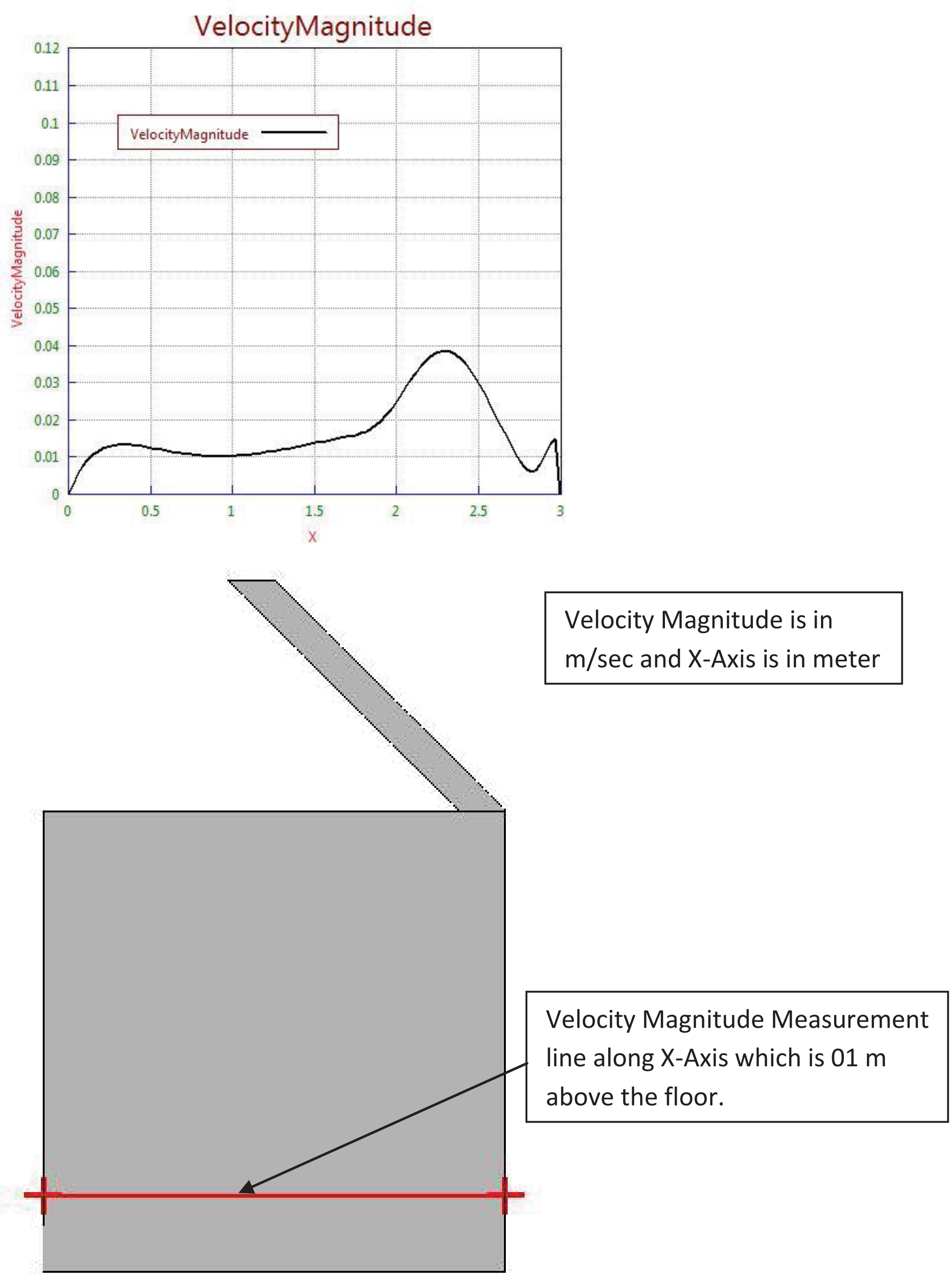

Figure :3.31: 2D Room with Inlet at Bottom of the Wall : Curve showing Velocity Magnitude Pattern along the Room (X-Axis).

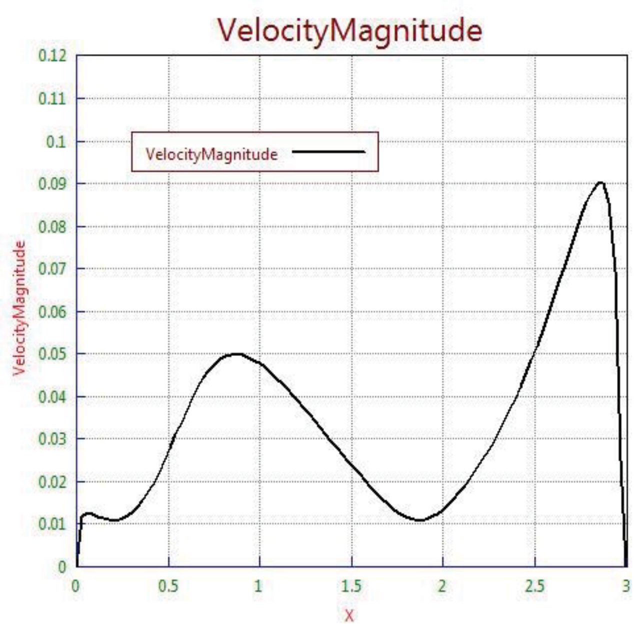

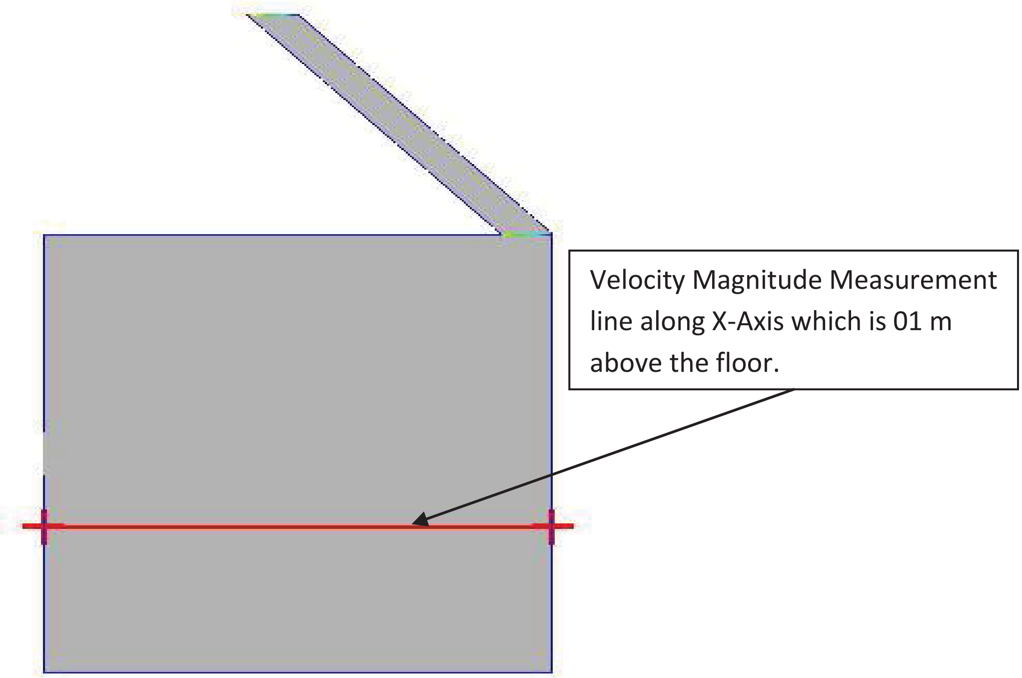

Figure :3.32: 2D Room with Inlet at Middle of the Wall : Curve showing Velocity Magnitude Pattern along the Room (X-Axis).

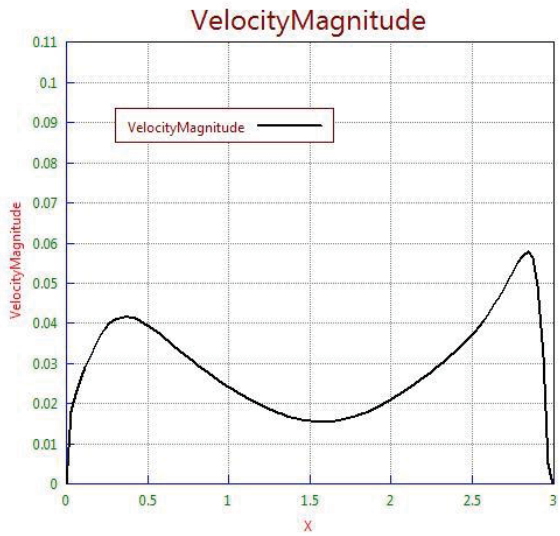

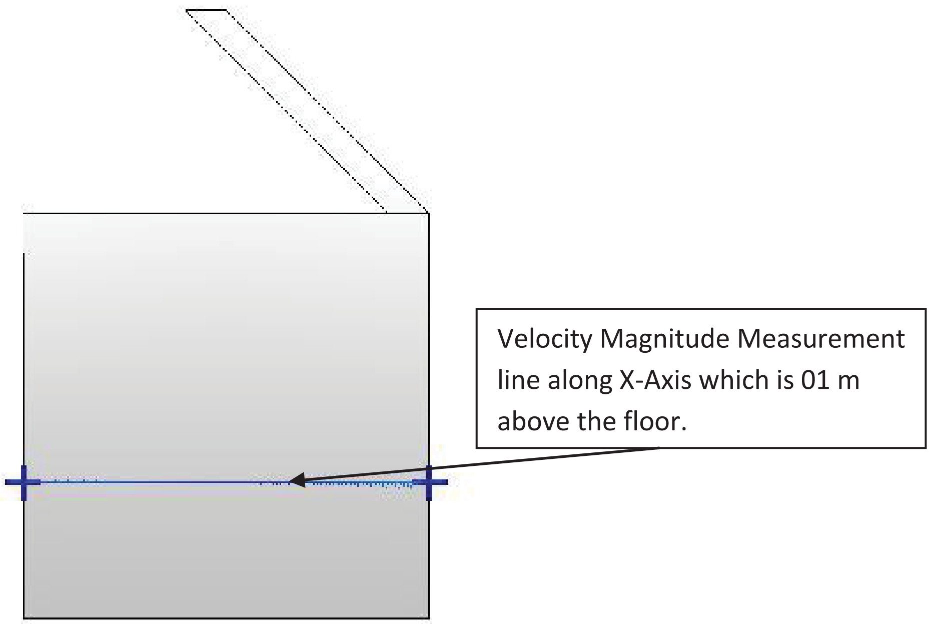

Figure :3.33: 2D Room with Inlet at Top of the Wall : Curve showing Velocity Magnitude Pattern along the Room (X-Axis).

By comparing above velocity magnitude curves of three models, it has been seen that the models with inlet at top side of the wall gives velocity magnitude value of 0.03 m/s along the width of the room. The model with room inlet at bottom is giving the variable velocity magnitude ranging from 0.1 to 0.3 m/s.

Chapter 4

Three-Dimensional Modeling and Simulation

4. Abstract

This chapter will cover the three dimensional modeling of the room fitted with solar chimney. Initially, a small scale model has been designed and simulated to get the idea and familiarization with three dimensional computations. After successful simulation on a small scale model, a real sized room fitted with solar chimney has been designed. An environment box has also been designed around room air inlet to study the air flow behavior at entrance of the room. The air flow pattern study has been carried out by changing solar chimney, room air inlet location and size of the environment box, in order to select the final model based on these analysis and previous research.

The selected model was further tested through grid convergence tests. After achieving the grid convergence, the final model was simulated with different air inlet locations and analysis were performed by putting pressure value of P = -0.22 N/m^2 at outlet boundary of the room i.e. solar chimney exit. This pressure value has been selected based on air flow analysis in inlet environment box; the detailed discussion on this is presented in this chapter.

The basic model has also been simulated by putting P = 0 N/m^2 (Natural condition) at outlet boundary of the room i.e. solar chimney exit and comparative analysis were performed with above model.

Additional analysis has also been performed by designing environment box around outlet boundary of the room i.e. solar chimney exit having same dimensions as that of inlet environment box. The comparative analysis has been performed with the first model. The important factor in natural ventilation is Air Change per Hour (ACH). The analysis based on this parameter has also been performed.

4.1. Designing / Modeling of a Three-Dimensional Room for Simulation

After simulation and analysis of 2D models, simulation of a real sized Three Dimensional (3D) room has been carried out. The purpose of analysis on a real sized 3D room is to get the physical conditions near to reality. The flow patterns achieved will be as per actual room size and will give us better idea of designing the chimney and inlet position.

In order to get the basic understanding of 3D simulation on CFD software, same idea as that of 2D computation has been adopted. First of all, a small size room with dimensions of 0.5m × 0.5m × 0.5m has been created for computation purpose. The inlet air opening and chimney width was taken as 0.025m × 0.025m each. The modeling and designing of 3D rooms has been carried out in GEOM Module of ESI group CFD software. The both geometry and grids were created in the CFD-GEOM. Structured meshes are used in each model. The model was simulated using CFD-ACE Module of ESI group software package.

4.2. 3D Modeling and Simulation of a Real Size Room

After getting the natural ventilation through 3D room at small scale, a real sized room with dimensions of 3m width, 3m length and 3m height was created. The room air inlet opening and the width of the solar chimney was 0.4m. The Chimney effective length was 2.12 meter and it was inclined chimney at an angle of 45^o from roof top.

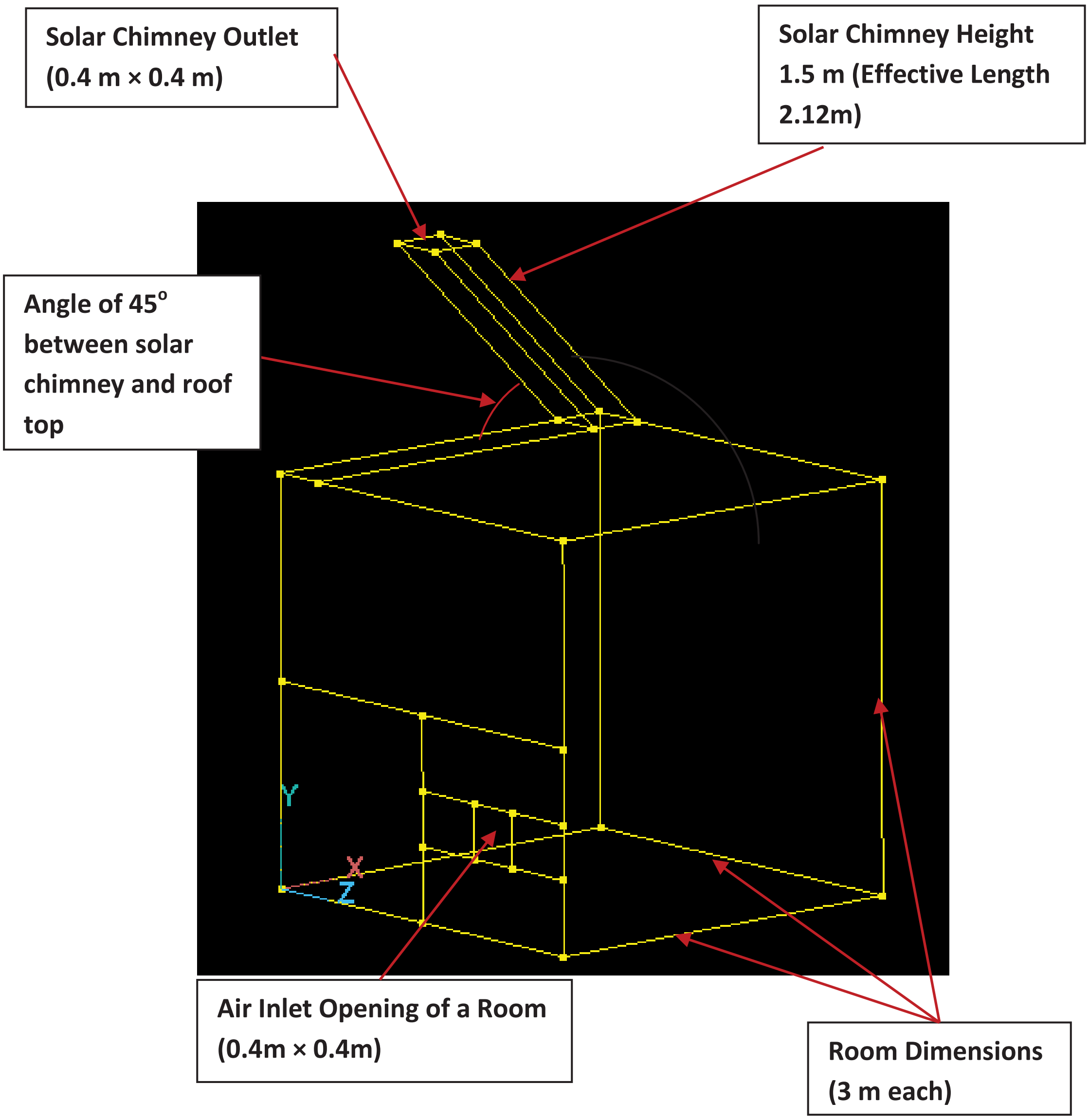

Figure: 4.1: Real Sized 3D Room created in CFD-GEOM

Initial analyses were performed on this model of a room fitted with Solar Chimney. But keeping in view the literature review and research already carried out on such type of room model, it was decided to make box around inlet opening of the room. The purpose of this box around inlet opening was to consider and analyze the behavior of air around and at inlet opening of the room, outside of the room boundary. Previously, most of the research has been carried out without giving much concentration on this point. The air flow rate and pattern at the entrance of the room inlet significantly affects the flow rates and patterns inside the room. In this scenario, the four faces of the inlet box (excluding bottom face which is kept as wall) will act as inlets while the actual room inlet will act as interface.

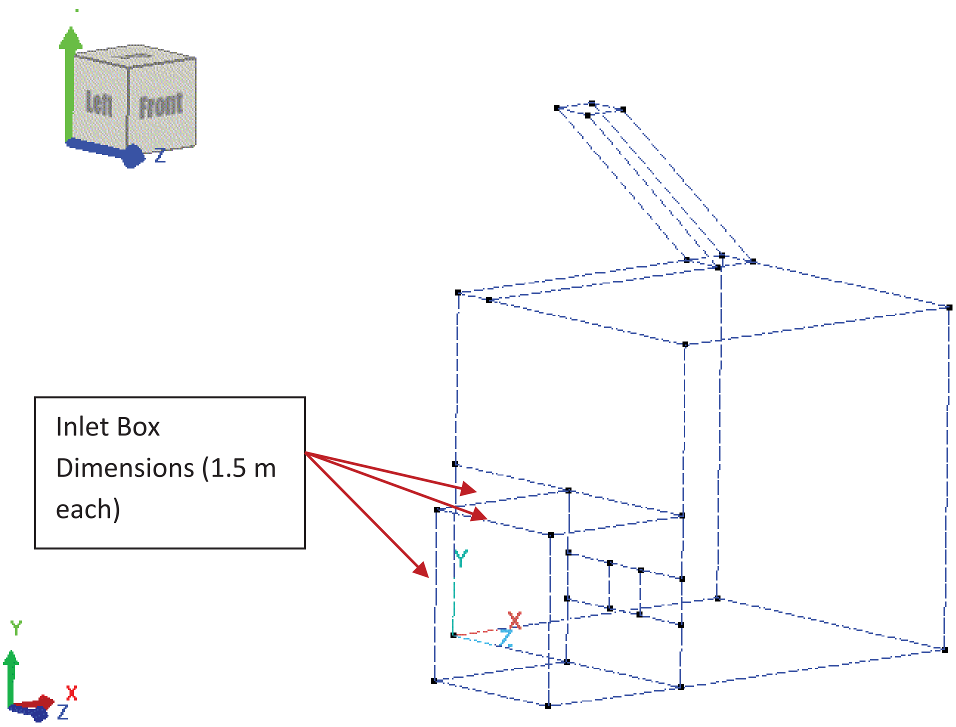

Figure: 4.2a: 3D Room created in CFD-GEOM with Inlet Box

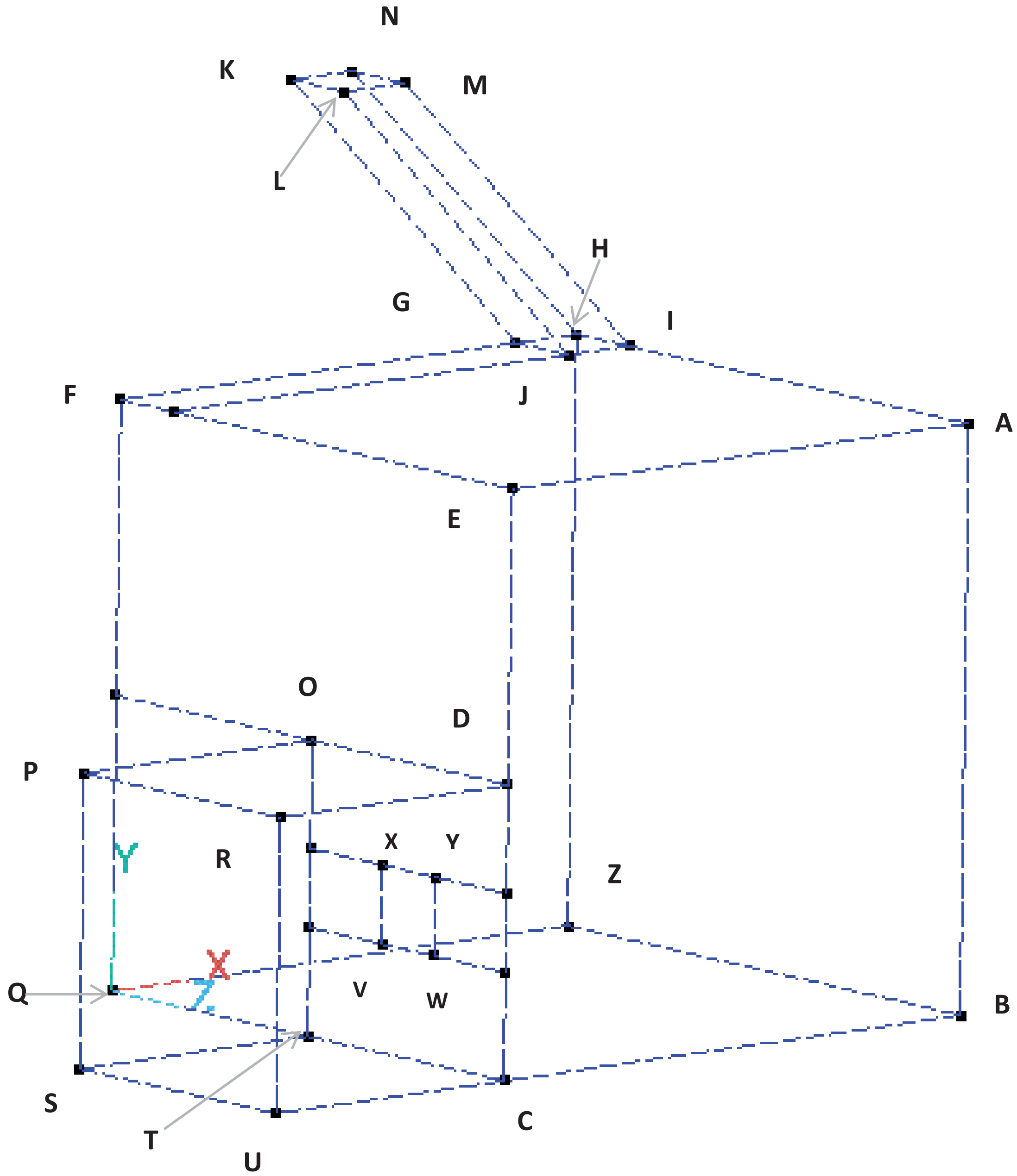

Figure: 4.2b: Defining different sections / faces of a 3D Room created in CFD-GEOM with Inlet Box

The above model is final 3D model created for simulation purpose and analysis. All the simulations were performed on this model. The different faces and parts of this model are explained below:

ABCE, ABZH, ZQFH and EFQC ---------------- Walls of the three dimensional room having dimension 3 meter × 3 meter each.

BZQC ---------------- Floor of the three dimensional room having dimensions 3 meter × 3 meter.

AEFH ---------------- Roof of the three dimensional room having dimensions 3 meter × 3 meter.

IJGH ---------------- Solar chimney inlet interface having dimension 0.4 meter × 0.4 meter.

KLMN ---------------- Solar chimney outlet having dimensions 0.4 meter × 0.4 meter.

XYVW ---------------- Room inlet interface having dimensions 0.4 meter × 0.4 meter.

OPDR ---------------- Roof of the inlet environment box having dimensions 1.5 meter × 1.5 meter and considered as inlet.

STCU ---------------- Floor of the inlet environment box having dimensions 1.5 meter × 1.5 meter and considered as wall.

PSUR, RDCU and OPST ---------------- Walls of the inlet environment box having dimensions 1.5 meter × 1.5 meter each and considered as inlets.

The inner wall ODCT of the inlet environment box and front wall EFQC of the room have been considered as solid wall except the portion XVWT which is inlet interface of the room and inlet environment box.

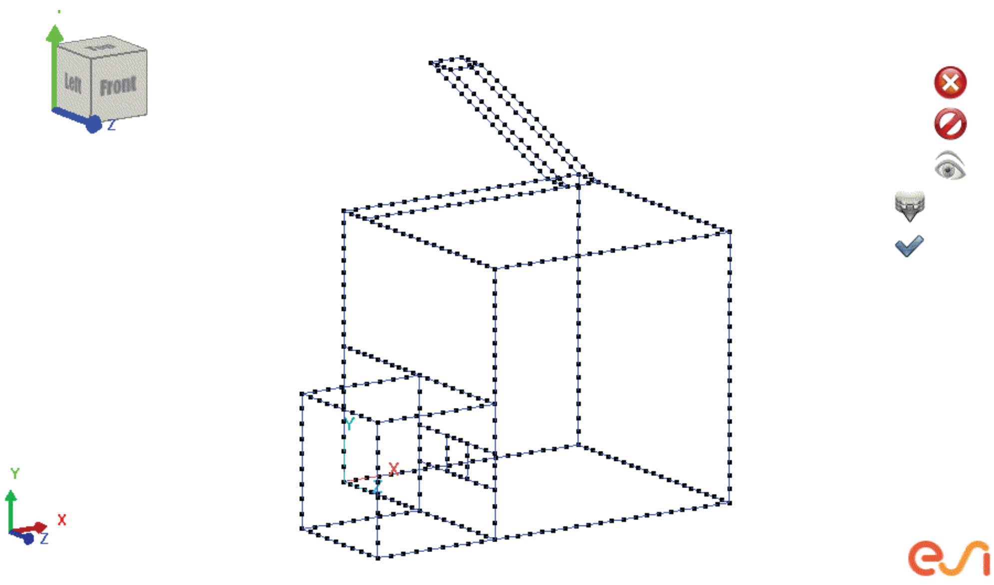

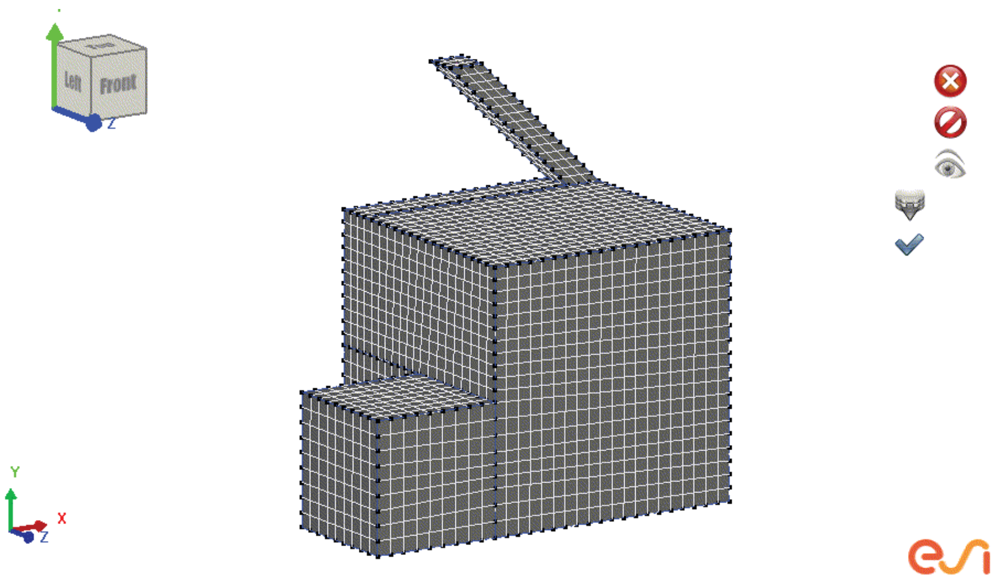

Figure: 4.3: 3D Room showing Edges and Faces created in CFD-GEOM

4.3. Designing of a Real Sized 3D Room in CFD GEOM

The models are designed in CFD-GEOM module of CFD ACE+ software. The both geometry and grids were created in the CFD-GEOM. Structured meshes are used in each model. The Figures 4.4 to 4.9 are showing steps during creation of a model of real sized room with structured mesh in CFD-GEOM.

First of all, a basic 3D room was created using point creation in CFD GEOM. The figure 4.4 below is showing this model.

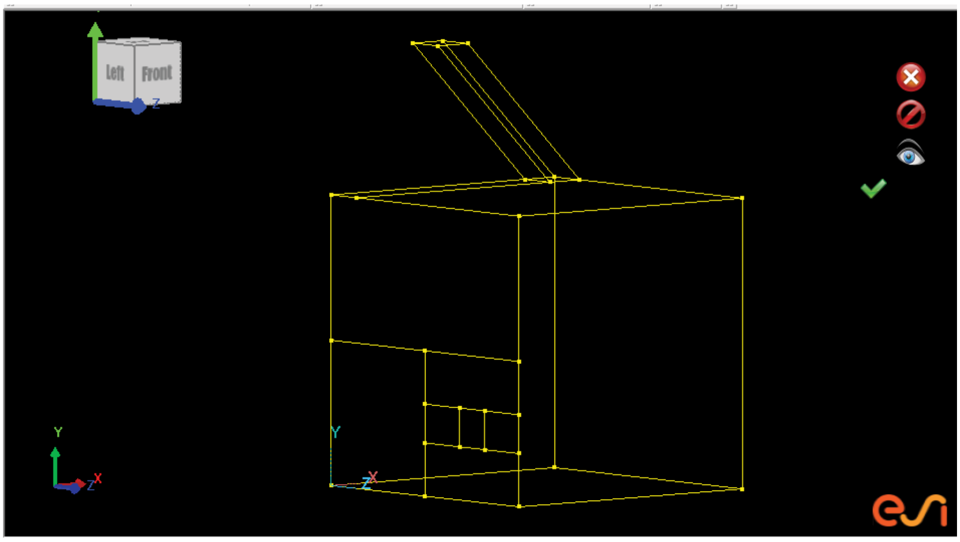

Figure: 4.4: Basic 3D Room model created in CFD-GEOM using points and lines

In order to further analyze the air flow characteristics at inlet opening, an inlet box has been designed around inlet opening with dimensions of 1.5 meter each. The figure 4.5 is showing inlet box around inlet opening.

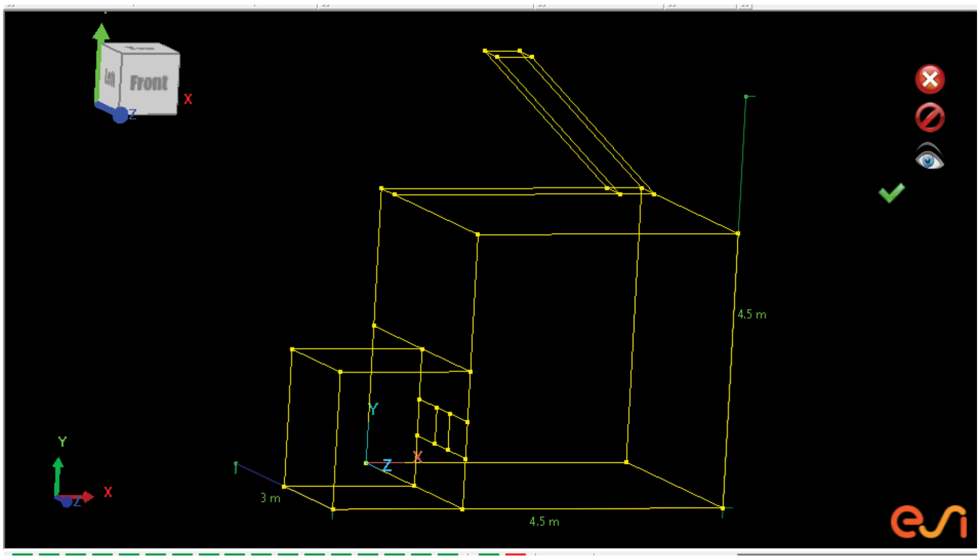

Figure: 4.5: Creation of box around inlet opening of the room

The Figure 4.6 below is showing finalized three-dimensional model with grids and meshes (structured mesh) in CFD-GEOM.

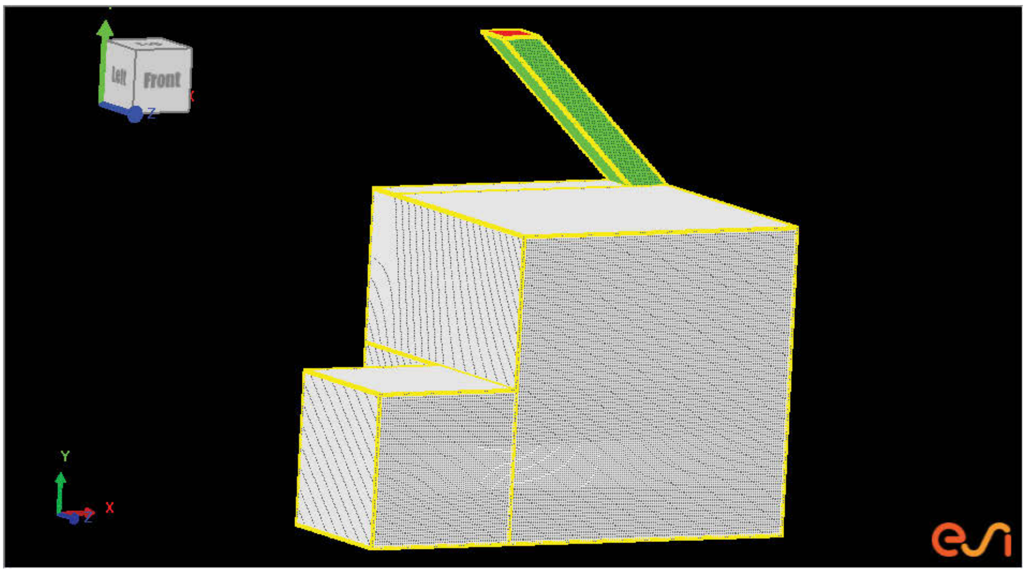

Figure: 4.6: Finalized Three Dimensional Model with Grids and Faces

4.4 Physical Conditions for the Model and Simulation in the CFD Solver

After the pre-processing stage in CFD-GEOM module by defining the geometry, mesh type and boundary conditions of the model, CFD-GUI module has been used as the graphical user interface of the CFD-ACE-SOLVER.

The air properties have been assumed against the normal atmospheric air temperature as 300 K and pressure as 101.3 kpa. There will be variation in density of the air due to change in temperature which will result in buoyancy force, therefore, boussinesq approximation has also been considered in the simulation of all cases. The following values of molecular properties have been used during simulation of all models (using common notation):

ρ (Density) = 1.161 kg/m^3, μ (Dynamic viscosity) = 1.846×10^{-05} kg/m-s

v (kinematic viscosity) = 1.5×10^{-05} m^2/s, Cp = 1007 J/kg-k

K (Thermal Conductivity) = 0.0263 W/m-k, Prandtl No. = 0.9

Reference Temperature = 297 K,

Thermal Expansion Coefficient = 0.003367 K^{-1}

All simulations have been considered turbulent with zero turbulence values which will act as of laminar conditions. There may not be much difference in the numerical results, if the cases will be simulated using turbulence model with above conditions (correspond to laminar flow). Based on previous research in the field [31], the value of Prandtl Number has been used as 0.9 during all simulations.

4.4.1 Boundary Conditions

The boundary conditions for the variables like velocity components, pressure and temperature are as follows:

- All openings on the flow domain's boundary i.e. room inlet openings (there are 04 inlet openings of the room due to inlet environment box around the actual inlet opening of the room) and solar chimney outlet opening (figure 1a & 1b) have been assigned with ambient conditions based on normal atmosphere around the room. The fluid has been considered at atmospheric pressure with a constant gauge pressure value of P = 0 N/m^2 and temperature as T = 297K.
- The value of heat flux "Q" for lower wall (heated face) of the chimney (wall facing roof of the room) has been fixed as 300 W/m^2 with Zero Velocity while the upper face (wall) has been designed as transparent to allow passing of solar heat up to lower face. Although, the higher value of solar heat flux favours the natural ventilation but this constant value of solar heat flux has been considered based on literature review, whereby, it has been analyzed that in most of the normalized area, the average heat flux provided by actual Sun radiation is around this value. So the consideration of this value keeps the research more practicable.
- The remaining surfaces of the room and chimney like walls of the room & chimney, roof & floor of the room and floor of the inlet environment box have been assumed as adiabatic walls with velocity value as zeros. The adiabatic condition has been considered based on the fact that walls of the buildings are normally constructed to avoid losses of internal cooling or to protect inner environment from outside harsh weather. So in case of concrete walls, the heat transfer is very negligible through walls and therefore, adiabatic conditions may be considered for walls.

- Based on the previous research in the field as explained in Chien [30] and to keep turbulence model results equaling to laminar model, the value of K and Ɛ have been taken as Zero for all solid surfaces. Where k is turbulent kinetic energy and Ɛ is its dissipation rate.
- At all openings, the constant value of Temperature, K and Ɛ shall apply only on those sections of an opening if inflow is occurring. If during computation, outflow is observed on any sections, the constant value of temperature, k and Ɛ shall be ignored and actual values shall be calculated. Similarly, the constant pressure condition applies only on those sections of an opening where there is outflow. If the computation reveals inflow on any sections, the constant pressure condition there will be ignored, and pressure will be computed instead.
- The important factor in natural ventilation is Pressure. There are two types of pressure values appearing in software / simulation results i.e. Static Pressure and Total Pressure. The concerned value in this research is Static Pressure. The value of static pressure at solar chimney exit plays a significant role in ventilation system. The detail discussion on Pressure is carried out in section 3.5.2.

  In natural ventilation systems, we keep pressure value as per atmospheric pressure but here we have studied both the conditions i.e. simulation with zero pressure value (atmospheric pressure) at solar chimney exit and simulation by putting –ve value of pressure at solar chimney exit.

Normally, it has been found that the small change in turbulence levels at the inlet / outlet openings has very minor effects on the simulation results.

The nomenclatures of other terminologies used in the study are given below:

Variable	Description	Variable	Description
X (meter)	Location in X Direction	U (m/s)	Velocity in Horizontal Direction
Y (meter)	Location in Y Direction	V (m/s)	Velocity in Vertical Direction
Z (meter)	Location in Z Direction	W (m/s)	Velocity in Z Direction
T (K)	Temperature	VM (m/s)	Velocity Magnitude
P (N/m^2)	Static Pressure		

All length values used / given in the study are in meters if otherwise specified.

The following three modules were selected in the CFD ACE+ Solver (CFD-GUI):

1) **Flow Module**
2) **Heat Transfer Module**
3) **Turbulence Module**

For the simulation analysis of the models, Reynolds-Averaged Navier-Stokes (RANS) approach has been used. The Low Reynolds Number $\boldsymbol{k}$ **-** $\boldsymbol{\varepsilon}$ turbulence model has been adopted as explained by Chien [30]. The governing equations which have been used for these analyses are Reynolds-averaged conservation of mass, momentum and balance of energy along with two transport equations for $\boldsymbol{k}$ and $\boldsymbol{\varepsilon}$ of the Chien model.

The other parameters considered for simulation are tabulated below:

Table:4.0: Physical Parameters Taken for Simulation of 3D Room Fitted with Inclined Solar Chimney

Modules		Body Forces	
Flow		Gravity in Y-Direction (m/s^2)	-9.81
Heat Transfer		**Boussinesq Approximation**	
Turbulance		Reference Temperature (K)	297
		Volume Coefficient of Thermal Expension (1/K)	0.003367
Turbulance Model			
K Epsilon Family			
Low Re (Chien)			
Standard Wall			

Convergence Criteria	0.0001

Boundary Conditions		Initial Conditions	
Room Inlet (Fixed Pressure)			
P (N/m^2)	0	P (N/m^2)	0
T (K)	297	T (K)	297
Kinetic Energy (m^2/s^2)	0.00E+00	Kinetic Energy (m^2/s^2)	0.00E+00
Dissipation Rate (m^2/s^3)	0.00E+00	Dissipation Rate (m^2/s^3)	0.00E+00
Room Outlet (Fixed Pressure)			
P (N/m^2)	0		
T (K)	297		
Kinetic Energy (m^2/s^2)	0.00E+00		
Dissipation Rate (m^2/s^3)	0.00E+00		
Chimney Inlet Wall			
Heat Flux (W/m^2)	300		

4.5. Simulation of a Real Sized 3D Room in CFD ACE+ GUI (Software Solver)

The all models created above have been simulated in CFD-ACE GUI module of CFD ACE+ software. The Figure 4.7 below is showing exported DTF file in CFD Solver for simulation.

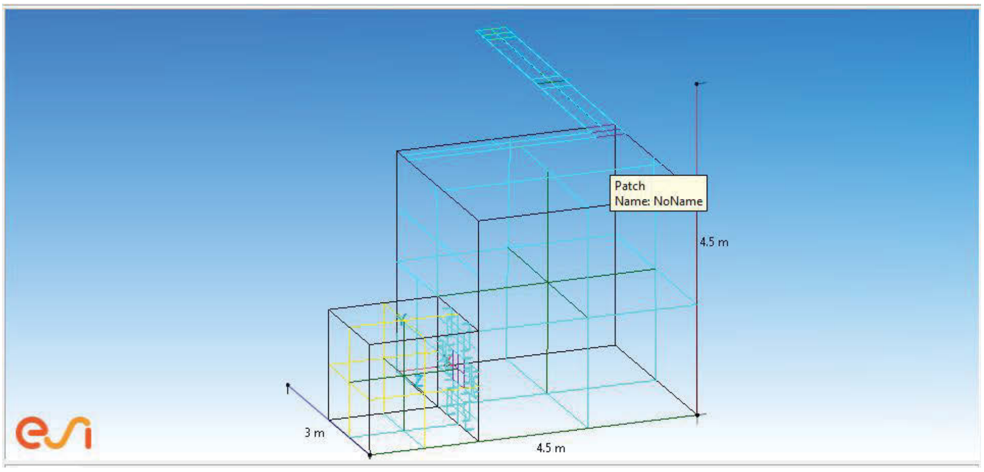

Figure: 4.7: Exported DTF model (Figure: 4.6) in CFD-ACE GUI Module for Simulation

The following major steps were involved during simulation of above model:

- **Selection of Modules in CFD-ACE GUI for simulation**
- **Gravity and Boussinesq Force Selection**
- **Turbulence Model Selection**
- **Selection of volume conditions / properties**
- **Defining Inlet Boundary Conditions**
- **Defining Chimney outlet Boundary Conditions**
- **Solar Chimney Heat Flux Rate**
- **Defining Initial Conditions**
- **Defining number of iterations and convergence criteria**

4.6. Designing and Simulation of Different Room Models

In order to study the effect of room air inlet opening design, location of box around inlet, its size and solar chimney location on air flow patterns, different room designs were created by changing inlet box size, inlet opening size and chimney location on roof top. These models were simulated in CFD Solver and their effects on air flow rate and patterns was analyzed.

The following models were created and simulated / analyzed in CFD Solver:

1. Room model with solar chimney on left side of the roof top (Figure 4.8)
2. Room model with solar chimney at the center of the roof top (Figure 4.9)
3. Room model with solar chimney on right side of the roof top – in front of room air inlet opening (Figure 4.10)
4. Room model with room air inlet opening at bottom right side of the wall – adjacent to room floor (Figure 4.11)
5. Room model with room air inlet opening at middle right side of the wall – with bigger inlet opening (Figure 4.12)
6. Room model by changing size of the box opening around inlet opening and location of inlet (Figure 4.13 to 4.18)

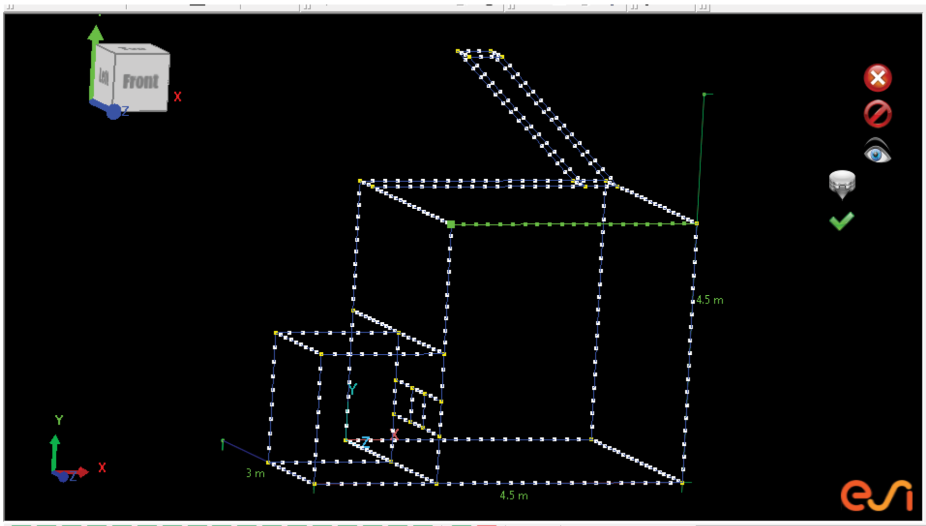

Figure: 4.8: Room model with solar chimney on left side of the roof top

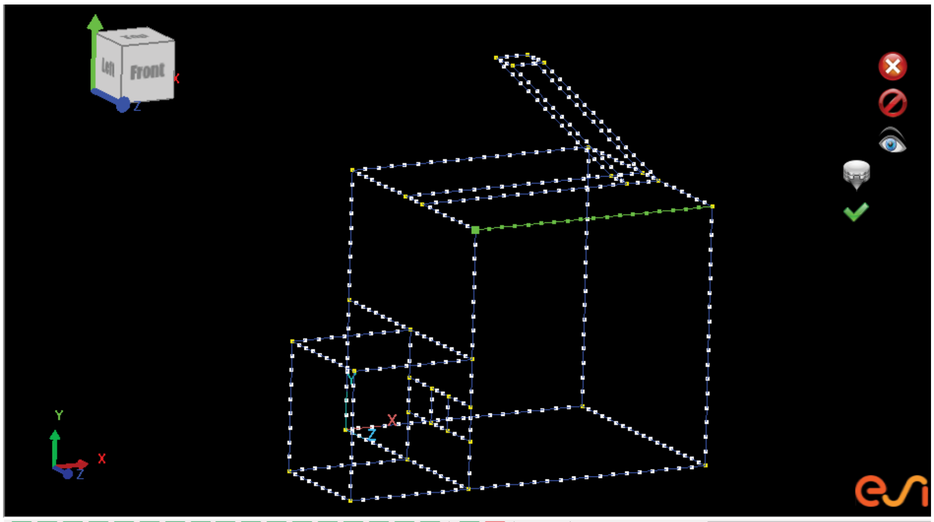

Figure: 4.9: Room model with solar chimney at the center of the roof top

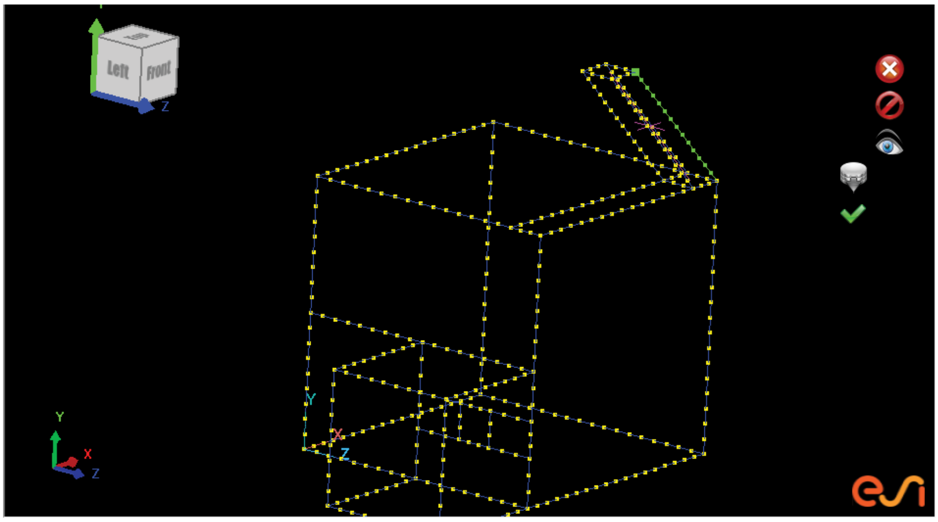

Figure: 4.10: Room model with solar chimney on right side of the roof top – in front of room air inlet opening

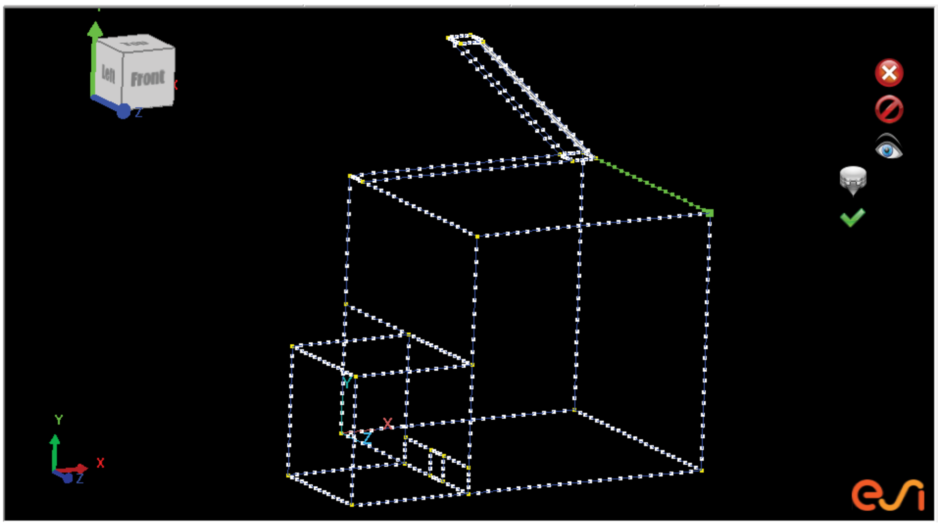

Figure: 4.11: Room model with room air inlet opening at bottom right side of the wall – adjacent to room floor

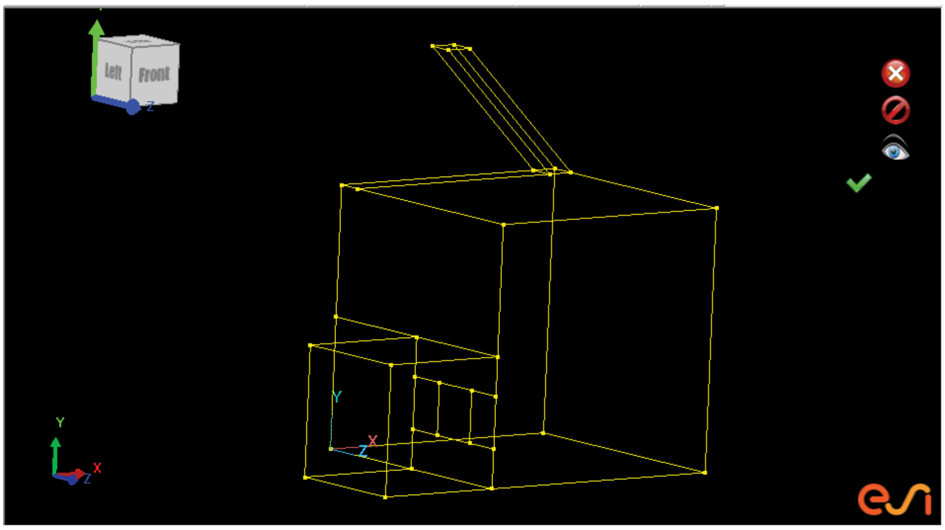

Figure: 4.12: Room model with room air inlet opening at middle right side of the wall – with bigger inlet opening

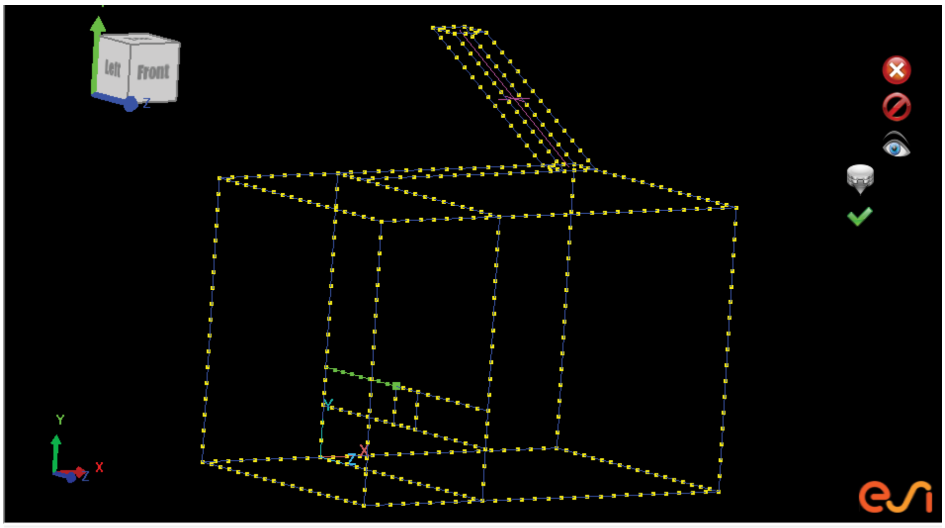

Figure: 4.13: Change in Size of Inlet Box

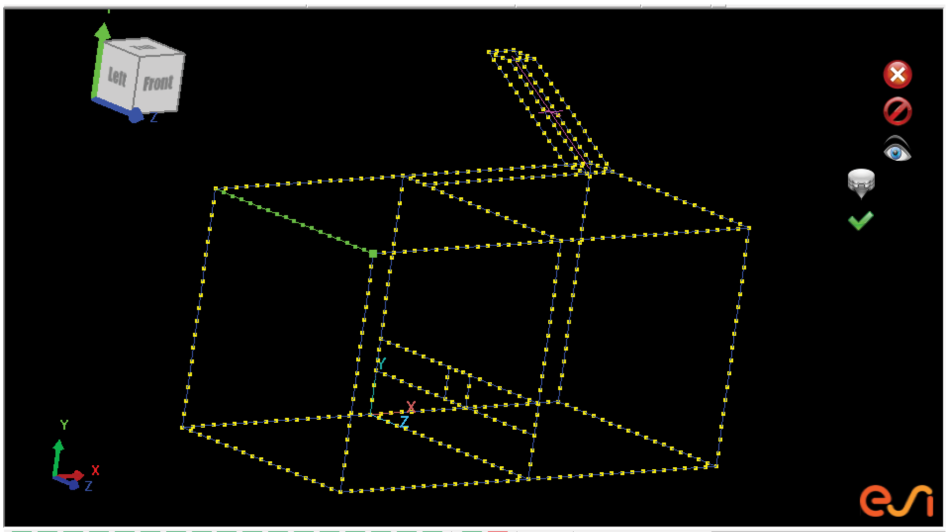

Figure: 4.14: Change in Size of Inlet Box

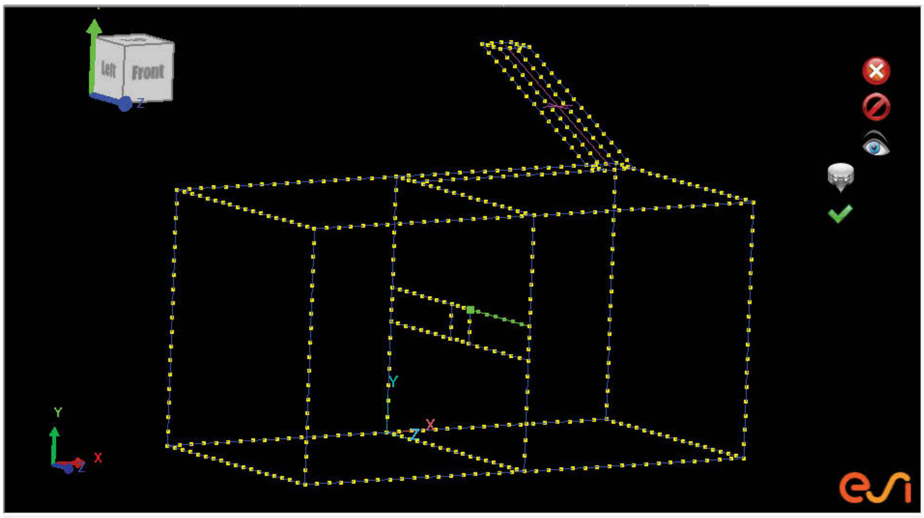

Figure: 4.15: Change in Size of Inlet Box and location of inlet opening

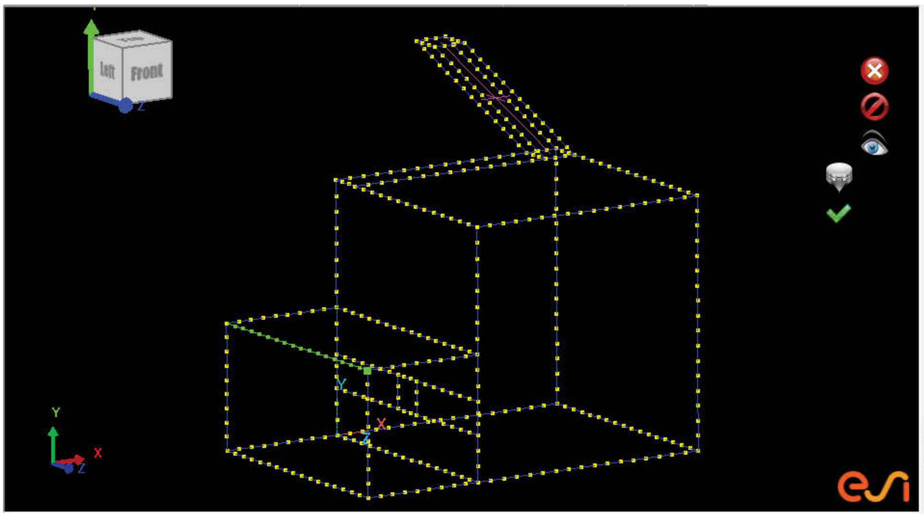

Figure: 4.16: Change in Size of Inlet Box

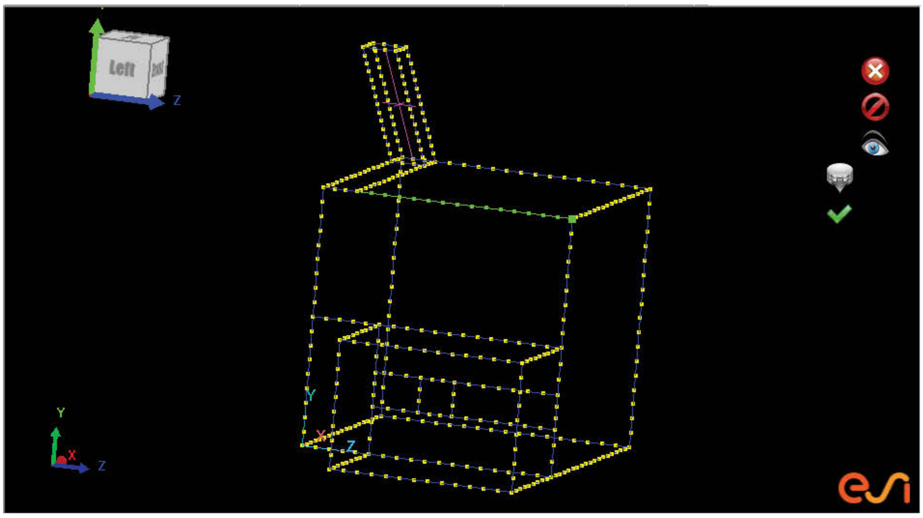

Figure: 4.17: Change in location of inlet opening

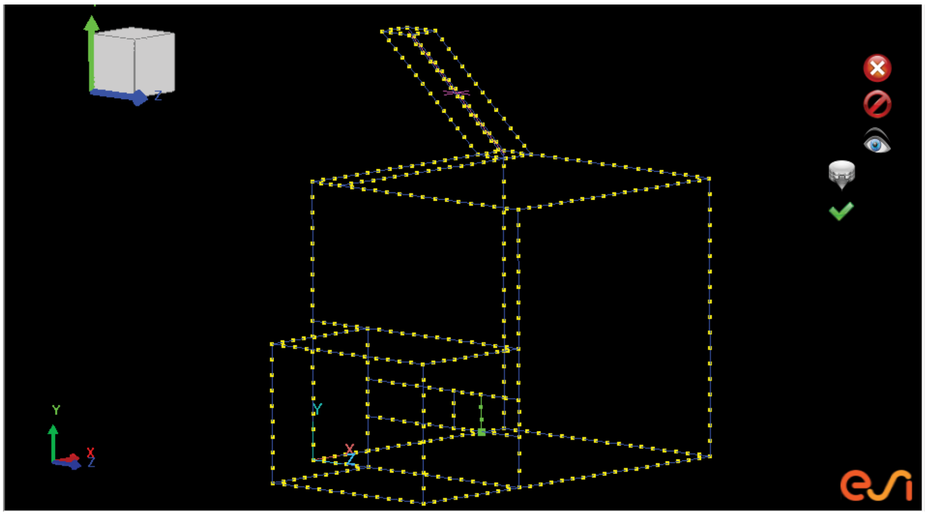

Figure: 4.18: Change in location of inlet opening

4.6.1 Grid Convergence Criteria

The Grid Convergence criteria of 0.0001 have been adopted for each simulation as shown in below screen shot:

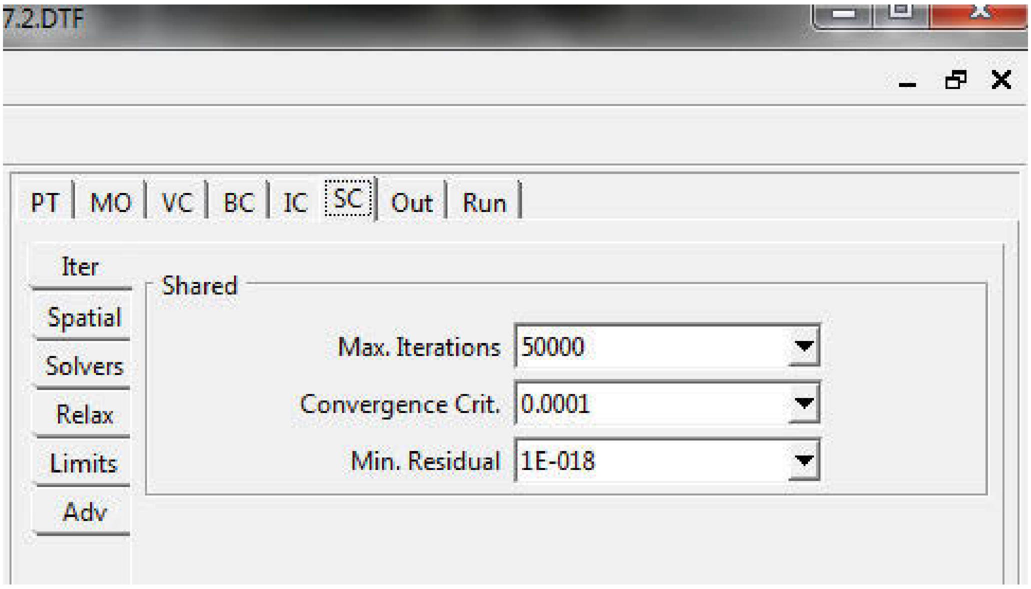

Figure 4.19: Showing number of Iterations and Grid Convergence Criteria for Simulation in the Solver

4.6.2 Normalized and Un-Normalized Residuals

The normalized and un-normalized residuals are used to measure the accuracy of the solution. The graphs below are showing the normalized and un-normalized solutions of one model.

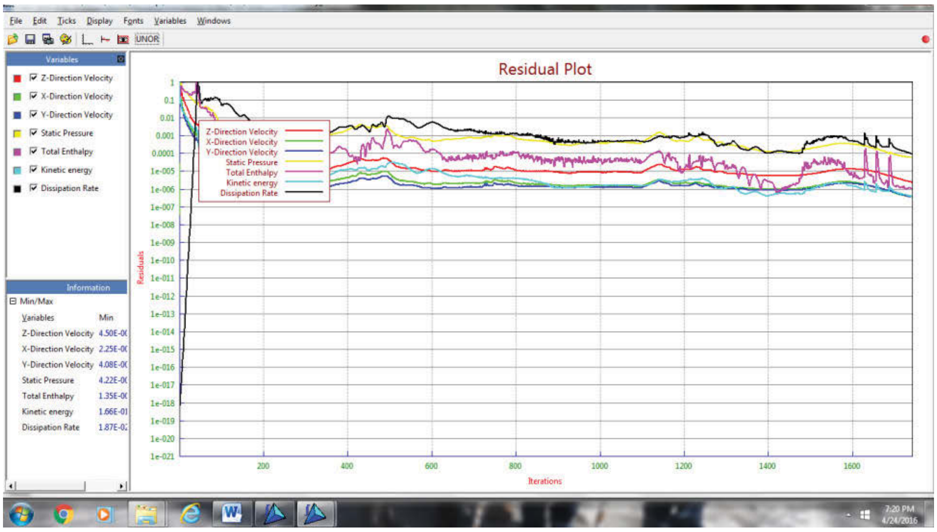

Figure:4.20: Graph showing Convergence of the one Model up to desired level (1.0×10^{-04}) with Normalized values

Figure:4.21: Graph showing Convergence of the one Model up to desired level (1.0×10^{-04}) with Actual values

4.7 Simulation Results and Analysis of Different Models

Initially, basic analyses were performed on above model (also shown in figure 4.2). The numerical and graphical results obtained from this model are tabulated below in Table 4.1. This data is against very basic model and may not be accurate unless grid convergence is achieved. The data of a model which will successfully pass grid convergence criteria shall be considered reliable:

Table: 4.1: Simulation Data of 3D Model-1 at Three Different Locations

Room Length	Room Width	Room Height	Chimney Height
3 m	3 m	3 m	1.5 m
Chimney Angle	Inlet / Outlet Opening		Chimney Length
45	0.4 m × 0.4 m		2.12 m
Nodes		No.	8071
Faces		No.	21351
Cells		No.	6687
Total In Flow		KG/S	1.16E+01
Total Out Flow		KG/S	-1.17E+01
Maximium Velocity in Whole Domain		Met/S	9.729
Maximum Temp. in whole domain		K	407.796
Converged at Iteration			817

Simulation Data (3D Model-1)											
At Center of the Room Inlet				At Chimney Inlet				At Chimney Outlet			
Location of Coordinates		Variable	Values	Location Coordinates		Variable	Values	Location Coordinates		Variable	Values
X (meter)	0.1	U (m/s)	0.027048	X (meter)	2.8	U (m/s)	-0.02573	X (meter)	1.29	U (m/s)	-0.505
Y (meter)	0.75	V (m/s)	0.018861	Y (meter)	2.85	V (m/s)	0.33161	Y (meter)	4.43	V (m/s)	0.5029
Z (meter)	2.25	VM (m/s)	0.06199	Z (meter)	0.2	VM (m/s)	0.4069	Z (meter)	0.2	VM (m/s)	0.7129
		P (N/m^2)	7.80E-01			P (N/m^2)	0.7433			P (N/m^2)	-0.00614
		Pt (N/m^2)	7.82E-01			Pt (N/m^2)	0.8577			Pt (N/m^2)	0.3529
		T (K)	297			T (K)	297.004			T (K)	305.215

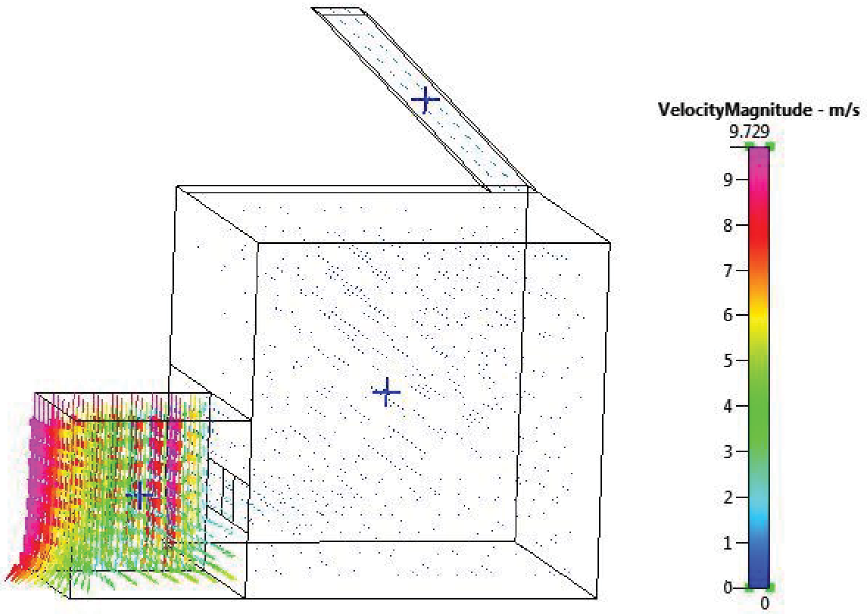

Figure: 4.22: Velocity Profile in CFD-View after Simulation of a 3D Room

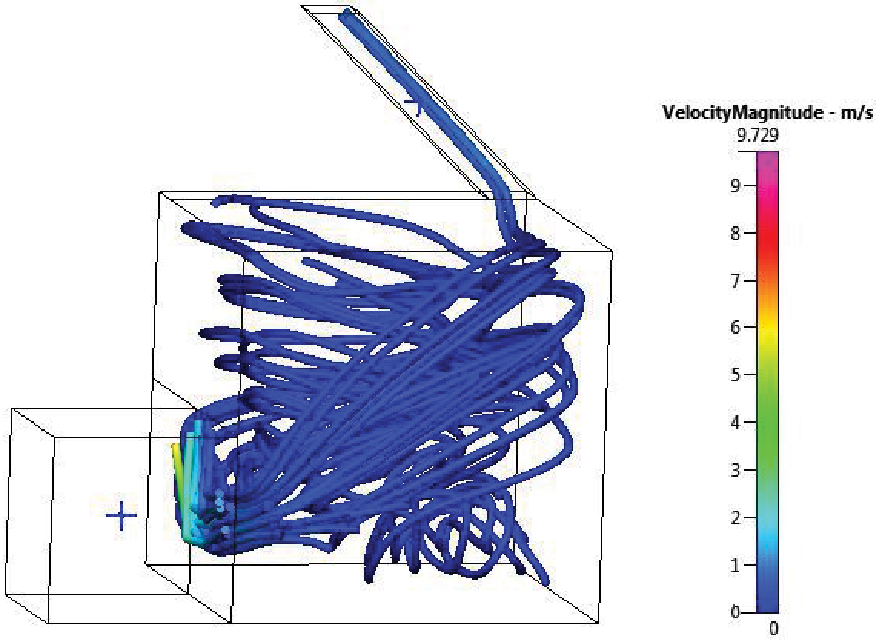

Figure: 4.23: Trace of air movement in CFD-View after Simulation of a 3D Room

It has been observed from analyses of above model (figure 4.27) that there is a significant amount of flow passes across the inlet box instead of going into the room. In order to get the actual values of flow rate going into the room, flows at individual boundary conditions and interfaces were obtained from the solver. The table below shows the summary of these individual flows at each inlet / outlets and interfaces:

Table: 4.2: Mass Balance Summary of 3D Model-1

Boundary-by-Boundary Mass Flow Rate Summary (kg/sec)				
Name	**Type**	**Inflow**	**Outflow**	**Sum**
Front Inlet	Inlet	6.57E-01	-3.16E-01	3.41E-01
Left Inlet	Inlet	0.00E+00	-1.34E+00	-1.34E+00
Right Inlet	Inlet	7.83E-02	-8.04E-01	-7.26E-01
Top Inlet	Inlet	1.86E+00	-6.05E-02	1.80E+00
Chimney Interface	Interface	6.95E-02	-6.95E-02	0.00E+00
Room Air Inlet	**Interface**	**7.09E-02**	**-7.09E-02**	0.00E+00
Chimney Outlet	Outlet	0.00E+00	-6.89E-02	-6.89E-02
Total Mass Flow Rate Summary		2.60E+00	-2.59E+00	1.75E-03

It can be seen from above mass flow rate summary that actual mass flow rate from room inlet (Inlet Interface) is only 7.09×10^{-2} kg/s which is much less as compared to total mass flow rate i.e. 2.60 kg/s. The most of the flow rate coming in total mass flow rate summary is passing across the inlet box. So our concentration and consideration will be actual mass flow rate going into the room through inlet interface.

In order to have better idea of flow rates and patterns, especially through inlet box, analyses were also carried out by changing the Solar Chimney location at roof top and positioning of air inlet opening, size of inlet opening and size of inlet box. The purpose was to get the idea about flow rates and air patterns in the real sized room. Analyses were carried out by changing different parameters for different simulation and their effect on the output parameters.

The following cases were considered for analysis:

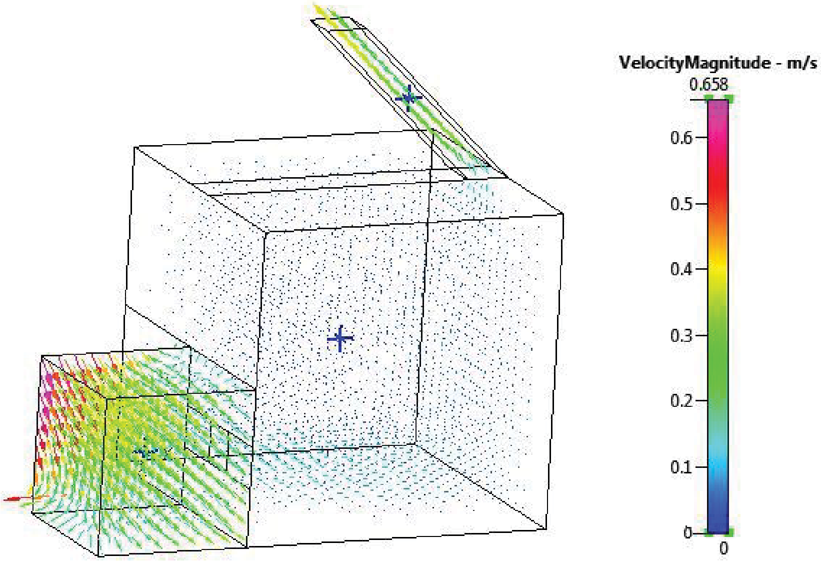

Figure:4.24: Velocity Profile after Simulation of a 3D Room with Solar Chimney Placed at Center of the Room

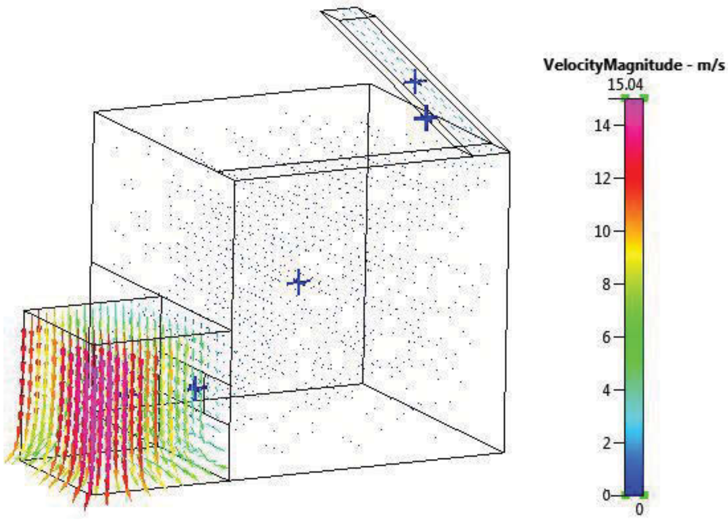

Figure:4.25: Velocity Profile after Simulation of a 3D Room with Solar Chimney Placed at Same Side of Room Inlet

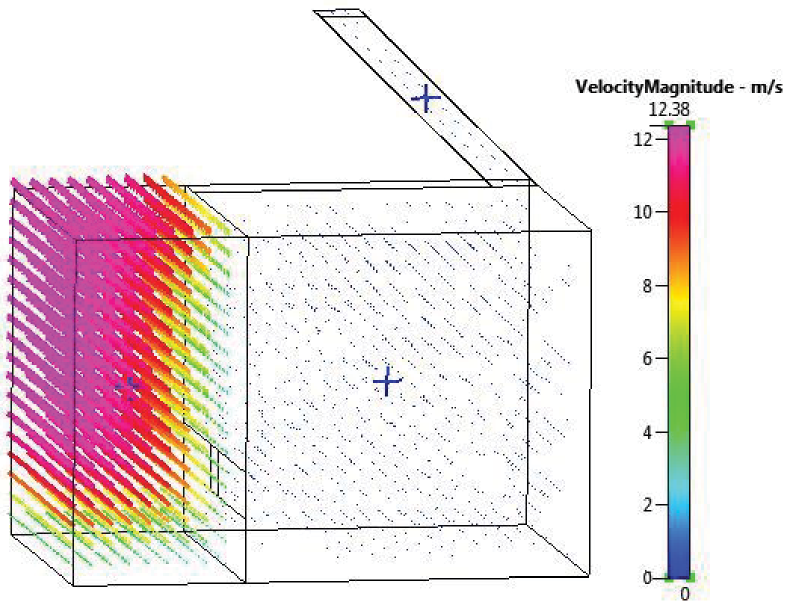

Figure:4.26: Velocity Profile after Simulation of a 3D Room with Bigger Inlet Box (1.5 meter × 3 meter × 3 meter) .

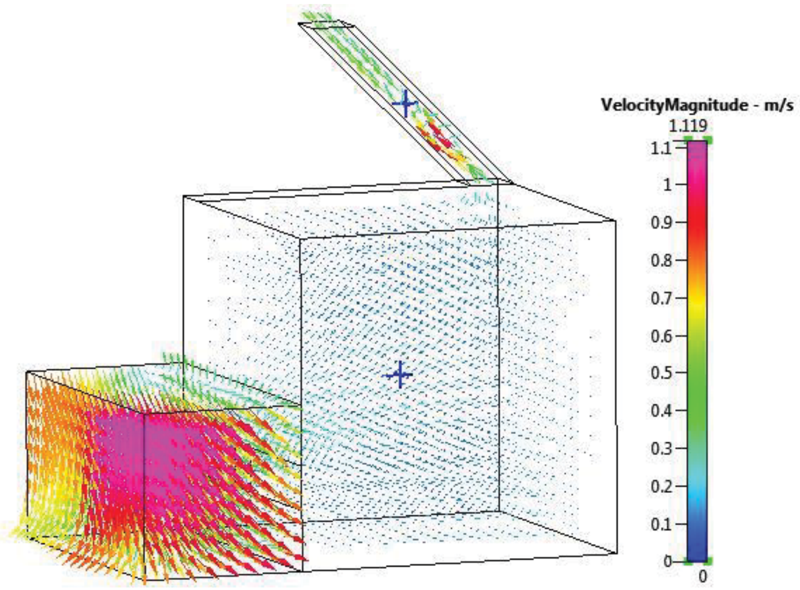

Figure:4.27: Velocity Profile after Simulation of a 3D Room with Bigger Inlet Box (1.5 meter × 3 meter × 1.5 meter).

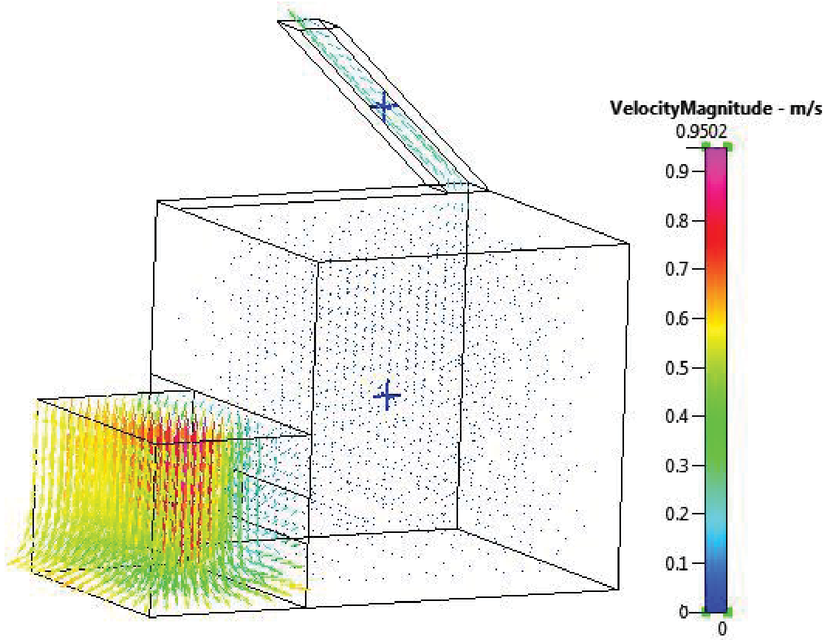

Figure:4.28: Velocity Profile after Simulation of a 3D Room with Bigger Inlet Box (1.5 meter × 2.25 meter ×1.5 meter).

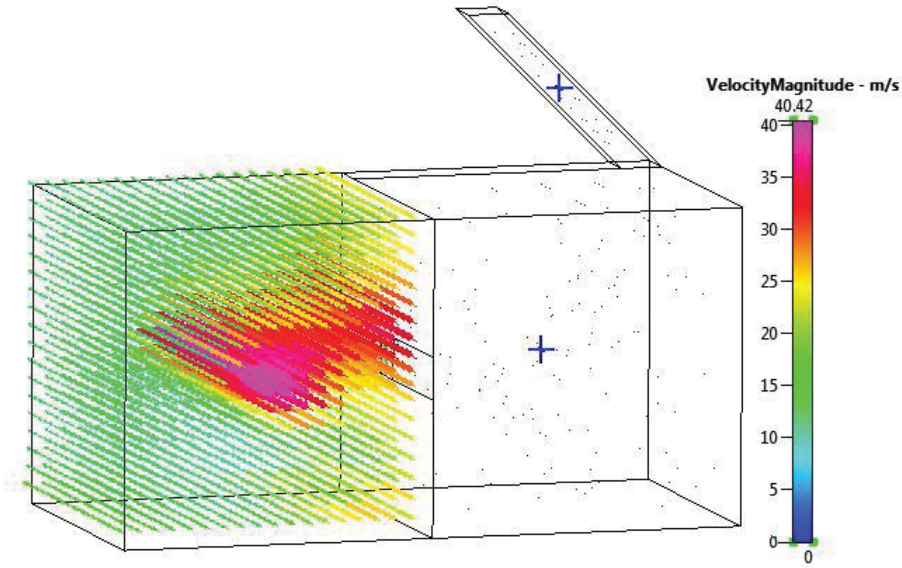

Figure:4.29: Velocity Profile after Simulation of a 3D Room with Bigger Inlet Box (3 meter × 3 meter × 3 meter) and Room Inlet at the Center of the Wall.

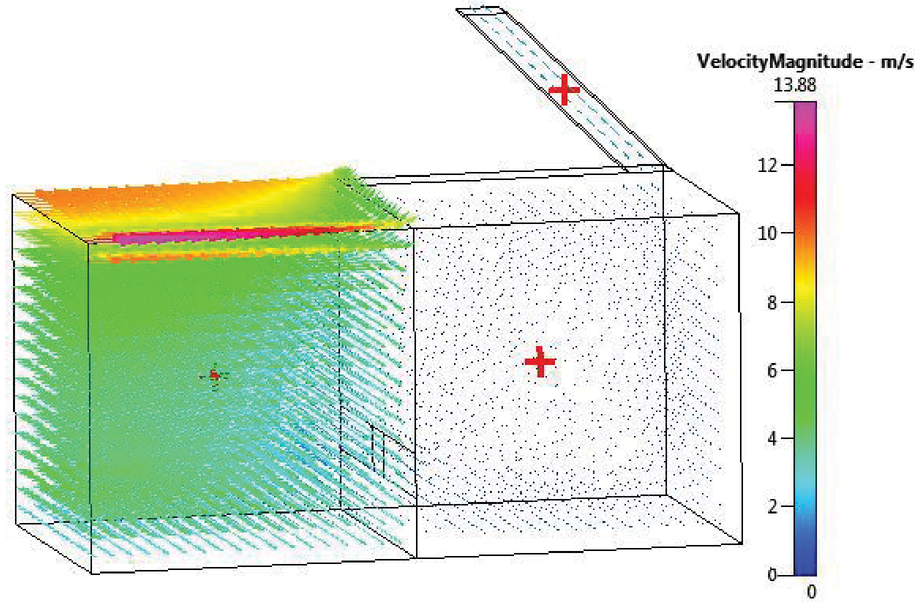

Figure:4.29a: Velocity Profile after Simulation of a 3D Room with Bigger Inlet Box (3 meter × 3 meter × 3meter) and Room Inlet at Bottom of the Wall.

In order to further investigate the behavior at room air inlet, the pressure profile has been studied along Z-Axis at following coordinates;

X = -0.02 ,Y = 0.75 , Z = 1.5

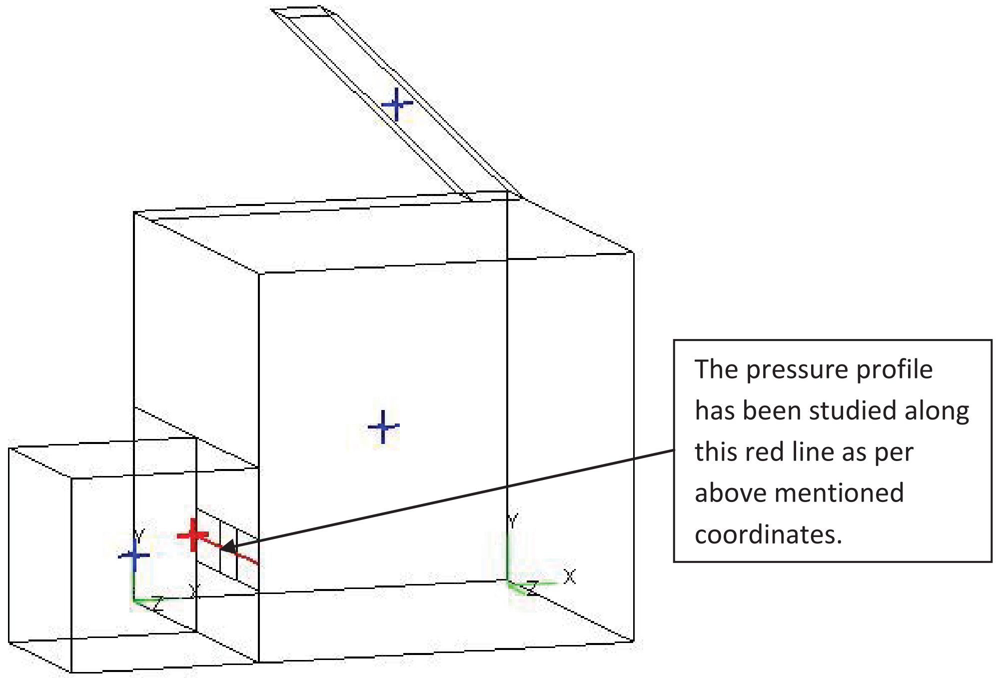

Figure: 4.30: Showing point at room air inlet where pressure profile has been studied.

The pressure profile trace and graph between P (Pressure) vs Z (Z-Axis) obtained at above coordinates are shown below:

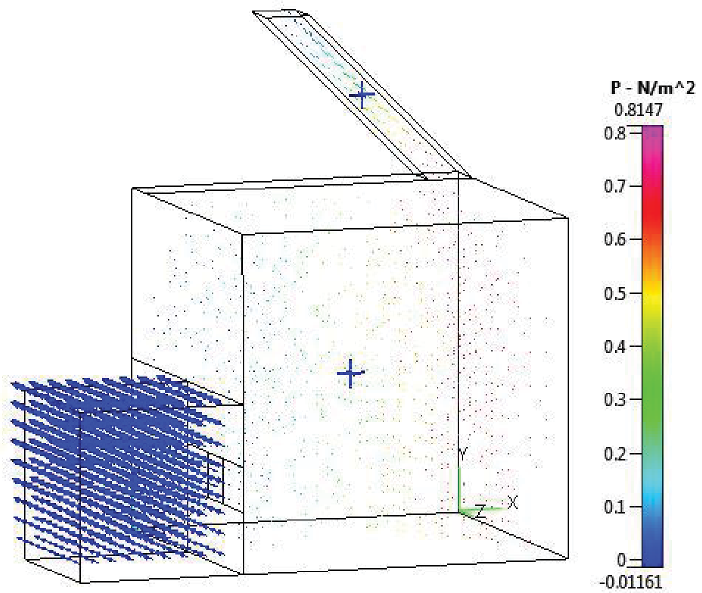

Figure: 4.30a: Pressure Trace in CFD-View after Simulation of a 3D Room with Pressure value of 0 N/m^2 at outlet i.e. solar chimney exit

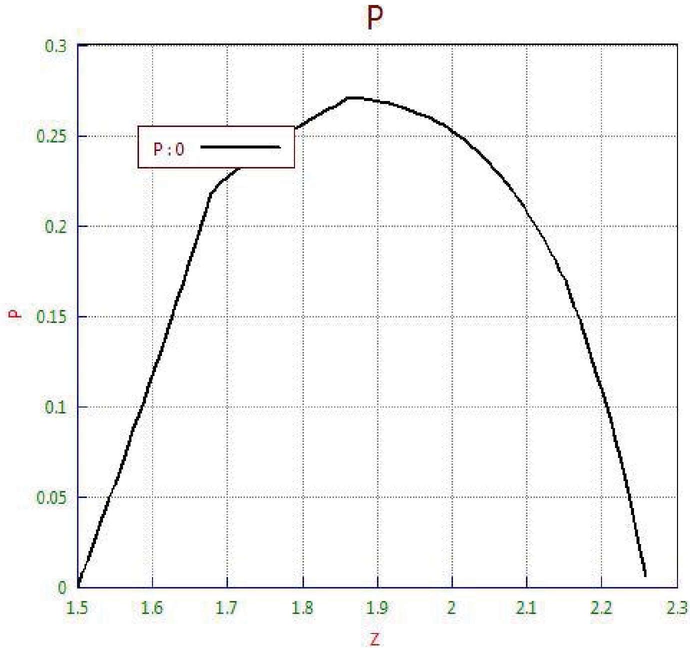

Figure: 4.31: Pressure vs Z axis graph just near inlet plane of the Room (with Pressure value of 0 N/m^2 at outlet i.e. solar chimney exit)

The following Legend / Notation have been used in above and all below graphs of Pressure vs Z-Axis.

P : 0--------	Legend showing that line in the graph is representing pressure values starting from Zero.
P	Pressure (N/m^2)
Z	Z - Axis

From above pressure trace and pressure values as seen in graph, it can be seen that the pressure at inlet opening of the room is greater as compared to right and left sides of the opening. Due to this higher positive pressure at inlet, most of the air flow is across the inlet box instead of going into the room. The same result can be seen in the Mass Flow Rate Summary shown above in Table : 4.2 where flow from actual room inlet is far less than the total mass flow rate from the model.

Keeping in view the above factors and in order to enhance the flow through room inlet opening, further study, simulation and analyses were carried out by giving negative (–ve) pressure value at chimney outlet. By giving fix –ve pressure value at outlet, the induce effect will increase which will create –ve pressure at inlet opening and ultimately, more air will pass through the room.

The main objective is to finalize Ideal Model / Physical conditions for further simulation where we will get equal (near to zero) pressures at right & left sides of the inlet box and –ve pressure at inlet opening so that air may go inside the room instead of cross flow across the inlet box.

The following table is showing data of models simulated with different pressure values at outlet:

Table:4.3: Simulation Data of 3D Model-1 with Different Pressure Values at Outlet

Simulation Results against Different Pressure Values at Outlet (solar chimney exit)					
Sr. No.	**Model Name**	**Pressure Fixed at Chimney Outlet (N/m^2)**	**Pressure at Center of the Inlet Opening - obtained after simulation (N/m^2)**	**Total Mass Flow Rate from the Model (Kg/Sec)**	**Mass Flow Rate from Room Air Inlet (Kg/Sec)**
1	3D Room Test 1.2	0	0.2807	2.59574	7.09E-02
2	3D Room Test 1.22	-0.35	-0.1618	1.4335	4.93E-02
3	3D Room Test 1.24	-0.4	-0.1565	1.021	5.68E-02
4	3D Room Test 1.26	-0.37	-0.1684	1.557	5.18E-02
5	3D Room Test 1.291	-0.32	-0.152	1.329	4.71E-02
6	3D Room Test 1.293	-0.25	-0.1098	1.029	4.56E-02
7	3D Room Test 1.294	-0.2	-0.0888	0.08823	4.24E-02
8	3D Room Test 1.295	-0.15	-0.0755	1.004	3.56E-02
9	3D Room Test 1.296	-0.1	-0.0472	0.499	3.42E-02
10	3D Room Test 1.297	-0.22	-0.063	0.4124	5.28E-02
11	3D Room Test 1.298	-0.23	-0.1082	1.1479	4.14E-02
12	3D Room Test 1.299	-0.21	-0.1004	1.104	4.15E-02

The following graphs showing pressure versus Z (length in Z direction) curves against different pressure values at chimney outlet. The pressure units are in N/m^2 and Z is in Meter.

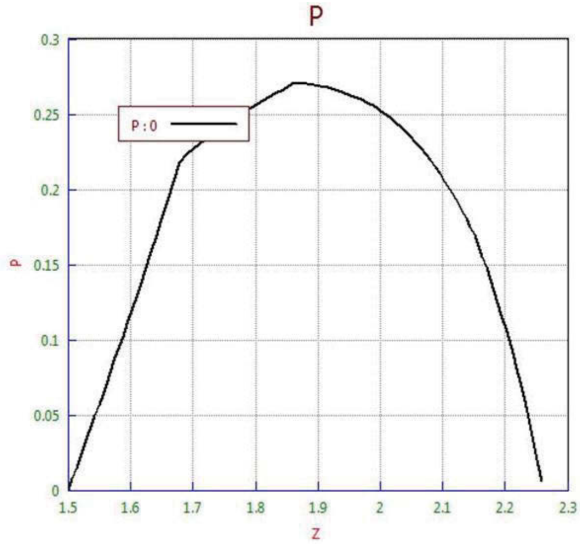

Figure: 4.32: Pressure vs Z graph just near inlet plane of Room against Sr. No.1 in Table : 4.2 (P= 0 N/m^2 at Outlet)

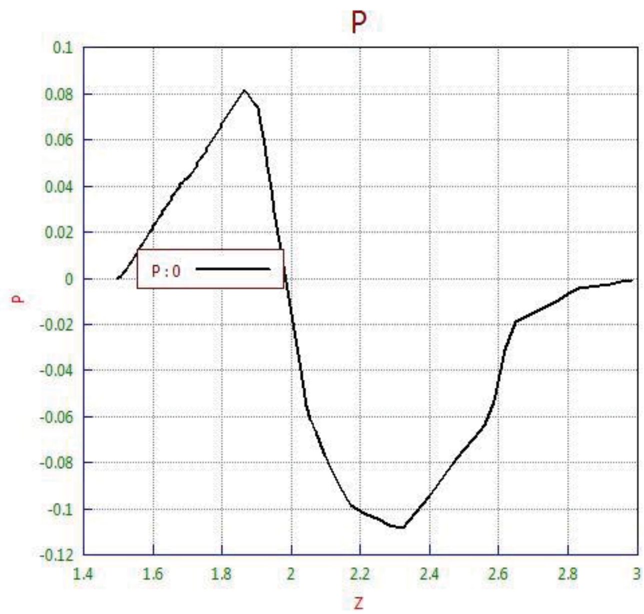

Figure: 4.33: Pressure vs Z graph just near inlet plane of Room against Sr. No.2 in Table : 4.2 (P= -0.35 N/m^2 at Outlet)

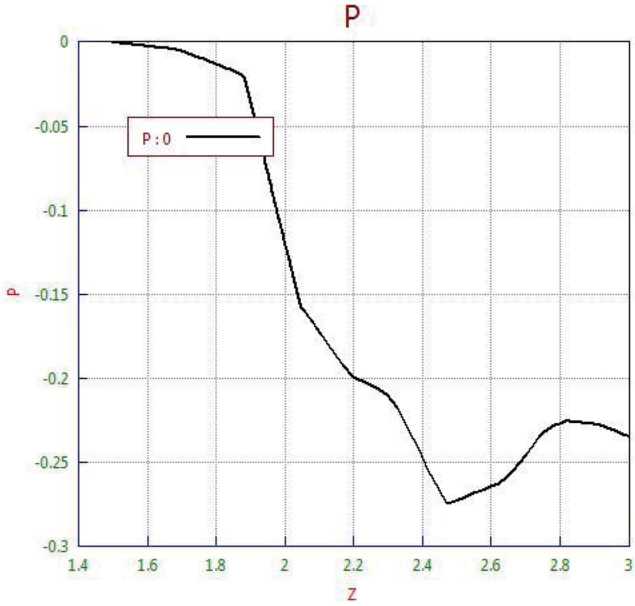

Figure: 4.34: Pressure vs Z graph just near inlet plane of Room against Sr. No.3 in Table : 4.2 (P= -0.4 N/m^2 at Outlet)

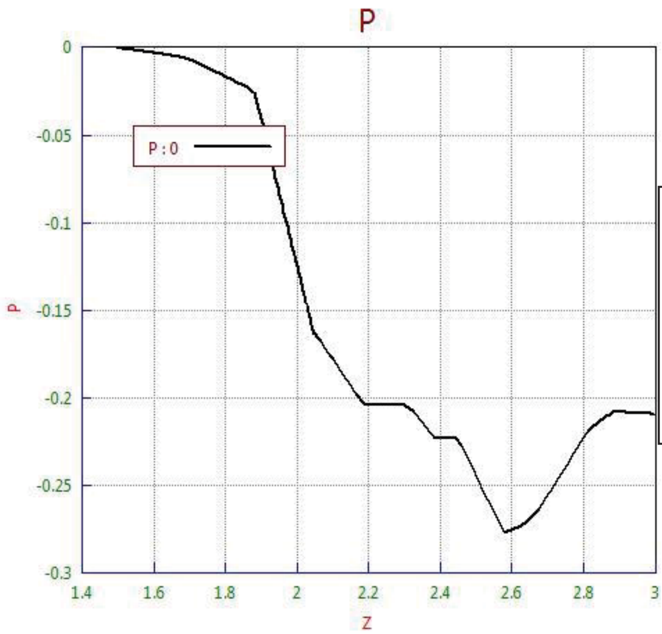

Figure: 4.35: Pressure vs Z graph just near inlet plane of Room against Sr. No.4 in Table : 4.2 (P= -0.37 N/m^2 at Outlet)

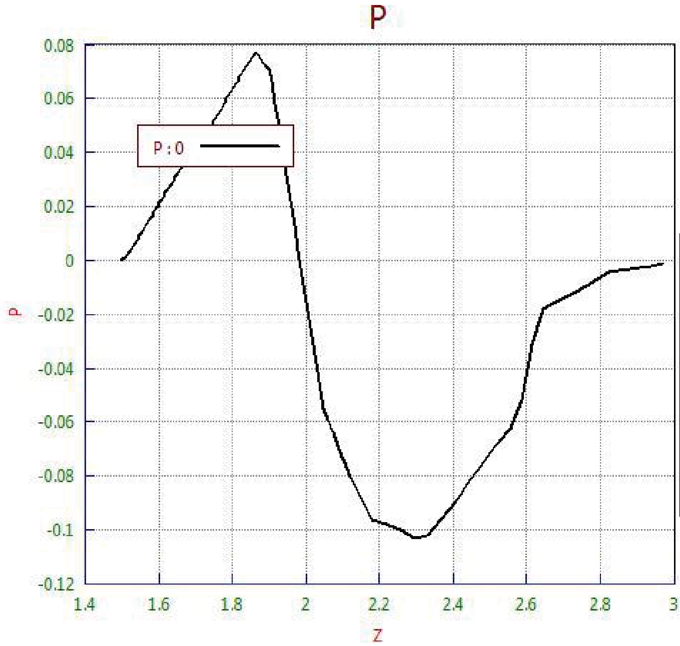

Figure: 4.36: Pressure vs Z graph just near inlet plane of Room against Sr. No.5 in Table : 4.2 (P= -0.32 N/m^2 at Outlet)

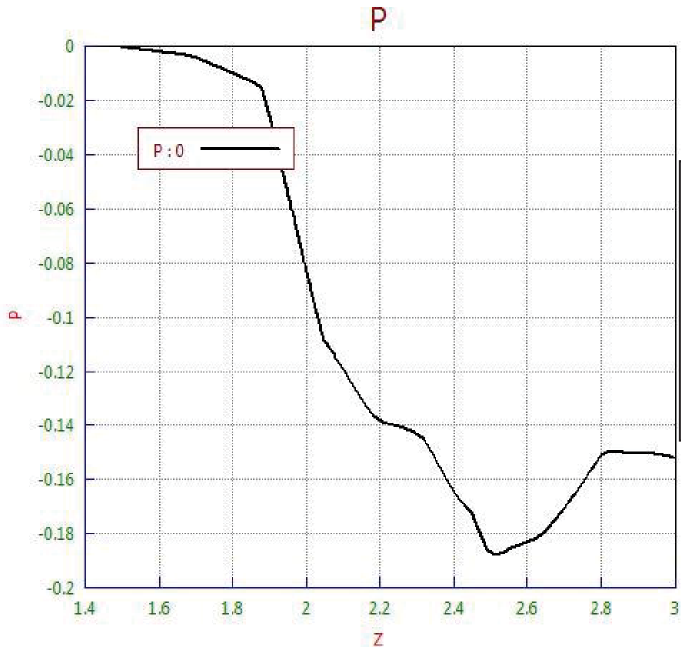

Figure: 4.37: Pressure vs Z graph just near inlet plane of Room against Sr. No.6 in Table : 4.2 (P= -0.25 N/m^2 at Outlet)

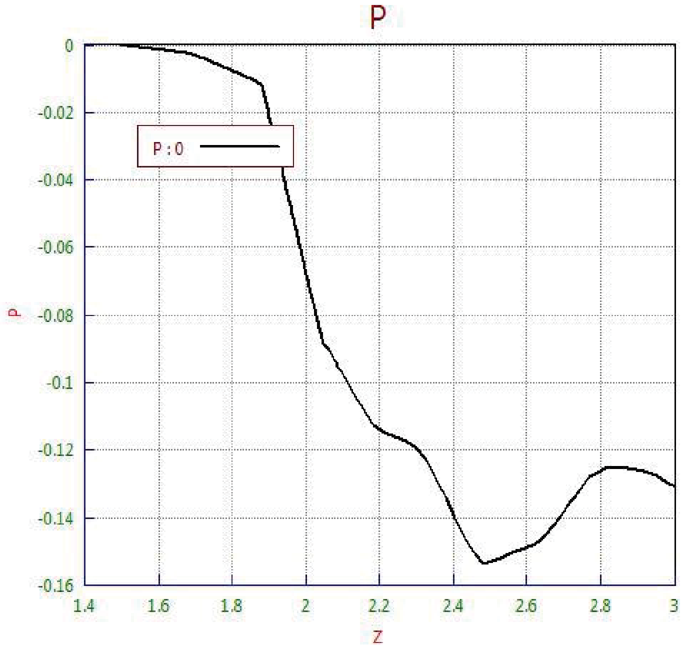

Figure: 4.38: Pressure vs Z graph just near inlet plane of Room against Sr. No.7 in Table : 4.2 (P= -0.2 N/m^2 at Outlet)

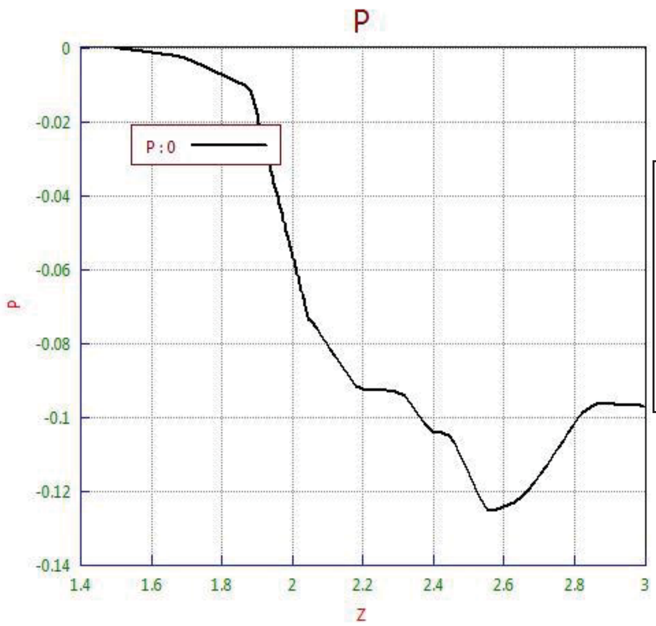

Figure: 4.39: Pressure vs Z graph just near inlet plane of Room against Sr. No.8 in Table : 4.2 (P= -0.15 N/m^2 at Outlet)

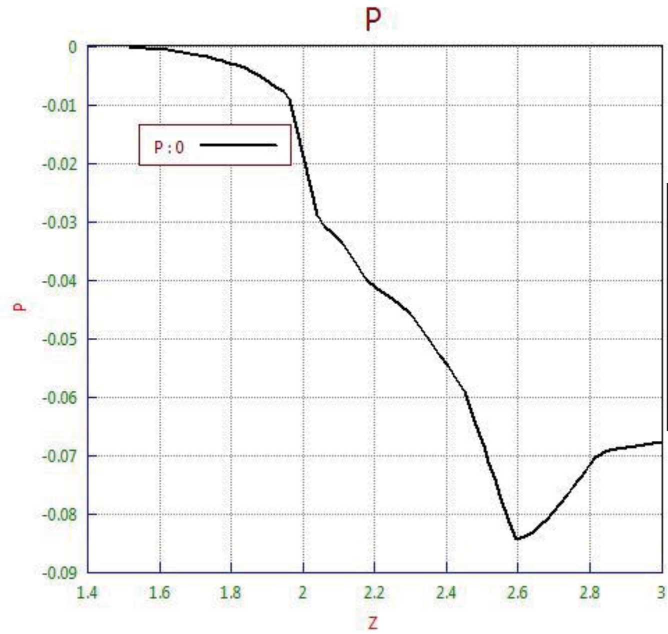

Figure: 4.40: Pressure vs Z graph just near inlet plane of Room against Sr. No.9 in Table : 4.2 (P= -0.1 N/m^2 at Outlet)

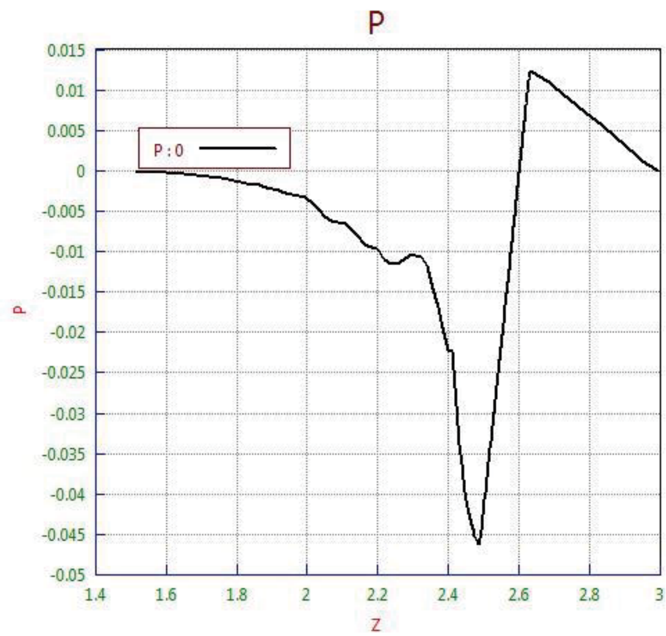

Figure: 4.41: Pressure vs Z graph just near inlet plane of Room against Sr. No.10 in Table : 4.2 (P= -0.22 N/m^2 at Outlet)

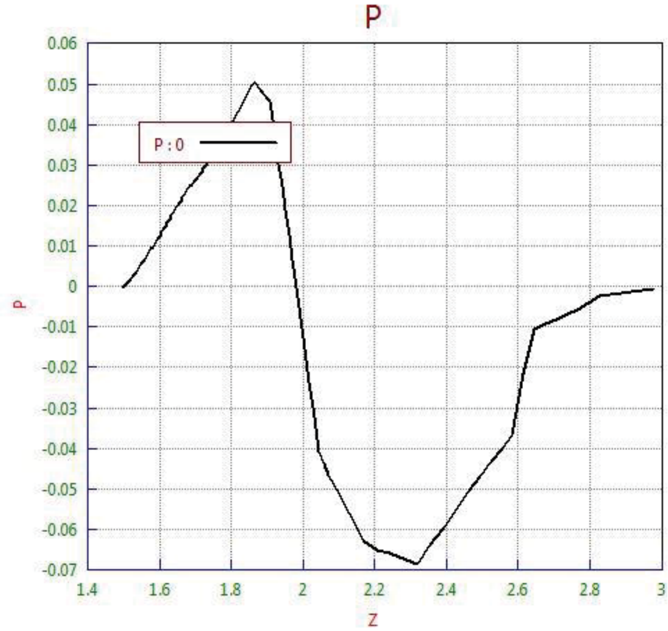

Figure: 4.42: Pressure vs Z graph just near inlet plane of Room against Sr. No.11 in Table : 4.2 (P= -0.23 N/m^2 at Outlet)

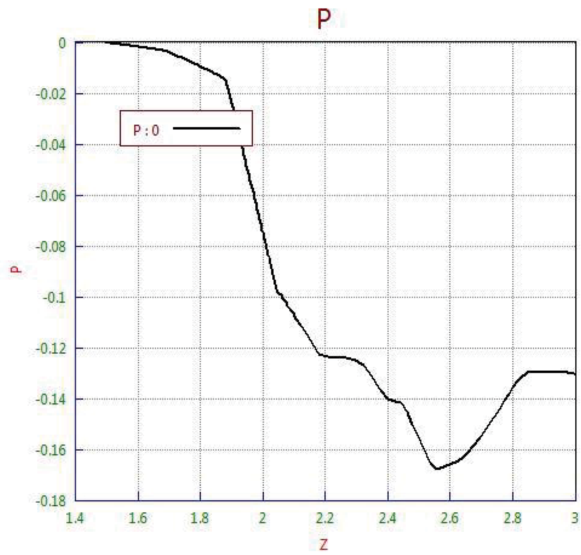

Figure: 4.43: Pressure vs Z graph just near inlet plane of Room against Sr. No.12 in Table : 4.2 (P= -0.21 N/m^2 at Outlet)

From the above simulations and analyses of results, the model at Sr. No. 10 where by the pressure at Chimney outlet was fixed at -0.22 N/m^2, gives the desired results. The pressure at left and right ends is zero while at the center is –ve pressure. The Pressure vs Z plane graph obtained after the simulation is reproduced below along with Velocity and Pressure profiles in the model. The Pressure profile clearly indicates proper and increased flow towards the room instead of cross flow across the inlet box.

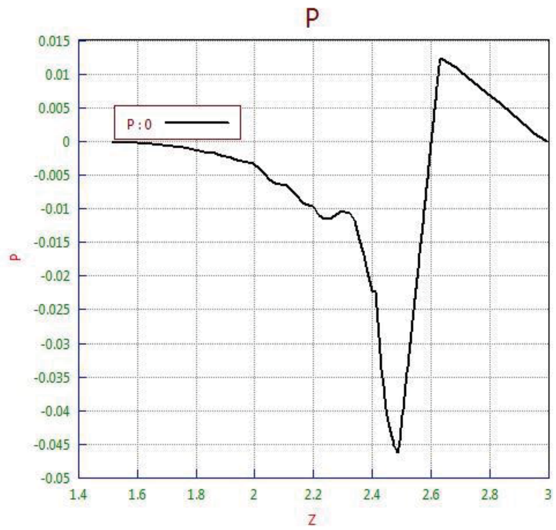

Figure: 4.44: Pressure vs Z graph just near inlet plane of Room against Sr. No.10 in Table : 4.2 (P= -0.22 N/m^2) at Outlet)

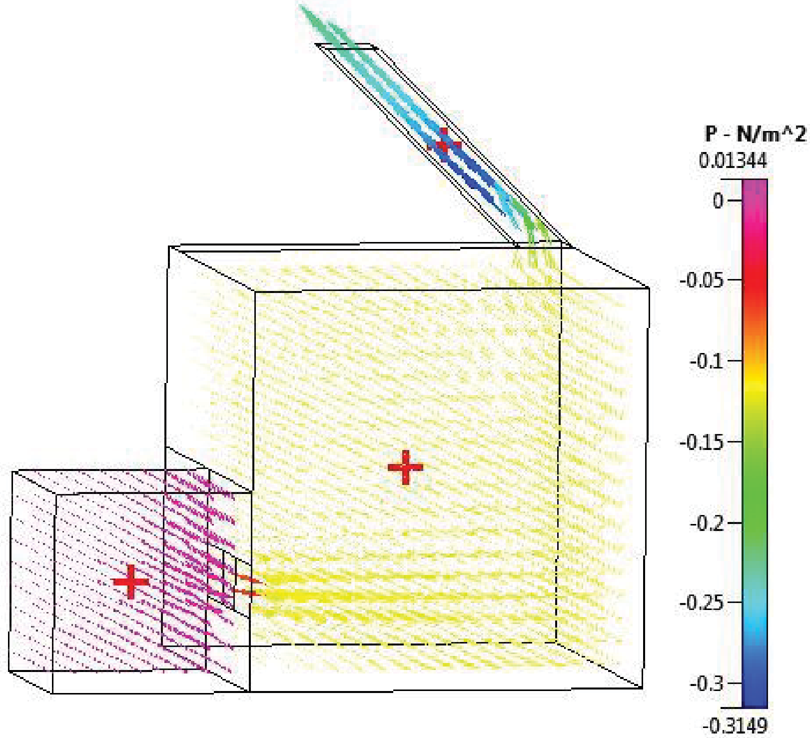

Figure: 4.46: Pressure Profile in a Room after Simulation (with Pressure value of -0.22 N/m^2 at outlet i.e. solar chimney exit)

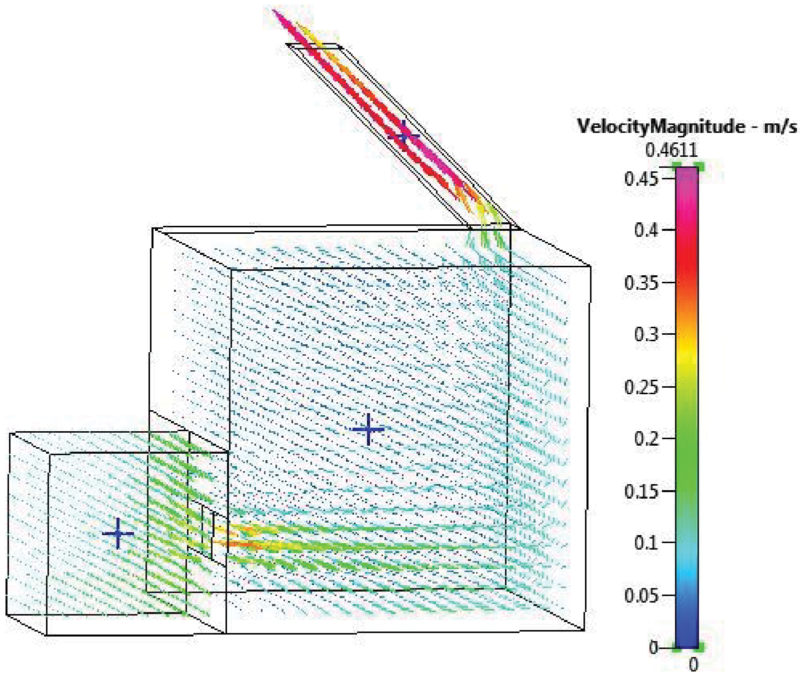

Figure: 4.47: Velocity Profile in a Room after Simulation (with Pressure value of -0.22 N/m^2 at outlet i.e. solar chimney exit)

Keeping in view the above factors and desired pressure profile achieved from this 3D Room Model, further analyses shall be carried out on this Room Models with chimney outlet pressure value fixed at -0.22 N/m^2.

4.8 Simulation and Validation of Results

Plenty of research has been carried out in the field of Solar Energy and particularly utilization of solar energy by employing solar chimney in the buildings to achieve natural ventilation with almost no consumption of energy. These include both experimental and computational studies. The solar chimneys are also being fitted in some modern buildings based on the extensive research in the field. The parameters and results of each research are different depending on the location of the physical experiments and parameters used. Similarly, computational results also depend on type / dimensions of the model, physical parameters used and most importantly, software package used. So it's really difficult to compare results of present research with some previous research as there may not be the experiment / computational that used exactly the same parameters with same software package. But on the other hand, a broader idea can be obtained from the previous researches which have been carried out almost with same parameters. In this research, the same idea has been obtained from the results / analysis of previous researchers and compared the results of this research with those of previous ones. The results of the basic factors, important in any natural ventilation like air mass flow rate, flow patterns, temperatures, pressures etc., have been found in-line with previous results. The exact comparison cannot be made as the models dimensions and some of the physical conditions are different as those of used in previous researches.

4.9 Grid Convergence Study

Grid Convergence test was employed to make sure that grids pattern employed for this simulation are adequate. More than 08 models were simulated with increased number of grid points and cells. Starting from 6,687 numbers of cells, the number of cells increased to 2,089,079 numbers. Each time, the convergence was achieved up to the desired level (1.0×10^{-04}) as shown in Figure:8 below and the results were analyzed.

Figure:4.48: Graph showing Convergence of the one Model up to desired level (1.0 × 10^{-04}). Above (Normalized values) and Below (Actual values)

To study the grid convergence, two points at different locations were taken and the important parameters at these points were noted. The percentage differences between values of same parameters in two simulations were analyzed. The process remains continues by making new models with increased number of cells unless grid convergence was achieved.

The table below shows a comparison of data against all these simulated models.

Table: 4.4: Table showing Comparison of Simulation Data of 3D Models – Values Taken at Three Different Locations

Room Length	Room Width	Chimney Height / Length	3D-1	3D-2	3D-2.1	3D-3	3D-4	3D-5	3D-6	3D-7
3 meter	3 meter	1.5 / 2.12 meter								
Chimney Angle	Inlet / Outlet Opening									
45 degree	0.4 meter × 0.4 meter									
Nodes		No.	8071	69115	136194	568411	867807	1256991	1673330	2145507
Faces		No.	21351	195228	389520	1655706	2537760	3686977	4923832	6323149
Cells		No.	6687	63152	126784	543842	835200	1215245	1625488	2089079
In Flow through the Domain		KG/S	0.412375	0.511374	0.253715	0.142086	0.0975369	7.69168	0.13275	0.114386
Out Flow through the Domain		KG/S	-0.412428	-0.511363	-0.253709	-0.142086	-0.0975363	-7.69148	-0.13192	-0.114316
Flow Through Room Air Inlet		KG/S	0.0506172	0.0524615	0.0537399	0.0455198	0.0482283	0.407384	0.0473381	0.0460977
Maximium Velocity in the Domain		Met/S	0.461119	0.666183	0.621556	0.487272	0.521485	6.18645	0.75194	0.678605
Maximum Temp. in the Domain		K	469.129	453.64	482.027	426.792	415.009	342.446	414.799	410.612
Converged at Iteration			984	2758	29917	35746	17732	15441	23139	38229
Data Locations										
At Center of the Room Inlet	Location	Variable								
X	0.1	U	0.234496	0.306009	0.366563	0.330459	0.355598	-2.23733	0.294489	0.00997998
Y	0.75	V	-0.038109	-0.126613	-0.0538946	-0.000806223	-0.00541679	0.204391	-0.00445365	-0.00310472
Z	2.25	VM	0.297762	0.375807	0.38069	0.332483	0.355674	2.25356	0.372419	0.339274
		P	-0.0953369	-0.109621	-0.0881073	-0.0608055	-6.94E-02	2.24E+01	-6.53E-02	-0.0529
		Pt	-0.0412965	-0.0258063	-0.00368553	0.00350077	0.00413107	25.3373	0.009317	0.0067861
		T	297	297	297	297	297	258.74	297	297
		K	4.05E-10							
At Chimney Inlet										
X	2.8	U	-0.0109065	-0.000923159	0.000532801	0.0259189	0.019089	6.43E-01	0.0490103	0.0173839
Y	2.85	V	0.180416	0.205313	0.160183	0.15575	0.164896	-2.5554	0.286529	0.216855
Z	0.2	VM	0.197677	0.20749	0.174691	0.164878	0.175505	2.64921	0.308031	0.176511
		P	-0.137439	-0.139335	-0.131897	-0.09597	-1.09E-01	2.76E+02	-1.27E-01	-0.110132
		Pt	-0.112215	-0.114034	-0.113553	-0.080032729	-0.0912468	271.697	-0.108671	-0.0617
		T	297.005	297	297	296.993	296.995	250.357	297	296.999
		K	5.97E-10							
At Chimney Outlet										
X	1.29	U	-0.261993	-0.323455	-0.311853	-0.259089	-0.284154	1.73582	-0.29216	-0.362486
Y	4.43	V	0.266126	0.400841	0.450417	0.256537	0.282733	-2.20705	0.26401239	0.358324
Z	0.2	VM	0.373573	0.516056	0.5482	0.364607	0.400852	2.80854	0.3194851	0.402726
		P	-0.224175	-0.223714	-0.224314	-0.223725	-0.225249	-200.822	-0.21369	-0.225035
		Pt	-0.0930767	-0.0544005	-0.0440442	-0.146521	-0.13191	-196.233	-0.125637	-0.0741293
		T	311.636	303.744	304.742	298.839	300.045	302.369	300.586	300.467
		K	1.08E-08							

The table above is showing a glimpse of data which has been collected after simulation of each model for analysis purpose. The data has been taken at three different locations against each model for the purpose of Grid Convergence Study.

The first measurement point has been taken at the entrance of room inlet with following axis locations:

Inlet at Bottom of the Wall	Inlet at Top Side of the Wall	Inlet at Bottom of the Wall Opposite to Chimney
1) X = 0.1 meter Y = 0.75 meter Z = 2.25 meter	1) X = 0.1 meter Y = 2.25 meter Z = 2.25 meter	1) X = 0.1 meter Y = 0.75 meter Z = 0.75 meter

The above location has been taken just after the entrance of the room inlet which will vary with the location of room air inlet location as shown above. This location is 0.1 meter away from entrance in X-Axis direction and at such height from the floor of the room which makes it in the front / middle of the inlet. This position comes out to be at the center of the room inlet opening.

The second measurement point has been taken at following axis locations:

2) X = 2.8 meter
Y = 2.85 meter
Z = 0.2 meter

The above location has been taken at the entrance of the solar chimney inlet. This location is 2.8 meter away from entrance in X-Axis direction, at the height of 2.85 meter from the floor of the room and 0.2 meter away from the walls.

The third measurement point has been taken at following axis locations:

3) X = 1.29 meter
Y = 4.43 meter
Z = 0.2 meter

The above location has been taken just before solar chimney outlet. This location is 1.29 meter away in X-Axis direction and at the height of 4.43

meter from the floor of the room. This position has been 0.07 meter before the solar chimney outlet and near the heated wall of the solar chimney in order to measure change in temperature due to heated wall.

All above mentioned data measurement locations has been shown in figure 4.48a below:

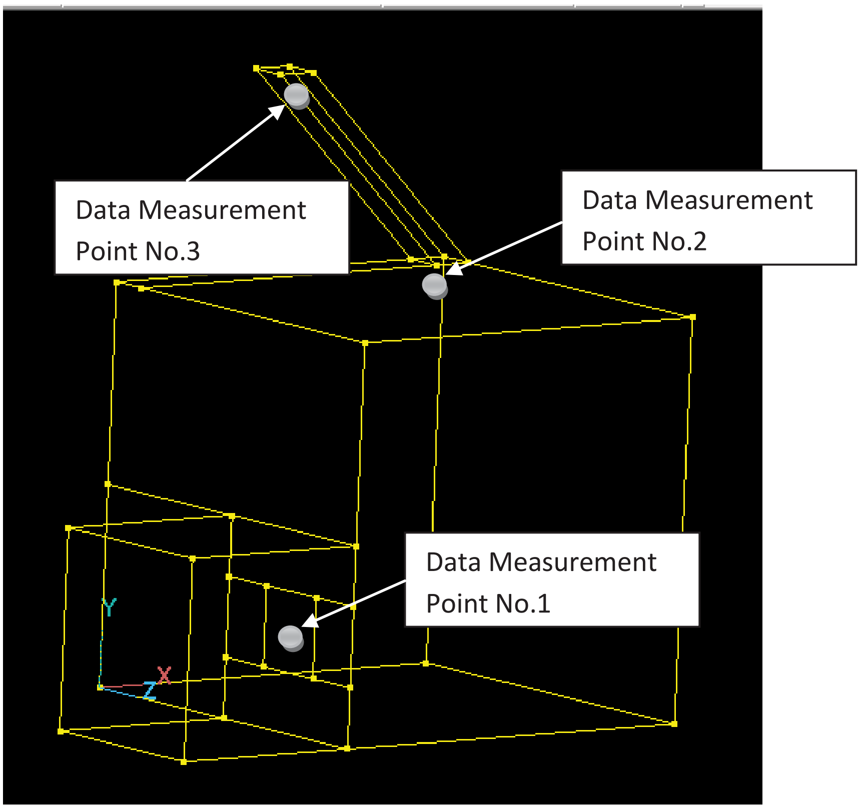

Figure 4.48a: Model with inlet opening at bottom of the side wall – Showing location of data measurement points for analysis

The following important parameters which are considered important in the study of natural ventilation through solar chimney have been noted at each measurement location:

U ---- Air velocity in horizontal direction (m/s)

V ---- Air velocity in vertical direction (m/s)

VM ---- Air velocity Magnitude at that location (m/s)

P ---- Point pressure at that location (N/m^2)

P_t ---- Total pressure at that location (N/m^2)

T ---- Air Temperature at that location (K)

The above data table has been given to give idea about the number of simulations carried out with increasing number of cells and what type of data has been collected against these simulations for further analysis. It is also giving the overview that the data has been collected at three different locations against each simulation.

In order to further explain above data table, the following two graphs in figures 4.48b and 4.48c have been drawn which shows change of flow through room inlet interface and maximum temperature in whole domain (***i.e. near heated surface of the Chimney***) with increasing number of cells. The inlet interface is a real room inlet opening of dimensions 0.4 × 0.4 meter and this has been shown in figure 4.48a where Data Measurement point No.1 is present. In CFD modeling, this opening is called as interface. The data has been measured at this point as this is a real opening of the room with which we are concerned for analysis.

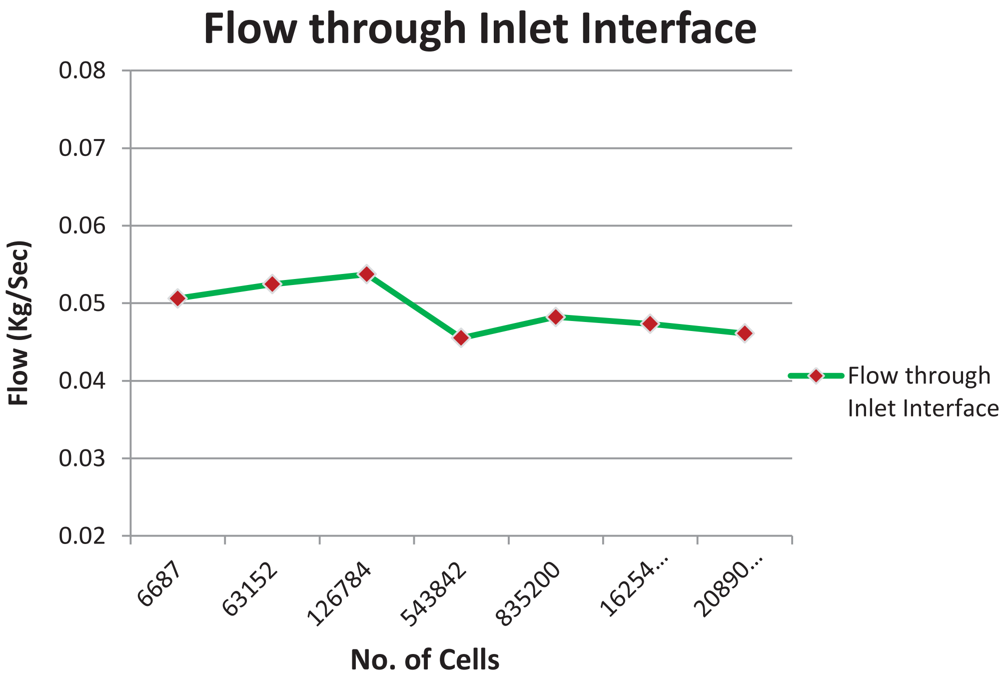

Figure:4.48b: Showing change in flow through inlet interface with increase in number of cells.

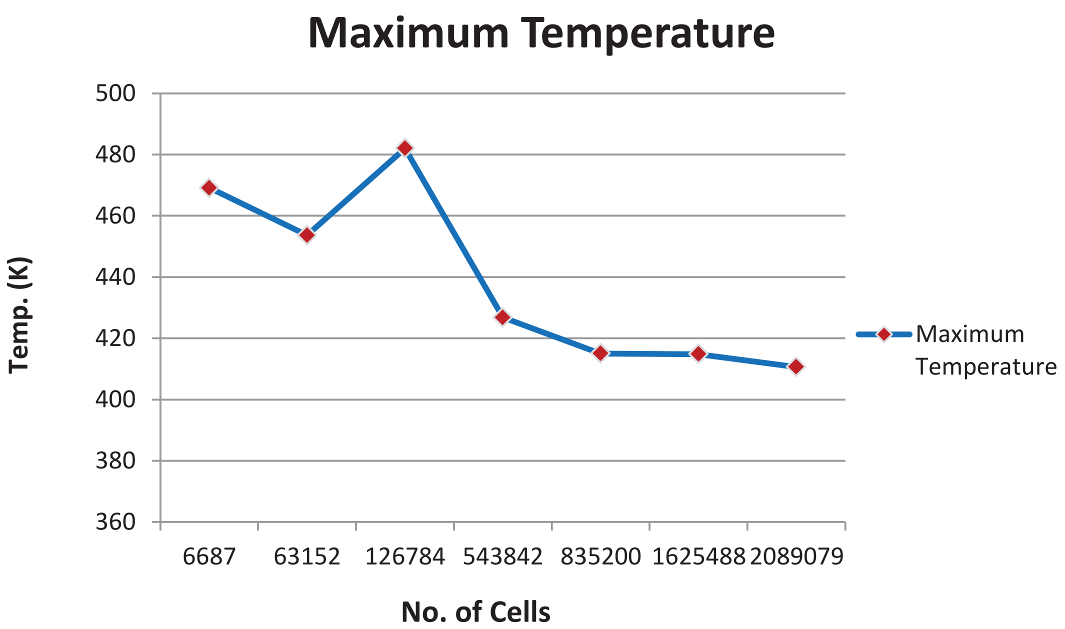

Figure:4.48c: Showing change in maximum temperature of domain (near Chimney's heated surface) with increase in number of cells.

The data of Model number 4 and Model number 7 against which grid convergence has been achieved are tabulated below:

Table: 4.5: Simulation Data of 3D Model-4 at Three Different Locations

Room Length	Room Width	Room Height	Chimney Height
3 m	3 m	3 m	1.5 m
Chimney Angle	Inlet / Outlet Opening		Chimney Length
45	0.4 m × 0.4 m		2.12 m
Nodes		No.	867807
Faces		No.	2537760
Cells		No.	835200
Total In Flow		KG/S	0.0975369
Total Out Flow		KG/S	-0.0975363
Maximium Velocity in Whole Domain		Met/S	0.521485
Maximum Temp. in whole domain		K	415.009
Flow Through Room Air Inlet		KG/S	0.0482283
Converged at Iteration			17732

Data Locations (3D Model-4)											
At Center of the Room Inlet				At Chimney Inlet				At Chimney Outlet			
Location Coordinates		Variable	Values	Location Coordinates		Variable	Values	Location Coordinates		Variable	Values
X	0.1	U	0.355598	X	2.8	U	0.019089	X	1.29	U	-0.28415
Y	0.75	V	-0.00542	Y	2.85	V	0.164896	Y	4.43	V	0.282733
Z	2.25	VM	0.355674	Z	0.2	VM	0.175505	Z	0.2	VM	0.400852
		P	-0.06939			P	-0.10931			P	-0.22525
		Pt	0.004131			Pt	-0.09125			Pt	-0.13191
		T	297			T	296.995			T	300.045

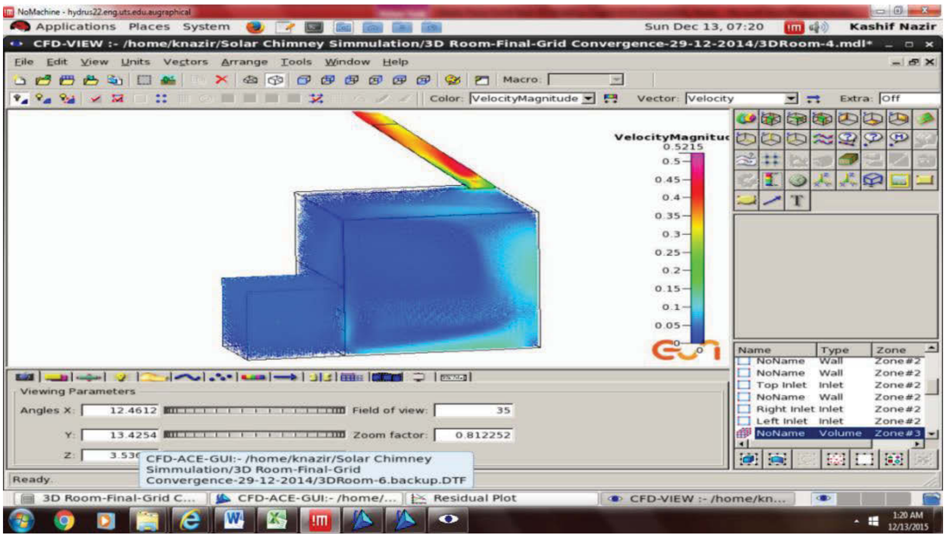

Figure: 4.49: Screen Shot of a 3D Room – 4 in CFD-View after Simulation

Table: 4.6: Simulation Data of 3D Model-7 at Three Different Locations

Room Length	Room Width	Room Height	Chimney Height
3 m	3 m	3 m	1.5 m
Chimney Angle	Inlet / Outlet Opening		Chimney Length
45	0.4 m × 0.4 m		2.12 m
Nodes		No.	2145507
Faces		No.	6323149
Cells		No.	2089079
Total In Flow		KG/S	0.377428
Total Out Flow		KG/S	-0.377089
Maximium Velocity in Whole Domain		Met/S	0.678605
Maximum Temp. in whole domain		K	410.612
Flow Through Room Air Inlet		KG/S	0.0460977
Converged at Iteration			38229

Data Locations (3D Model-7)											
At Center of the Room Inlet				At Chimney Inlet				At Chimney Outlet			
Location Coordinates		Variable	Values	Location Coordinates		Variable	Values	Location Coordinates		Variable	Values
X	0.1	U	0.00998	X	2.8	U	0.017384	X	1.29	U	-0.36249
Y	0.75	V	-0.0031	Y	2.85	V	0.216855	Y	4.43	V	0.358324
Z	2.25	VM	0.339274	Z	0.2	VM	0.176511	Z	0.2	VM	0.402726
		P	-0.0529			P	-0.11013			P	-0.22504
		Pt	0.006786			Pt	-0.0617			Pt	-0.07413
		T	297			T	296.999			T	300.467

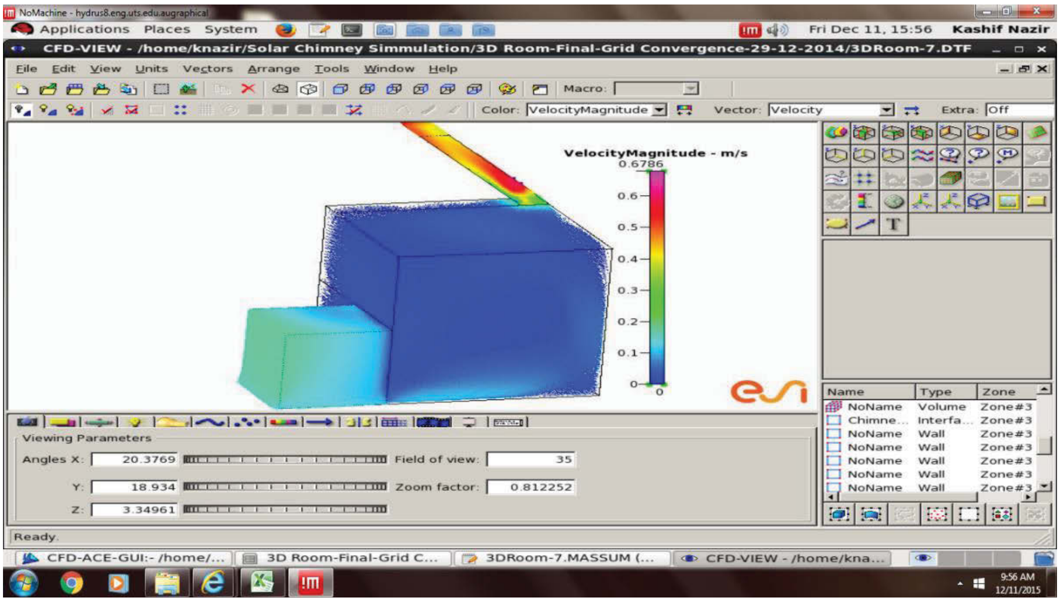

Figure: 4.50: Screen Shot of a 3D Room – 7 in CFD-View after Simulation

The table below is showing analysis of a selected data taken at two different points for grid convergence study:

Table: 4.7: Comparison of Velocity Magnitudes and Pressure at two selected points for two different cases

Variable	Case -4 (G1)	Case -7 (G2)	Difference (%age)
Grid Patterns (Number of Cells)	835200	2089079	150.13
Velocity Magnitude (m/s) at Chimney inlet	0.175505	0.176511	0.57
Velocity Magnitude (m/s) at chimney Outlet	0.400852	0.402726	0.47
Pressure (N/m^2) at Chimney Inlet	-0.109313	-0.110132	0.75
Pressure (N/m^2) at Chimney Outlet	-0.225249	-0.225035	-0.10

From the above data, it is cleared that the difference of velocity magnitude at same location i.e. Chimney inlet between two different cases is only 0.57% against 150% increased number of cells. To study grid independency more rigorously, another location was taken at chimney outlet. The difference of velocity magnitude at this location between above two cases is only 0.47%. Also, the difference of Pressure, at above mentioned points, between two cases is only 0.75% and 0.10%. The above results are showing good grid convergence.

4.9.1 Richardson Extrapolation Method for Grid Convergence Test

The best known way to demonstrate grid convergence is to repeat a computation with same model but with increased number of grid points and then compare the two solutions. Using results of simulation with two different grids, techniques such as Richardson Extrapolation (Roache 1998) can be used. Richardson Extrapolation is the discretization error estimator and is a recovery method. Discretization error is estimated by varying the grid spacing uniformly in all directions. This method is very simple to implement and should be used whenever possible.

The explanation of this method has already been explained in section 3.7.6 above.

Table-4.8 shows the amount of estimated fractional error, using the Generalization of Richardson Extrapolation, for velocity magnitude and temperature at two different selected points.

Table: 4.8: Estimated fractional error by using Generalization of Richardson Extrapolation for velocity magnitude and pressure at two different selected points

Grid Patterns (Number of Cells)	Selected Point 1		Selected Point 2	
	E_1 for Velocity Magnitude	E_1 for Pressure	E_1 for Velocity Magnitude	E_1 for Pressure
G1 (835200) G2 (2089079)	0.001090473	0.001425341	0.001425341	-0.000180741

As it is evident from the above table and graph that by increasing the number of grid cells, the amount of estimated fractional error E_1 for velocity and pressure at two selected points are much less than 1 (E_1<< 1) which verifies the reasonable accuracy of the solutions.

Based on above grid convergence study, Model number 4 was selected for further analysis with reference to change in room air inlet location.

4.10 Effect of Room Air Inlet Location

The change of room air inlet location significantly effects air flow rate and pattern in a room. In the previous chapter, effect of room air inlet on 2D model was studied / analyzed. In order to study this affect in a real sized 3D room, following three models, with different room inlet location, were considered for further analysis and comparison of results.

The purpose was to compare air flow rate and flow patterns with changing inlet location in order to suggest best location for room air inlet to get maximum air flow rate.

4.10.1 Room with Air Inlet at Bottom of the Side Wall

Below are the simulation results of a basic model with room air inlet location at bottom of the side wall and which has been successfully fall in the criteria of grid convergence test i.e. Model-4. The graphical and numerical results obtained against this simulation are presented below.

Table: 4.9: Simulation Data of 3D Model-4 at Three Different Locations having Inlet at Bottom of the Wall

Room Length	Room Width	Room Height	Chimney Height
3 m	3 m	3 m	1.5 m
Chimney Angle	Inlet / Outlet Opening		Chimney Length
45	0.4 m × 0.4 m		2.12 m
Nodes		No.	867807
Faces		No.	2537760
Cells		No.	835200
Total In Flow		KG/S	0.0975369
Total Out Flow		KG/S	-0.0975363
Maximium Velocity in Whole Domain		Met/S	0.521485
Maximum Temp. in whole domain		K	415.009
Flow Through Room Air Inlet		KG/S	0.0482283
Converged at Iteration			17732

Data Locations (3D Model-4) Inlet at Bottom of the Wall											
At Center of the Room Inlet				At Chimney Inlet				At Chimney Outlet			
Location Coordinates		Variable	Values	Location Coordinates		Variable	Values	Location Coordinates		Variable	Values
X	0.1	U	0.355598	X	2.8	U	0.019089	X	1.29	U	-0.28415
Y	0.75	V	-0.00542	Y	2.85	V	0.164896	Y	4.43	V	0.282733
Z	2.25	VM	0.355674	Z	0.2	VM	0.175505	Z	0.2	VM	0.400852
		P	-0.06939			P	-0.10931			P	-0.22525
		Pt	0.004131			Pt	-0.09125			Pt	-0.13191
		T	297			T	296.995			T	300.045

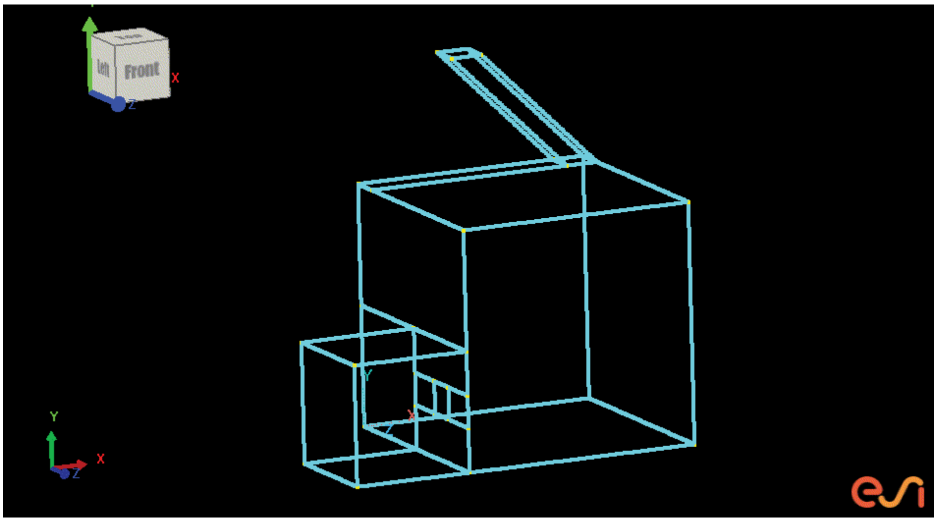

Figure: 4.51: 3D Room Model in CFD GEOM with Inlet at Bottom of the Wall.

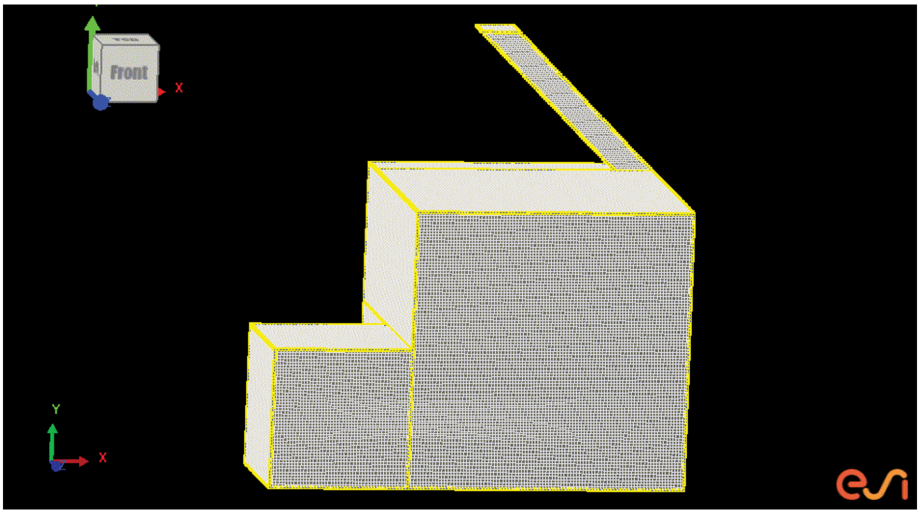

Figure: 4.52: 3D Room Model after Structured Meshing in CFD GEOM with Inlet at Bottom of the Wall.

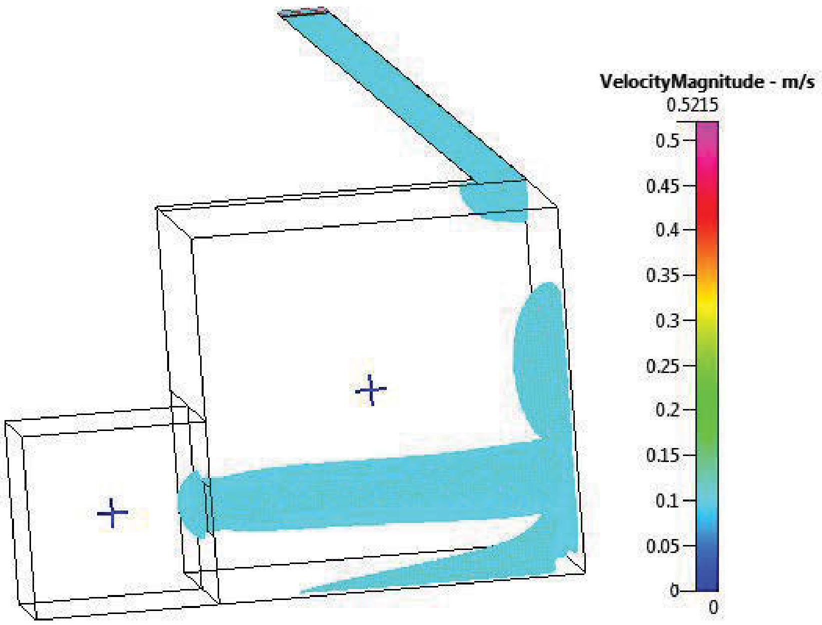

Figure: 4.53: 3D Room Model with Inlet at Bottom of the Wall in CFD View after Simulation showing Isocurve with Velocity Value of 0.1 m/s.

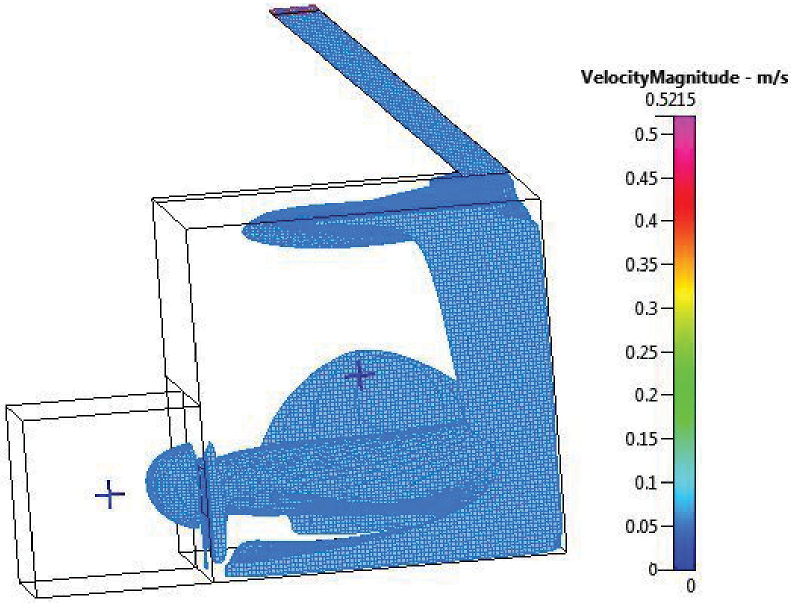

Figure: 4.53a: 3D Room Model with Inlet at Bottom of the Wall in CFD View after Simulation showing Isocurve with Velocity Value of 0.05 m/s.

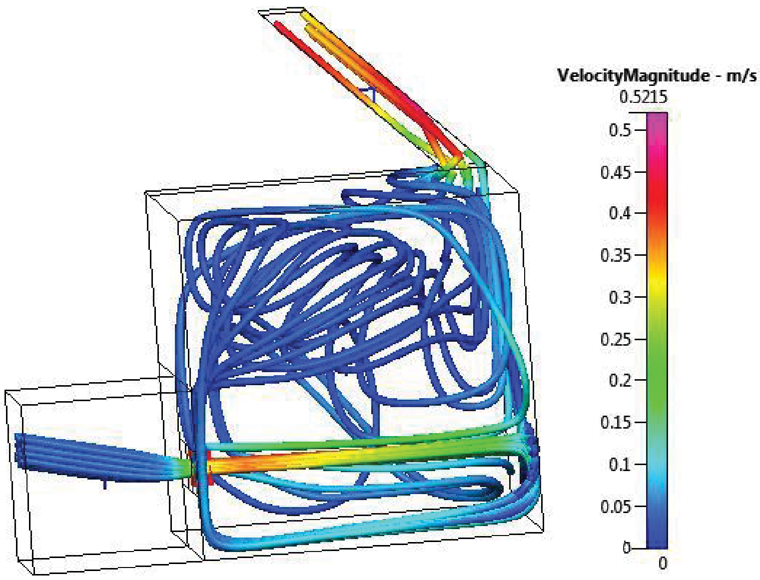

Figure: 4.54: 3D Room Model with Inlet at Bottom of the Wall in CFD View after Simulation showing trace of air parcel.

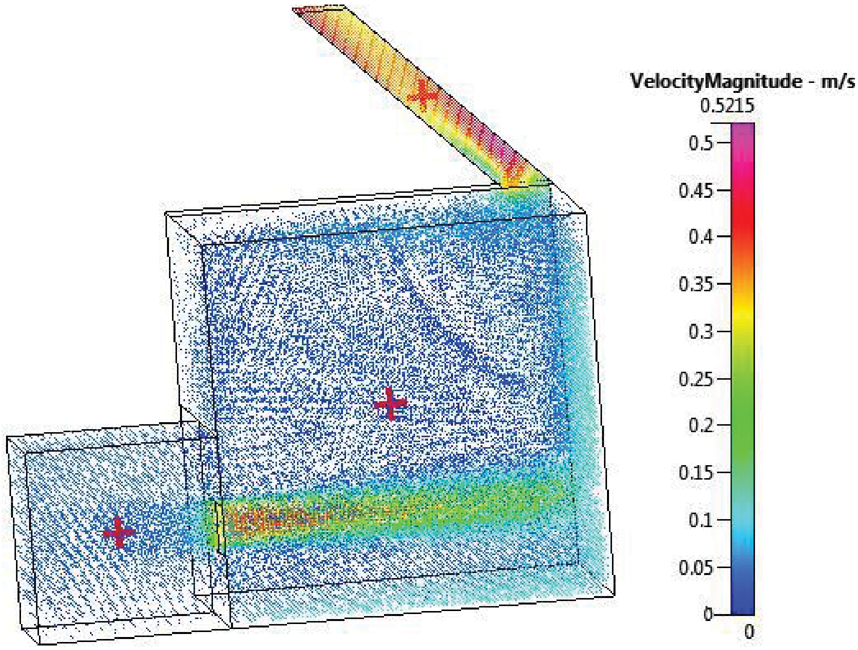

Figure: 4.55: 3D Room Model with Inlet at Bottom of the Wall in CFD View after Simulation showing Velocity Vectors.

4.10.2 Room with Air Inlet at Top of the Side Wall

A new model with room air inlet location at top of the wall was made having the same number of cells where grid convergence was achieved i.e. Model-4. The Model was simulated using the same parameters in order to compare results. The graphical and numerical results obtained against this simulation are presented below.

Table: 4.10: Simulation Data of 3D Model-4 at Three Different Locations having Inlet at Top Side of the Wall

Room Length	Room Width	Room Height	Chimney Height
3 m	3 m	3 m	1.5 m
Chimney Angle	Inlet / Outlet Opening		Chimney Length
45	0.4 m × 0.4 m		2.12 m
Nodes		No.	865943
Faces		No.	2535960
Cells		No.	835200
Total In Flow		KG/S	0.099351
Total Out Flow		KG/S	0.099294
Maximium Velocity in Whole Domain		Met/S	0.5476
Maximum Temp. in whole domain		K	418.61
Flow Through Room Air Inlet		KG/S	0.04927
Converged at Iteration			14632

Data Locations (3D Model-4) Inlet at Top Side of the Wall											
At Center of the Room Inlet				At Chimney Inlet				At Chimney Outlet			
Location Coordinates		Variable	Values	Location Coordinates		Variable	Values	Location Coordinates		Variable	Values
X	0.1	U	0.186741	X	2.8	U	0.005374	X	1.29	U	-0.24698
Y	2.25	V	-0.30827	Y	2.85	V	0.17042	Y	4.43	V	0.25369
Z	2.25	VM	0.36136	Z	0.2	VM	0.18206	Z	0.2	VM	0.35415
		P	-0.11144			P	-0.15496			P	-0.22456
		Pt	-0.02355			Pt	-0.13372			Pt	-0.1056
		T	297			T	296.999			T	302.244

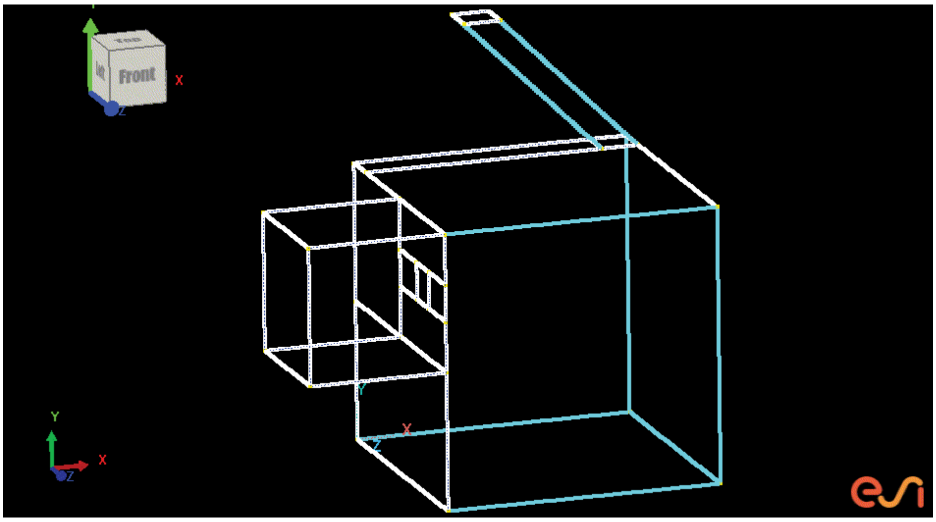

Figure: 4.56: 3D Room Model in CFD GEOM with Inlet at Top Side of the Wall.

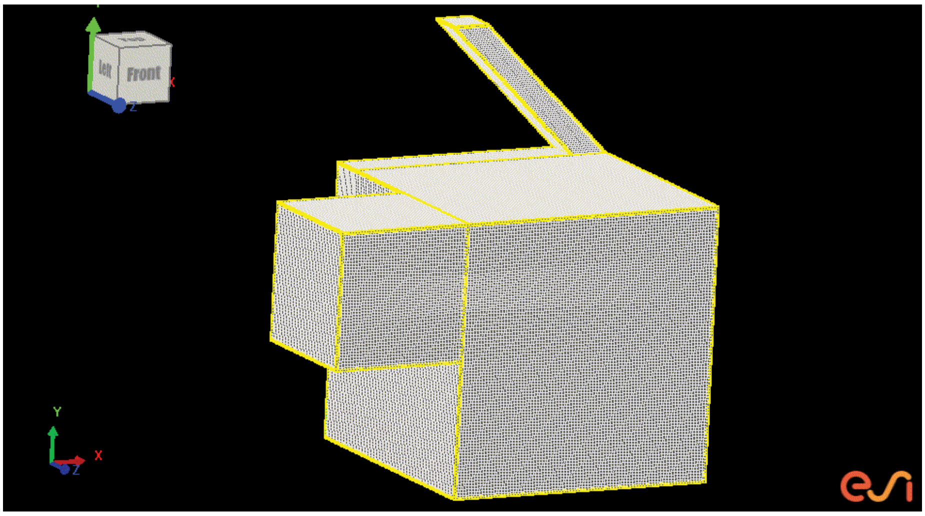

Figure: 4.57: 3D Room Model after Structured Meshing in CFD GEOM with Inlet at Top Side of the Wall.

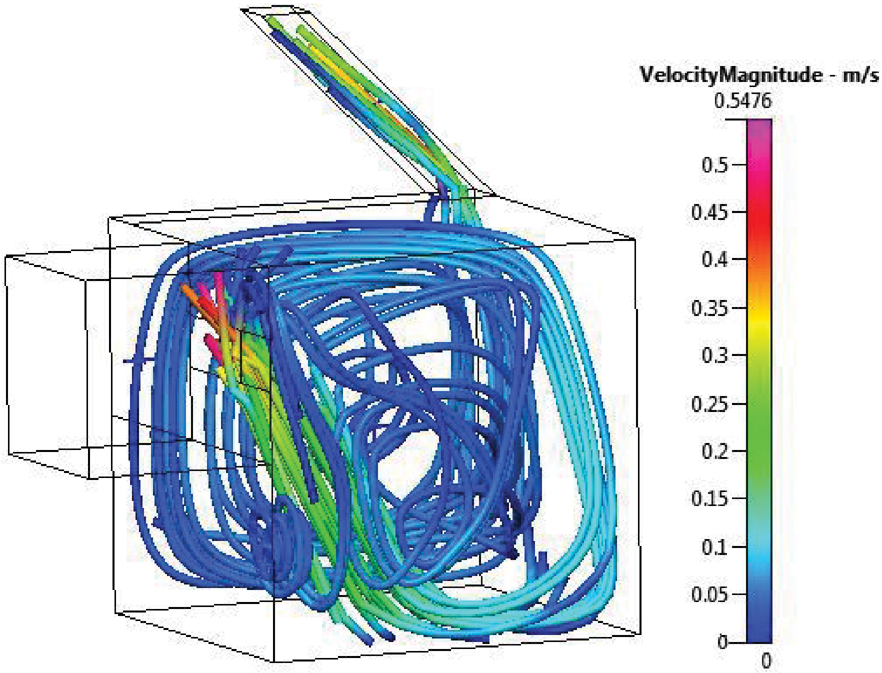

Figure: 4.58: 3D Room Model with Inlet at Top Side of the Wall in CFD View after Simulation showing trace of air parcel.

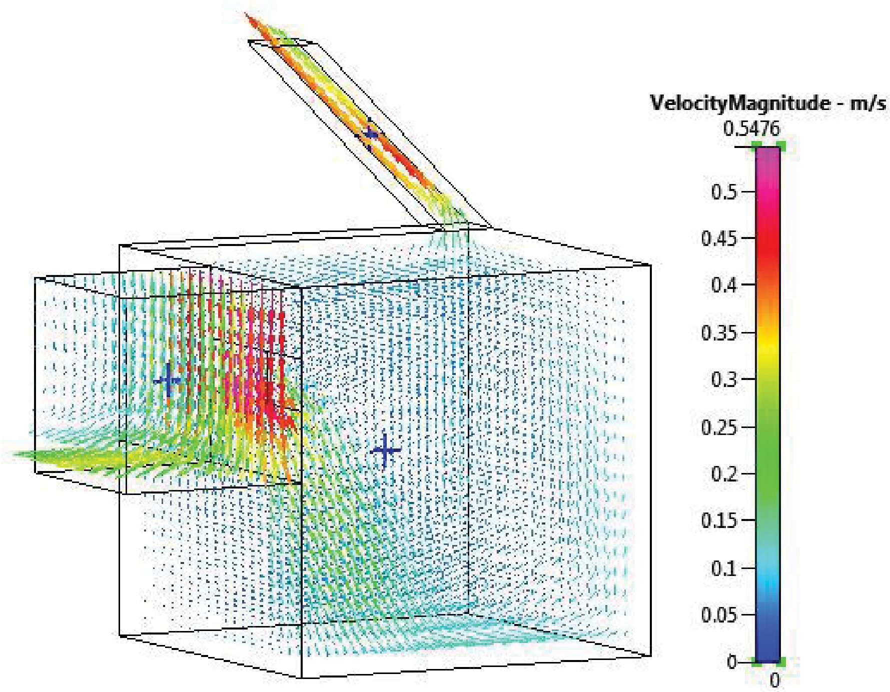

Figure: 4.59: 3D Room Model with Inlet at Top Side of the Wall in CFD View after Simulation showing Velocity Vectors.

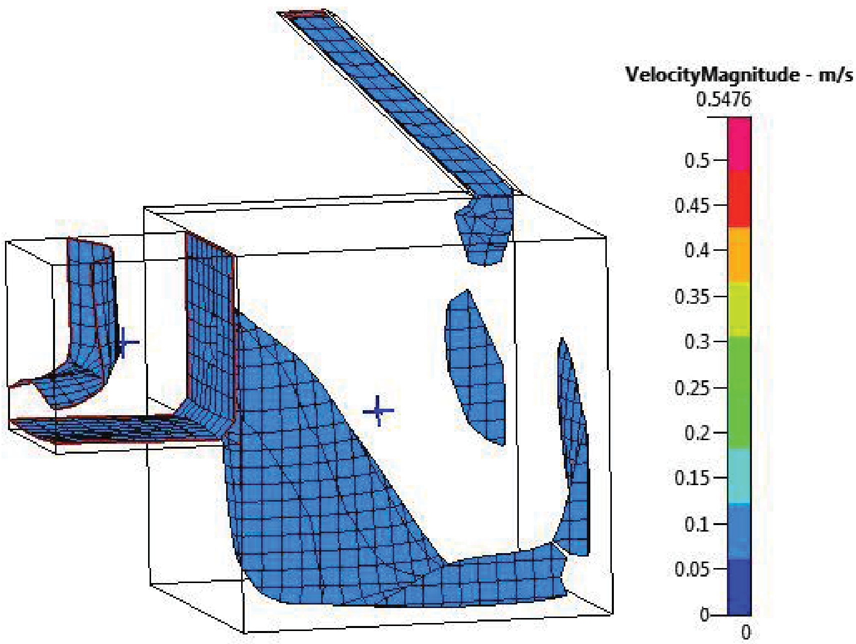

Figure: 4.60: 3D Room Model with Inlet at Top Side of the Wall in CFD View after Simulation showing Isocurve with Velocity Value of 0.1 m/s.

4.10.3 Room with Air Inlet at Opposite of the Chimney Wall

Another model with room air inlet location at bottom of the wall but opposite to Chimney side was made having the same number of cells where grid convergence was achieved i.e. Model-4. The Model was simulated using the same parameters in order to compare results. The graphical and numerical results obtained against this simulation are presented below.

Table: 4.11: Simulation Data of 3D Model-4 at Three Different Locations having Inlet Opposite to Chimney

Room Length	Room Width	Room Height	Chimney Height
3 m	3 m	3 m	1.5 m
Chimney Angle	Inlet / Outlet Opening		Chimney Length
45	0.4 m × 0.4 m		2.12 m
Nodes		No.	867807
Faces		No.	2537760
Cells		No.	835200
Total In Flow		KG/S	0.12618
Total Out Flow		KG/S	-0.12603
Maximium Velocity in Whole Domain		Met/S	0.5381
Maximum Temp. in whole domain		K	417.441
Flow Through Room Air Inlet		KG/S	0.04973
Converged at Iteration			21339

Data Locations (3D Model-4) Inlet at Bottom of the Wall Opposite to Chimney											
At Center of the Room Inlet				At Chimney Inlet				At Chimney Outlet			
Location Coordinates		Variable	Values	Location Coordinates		Variable	Values	Location Coordinates		Variable	Values
X	0.1	U	0.19218	X	2.8	U	0.02558	X	1.29	U	-0.24985
Y	0.75	V	-0.30497	Y	2.85	V	0.1797	Y	4.43	V	0.25935
Z	0.75	VM	0.36257	Z	0.2	VM	0.18778	Z	0.2	VM	0.3623
		P	-0.11125			P	-0.16312			P	-0.2265
		Pt	-0.02492			Pt	-0.14038			Pt	-0.11537
		T	297			T	296.998			T	301.756

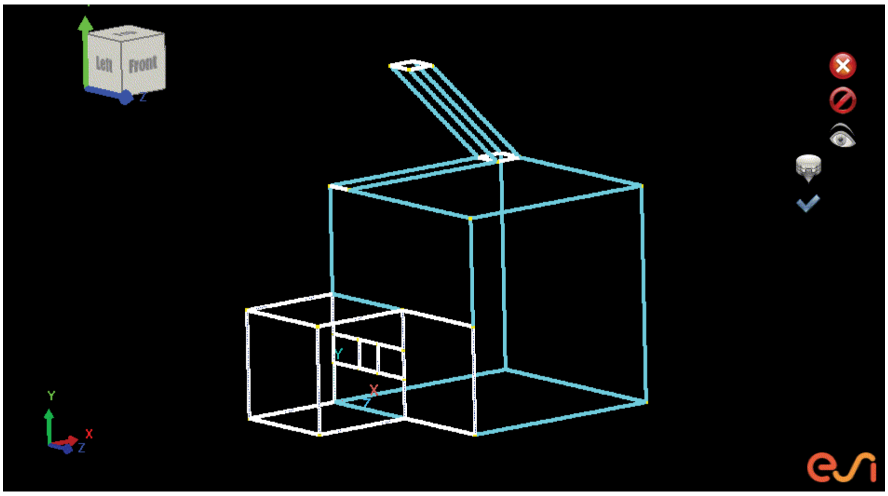

Figure: 4.61: 3D Room Model in CFD GEOM with Inlet Opposite to Chimney Side.

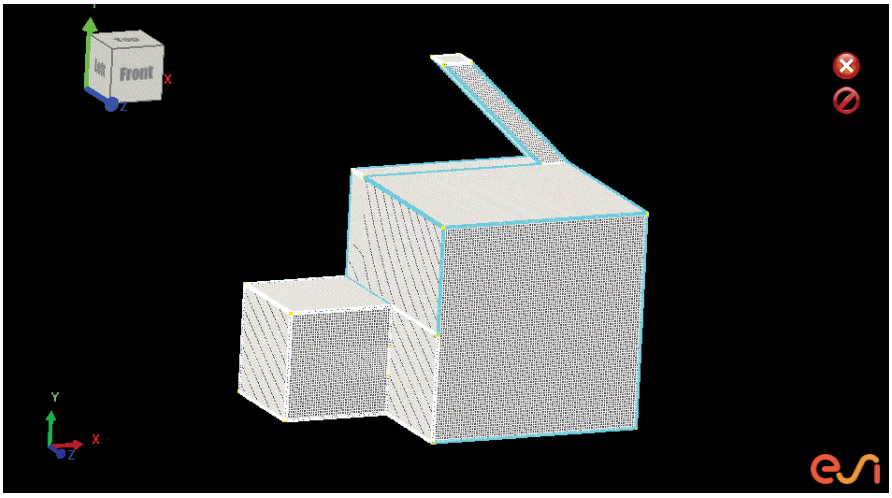

Figure: 4.62: 3D Room Model after Structured Meshing in CFD GEOM with Inlet Opposite to Chimney Side.

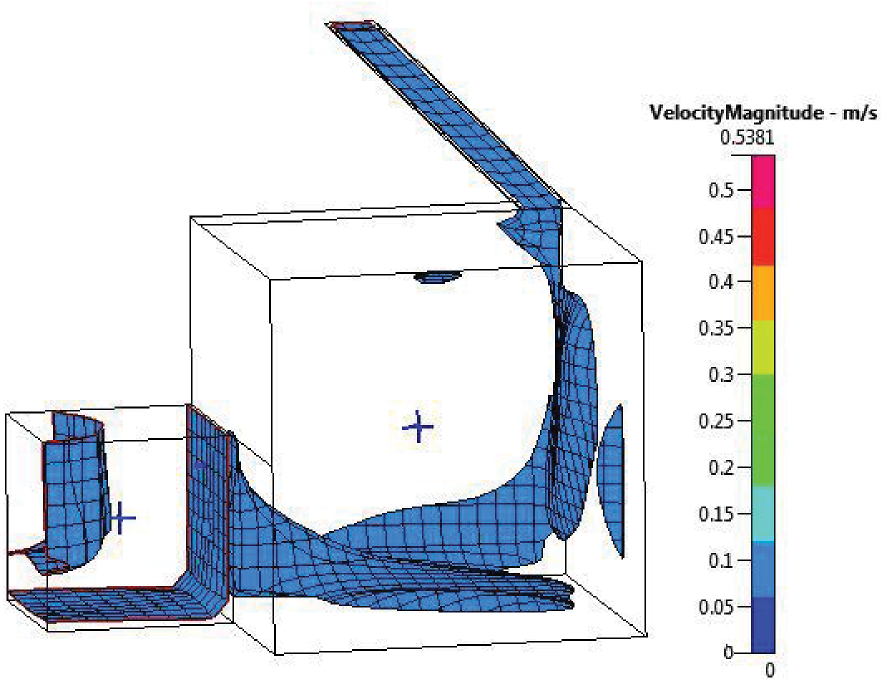

Figure: 4.63: 3D Room Model with Inlet Opposite to Chimney Side in CFD View after Simulation showing Isocurve with Velocity Value of 0.1 m/s.

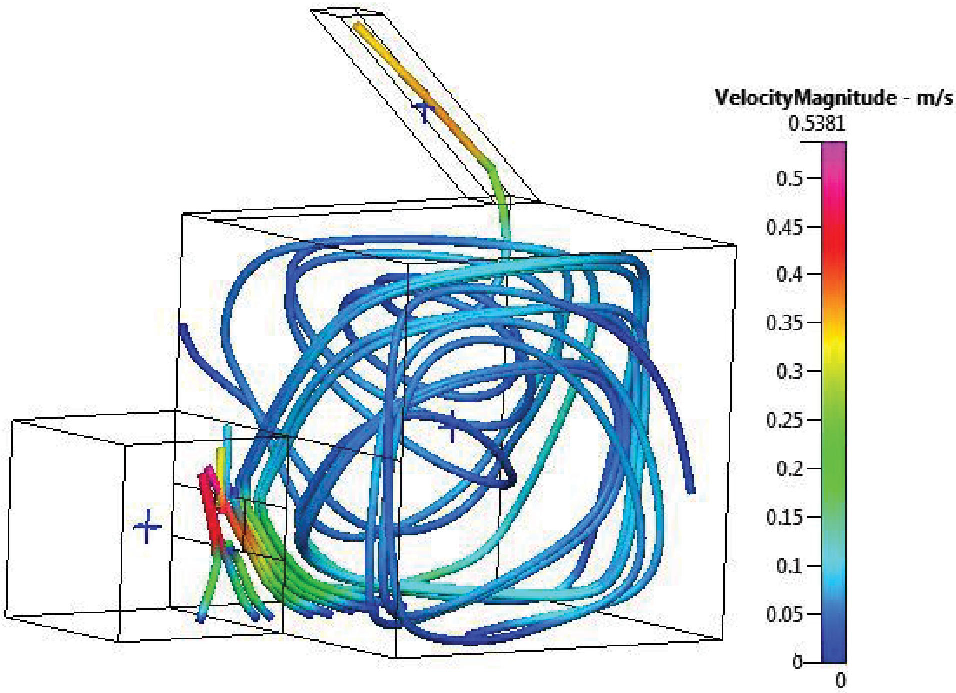

Figure: 4.64: 3D Room Model with Inlet Opposite to Chimney Side in CFD View after Simulation showing trace of air parcel.

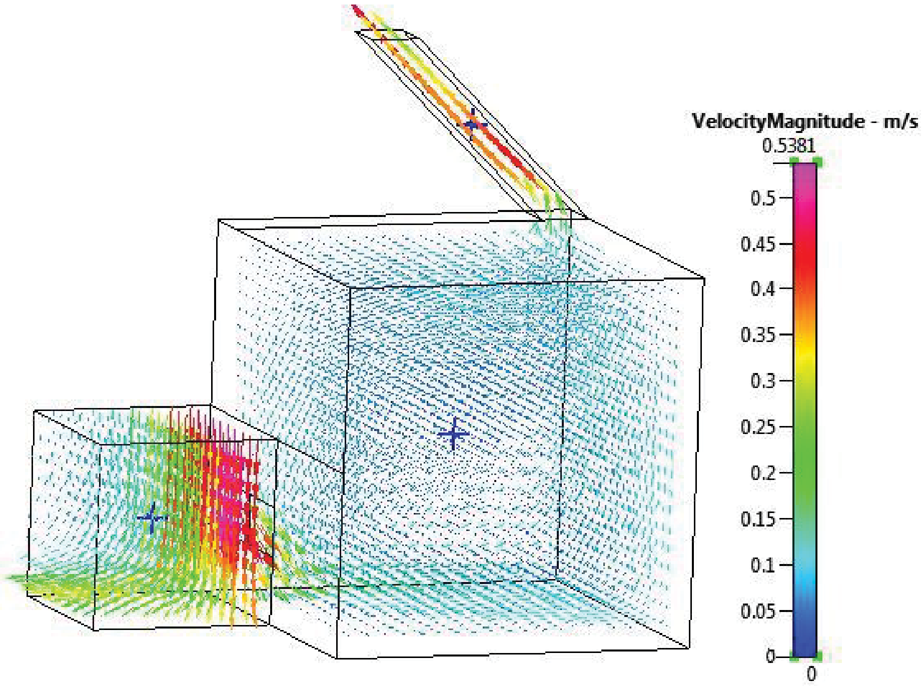

Figure: 4.65: 3D Room Model with Inlet Opposite to Chimney Side in CFD View after Simulation showing Velocity Vectors.

4.10.4 Solution Convergence and Mass Flow Rate Analysis

The above 3-Dimensional models have been simulated using physical parameters explained previously. The convergence criterion was kept at 0.0001 for each simulation and acceptable mass flow rate balance has been achieved in each model. The table and graph below in figure 4.65aare explaining the mass flow rate balance achieved in each three cases where room air inlet location has been changed.

Model Description	Air Mass Flow Rate at Inlet (Kg/sec)	Air Mass Flow Rate at Outlet (Kg/sec)	Difference (Kg/sec)
Model with room air inlet at bottom of the side wall	0.0975369	-0.0975363	0.0000006
Model with room air inlet at top of the side wall	0.099351	-0.099294	0.000057
Model with room air inlet at opposite of the chimney wall	0.12618	-0.12603	0.00015

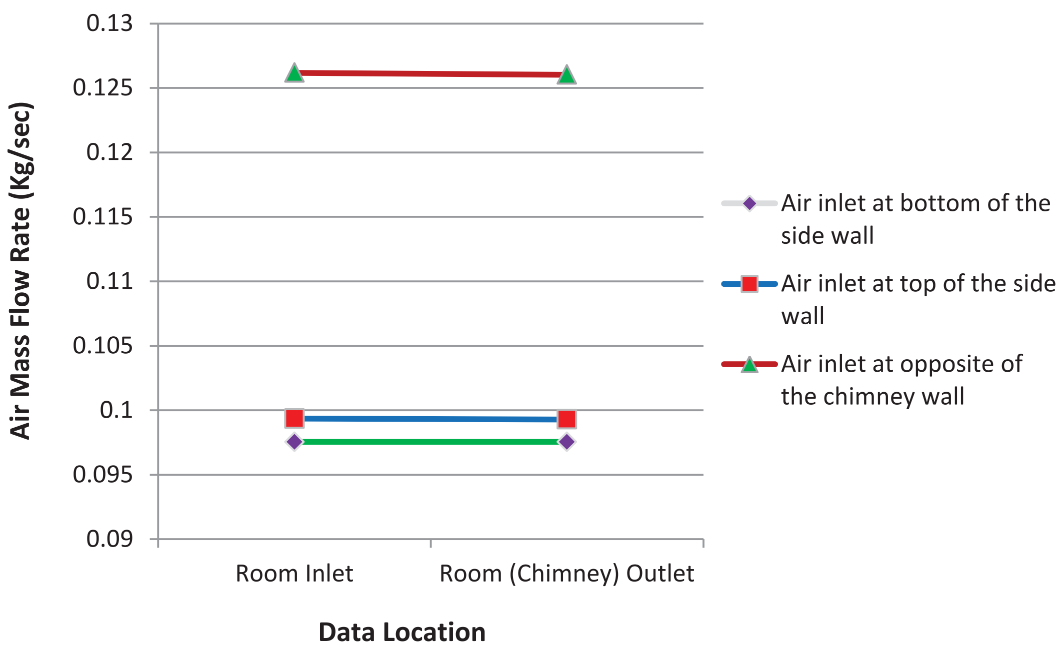

Figure:4.65a: Graph showing comparison of Total Mass Air Flow Rate at Room inlet and outlet.

Through above tabulated and graphical analysis, it is clear that after achieving convergence as per defined criteria, balance of mass is well verified with a minimum inlet and outlet difference of 0.00015.

The relative difference also comes well within acceptable limits i.e.

(In Flow – Out Flow) / Inflow

Model	Relative Difference
Model with room air inlet at bottom of the side wall	0.00000615
Model with room air inlet at top of the side wall	0.000571
Model with room air inlet at opposite of the chimney wall	0.001188

4.11 Analysis and Discussion on Simulation Results

The graphical and numerical analysis shows that with change of room air inlet location, while keeping all other parameters same, air flow rate through inlet interface almost remained same in all three models. The velocity magnitude slightly increases by taking inlet to top side of the wall and further increases when inlet is opposite to chimney side.

Another important factor in room ventilation is air flow pattern. The best pattern will be the one which will evenly circulate in the room and must pass through the sitting area of the occupants which is the floor of the room. Keeping this important factor in view, the best air flow pattern has been seen in a model where air inlet location is at the bottom of the wall at opposite corner of the Chimney (figures 4.53, 4.54 & 4.55) and model with air inlet location at top of the wall (figures 4.63, 4.64 & 4.65). In these models, air is more evenly distributing in whole room as compared to third model, which will give comfort to the occupants of the room.

With the change in room air inlet location, the air flow rate and pattern significantly changes. The Table:4.12 and graph in figure 4.65b below summarizes and give comparison of some important parameters noted after simulation with each type of room model:

Table:4.12: Comparison of Important Parameters obtained after Simulation of Different Models

Room Air Inlet location	Air Inflow Rate (Kg/sec)	Air Inflow Rate Through Inlet Interface (Kg/sec)	Maximum Velocity (m/s)
Bottom of the side wall	0.09754	0.04823	0.5215
Top of the side wall	0.09935	0.04927	0.5476
In front of the Chimney	0.12618	0.04973	0.5381

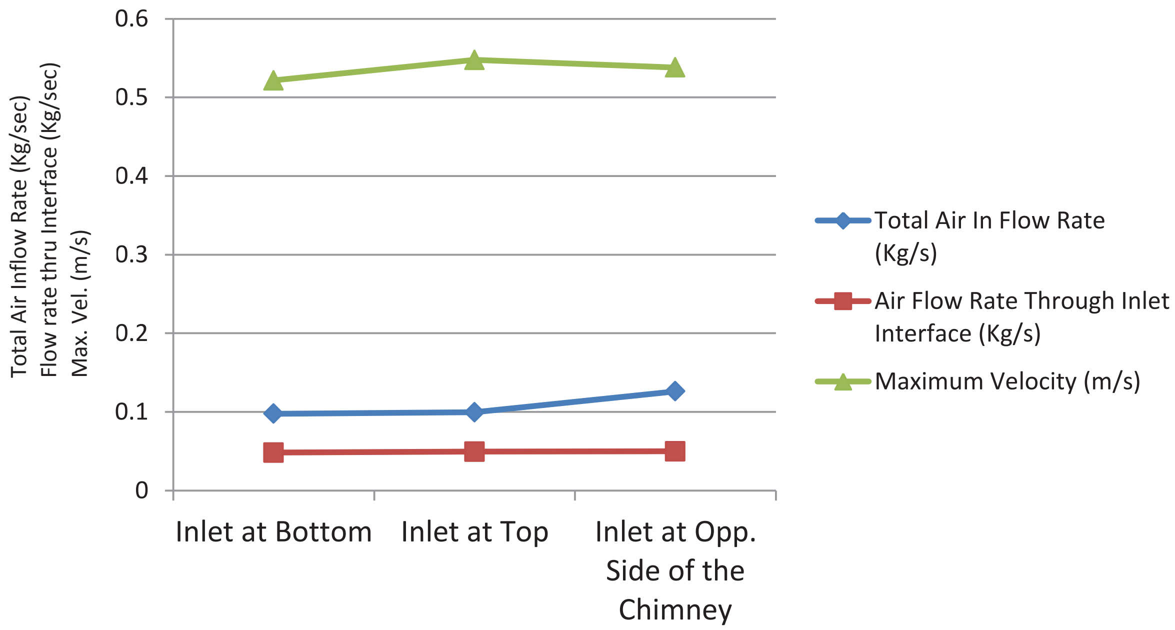

Figure:4.65b: Graph showing comparison of Total Mass Air Flow Rate, Flow Rate through Inlet Interface and Velocity with change in inlet location.

In order to further analyze the behavior of air flow rate and velocity in above three models, data of velocity magnitude measured along the center of the each room model and curves drawn to identify the difference. The data points has been taken along the straight line in the center of the room from right to left with a height of 01 meter from the floor. The data points has been taken at this level keeping in view the fact that this level is normally sitting area of the occupants and any better air flow / velocity at this level will directly provide comfort along with desired ventilation.

The figures and curves below are showing points in the room where data has been taken and value / trend of the data respectively.

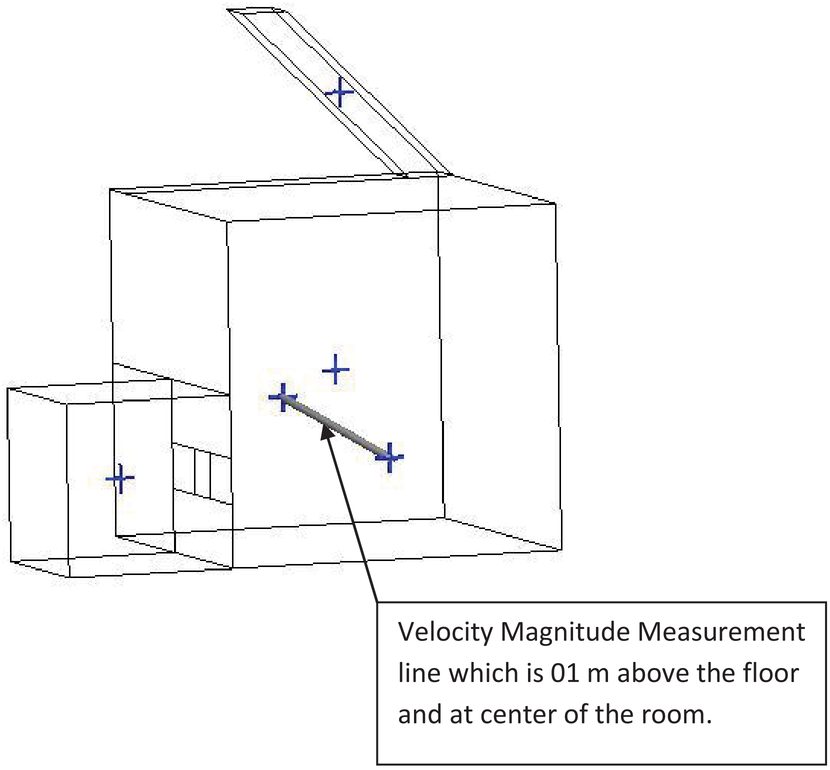

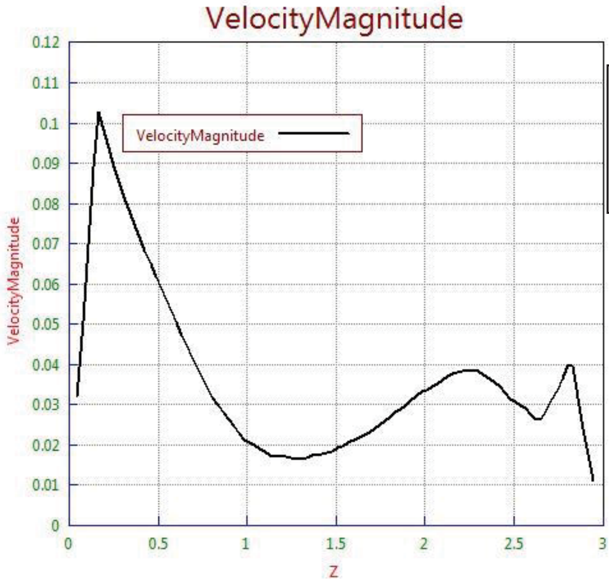

Velocity Magnitude is in m/sec and Z-Axis is in meter.

Figure :4.66: 3D Room with Inlet at Bottom of the Wall : Curve showing Velocity Magnitude Pattern along the Center of the Room.

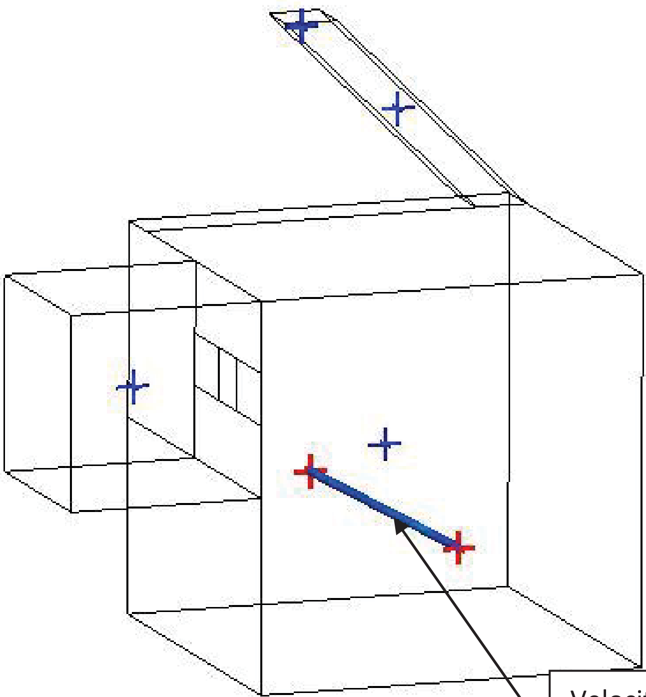

Velocity Magnitude Measurement line which is 01 m above the floor and at center of the room.

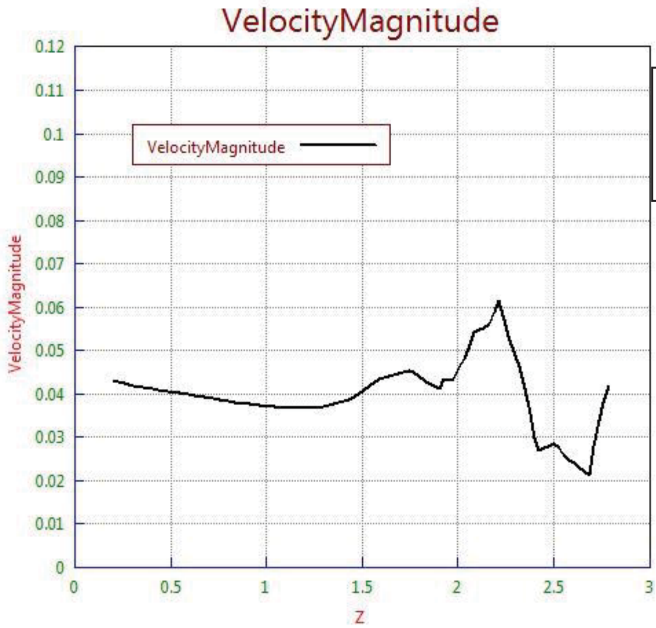

Velocity Magnitude is in m/sec and Z-Axis is in meter.

Figure :4.67: 3D Room with Inlet at Top Side of the Wall : Curve showing Velocity Magnitude Pattern along the Center of the Room.

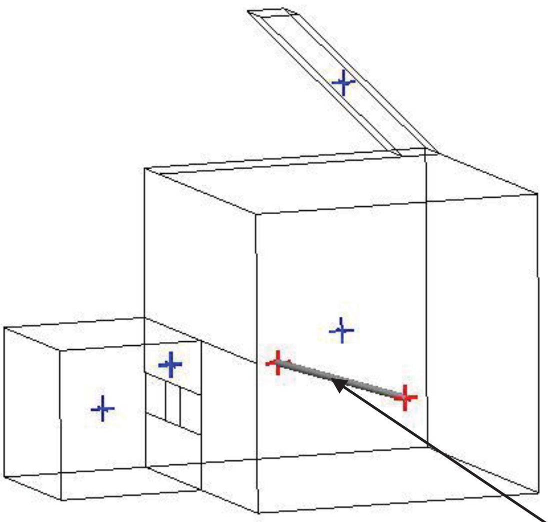

Velocity Magnitude Measurement line which is 01 m above the floor and at center of the room.

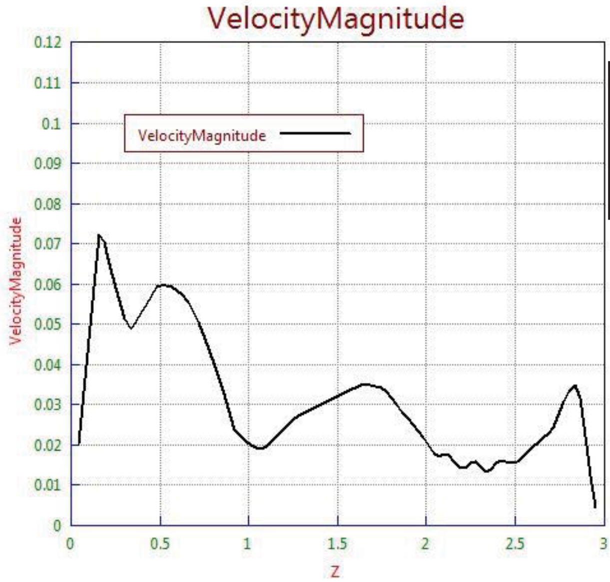

Velocity Magnitude is in m/sec and Z-Axis is in meter.

Figure :4.68: 3D Room with Inlet at Opposite Side of the Chimney : Curve showing Velocity Magnitude Pattern along the Center of the Room.

By comparing above velocity magnitude curves of three models, it has been seen that the models with inlet at top side of the wall gives steady velocity magnitude pattern along the width of the room. The value of velocity magnitude is around 0.04 m/s. The model with room inlet at bottom is giving the variable velocity magnitude along the width of the room. It gives a peak value of 0.1 m/s in front of the inlet opening.

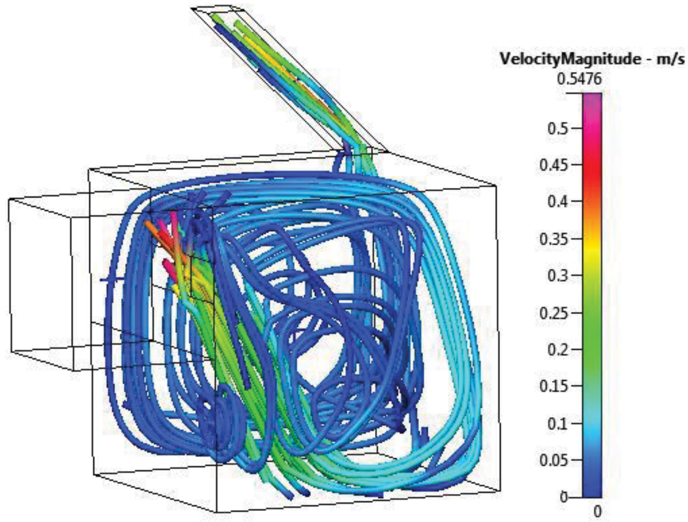

Figure: 4.69: 3D Room Model with Inlet at Top Side of the Wall in CFD View after Simulation showing Velocity Trace.

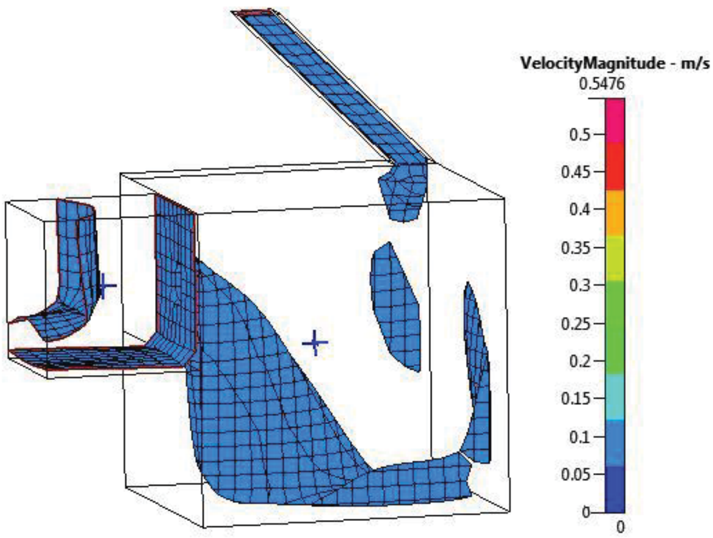

Figure:4.70: 3D Room Model with Inlet at Top Side of the Wall in CFD View after Simulation showing Isocurve with Velocity Value of 0.1 m/s.

4.12 Study of Air Behavior and Pressure at Exit of the Solar Chimney

The above models of rooms fitted with solar chimney were simulated by making environment box around inlet opening of the room and defining -0.22 N/m^2 pressure at chimney exit. The environment box around inlet opening has been designed to study the air behavior and trend at inlet of the room. The analysis of environment box disclosed that maximum portion of the air present around the inlet opening is not going in to the room, instead, it is travelling across the environment box. Only very short portion of air enters into the room through inlet opening of the room.

In order to enhance the air intake into the room through inlet opening, pressure variation study carried out above in section 4.7, which reveals that –ve pressure at inlet opening is not strong enough to pull the much quantity of the air into the room. In order to properly study the air ventilation behavior in the room and chimney, value of P = -0.22 N/m^2 was imposed at chimney exit. This imposed value of pressure created the sufficient –ve pressure at room inlet (equal to that of environment box surroundings), which resulted in almost equal flow of air through inlet opening and across the environment box (based on percentage of air flow with respect to size of opening)

4.12.1 Simulation of 3D Model with Zero Pressure Value (Atmospheric) at Solar Chimney Exit

The above simulations were performed based on of P = -0.22 N/m^2 at chimney exit. But in natural scenario, natural ventilation through solar chimney is considered with zero pressure at solar chimney exit, the above same model has been simulated without putting any value of pressure at exit i.e. P = 0 N/m^2 (pressure at exit will be calculated by solver).

All other physical parameters and boundary conditions (other than pressure at solar chimney exit which is P = 0 N/m^2) were same as that of previous model. The graphical and numerical results obtained are presented below:

Table: 4.13: Simulation Data of 3D Model (P=0 N/m^2 at exit) at Three Different Locations having Inlet at Bottom of the Wall

Room Length	Room Width	Room Height	Chimney Height
3 m	3 m	3 m	1.5 m
Chimney Angle	Inlet / Outlet Opening		Chimney Length
45	0.4 m × 0.4 m		2.12 m
Nodes		No.	867807
Faces		No.	2537760
Cells		No.	835200
Total In Flow		KG/S	0.241738
Total Out Flow		KG/S	-0.241736
Maximium Velocity in Whole Domain		Met/S	0.659578
Maximum Temp. in whole domain		K	419.239
Flow Through Room Air Inlet		KG/S	0.0244203
Converged at Iteration			8369

Simulatio Data (3D Model with P=0 N/m^2 at Solar Chimney Exit) and Inlet at Bottom of the Wall											
At Center of the Room Air Inlet				At Chimney Inlet				At Chimney Outlet			
Location of Coordinates		Variable	Values	Location of Coordinates		Variable	Values	Location of Coordinates		Variable	Values
X	0.1	U	0.142533	X	2.8	U	0.00523	X	1.29	U	-0.05331
Y	0.75	V	-0.129688	Y	2.85	V	0.07704	Y	4.43	V	0.0449
Z	2.25	VM	0.192735	Z	0.2	VM	0.0786	Z	0.2	VM	0.1255
		P	-0.022226			P	-0.0296			P	-0.01256
		Pt	-0.0004669			Pt	-0.026			Pt	0.00572
		T	297			T	297			T	301.729

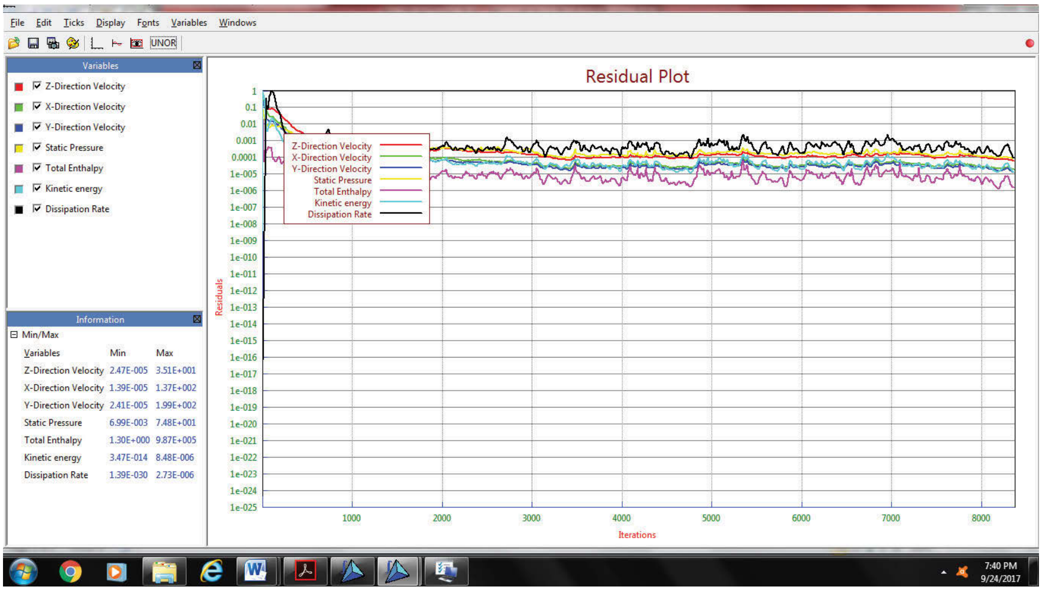

Figure:4.71: Graph showing Convergence of the Model (P = 0) up to desired level (1.0×10^{-04}).

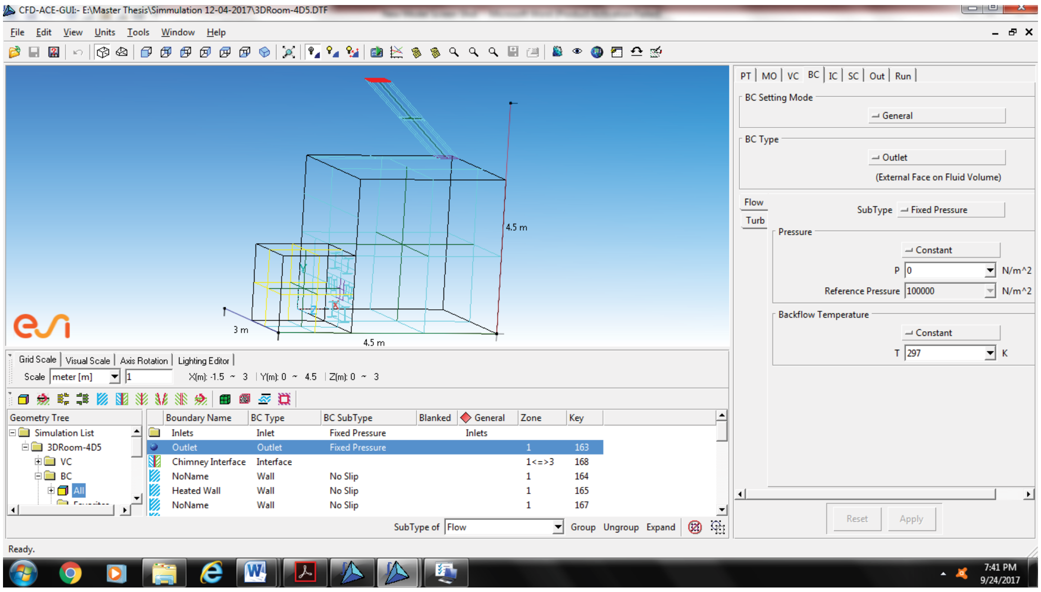

Figure: 4.72: Screen Shot of a 3D Room Model in CFD ACE+ with P = 0 N/m^2 at solar chimney exit.

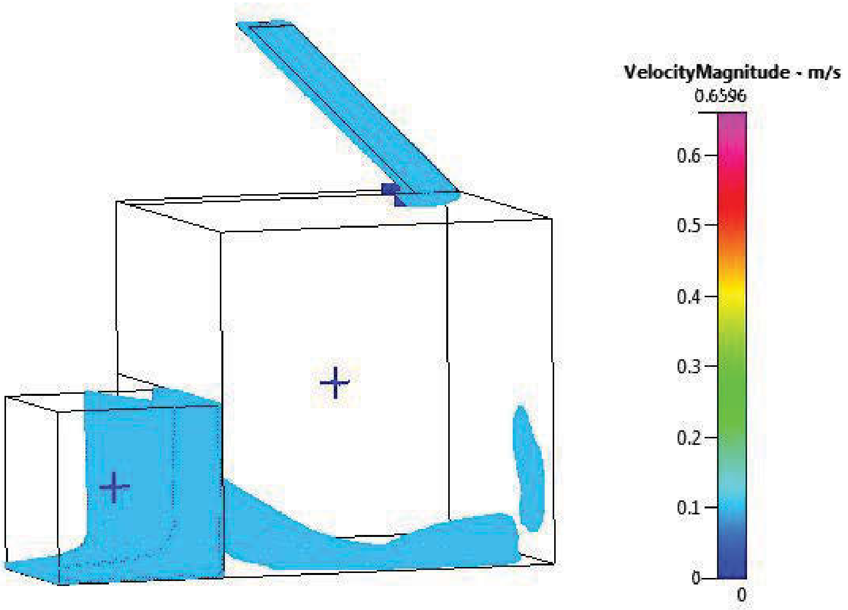

Figure: 4.73: 3D Room Model (P = 0 N/m^2 at exit) with Inlet at Bottom of the Wall in CFD View after Simulation showing Isocurve with Velocity Value of 0.1 m/s.

.

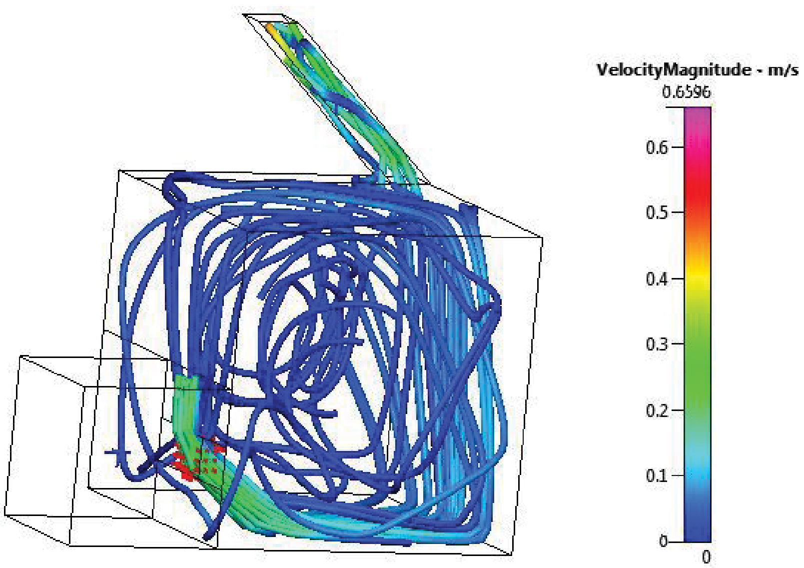

Figure: 4.74: 3D Room Model (P = 0 N/m^2 at exit) with Inlet at Bottom of the Wall in CFD View after Simulation showing trace of air parcel.

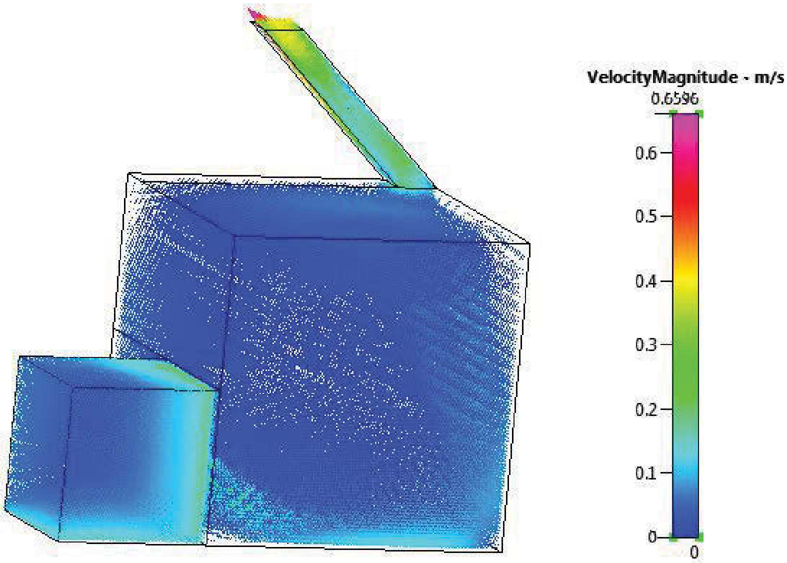

Figure: 4.75: 3D Room Model (P = 0 N/m^2 at exit) with Inlet at Bottom of the Wall in CFD View after Simulation showing Velocity Vectors.

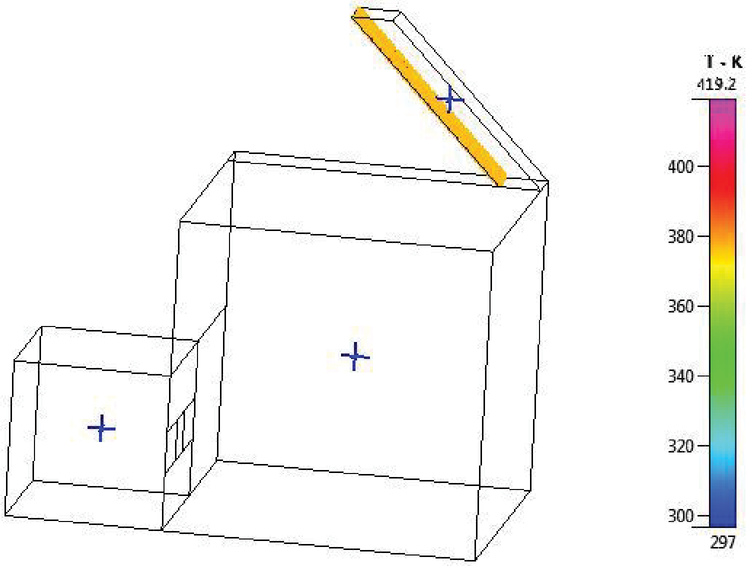

Figure: 4.76: 3D Room Model (P = 0 N/m^2 at exit) with Inlet at Bottom of the Wall in CFD View after Simulation showing Isocurve of Temperature on heated wall of Chimney.

4.12.2 Comparison of Results: Simulation of 3D Model with P = 0 N/m^2 and P = -0.22 N/m^2 at Solar Chimney Exit

The simulation of both models i.e. with P = 0 N/m^2 and P = -0.22 N/m^2 at Solar Chimney Exit, has been carried out and convergence has been achieved as per desired criteria. The analysis / comparison of results obtained through both models will further give us the idea about importance of change in pressure at solar chimney exit.

There could be many reasons of increased / decreased pressure at solar chimney exit and change in this pressure may significantly effects the air ventilation behaviour in the room.

Below is the the table showing comparison of results obtained through simulation of two models only by changing pressure value at the exit of the solar chimney:

Table: 4.14: Comparison of Results obtained after Simulation of 3D Models with P = 0 N/m^2 & P= -0.22 N/m^2 at solar chimney exit, with all other parameters remained same

Room Length	Room Width	Chimney Height / Length		Model 3D-4 with P=-0.22 N/m^2 at Solar Chimney Exit	Model 3D-4 with P=0 N/m^2 at Solar Chimney Exit
3 meter	3 meter	1.5 / 2.12 meter			
Chimney Angle	Inlet / Outlet Opening				
45	0.4 meter × 0.4 meter				
Nodes		No.		867807	867807
Faces		No.		2537760	2537760
Cells		No.		835200	835200
In Flow		KG/S		0.0975369	0.241738
Out Flow		KG/S		-0.0975363	-0.241736
Flow Through Room Air Inlet		KG/S		0.0482283	0.024423
Maximium Velocity		Met/S		0.521485	0.659578
Maximum Temp.		K		415.009	419.239
Converged at Iteration				17732	8369
Data Locations					
At Center of Room Air Inlet	Location	Variable			
X	0.1	U		0.355598	0.142533
Y	0.75	V		-0.00541679	-0.129688
Z	2.25	VM		0.355674	0.192735
		P		-6.94E-02	-2.22E-02
		Pt		0.00413107	-0.000466895
		T		297	297
At Chimney Inlet					
X	2.8	U		0.019089	0.00522961
Y	2.85	V		0.164896	0.0770421
Z	0.2	VM		0.175505	0.0786147
		P		-1.09E-01	-2.96E-02
		Pt		-0.0912468	-0.0260102
		T		296.995	297
At Chimney Outlet					
X	1.29	U		-0.284154	-0.0533063
Y	4.43	V		0.282733	0.0449332
Z	0.2	VM		0.400852	0.125458
		P		-0.225249	-0.0125577
		Pt		-0.13191	0.00572307
		T		300.045	301.729

4.12.3 Simulation of 3D Model with Environment Box at Outlet and Pressure Value of Zero at Solar Chimney Exit

In order to further analyze the air flow behaviour at the exit of the chimney with natural pressure conditions i.e. P = 0 N/m^2, an environment box has also been designed with almost same dimensions as that of inlet environment box

The purpose of this box around solar chimney exit is to consider and analyze the behavior of air around outlet of the chimney and outside of the room boundary when heated air leaves the room. Previously, most of the research has been carried out without giving much concentration on this point. The air flow rate, pattern and pressure at the exit of the room significantly affect the flow rates and patterns inside the room. In this scenario, all the faces of the outlet environment box will act as Outlets while the actual chimney outlet will act as interface (chimney outlet). The interface is a term used in CFD software but this interface (chimney outlet) is actual outlet of the room. The flow through this outlet is our prime concern.

Below is the model of the 3D room fitted with inlet and outlet environment boxes:

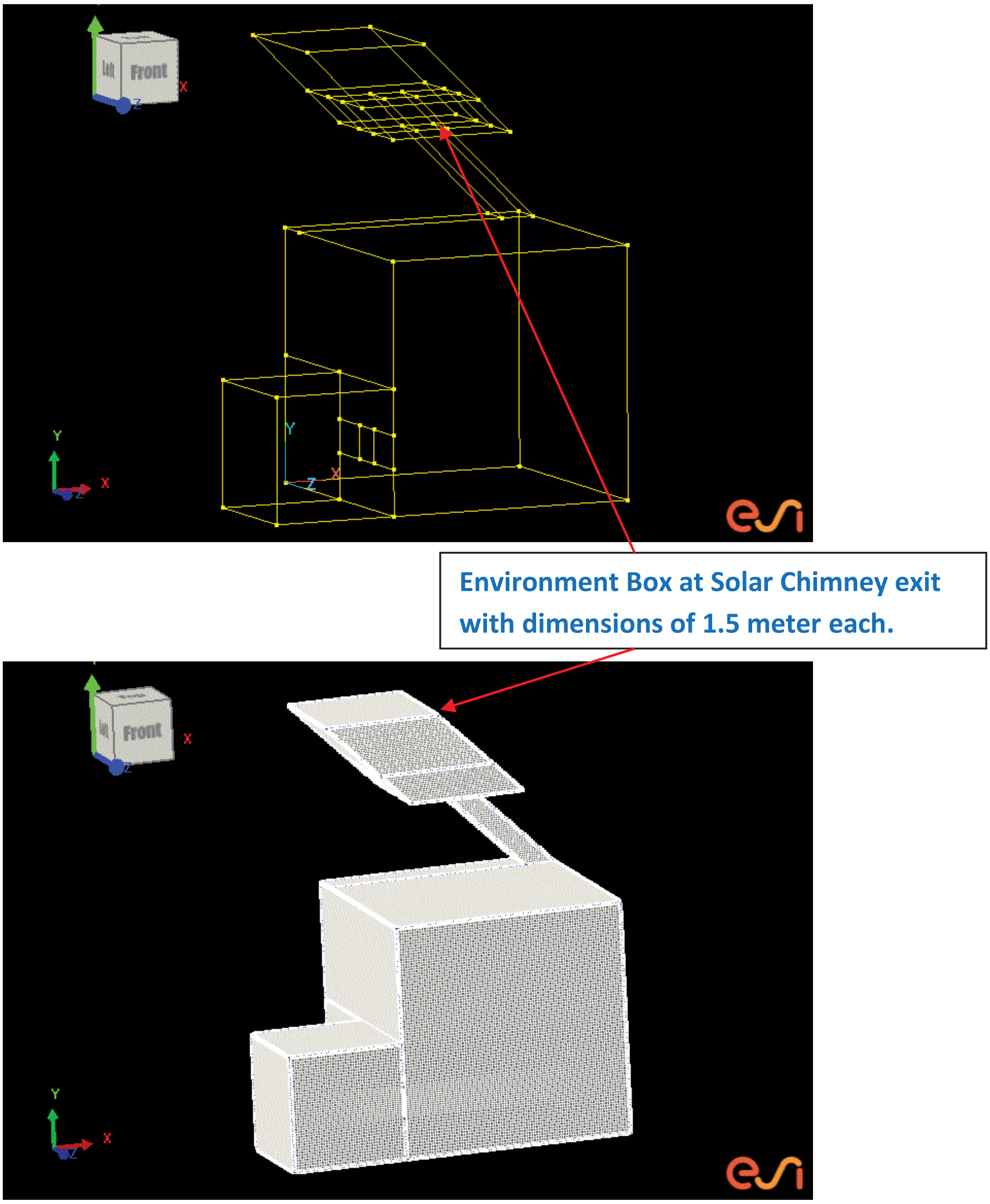

Figure: 4.77: Screen Shots of a 3D Room Model in CFD GEOM with Environment Box at outlet.

All parameters like number of edges, grids spacing have been kept same as that of inlet environment box, during construction of environment box at outlet.

The above model was then simulated with same parameters / conditions as that of model in section 4.12.1 (with pressure value of P = 0 at exit). All other physical parameters and boundary conditions were same as that of previous model.

Boundary Conditions of Outlet Environment Box

The boundary conditions for the variables like velocity components, pressure and temperature have been taken as same as that of inlet environment box.

All outlet openings on the environment box around the solar chimney outlet opening have been assigned with ambient conditions based on normal atmosphere around the room. The fluid has been considered at atmospheric pressure with a constant gauge value of P = 0 N/m^2 and temperature as T = 297 K.

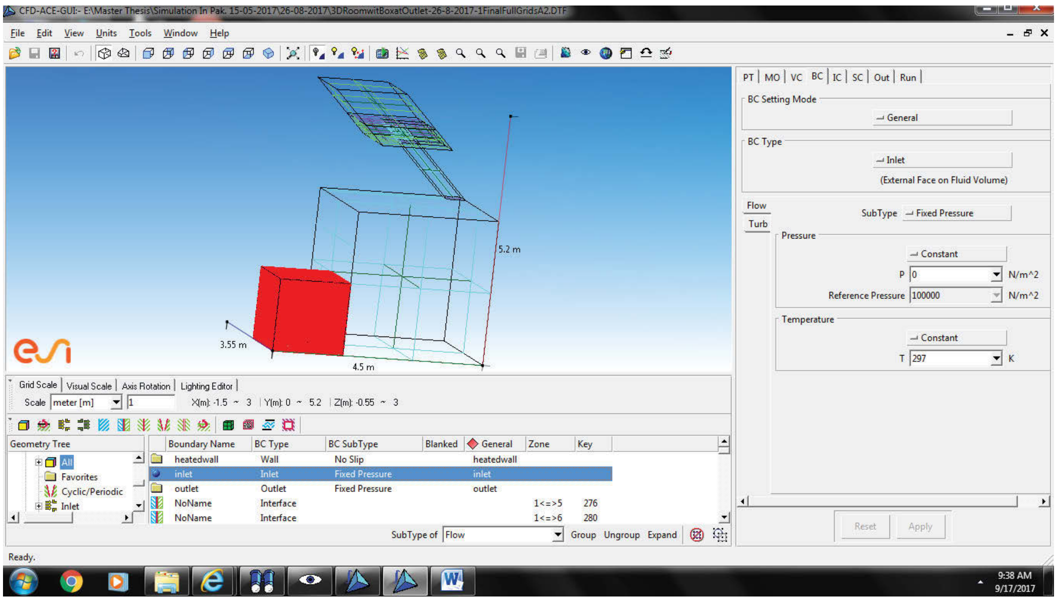

Figure: 4.78: Screen Shot of a 3D Room Model in CFD Solver (ACE+) showing boundary conditions for inlet environment box.

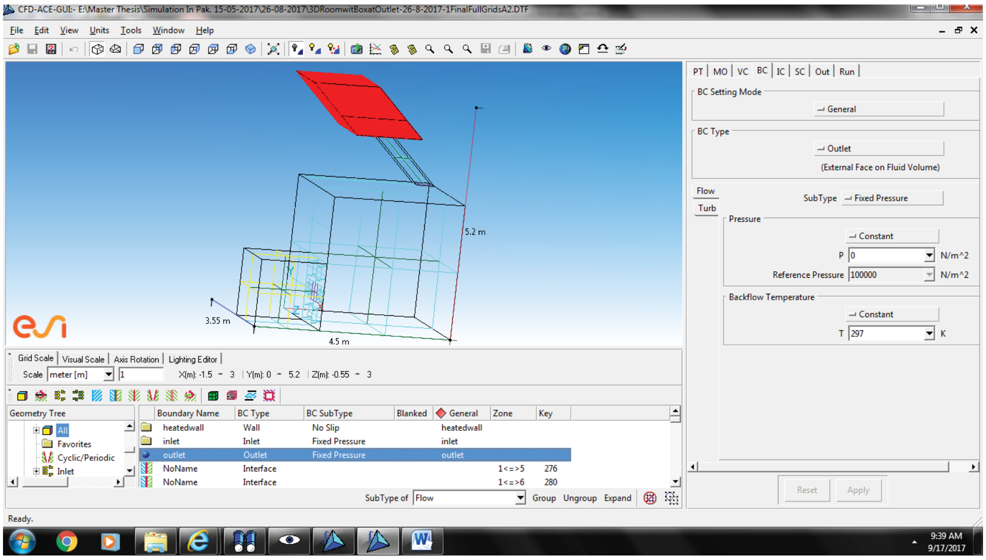

Figure: 4.79: Screen Shot of a 3D Room Model in CFD Solver (ACE+) showing boundary conditions for outlet environment box.

The graphical and numerical results obtained are presented below:

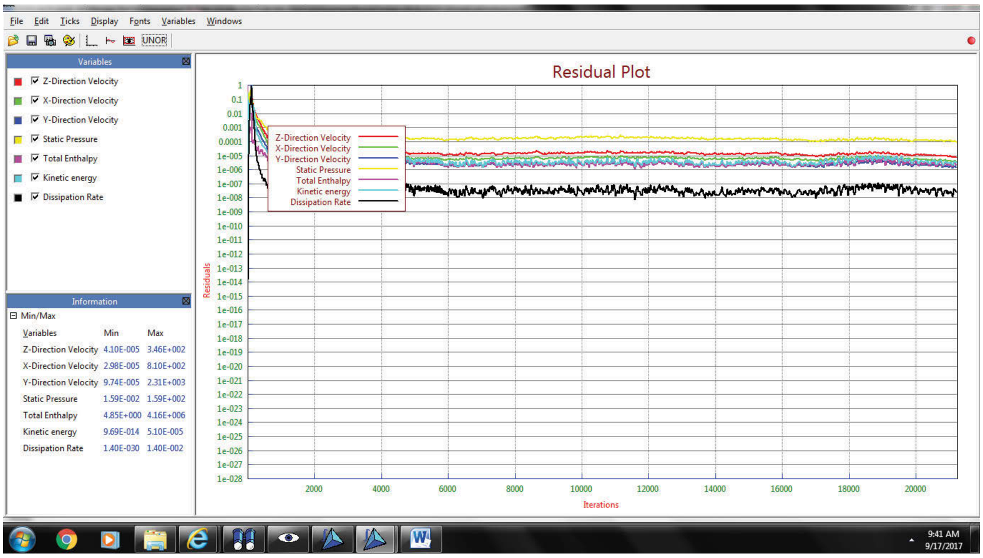

Figure:4.80: Graph showing Convergence of the Model (with environment box at outlet) up to desired level (1.0×10^{-04}).

Below table is presenting model data and results obtained after simulation:

Table: 4.15: Simulation Results of 3D Model (with environment box at outlet & P = 0 N/m^2 at outlets i.e. faces of outlet environment box) at Four Different Locations

Room Length	Room Width	Room Height	Chimney Height
3 m	3 m	3 m	1.5 m
Chimney Angle	Inlet / Outlet Opening		Chimney Length
45	0.4 m × 0.4 m		2.12 m
Nodes		No.	958051
Faces		No.	2796210
Cells		No.	919350
Total In Flow		KG/S	0.358493
Total Out Flow		KG/S	-0.358467
Maximium Velocity in Whole Domain		Met/S	0.6056
Maximum Temp. in whole domain		K	454.365
Flow Through Room Air Inlet		KG/S	0.02728
Converged at Iteration			21227

Simulation Data (3D Model with Environment Box at Outlet and P=0 N/m^2 at Faces of Outlet Environment Box)												
Variable	At Center of the Room Inlet			At Chimney Inlet			At Chimney Outlet (inside chimney)			In Outlet Environment Box Near Chimney Exit		
	Location of Coordinates		Values	Location of Coordinates		Values	Location of Coordinates		Values	Location of Coordinates		Values
U	X	0.1	0.18868	X	2.8	-0.01912	X	1.29	-0.0392272	X		-0.224278
V	Y	0.75	-0.05249	Y	2.85	0.091553	Y	4.43	0.00124117	Y		0.17689
VM	Z	2.25	0.221771	Z	0.2	0.109741	Z	0.2	0.143713	Z		0.291065
P			-2.79E-02			-3.85E-02			-0.034518			-0.0019227
Pt			0.000723			-0.03149			-0.02111			0.0495877
T			297			297			299.579			299.537

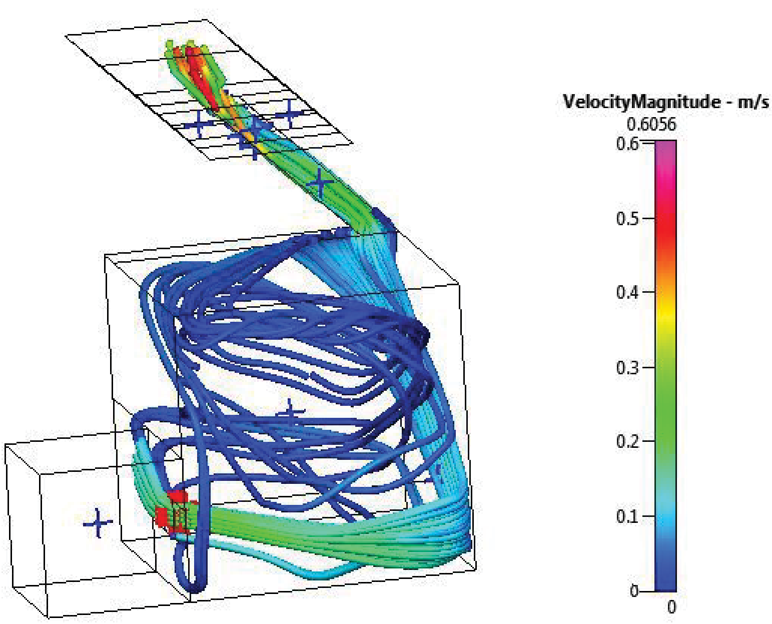

Figure: 4.81: 3D Room Model (with environment box at outlet & P = 0 N/m^2 at outlets i.e. faces of outlet environment box) in CFD View after Simulation showing trace of air parcel.

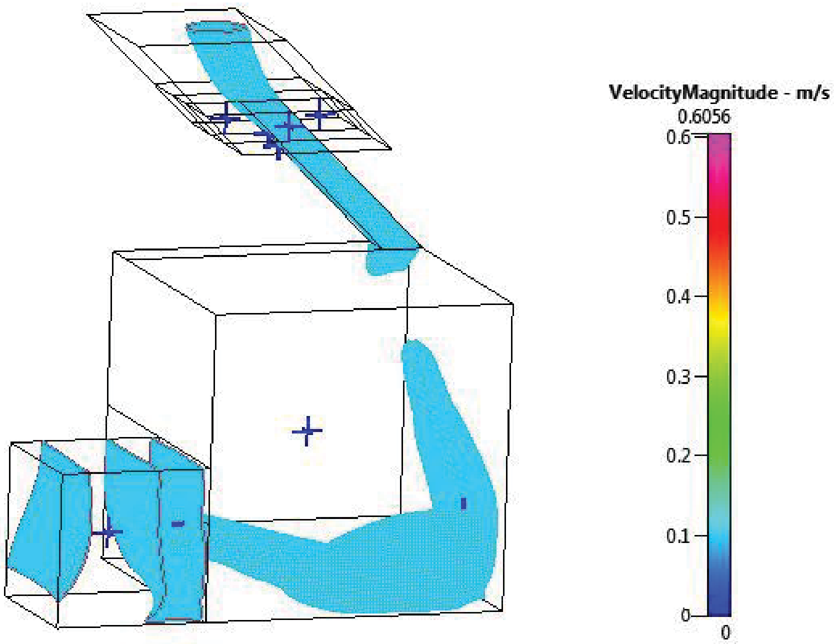

Figure: 4.82: 3D Room Model (with environment box at outlet & P = 0 N/m^2 at exit) in CFD View after Simulation showing Isocurve with Velocity Value of 0.1 m/s.

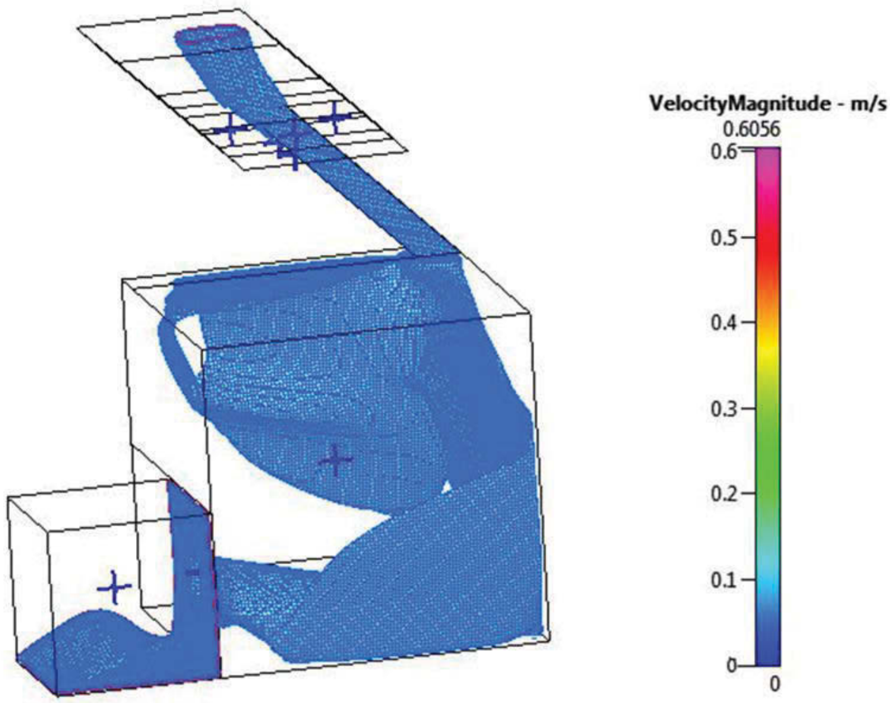

Figure: 4.82a: 3D Room Model (with environment box at outlet & P = 0 N/m^2 at exit) in CFD View after Simulation showing Isocurve with Velocity Value of 0.05 m/s.

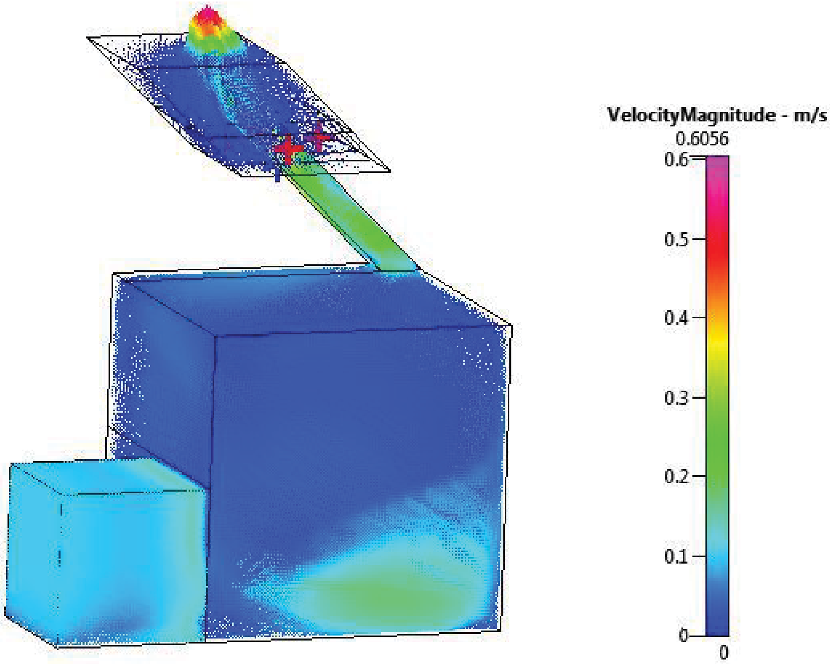

Figure: 4.83: 3D Room Model (with environment box at outlet & P = 0 N/m^2 at exit) in CFD View after Simulation showing Velocity Vectors.

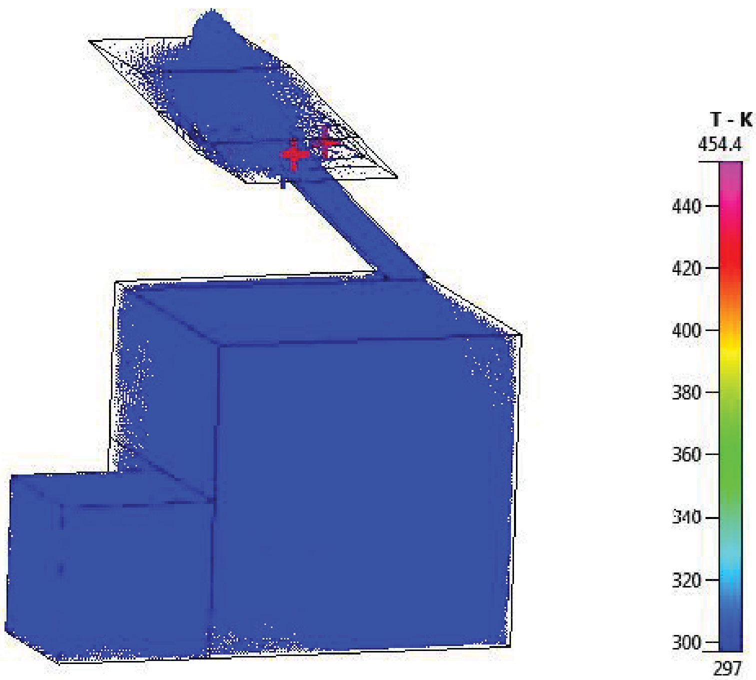

Figure: 4.84: 3D Room Model (with environment box at outlet & P = 0 N/m^2 at exit) in CFD View after Simulation showing Temperature profile.

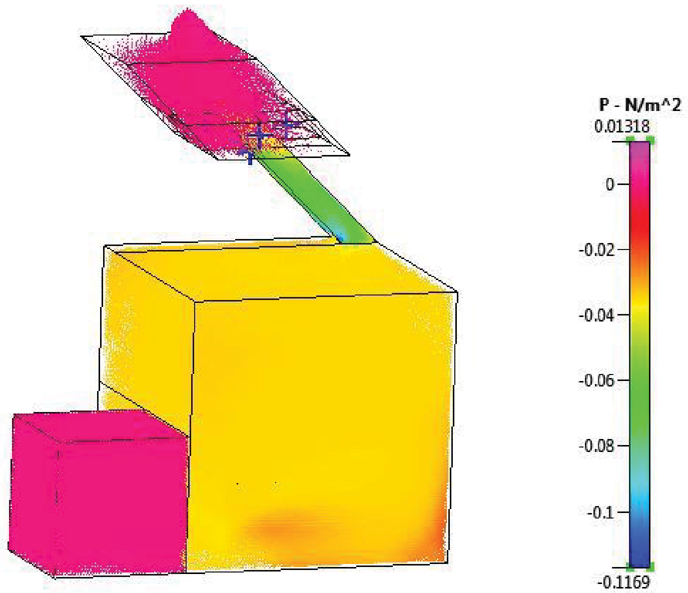

Figure: 4.85: 3D Room Model (with environment box at outlet & P = 0 N/m^2 at exit) in CFD View after Simulation showing Pressure Profile.

4.12.4 Comparison and Discussion of Results:

3D Model with P = 0 N/m^2 (*with environment box at outlet*) and P = -0.22 N/m^2 (*without environment box at outlet*) at Solar Chimney Exit

The simulation of both models i.e. Model with environment box at outlet & with P=0 N/m^2 at outlet boundary conditions and Model without environment box at outlet & P = -0.22 N/m^2 at Solar Chimney Exit, has been carried out and convergence has been achieved as per desired criteria. The analysis / comparison of numerical and graphical results obtained through both models has been given below.

Below is the the table showing comparison of results obtained through simulation of two models only by addition of environment box at outlet and changing pressure value at the exit of the solar chimney:

Table: 4.16: Comparison of Results obtained after Simulation of 3D Models: Model without box at outlet with P= -0.22 N/m^2 at Exit (solar chimney exit) and Model with box at outlet with P = 0 N/m^2 at Exit (Faces of Outlet Environment Box), with all other parameters remained same.

Room Dimensions		Chimney Effective Length	3DRoom4 without Box at outlet & P= -0.22 at Exit (Exit is Solar chimney outlet)	3DRoom4 with Box at Outlet and P= 0 at Exit (Exits are outlet environment box faces)
3m × 3m × 3m		2.12 m		
Chimney Angle	Inlet / Outlet Opening			
45	0.4m × 0.4m			
Nodes		No.	867807	958051
Faces		No.	2537760	2796210
Cells		No.	835200	919350
In Flow		KG/S	0.0975369	0.358493
Out Flow		KG/S	-0.0975363	-0.358467
Flow Through Room Air Inlet		KG/S	0.0482283	0.0272811
Maximium Velocity		Met/S	0.521485	0.605562
Maximum Temp.		K	415.009	454.365
Converged at Iteration			17732	21227
Data Locations				
At Center of the Room Air Inlet	Location	Variable		
X	0.1	U	0.355598	0.18868
Y	0.75	V	-0.00541679	-0.0524876
Z	2.25	VM	0.355674	0.221771
		P	-6.94E-02	-2.79E-02
		Pt	0.00413107	0.000723404
		T	297	297
At Chimney Inlet				
X	2.8	U	0.019089	-0.0191234
Y	2.85	V	0.164896	0.0915532
Z	0.2	VM	0.175505	0.109741
		P	-1.09E-01	-3.85E-02
		Pt	-0.0912468	-0.0314906
		T	296.995	297
At Chimney Outlet				
X	1.29	U	-0.284154	-0.0392272
Y	4.43	V	0.282733	0.00124117
Z	0.2	VM	0.400852	0.143713
		P	-0.225249	-0.034518
		Pt	-0.13191	-0.02111
		T	300.045	299.579
At Outlet Box just near Chimney Exit				
X	1.2	U		-0.224278
Y	4.7	V		0.17689
Z	0.2	VM		0.291065
		P		-0.00192271
		Pt		0.0495877
		T		299.537
		K		1.45E-09

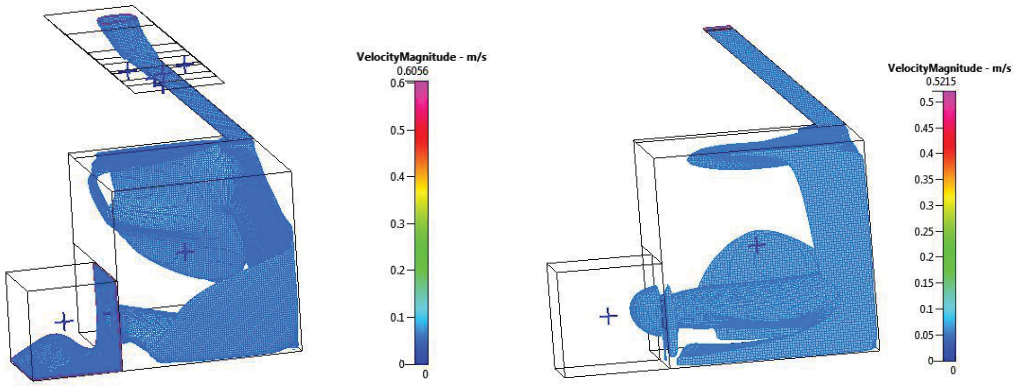

Figure: 4.86: Comparison of Velocity Magnitude Isocurve with velocity value of 0.05 m/s: Model with box at outlet & P = 0 N/m^2 and Model without box at outlet & P = -0.22 N/m^2

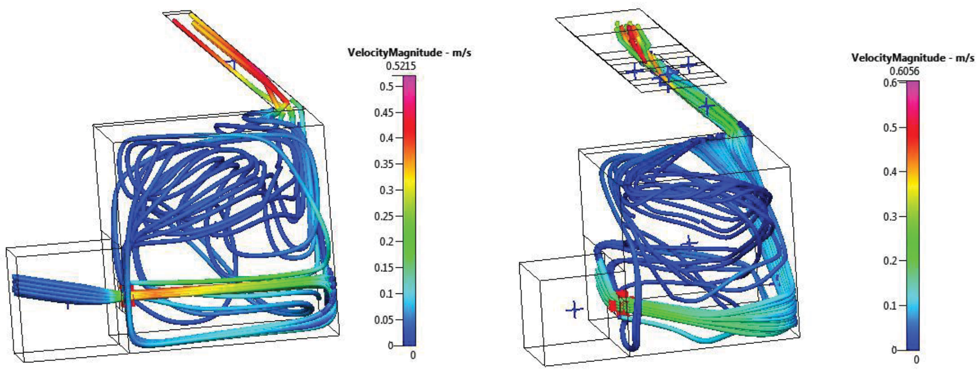

Figure: 4.87: Comparison of Velocity Magnitude Air Parcel Trace: Model with box at outlet & P = 0 N/m^2 and Model without box at outlet & P= -0.22 N/m^2

The purpose of addition of environment boxes around inlet and outlet openings of the room is to get idea about the behavior of air flow rate around these important and critical areas in a natural ventilation scenario.

There has been a slight change in numerical values of pressure and temperature with in the room domain but if we see the graphical output of the air circulation and velocity in the domain, there is not much difference in both models. In both cases, we are getting desired air circulation / ventilation all around the domain.

4.13 Analysis of Air Flow Rate in Terms of "Air Changes per Hour (ACH)

Air is continuously exchanged within buildings and their surroundings as a result of mechanical and passive ventilation and infiltration through the building envelope. The rate at which air is exchanged is an important property for the purposes of ventilation design and heat loss calculations. This property is normally measured in terms of flow rate which can also be presented in terms of Air Changes per Hour (ACH). **Air changes per hour**, or **air change rate**, abbreviated ACH or ACPH, is a measure of the air volume added to or removed from a space (normally a room or house) divided by the volume of the space. If the air in the space is either uniform or perfectly mixed, air changes per hour is a measure of how many times the air within a defined space is replaced. If a building has an air change rate of 1 ACH, this equates to all of the air within the internal volume of the building being replaced over a 1 hour period.

A number of techniques are available for calculating the air change rate of a building. The choice of method depends on the accuracy required. The most straight forward method relies on the use of a simple mathematical equation, while the most complex methods use computational analysis and consider many different variables (such as computational fluid dynamics).

The normally used method to calculate Air Change per Hour is presented below.

$$\mathbf{ACH} = \frac{\mathbf{Q} \times \mathbf{3600}}{\mathbf{V'}}$$

The above expression has been defined by ASHRAE, where $\mathbf{Q}$ *is volumetric flow rate of air in* m^3/s and $\mathbf{V'}$ is room volume in m^3.

4.13.1 Study of "Air Changes per Hour (ACH)" for Three Models with Different Air Inlet Locations:

The following three models with different air inlet opening locations have been analyzed with reference to change in ACH value.

1. **Room with Air Inlet at Bottom of the Side Wall (explained in section 4.10.1 & Figure 4.51)**
2. **Room with Air Inlet at Top of the Side Wall (explained in section 4.10.2 & Figure 4.56)**
3. **Room with Air Inlet at Opposite of the Chimney Wall (explained in section 4.10.3 & Figure 4.61)**

For calculation of Air Changes per Hour (ACH) in above three models with different air inlet locations, the following values of different parameters have been taken.

Air Flow Rate $(\mathbf{Q})$**:** Flow rate through room air inlet (given in Tables 4.9 / 4.10 / 4.11 above) has been taken. The value of flow rate is being calculating by software in Kg/s and is reliable for calculation of ACH.

Density of the Air: Air density has been taken as 1.16 kg/m^3. This value will be used to convert air flow rate from kg/s to m^3/s.

Volume of the Room $(\mathbf{V'})$**:** Room volume has been taken as 27 m^3 (3m × 3m × 3m) to calculate the ACH.

The table below is giving the values used and ACH valued obtained against three models with different room air inlet locations.

Table:4.17: Data showing calculation of ACH with different room air inlet locations.

Location of Room Air Inlet	Air Flow Through Room Air Inlet (Kg/s)	Air Flow Through Room Air Inlet (m^3/s)	Air Flow Through Room Air Inlet (m^3/hr)	Volume of the Room (m^3)	ACH Value
At Bottom of the side Wall	0.0482	0.0416	149.6740	27	**5.54**
At Top of the side Wall	0.0493	0.0425	152.9069	27	**5.66**
At Bottom of the side Wall Opposite to Solar Chimney	0.0497	0.0429	154.3345	27	**5.72**

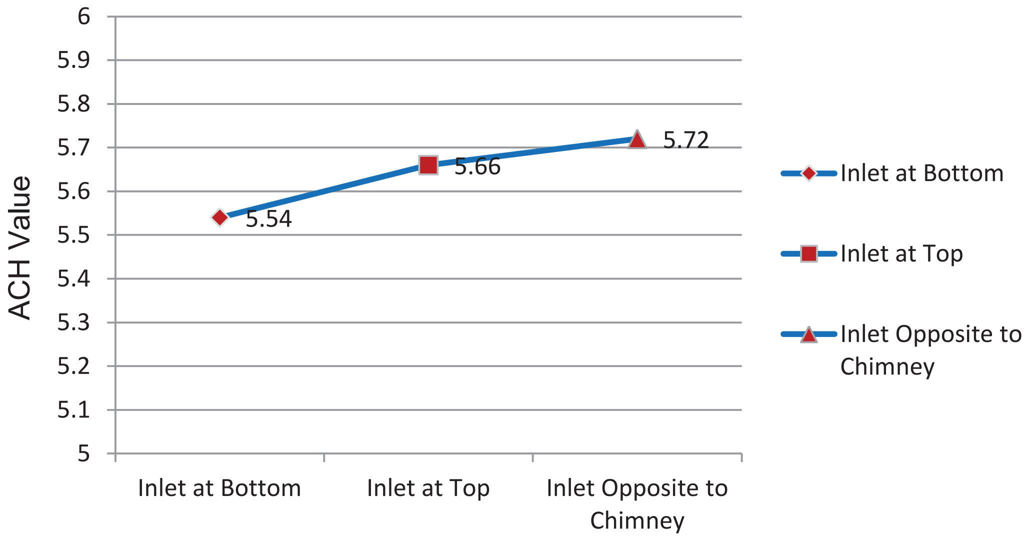

Figure:4.88: Graph showing change in ACH value with change in Room Air Inlet Location against above data table.

The analysis of above data / graph reveals that there is no considerable change in ACH value by changing room air inlet locations. The most appropriate results are obtained in a model with inlet opening opposite to solar chimney i.e. ACH value of 5.72.

4.13.2 Study of "Air Changes per Hour (ACH)" for Models with P= -0.22 N/m^2 and P = 0 N/m^2 at the exit of Solar Chimney:

In this chapter, we performed analysis initially on a model with P = -0.22 N/m^2 at the exit of solar chimney and then performed simulation of a model by putting P = 0 N/m^2 at the exit of solar chimney. With change in pressure value, the velocity value and air flow rate at room air inlet also changed considerably.

To analyze the effect of chimney exit pressure on ACH, the following two models with different pressure values, at solar chimney outlet, have been analyzed with reference to change in ACH value.

1. **Room with Air Inlet at Bottom of the Side Wall with pressure value of -0.22 N/m^2 (explained in section 4.10.1 & Figure 4.51)**
2. **Room with Air Inlet at Bottom of the Side Wall with pressure value of 0 N/m^2 (explained in section 4.12.1 & Figure 4.73)**

The value of room air inlet flow rate for below calculations has been taken from table 4.9 and 4.13. All other parameters are same as explained above.

The table and graph below is showing change in ACH with change in solar chimney exit pressure.

Table:4.18: Data showing calculation of ACH with different value of pressure at solar chimney exit.

Pressure value at Solar Chimney Exit	Air Flow Through Room Air Inlet (Kg/s)	Air Flow Through Room Air Inlet (m^3/s)	Air Flow Through Room Air Inlet (m^3/hr)	Volume of the Room (m^3)	ACH Value
Model 4.73 P = 0 N/m^2	0.0244	0.0211	75.7955	27	**2.81**
Model 4.51 P = -0.22 N/m^2	0.0482	0.0416	149.6740	27	**5.54**

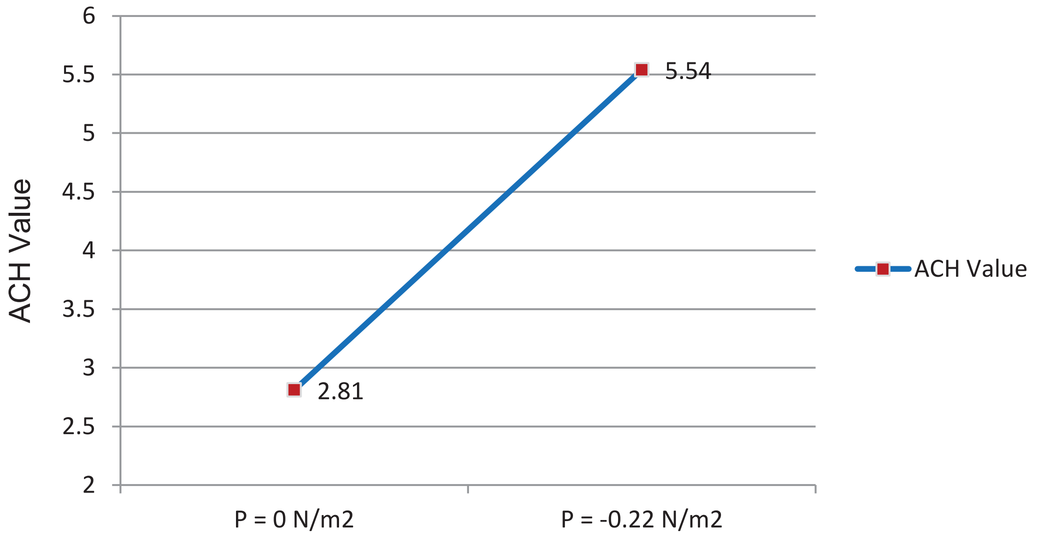

Figure:4.89: Graph showing change in ACH value with change in value of pressure at solar chimney exit against above data table.

It is evident from above results and analysis that ACH considerably increases with change (reduction) in solar chimney exit pressure. The value of this pressure ultimately depends on the performance of solar chimney. The higher performance of solar chimney will result in higher pressure difference between room inlet and outlet and resultantly, higher value of ACH will be obtained. The performance of solar chimney depends on many factors like height / width / length of the chimney, absorber efficiency, angle of solar chimney etc. The proper manipulation of theses parameters may result in higher performance of solar chimney and more ACH value. In this research, we have already taken those values of solar chimney parameters which have already been researched extensively like solar chimney inclination angle from roof top, solar chimney width and height / length of solar chimney but still more research / experimentation is required on solar chimney particularly at the exit area of solar chimney to improve flow / pressure conditions.

Chapter 5

CONCLUSION AND DISCUSSION

5.1. Simulation and Validation of Results

Extensive research has been carried out in the field of Solar Energy and particularly utilization of solar energy by employing solar chimney in the buildings to achieve natural ventilation with almost no consumption of energy. These include both experimental and computational studies. The solar chimneys are also being fitted in some modern building based on the widespread research in the field.

The parameters and results of each research are different depending on the location of the physical experiments and parameters used. Similarly, computational results also depend on type / dimensions of the model, physical parameters used and most importantly, software package used. So it's really difficult to compare results of present research with some previous research as there may not be the experiment / computation that used exactly the same parameters with same software package. But on the other hand, a broader idea can be obtained from the previous researches which have been carried out almost with same parameters.

In this research, the same idea has been obtained from the results / analysis of previous researchers and compared the results of this research with those of previous ones. The results of the basic factors, important in any natural ventilation like air mass flow rate, flow patterns, temperatures, pressures etc., have been found in-line with previous studies. For example, the ventilation performance of the chimney increases with increased heat absorption, width of the chimney etc. in general but with certain limitations / conditions. The exact comparison cannot be made as the models dimensions and some of the physical conditions are different as those of used in previous researches.

5.2 Importance of Grid Convergence

Grid Convergence study of the models to be simulated is highly imported in any software package where simulation activity is being performed. The application of grid convergence test as per proven methods guarantees the accurate results of simulation.

Keeping in view this fact in mind, Grid Convergence test was employed to make sure that grids pattern employed for this simulation are adequate. More than 08 models (three dimensional) were simulated with increased number of grid points and cells. Starting from 6,687 numbers of cells, the number of cells increased to 2,089,079 numbers. Each time, the convergence was achieved up to the desired level (1.0×10^{-04}) as shown in Figure: 5.1 below and the results were analyzed.

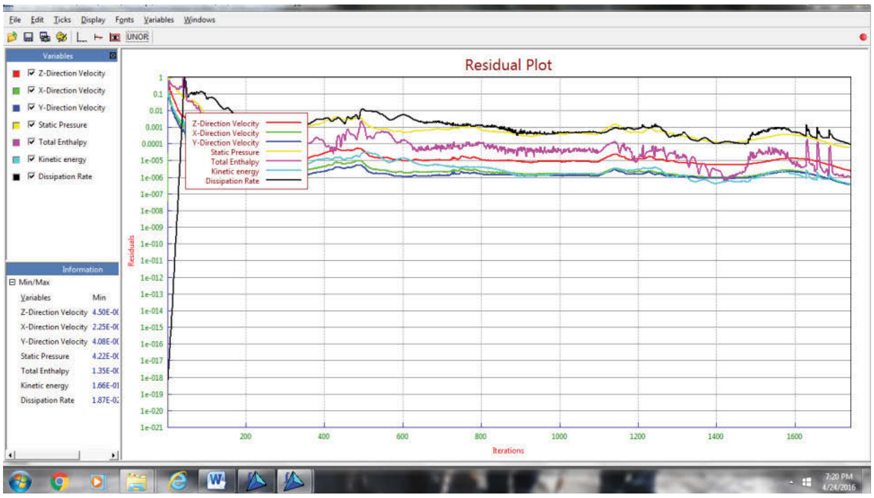

Figure:5.1: Graph showing Convergence of the one Model up to desired level (1.0×10^{-04}). Above (Normalized values) and Below (Actual values)

To study the grid convergence, two points at different locations were taken and the important parameters at these points were noted. The percentage differences between values of same parameters in two simulations were analyzed. The process remains continues by making new models with increased number of cells unless grid convergence was achieved.

5.3 Analysis of Simulation Results

The two most important factors in case of natural ventilation are air mass flow rate and circulation pattern. The best pattern will be the one which will evenly circulate in the room and must pass through the sitting area of the occupants which is the floor of the room. Keeping in view the previous research, numerical and experimental, the most of the parameters were kept constant like:

- Solar Chimney Inclination Angle of 45 degree
- Heat flux rate of 300 W/m^2 for chimney inner surface

The concentration of this research was on one basic point which is:

- Effect of Room air inlet location on the Natural Ventilation parameters

Therefore, the present research was majorly focused to find improvements in air mass flow rate and circulation pattern with reference to room air inlet location. The following key points have been noted against two-dimensional and three-dimensional simulation analysis of a real sized room fitted with inclined solar chimney.

5.4 Modeling and Simulation of 2D Real Sized Room

The graphical and numerical analysis shows that with change of room air inlet location, while keeping all other parameters same, air flow rate and velocity significantly changes. It can be clearly observed from above graphical outputs, comparison table and graph that by taking air inlet location towards top side of the room, the air flow rate increases and velocity decrease.

Another important factor in room ventilation is air flow pattern. Keeping this important factor in view, the desired air flow pattern has been seen in models where air inlet location is at the bottom and top of the wall.

The detailed discussion on above mentioned cases has been carried out in Chapter: 3 Results and Analysis section.

5.5 Modeling and Simulation of 3D Real Sized Room

Before going into detailed simulation of the models with reference to change in room air inlet location, a comprehensive study has been carried out on the area around room air inlet opening. Normally air flow properties and patterns are not considered for detailed study in natural ventilation. For this purpose, an environment box of dimensions 1.5 meter × 1.5 meter × 1.5meter was made around air inlet opening of the room as shown in figure 5.2 below:

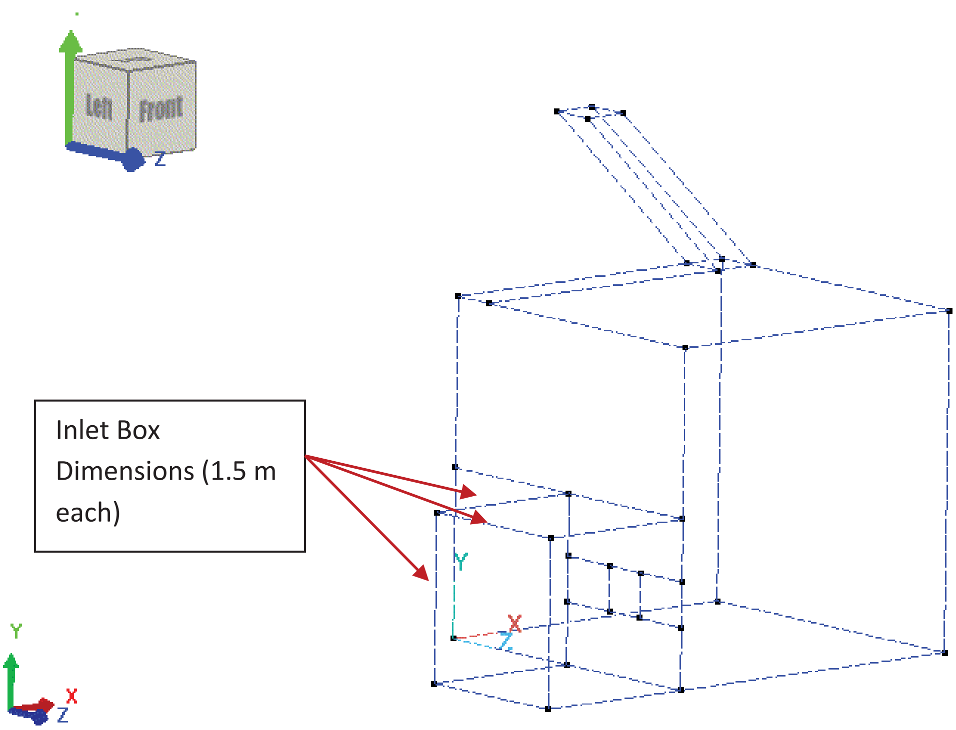

Figure: 5.2: 3D Room created in CFD-GEOM with Inlet Box

Initially, detailed analysis was performed on this model. The simulation of above room in the presence of inlet environment box has given the very clear idea about the air flow patterns just before the inlet of the room. It has been noted that majority of outside air does not enter the room and passes across the inlet. The detailed analysis and results obtained against this inlet environment box has been discussed in Chapter: 4.

Further analysis has been performed on a real sized room to keep the simulation as per practical situation. The graphical and numerical analysis showed that with change of room air inlet location, air flow rate through inlet interface almost remained same in all three models. The velocity magnitude slightly increases by taking inlet to top side of the wall and further increases when inlet is opposite to chimney side.

Another important factor in room ventilation is air flow pattern. Keeping this important factor in view, the best air flow pattern has been seen in a model where air inlet location is at the bottom of the wall at opposite corner of the Chimney (figures 4.63, 4.64 & 4.65) and model with air inlet location at top of the wall (figures 4.58, 4.59 & 4.60). In these models, air is more evenly distributing in whole room as compared to third model, which will give comfort to the occupants of the room. The detailed discussion on above mentioned cases has been carried out in Chapter:4 Results and Analysis section.

After studying the behavior of air circulation at inlet of the room through designing of environment box, same approach has been adopted at outlet of the room. An environment box of same dimension as that of inlet was designed and model was put up for simulation. The basic purpose of designing of environment box at outlet is to study of air ventilation behavior at exit of the solar chimney. For this purpose, an environment box of dimensions 1.5 meter × 1.5 meter × 1.5 meter was made around air outlet (chimney exit) opening of the room as shown in figure 5.3 below:

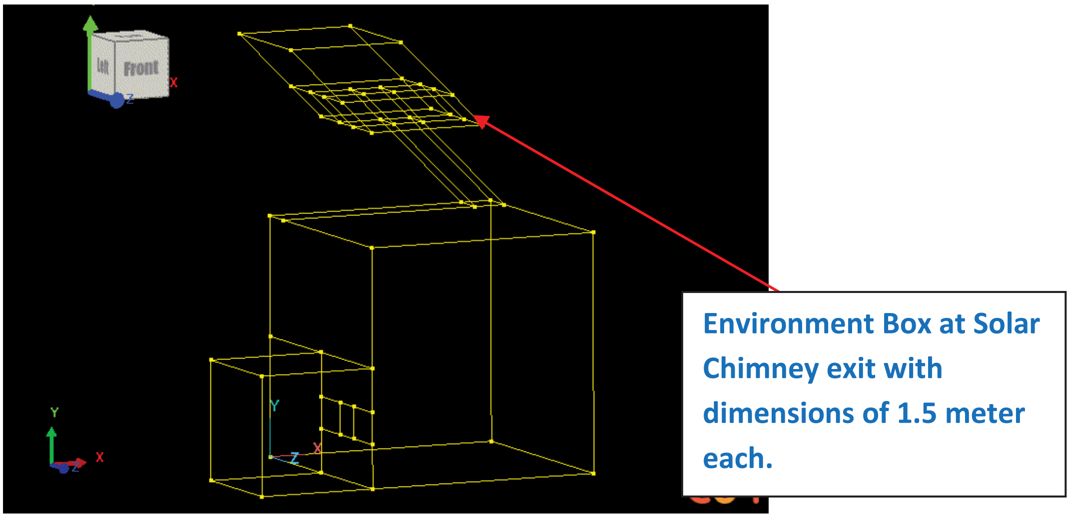

Figure: 5.3: 3D Room created in CFD-GEOM with Inlet and outlet environment Boxes

The detailed analysis and discussion on results obtained after simulation of above model has been discussed in chapter : 4, Section : 4.12.3.

5.6 Analysis of Air Flow Rate in Terms of “Air Changes per Hour (ACH)

An important factor in performance and analysis of air ventilation systems is Air Changes per Hour. This factor gives idea about the quantity of exchange of air through a particular space over a 1 hour period.

The above factor has been graphically analyzed with following two conditions;

a) **Three models with different inlet opening locations have been analyzed with reference to change in ACH value.**

The results / analysis obtained after simulation / analysis of data reveals that there is no considerable change in ACH value by changing room air inlet locations. The most appropriate results are obtained in a model with inlet opening opposite to solar chimney i.e. ACH value of 5.72. The detailed results and analysis has been discussed in previous chapter / section 4.13.

b) Effect of solar chimney exit pressure on ACH value.

The analysis of model with change in solar chimney exit pressure has shown considerable increase in ACH value with change (reduction) in solar chimney exit pressure. By improving induced pressure in solar chimney, very effective room ventilation rate can be achieved. The detailed results and analysis has been discussed in previous chapter / section 4.13.

5.7 Contribution and Achievement

The field of natural ventilation is very huge and there is much scope of research in this field. Each and every aspect has been studied extensively by different researchers but with the passage of time, new phases of development are arising.

In the present research, concentration has been given on inlet location of the room opening and studied the behavior of air around inlet opening. It is really necessary to study and understands the behavior of air around room inlet with different locations of the room inlet. For this purpose, an environmental box has been considered around room air inlet for each model. By considering this type of model, the broader understanding has been achieved about behavior of air flow through room inlet.

The idea and purpose of designing of environment boxes around inlet opening of the room and chimney outlet opening is to study the behavior of air ventilation rate / magnitude around these important areas in a natural ventilation scenario of a room / building.

It is clear from the simulation results that:

- The much of the air present at the entrance of the room does not enter the room in normal scenario.
- The direction of the air flow, room air inlet and location of room air inlet plays vital role in air flow rate inside the room.
- Air flow at bottom of the room (sitting area) is achieved by keeping room air inlet location at bottom of the room while more air flow rate is achieved by keeping inlet location at top of the wall.
- The position of room air outlet i.e. solar chimney exit and magnitude of pressure value at exit of chimney plays important role in ventilation rate of air but flow pattern of the air in the room remains almost same.
- The high air flow intake in the room can be achieved by choosing the proper air inlet location keeping in view the historical environmental trends / direction of air in that particular area. Similarly, low pressure at exit of the solar chimney through adjustment of chimney inclination angle, height of the chimney etc.
- Another important factor in any building ventilation system is that how much air passes through a space in a specified time. This factor is normally measured in terms of Air Changes per Hour (ACH). This factor has been studied and analyzed in detail against simulated models. The results / analysis show that room air inlet location has minor effect on ACH value compared to solar chimney exit pressure value. The change in later considerably changes ACH value.

5.8 Recommendations

- The room air inlet opening plays a vital role in getting the desired natural ventilation. Before actual installation of the solar chimney on any building, the appropriate room air inlet location should be chosen based on physical environment, historical air flow velocities and directions. The appropriate location of the room air inlet will certainly boost the performance of solar chimney and ultimately natural ventilation.

  If the appropriate location / direction of the inlet opening is not chosen, very less air may enter the room and much induced pressure will be required to achieve the desired ventilation.

- The analysis of inlet environment box has also raised the need of further research about the pattern of air just before inlets. The further research will help to induce maximum air into the room either with the improvement of room air inlet opening design / shape or by making some geometry around inlet opening so that the maximum air may be directed into the room.

- The environmental conditions around outlet of the room i.e. solar chimney exit, also plays vital role in controlling air ventilation rate and magnitude. Further research is required around outlet opening of the room to dig out the ways for enhancement of induced pressure, which will certainly give more air ventilation and higher value of ACH.

- The Air Change per Hour (ACH) value, which is an important parameter in building ventilations, is much dependent on solar chimney exit pressure. The conditions at solar chimney exit may be manipulated to get desired results and enhanced ventilation, This again requires further investigation at exit area of solar chimney.

Bibliography

[1] J. Arce, *et al.* "**Experimental study for natural ventilation on a solar chimney",** Renewable Energy, 34 (12) (2009), pp. 2928–2934

[2] T. Miyazaki, A. Akisawa, T. Kashiwagi, "**The effects of solar chimneys on thermal load mitigation of office buildings under the Japanese climate",** Renewable Energy, 31 (7) (2006), pp. 987–1010

[3] N.K. Bansal, R. Mathur, M.S. Bhandari, "**Solar chimney for enhanced stack ventilation",** Building and Environment, 28 (3) (1993), pp. 373–377

[4] N.K. Bansal, R. Mathur, M.S. Bhandari, "**A study of solar chimney assisted wind tower system for natural ventilation in buildings",** Building and Environment, 29 (4) (1994), pp. 495–500

[5] B. P. Huynh, **"Natural ventilation induced by solar chimneys",** 17th Australasian Fluid Mechanics Conference, Auckland, 5-9 December, 2010.

[6] K.H. Lee, R.K. Strand, "**Enhancement of natural ventilation in buildings using a thermal chimney",** Energy and Buildings, 41 (6) (2009), pp. 615–621

[7] K. Pavlou, K. Vasilakopoulou, M. Santamouris, "**The impact of several construction elements on the thermal performance of solar chimneys",** International Journal of Ventilation, 8 (3) (2009), pp. 277–285

[8] K. Goriel, V. Avakian, B. P. Huynh, **"Study of Natural ventilation flow in a room fitted with a solar chimney",** IMECE2012, Houston, 9-15 November, 2012

[9] ClitoAfonso, Armando Oliveira, **"Solar Chimneys: Simulation and experiment",** Energy and Buildings, 32 (2000), pp. 71–79

[10] Rakesh Khanal, Chengwang Lei, **"Flow Reversal Effects on buoyancy induced air flow in a solar chimney",** Solar Energy, 86 (2012), pp. 2783–2794

[11] Roache P.J. (1998), **"Verification and Validation in Computational Science and Engineering"**, pp 107-142.

[12] Yau R. (2002) **'Building environmental and sustainable design approach to housing developments'**, Housing Conference, Hong Kong Housing Authority.

[13] Yau R. and Lee S. (2003) **"Building environmental and sustainable design by advanced simulation techniques"**, Proceedings of Shandong-Hong Kong Joint Symposium.

[14] Versteeg H. K. and Malalasekera W. (1995), " **An Introduction to Computational Fluid Dynamics – The Finite Volume Method"**, Longman, Harlow, UK.

[15] Emmerich S. J. and McGrattan K. B. (1998), **"Application of a large eddy simulation model to study room airflow"**, ASHRAE Transactions, vol 104, pp 1128–1140.

[16] Murakami S. (1998), **"Overview of turbulence models applied in CWE-1997"**, Journal of WindEngineering and Industrial Aerodynamics, vol 74–76, pp 1–24.

[17] Zhang W. and Chen Q. (2000**), "Large eddy simulation of indoor airflow with a filtered dynamic sub grid scale model"**, International Journal of Heat and Mass Transfer, vol 43, no 17, pp 3219–3231.

[18] Wang J.C.Y., Jiang Z. and Haghighat F.(1991) **"Influence of air infiltration on airflow in a ventilated isothermal two-zone enclosure"**, Energy and Buildings, vol 17, pp 43–54.

[19] Li Y. and Fuchs L.(1993), **"'Numerical prediction of airflow and heat–radiation interaction in a room with displacement Ventilation"**, Energy and Buildings, vol 20, pp 27–43.

[20] Borchiellini G. V., Fracastoro M. and Perino L.(1994) **, "Analysis of IAQ in a university auditorium', in Proceedings of Roomvent '94, 4th International Conference on Air Distribution in Rooms"**, Cracovia, 15–17 June, vol 2, pp 47–62.

[21] Chen Q. (1996), **"Prediction of room air motion by Reynolds-stress models"**, Building andEnvironment, vol 31, no 3, pp 233–244.

[22] Chen Q. (2009), **"Ventilation performance prediction for buildings: A method overview and recent applications",** Building and Environment, vol 44, no 4, pp 848–858.

[23] R. Bassiouny, N.S.A. Koura, **"An analytical and numerical study of solar chimney use for room natural ventilation"**, Energy and Buildings, 40 (5) (2008), pp. 865–873

[24] K.S. Ong, C.C. Chow, **"Performance of a solar chimney"**, Solar Energy, 74 (1) (2003), pp. 1–17

[25] J. Mathur, *et al., "***Experimental investigations on solar chimney for room ventilation"**, Solar Energy, 80 (8) (2006), pp. 927–935

[26] J. Mathur, Anupama, S. Mathur**, "Experimental investigation on four different types of solar chimneys"**, Advances in Energy Research (2006), pp. 151–156

[27] J. Mathur, S. Mathur, Anupma**, "Summer-performance of inclined roof solar chimney for natural ventilation"**, Energy and Buildings, 38 (10) (2006), pp. 1156–1163

[28] Z.D. Chen, et al., **"An experimental investigation of a solar chimney model with uniform wall heat flux"**, Building and Environment, 38 (7) (2003), pp. 893–906

[29] J. Hirunlabh, et al., **"Study of natural ventilation of houses by a metallic solar wall under tropical climate"**, Renewable Energy, 18 (1) (1999), pp. 109–119

[30] N.K. Bansal, *et al.,* **"Modeling of window-sized solar chimneys for ventilation"**, Building and Environment, 40 (10) (2005), pp. 1302–1308

[31] P. Chantawong, *et al.,* **"Investigation on thermal performance of glazed solar chimney walls"**, Solar Energy, 80 (3) (2006), pp. 288–297

[32] S. Punyasompun, *et al.,* **"Investigation on the application of solar chimney for multi-story buildings"**, Renewable Energy, 34 (12) (2009), pp. 2545–2561

[33] B. Zamora, A.S. Kaiser, **"Optimum wall-to-wall spacing in solar chimney shaped channels in natural convection by numerical investigation"**, Applied Thermal Engineering, 29 (4) (2009), pp. 762–769

[34] S.A.M. Burek, A. Habeb**, "Air flow and thermal efficiency characteristics in solar chimneys and trombe walls",** Energy and Buildings, 39 (2) (2007), pp. 128–135

[35] D.J. Harris, N. Helwig, **"Solar chimney and building ventilation"**, Applied Energy, 84 (2) (2007), pp. 135–146

[36] E.P. Sakonidou, et al., **"Modeling of the optimum tilt of a solar chimney for maximum air flow"**, Solar Energy, 82 (1) (2008), pp. 80–94

[37] Chien, K.-Y., **"Predictions of Channel and Boundary Layer Flows with a Low-Reynolds-Number Turbulence Model"**, AIAA Journal, 20, 1982, 33-38.

[38] B. P. Huynh, **"Natural-Ventilation Flow in a 3-D Room Fitted With Solar Chimney"**, Proceedings of the ASME 2012 InternationalMechanical Engineering Congress & Exposition, Houston, Texas, USA, 9-15 November 2012.

[39] Nadia Saifi, Settou, Dokkar, Negrou, Chennouf, **“Experimental Study and Simulation of Air Flow in Solar Chimney”**, Energy Procedia 18 (2012), 1289 – 1298

[40] Leticia Neves, Roriz, Marques de Silva, **“Modeling a Solar Chimney for Maximum Solar Irradiation and Maximum Air Flow, for Low Latitude Locations”**, Proceedings of Building Simulation 2011.12th Conference ofBuilding Performance Simulation Association, Sydney, 14-16 November 2011.

[41] TayebiTahar et al, **“Numerical Simulation of Natural Convection in a Solar Chimney”**, International Journal of Renewable Energy Research, Vol 2, No. 4, 2012.

[42] Y. Kaneko, K. Sagara, T. Yamanaka, H. Kotani, **“Ventilation Performance of Solar Chimney With Built-in Latent Heat Storage”**, CSEM - UAE Innovations Inc.

[43] M. Santamouris, “**Advances in Building Energy Research**”, Volume 1, Published by Earthscan.

[44] ISSEI KATO/Reuters/File, LNG storage tanks and a membrane-type tanker at Tokyo Electric Power Co's Futtsu Thermal Power Station in Futtsu, east of Tokyo, Photograph, viewed October 2016.

<https://www.csmonitor.com/Environment/Energy-Voices/2013/0301/Japan-should-invest-in-European-shale-gas>

[45] BP 2015 Data, Global Energy Consumption 2014, Pie Chart viewed November 2017 in “Energy Matters”.

<http://euanmearns.com/global-energy-trends-bp-statistical-review-2015/>

[46] COLIN J. CAMPBELL, depletion model of conventional energy resources, Graph viewed October 2016 in “Changing in Human Circumstances”

<http://www.resilience.org/stories/2015-04-09/changing-human-circumstances/>

[47] Barry Saxifrage, Analysis, Energy, Photo by Kris Krug seen in “These 'missing charts' may change the way you think about fossil fuel addiction” Viewed November 2017.

<https://www.nationalobserver.com/2017/07/13/analysis/these-missing-charts-may-change-way-you-think-about-fossil-fuel-addiction>